UNIVERSITY OF LIVERPOOL | INSTITUTE OF TRANSLATIONAL MEDICINE

Advanced Magnetic Resonance Imaging Studies in Patients with Refractory and Non-refractory Focal Epilepsy

Lorna Bryant

Ph.D. **2021**

Advanced Magnetic Resonance Imaging Studies in Patients with Refractory and Non-refractory Focal Epilepsy

This thesis is submitted in accordance with the requirements of the University of Liverpool for the Degree of Doctor in Philosophy

by

Lorna Bryant BSc, MSc (*Distinction*)

June 2021

In memory of

Warren Mark Bryant, who will see me become a Dr from above

Declaration

This thesis is the result of my own work. The material contained in this thesis has not been presented, nor is currently being presented, either wholly or in part, for any other degree or qualification.

Lorna Bryant

Acknowledgements

There are many people to thank in supporting me throughout this incredibly long journey. First my supervisors, Simon Keller, Tony Marson, Harish Poptani, and Lauren Walker for providing me with skills, opportunities, and knowledge which has been invaluable. Also, to Val Adams, for giving me so much support in setting up my study, and especially to Kieran Murphy for helping in every possible way and for our ridiculous discussions during scanning. Guleed, thank you for helping me get my recruitment over the line, and to the rest of the clinicians at the Walton Centre for all your support. To the research nurses and doctors who helped me out when I really needed it and to the rest of the Keller lab and to everyone in MARIARC/LiMRIC who has supported me when it got tough. Amal, Alanood, Manal, Dan, Nikki, Christophe, Liv – thanks for everything. Thanks to the MRC and to DiMEN for my funding and for the support over years. Particularly Emily for arranging the training, and to the original Liverpool cohort for the laughs. To the group at MUSC, especially Leo, Emilie, and Andrew – thank you for the week you allowed me to spend with you and for answering my constant questions, you all taught me more than I would have thought possible in such a short time. Of course, thank you to the patients, who gave up their time to take part in my work.

I want to say an extra special thank you to Barbara Kreilkamp and Yachin Chen, without both of you, this thesis would not be where it is today. I admire you both as friends and as scientists, and I know you'll both go far.

To my family, thanks for supporting me in the past 25(!) years of my education. To my mum and Dave who sorted me out when I needed it, and to Aimee and Ash for dog walking with me. A special thank you to Kay, Geoff, and the rest of the Deakin/Cannons, for adopting me into your family and supporting me in ways I never expected you to. To my other family, Georgia – I couldn't do any of it without you, and I will always follow you around the country.

To all my friends, you know who you are – thank you, really. A special thank you to Andrea (and Fionnian), and Sarika, for everything you do for me. And finally, to Bonelli, for keeping me going.

Abstract

Epilepsy is the most common serious neurological disorder affecting over 50 million people worldwide, with 87 people in the UK being diagnosed with epilepsy every day. Approximately 30% of patients with epilepsy will continue to experience persistent seizures despite treatment with anti-epileptic drugs (AEDs) and will go on to develop chronic pharmacoresistant epilepsy. Patients who do not achieve complete seizure control following the first two regimens of AEDs, and within the first two years of starting treatment, have a very small chance of achieving seizure freedom and may be considered to have pharmacoresistant epilepsy. Currently, predictors of achieving seizure control are lacking.

This aims of this thesis were to identify biomarkers of pharmacoresistant epilepsy using two main methods: (1) advanced diffusion magnetic resonance imaging to investigate underlying microstructural pathology and; (2) identifying markers of brain and peripheral inflammation to further understand the biological mechanisms underlying diffusional changes.

Two datasets were analysed, both including a cohort of age-matched controls: patients with newly diagnosed focal epilepsy who were followed up 12 months after undergoing MRI scanning to assess response to AED treatment (cohort 1), and patients with chronic epilepsy who were either experiencing persistent seizures despite AED treatment at time of MRI, or who were seizure free for at least six months at time of MRI (cohort 2).

We revealed significant diffusional changes in both grey and white matter in patients with newly diagnosed and longstanding focal epilepsy. Despite being long considered a disorder of grey matter, we were able to identify changes in white matter in both cohorts suggesting of a perturbed network at the onset of disease and later in disease progression. The use of advanced Fiber Ball Imaging enabled inference of biological mechanisms underlying diffusional changes and has highlighted the importance of advanced imaging methods in the study of focal epilepsy.

Contents

List of Figures

List of Tables

List of Abbreviations

3T	3 Tesla
AD	Axonal diffusivity
AED	Anti-epileptic drugs
AFQ	Automated fibre quantification
AK	Axonal kurtosis
AWF	Axonal water fraction
BBB	Blood-brain barrier
BOLD	Blood oxygenation dependent level
CHARMED	Composite hindered and restricted model of diffusion
CSD	Constrained spherical deconvolution
CSF	Cerebrospinal fluid
CSI	Chemical shift imaging
DKE	Diffusion kurtosis estimator
DKI	Diffusion kurtosis imaging
DMN	Default mode network
DTI	Diffusion tensor imaging
DWI	Diffusion weighted imaging
EEG	Electroencephalography
ELISA	Enzyme-linked immunoabsorbent assay
FA	Fractional anisotropy
FAA	Intra-axonal fractional anisotropy
FAE	FA of the extra-axonal space
FBI	Fiber ball imaging
FBWM	Fiber ball white matter
FCD	Focal cortical dysplasia
FLAIR	Fluid-attenuated inverstion recovery
FLE	Frontal lobe epilepsy
FLIRT	FMRIB's linear image registration tool
FODF	Fiber orientation dispersion index
FOV	Field of view
FWI	Free-water imaging
GGE	Genetic generalised epilepsy
GM	Grey matter
HMGB1	High-mobility box group 1
HS	Hippocampal sclerosis
ICVF	Intra cranial volume fraction
IL-1β	Interleukin 1 beta
ILAE	International League Against Epilepsy
IRAS	Integrated research application system
KFA	Kurtosis fractional anisotropy

MCD	Malformations of cortical development
mcDESPOT	Multi-compartment driven equilibrium single pulse observation of T1/T2
MD	Mean diffusivity
MK	Mean kurtosis
MNI	Montreal Neurological Institute
MPRAGE	Magnetisation-prepared rapid acquisition gradient echo
MR	Magnetic resonance
MRI	Magnetic resonance imaging
MRS	Magnetic resonance spectroscopy
MTI	Magnetic transfer imaging
MTS	Mesial temrporal sclerosis
MWF	Myelin water fraction
NICE	National Institute for Health and Care Excellence
NMR	Nuclear magnetic resonance
NODDI	Neurite orientation dispersion and density imaging
ODI	Orientation dispersion index
PET	Positron emission tomography
PRESS	Point-resolved spectroscopy
RAGE	Receptor for advanced glycation endproducts
RD	Radial diffusivity
RK	Radial kurtosis
ROI	Region of interest
SE	Status epilepticus
SUDEP	Sudden unexplained death in epilepsy
T1	T1-weighted
T2	T2-weighted
TBI	Traumatic brain injury
TE	Time to echo
TI	Time to inversion
TLE	Temporal lobe epilepsy
TMS	Transcranial magnetic stimulation
TNF-α	Tumor necrosis factor alpha
TR	Time to repetition
TRACULA	TRActs Constrained by UnderLying Anatomy
TSPO	Translocator protein
WM	White matter
WMTI	White matter tract integrity

1 Introduction

1.1 Background

Epilepsy is a neurological disorder which is characterised by recurrent spontaneous seizures. The International League Against Epilepsy (ILAE) define epilepsy as "a disease of the brain defined by any of the following conditions: (1) At least two unprovoked (or reflex) seizures occurring >24 hours apart; (2) one unprovoked (or reflex) seizure and a probability of further seizures similar to the general recurrence risk (at least 60%) after two unprovoked seizures, occurring over the next 10 years; (3) diagnosis of an epilepsy syndrome" (Fisher *et al*., 2014). Approximately 1% of the population in the UK have epilepsy, making it the most common serious neurological disorder, with 87 people being diagnosed daily (Epilepsy Action UK, 2019). For a diagnosis to be made, a patient typically needs to have experienced a minimum of two unprovoked seizures. Epilepsy can severely affect quality of life, with patients often

losing independence through inability to drive or needing assistance with daily living. Around 50% of patients with epilepsy have at least one medical comorbidity (Keezer, Sisodiya and Sander, 2016), with between 37-60% of patients experiencing a psychiatric comorbidity, depending on type of epilepsy (Josephson, Jetté and Jett, 2017). There is also an increased risk of death from SUDEP (sudden unexplained death in epilepsy), with an incidence rate of 0.35 per 1000 person-years. This exceeds the expected sudden death rate of the general population by around 24 times (Ficker *et al*., 1998). There are a range of different seizure types affecting patients with epilepsy, which have been described by the ILAE. Seizures are characterised by type, cause, age of onset and electroencephalographic patterns (ILAE, 1989). These seizure classifications continue to be adapted and revised, with the most recent revision being published in 2017. This allows new knowledge and research into epilepsy to be brought into diagnosis.

1.1.1 Epileptic seizures

A seizure is an episode of excessive synchronous neuronal activity in the brain, temporarily disrupting its normal functioning. The clinical presentation of a seizure depends on the region and extent of brain involved and can affect motor function, awareness, perception, autonomic function or a combination of these (Miller and Goodkin, 2014). Epilepsy is a condition involving recurrent, spontaneous seizures, and as such is usually diagnosed following two or more seizures. An epilepsy syndrome refers to a group of symptoms, of which seizures are the primary manifestation, which consistently occur together. These symptoms may be defined by seizure focus, age of onset, seizure type, electroencephalogram (EEG) findings, response to anti-epileptic drugs (AEDs), aetiology, and prognosis.

1.1.2 Epileptic seizure subtypes

There are broadly two types of epileptic seizure; focal onset and generalised onset. Focal onset seizures, previously termed partial onset seizures, are defined by the ILAE (2017) as "originating within networks limited to one hemisphere. They may be discretely localized or more widely distributed. Focal seizures may originate in subcortical structures" (Fisher *et al*., 2017). Further classification of focal seizures then depends on whether awareness remains (focal aware, previously simple partial)

during a seizure or is impaired (focal with impaired awareness, previously complex partial). Awareness is defined by the ILAE in this instance as knowledge of the self and environment, and awareness does not need to be impaired for the duration of the seizure for it to be classified as focal with impaired awareness. Further, a focal seizure may spread to involve the whole brain, this is termed a focal to bilateral tonic-clonic seizure (previously partial seizure with secondary generalisation). Generalised onset seizures are defined as "originating at some point within, and rapidly engaging, bilaterally distributed networks" (Fisher *et al*., 2017). Finally, seizures can be classified as unknown onset if the focus is unclear but may be later classified as focal or generalised with further evidence. Regardless of seizure onset, all types can be additionally classified into motor or nonmotor onset. Specific motor and nonmotor seizures for each type can be seen in Figure 1.1, and the reader is referred to Fisher *et al*. (2017) for detailed descriptions of these seizure types.

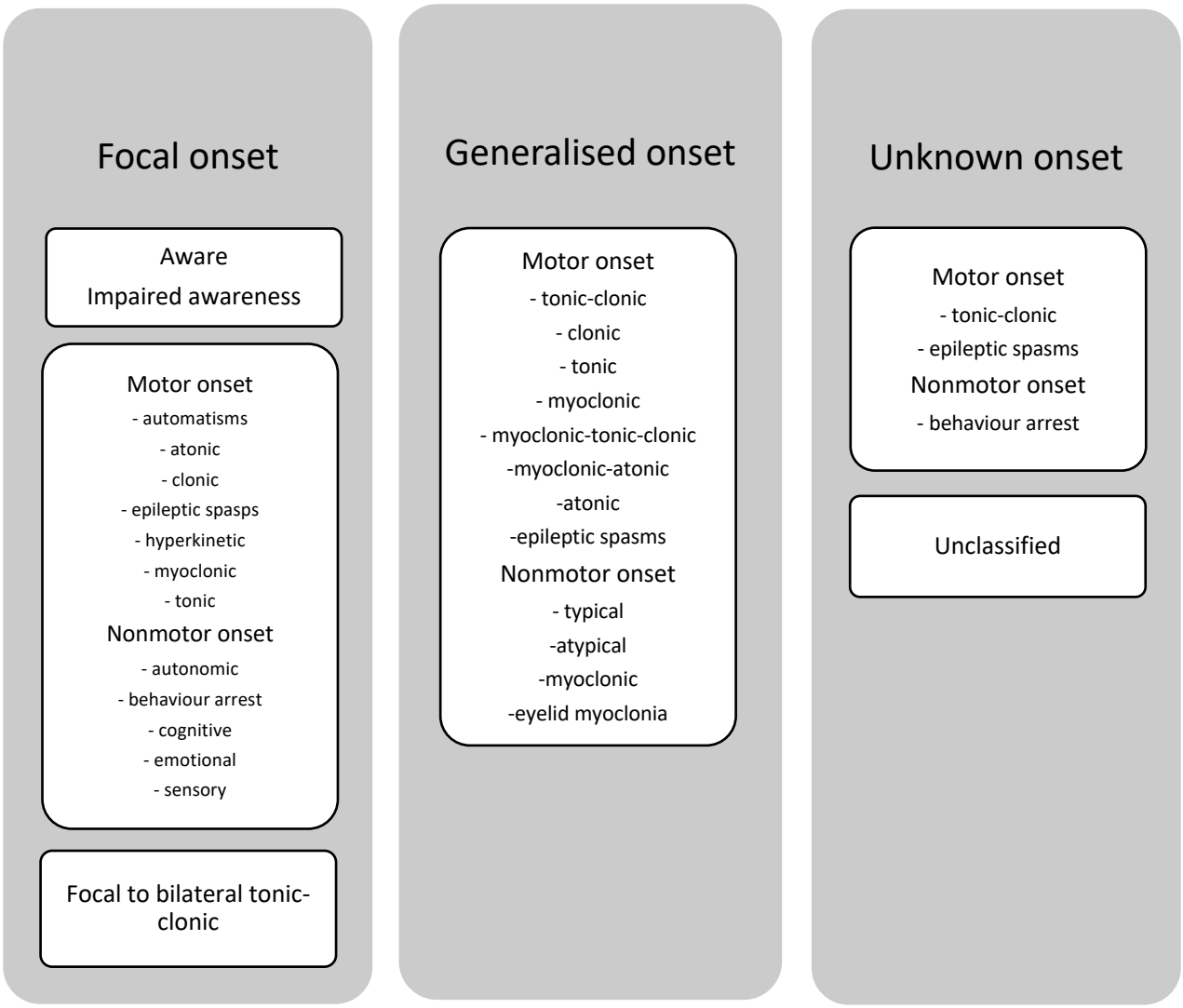

Figure 1.1: Classification of epileptic seizures according to ILAE 2017. Note that the organisation is not hierarchical, as naming the awareness level is optional. Adapted from Fisher *et al*. (2017)

1.2 Diagnosis, treatment, and management of epilepsy

The National Institute for Health and Care Excellence (NICE) publish guidance for the diagnosis, treatment, and management of patients with epilepsy in the UK, to which the reader is referred for detailed information[1]. A diagnosis of epilepsy is made usually following two or more seizures by a specialist medical practitioner. However,

[1] https://www.nice.org.uk/guidance/cg137/chapter/1-Guidance#diagnosis-2

epilepsy may be diagnosed following one seizure if the probability of further unprovoked seizures is greater than 60%, which may be the case following stroke or in the presence of a structural abnormality (Rugg-Gunn and Stapley, 2017). See Figure 1.2 for details on diagnosis and management of epilepsy.

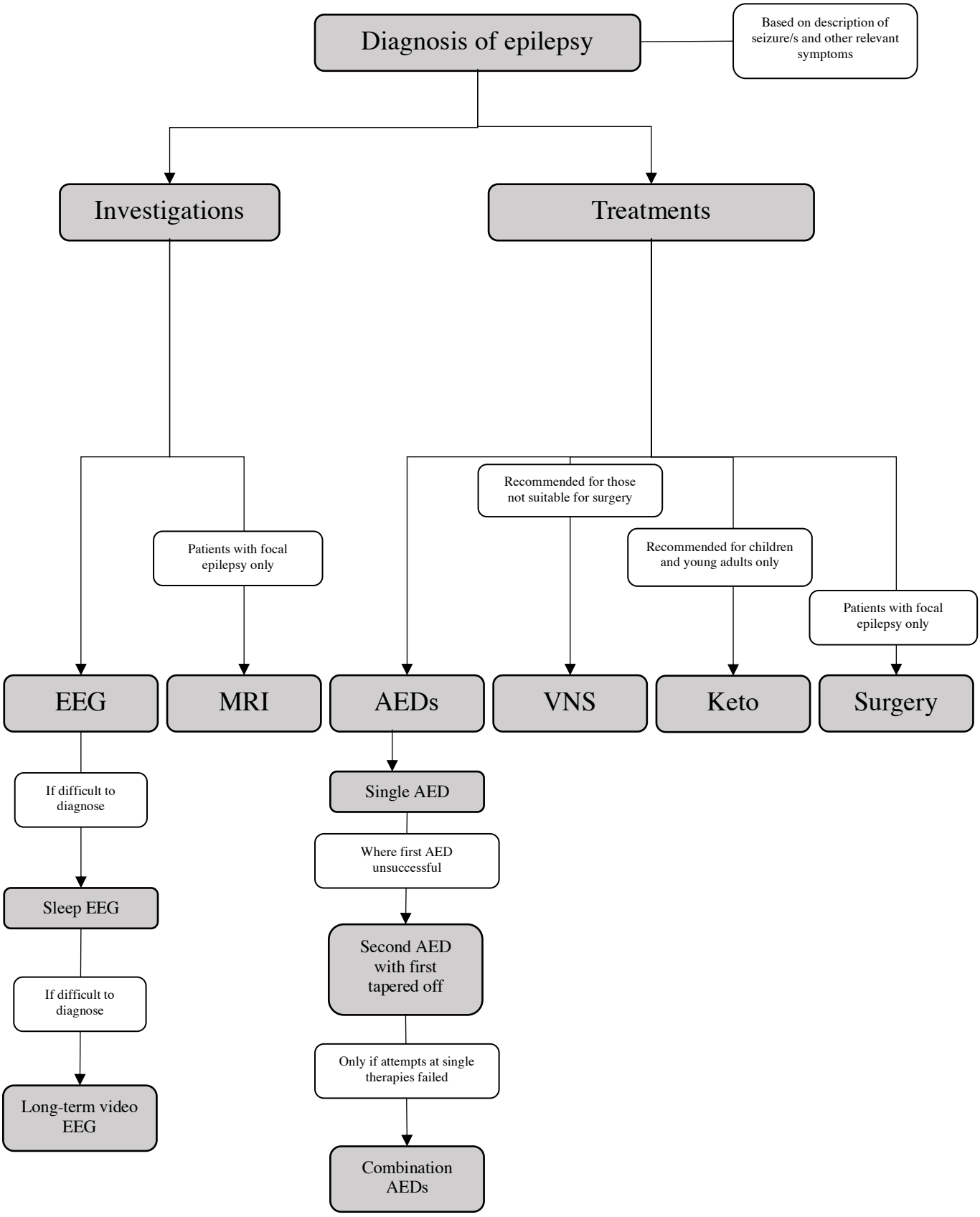

Figure 1.2: Flowchart detailing diagnosis, treatment, and management of epilepsy, according to NICE guidelines (https://www.nice.org.uk/guidance/cg137/chapter/1-Guidance#diagnosis-2)

1.2.1 Clinical MRI

Patients with focal seizures will typically undergo structural MRI for the detection of potential lesions. MRI is performed in two situations in patients with focal epilepsy. The first is in those with newly diagnosed epilepsy and those with longstanding epilepsy who require more detailed investigation. The second is for patients who have refractory epilepsy and are being considered for resective surgery (Cendes *et al*., 2016). MRI is useful for identifying abnormalities which may be related to epilepsy, such as hippocampal sclerosis or focal cortical dysplasia. Importantly, MRI can also offer information on pathology which may be related to seizures but would rule out a diagnosis of epilepsy such as tumour, infection, or vascular malformations. While epileptogenic lesions may be identified through standard MRI protocols, small or subtle lesions may be missed and so it is recommended to use an optimised epilepsy protocol (Cendes *et al*., 2016). The specifics of this protocol will depend on the likely diagnosis or suspected lesion. For example, for patients with suspected neocortical lesions, commonly acquired scans include a coronal T1-weighted (T1-w) perpendicular to the long axis of the hippocampus, a high resolution volume (3D) T1-w scan with isotropic voxels, coronal T2-weighted (T2-w), and a coronal and axial or 3D fluid-attenuated inversion recovery (FLAIR) scan (Cendes *et al*., 2016). Common features seen on MRIs in the presence of dysplasia include abnormally thick grey matter and blurring of the white/grey boundary on T1-w scans and grey matter hyperintensity of lesions seen on T2-w images with an increased sensitivity to this on FLAIR images (So and Ryvlin, 2015).

1.3 Additional research MRI

Along with standard MRI sequences used primarily as diagnostic tools, several more advanced imaging techniques are beginning to be employed in the clinical environment, most commonly for surgical planning.

1.3.1 Diffusion imaging

Diffusion imaging allows for the visualisation of white matter (WM) tracts and measures of structural connectivity using diffusion tensor imaging (DTI) tractography (Chapter 2). Briefly, this technique allows the reconstruction of white matter (WM) pathways through the quantification of water diffusivity along the main and

perpendicular axes of axons. This allows for inference of structural brain connections and WM fibre integrity and is thus extremely useful for surgical planning and decision-making prior to and during surgery (Sivakanthan *et al*., 2016). For example, tractography of the optic radiations has been used for the surgical planning of mesial temporal resections including selective amygdalohippocampectomy in order to reduce visual field deficits. Thudium *et al*. (2010) verified the value of this in a study of 12 patients who underwent preoperative DTI tractography prior to selective amygdalohippocampectomy. Nine of the 12 patients had no postoperative field deficits and the authors concluded tractography was a useful tool for preoperative planning (Thudium *et al*., 2010). Additionally, Yogarajah *et al*. (2009) demonstrated the utility of DTI in assessing a patient's individual risk of developing postoperative visual field deficits following anterior temporal lobe resection.

1.3.2 Functional MRI

Similarly, functional MRI (fMRI) has also been used to aid surgical planning. fMRI quantifies the blood oxygen level dependent (BOLD) signal and this can be measured during a task (task-based fMRI) or at rest (rsfMRI). Task-based fMRI has been used extensively to non-invasively localise language function prior to surgery (Abou-Khalil, 2007), with a typical task involving word generation or recognition. During these tasks, the BOLD signal increases in the areas involved in the task and provides localisation of brain regions involved in performing the task. Alternatively, rsfMRI does not use tasks and measures the BOLD signal during rest. This allows for visualisation of resting networks within the brain which can be useful for localisation of regions involved in various cognitive functions. A study of 16 patients with refractory medial temporal lobe epilepsy (TLE) was able to identify regions involved in the epileptogenic network with an average sensitivity of 77.2% and specificity of 83.86% (Zhang *et al*., 2011). A study using seed-based methods was able to successfully identify sensorimotor areas in patients with tumours or epileptic foci in this region; the areas identified using rsfMRI agreed with task-based fMRI and intraoperative cortical stimulation (Liu *et al*., 2009). Similarly, a study which compared task-based- and rs-fMRI found that language activation can be reliably mapped from rsfMRI even in young paediatric patients (Suarez *et al*., 2014). The

utility of rsfMRI to guide surgical planning has important implications for sedated young patients, for which task-based fMRI would not be appropriate.

Along with surgical planning, rsfMRI has also been used in research environments. Recent studies have demonstrated altered resting state networks in patients with idiopathic generalised epilepsy (IGE) (Chen *et al*., 2021). In this study, patients with refractory IGE demonstrated increased functional connectivity between specific thalamic nuclei and cortical regions compared to patients with non-refractory IGE. Alternatively, in a network based study, no differences were found between patient groups, however, patients in general demonstrated higher global connectivity compared to patients (Pegg *et al*., 2021). Together, these studies suggest an increase in functional connectivity in patients with IGE. Abnormalities in functional connectivity have also been demonstrated in patients with focal epilepsy. In patients with TLE, more abnormal connections were seen in patients compared to controls (Pereira *et al*., 2010). Interestingly, numerous studies have reported reduced functional connectivity in multiple pre-defined networks (Zhang *et al*., 2009; Liao *et al*., 2011; Moeller *et al*., 2011; Masterton, Carney and Jackson, 2012; McGill *et al*., 2012).

1.4 Causes of epilepsy & pathology

Epileptogenesis – the process of a non-epileptic brain developing into an epileptic one (Pitkänen and Engel, 2014) - is thought to be caused by an imbalance between excitatory and inhibitory activity within neurons (Thijs *et al*., 2019). This imbalance causes the neuronal network to behave in an excessive and hypersynchronous manner which leads to the disruption of other networks in the brain (Fisher *et al*., 2005). In patients with generalised epilepsy, and those with focal to bilateral tonic-clonic epilepsy, these networks are widely distributed and involve both hemispheres. In those with focal epilepsies these networks involve one hemisphere and often one localised region of this hemisphere.

1.4.1 Genetic contributions

Generalised epilepsy is widely considered to have a genetic basis (Helbig *et al*., 2008). There are more than 30 different mutated genes which have been found in familial monogenic – where a single genetic mutation accounts for a phenotype - epilepsies

(Steinlein *et al*., 1995; Gourfinkel-An *et al*., 2004). These are primarily in genes coding for ion channels but also in those for neuronal receptors, transcription factors, and enzymes (Thijs *et al*., 2019). However, the majority of inherited epilepsies are not monogenic, rather they have a complex inheritance pattern suggesting that the phenotype is determined by more than one gene – oligogenic or polygenic (Thomas and Berkovic, 2014). Further, it is suggested that there may be a gene-environment interaction in many epilepsies (Berkovic *et al*., 2006), particularly following a major brain insult such as traumatic brain injury (TBI; Christensen *et al*., 2009). Though generalised epilepsies are traditionally thought of as being the only epilepsies with a genetic basis, there is some evidence supporting the role of genetics in focal epilepsies. Previously, focal epilepsies were thought of as being only acquired (Thomas and Berkovic, 2014). However, in a study of 40 patients with focal epilepsies suspected to have a genetic basis, 12.5% of cases were found to have a pathogenic or likely pathogenic variant (Perucca *et al*., 2017). Indeed, mutations in DEPDC5 have been found to be a major cause of multiple focal epilepsies including familial temporal lobe epilepsy, familial focal epilepsy with variable foci (Dibbens *et al*., 2013), autosomal dominant nocturnal frontal lobe epilepsy (Ishida *et al*., 2013; Picard *et al*., 2014), and other non-lesional focal epilepsies (Perucca *et al*., 2017), as well as in focal epilepsy with brain malformations (Baulac *et al*., 2015). While the genetic basis of many focal epilepsies is poorly understood, it is important to assess these patients for genetic mutations particularly in those showing pharmacoresistance. Perucca *et al*. (2017) identified a patient in their study with refractory TLE who showed a mutation in SCN1A. This patient was previously being investigated for surgical intervention, which was stopped on discovery of this mutation as SCN1A mutations have been associated with poor surgical outcome (Skjei *et al*., 2015). Further, this patient was taking carbamazepine, which is known to provoke seizures in patients with epilepsy and a SCN1A mutation. The patient stopped taking carbamazepine and subsequently achieved complete seizure control (Perucca *et al*., 2017). The benefits of further understanding the genetic contribution to focal epilepsies are clear, particularly for those patients with non-lesional refractory epilepsies.

1.4.2 Brain lesions, TBI, & infection

Patients with focal epilepsy often present with a brain lesion. In those where a lesion is present, the most common are hippocampal sclerosis, brain tumours, and malformations of cortical development which, in a study by of 9,523 complex and refractory patients from the European Epilepsy Brain Bank, were found in 78% of patients. Additionally, 72% of all lesions were located in the temporal lobe, with 13% in the frontal lobe and 9% in multiple lobes (Blumcke *et al*., 2017). Histopathological investigations found that there were common structural abnormalities in these lesions including reactive gliosis – a process involved in inflammation, an excess of heterotopic neurons in white matter, white matter angiopathy, and inflammatory cellular infiltrates (Blumcke *et al*., 2017; Klein *et al*., 2018). Lesions can be caused by TBI, infection, early febrile seizures, or may have a genetic component (Walker, 2015). In patients with TBI, severity of injury is a key predictor for the development of post-traumatic epilepsy, ranging from 2.1% in patients with mild TBI to 16.7% for those with severe TBI ten years post injury (Annegers *et al*., 1998). Again, genetics may play a role in the development of epilepsy post TBI with the apolipoprotein E epsilon 4 allele being associated with a 2.4 times increased risk (Diaz-Arrastia *et al*., 2003). Infection is among the most common risk factor for acquired epilepsy, particularly in countries with limited resources. Infections which can result in acute seizures (Beghi *et al*., 2010) and later epilepsy include acute bacterial meningitis, intracranial abscesses and empyemas, central nervous system tuberculosis, parasitic infections (Vezzani *et al*., 2016), herpes simplex virus encephalitis, neurocysticerosis (Ramantani and Holthausen, 2017) and many of these can cause lesions, though a lesion does not have to be present for a patient to develop epilepsy. Seizures early on in the infection are a risk factor for the later development of epilepsy, though not all patients who experience seizures during infection will go on to develop epilepsy (Lowenstein, 2009). Finally, seizures occurring early on in the infection course are not considered epileptic in nature due to the cause being attributed to the infection and thus not spontaneous (Vezzani *et al*., 2016).

1.4.3 Neuroinflammation

While there are a wide range of pathologies underlying the causes of epileptogenesis, linking almost all of these together is neuroinflammation. Inflammatory processes are

seen in histopathological investigations of resected tissue from patients with lesional epilepsy (Blumcke *et al*., 2017), TBI can lead to inflammation which can remain elevated more than eight days post-TBI (Kovesdi *et al*., 2012), many brain infections lead to increased neuroinflammation (Vezzani *et al*., 2016), and in experimental rat models, febrile seizures have been shown to trigger inflammation (Dubé *et al*., 2010).

A well-studied neuroinflammatory pathway is the HMGB1-TLR4 regulatory axis (Figure 1.3). High-mobility group box-1 (HMGB1) is a ubiquitous nuclear DNA-binding protein (Jong *et al*., 2006), which is released by glial cells and neurons as a result of epileptogenic insult (Paudel *et al*., 2018). Its function in neuroinflammation in epilepsy comes from its role as a pathogenic proinflammatory cytokine during the neuroinflammatory signalling cascade in epileptogenesis (Wu *et al*., 2018). HMGB1 in epilepsy has been widely studied in both mouse models and recently in human epilepsy. In mice, HMGB1 translocation and release has been shown to be triggered by seizure activity (Maroso *et al*., 2010), and seizures have been shown to cause the up-regulation of Toll-like receptor 4 (TLR-4) and the receptor for advanced glycation endproducts (RAGE; Maroso *et al*., 2010; Zurolo *et al*., 2011; Iori *et al*., 2013), both of which are interacted with by HMGB1 (Wu *et al*., 2018), in both neurons and astrocytes. Further, the injection of HMGB1 in mice has been shown to speed up onset of acute seizures by convulsive drugs, also increasing their severity and number (Maroso *et al*., 2010; Fu *et al*., 2017). Similarly, Zhao *et al*. (2017) demonstrated that HMGB1 inactivation during epileptogenesis reduced seizure number in animals which went on to develop epilepsy. In human epilepsy, the activation of the HMGB1-TLR4-RAGE axis has been shown in brain tissue resected during surgery of refractory patients (Maroso *et al*., 2010; Zurolo *et al*., 2011; Iori *et al*., 2013; Pauletti *et al*., 2017). Similarly, in surgically resected hippocampal slices also from refractory patients, HMGB1 has been shown to contribute to spontaneous epileptic discharges (Zhao *et al*., 2017). Brain changes in HMGB1 are reflected in changes in HMGB1 serum levels (Ravizza and Vezzani, 2018), allowing for the potential of a non-invasive marker of neuroinflammation. However, there are questions surrounding the role of HMGB1, and whether it is a marker of neuroinflammation or neuronal loss. The secretion of HMGB1 extracellularly has two suggested mechanisms either actively as a result of inflammatory stimulation, or passively from necrotic cells (Li, Liang and

Lotze, 2013). Thus, an increase in HMGB1 in a patient population cannot be attributed definitively to either inflammation or cell loss.

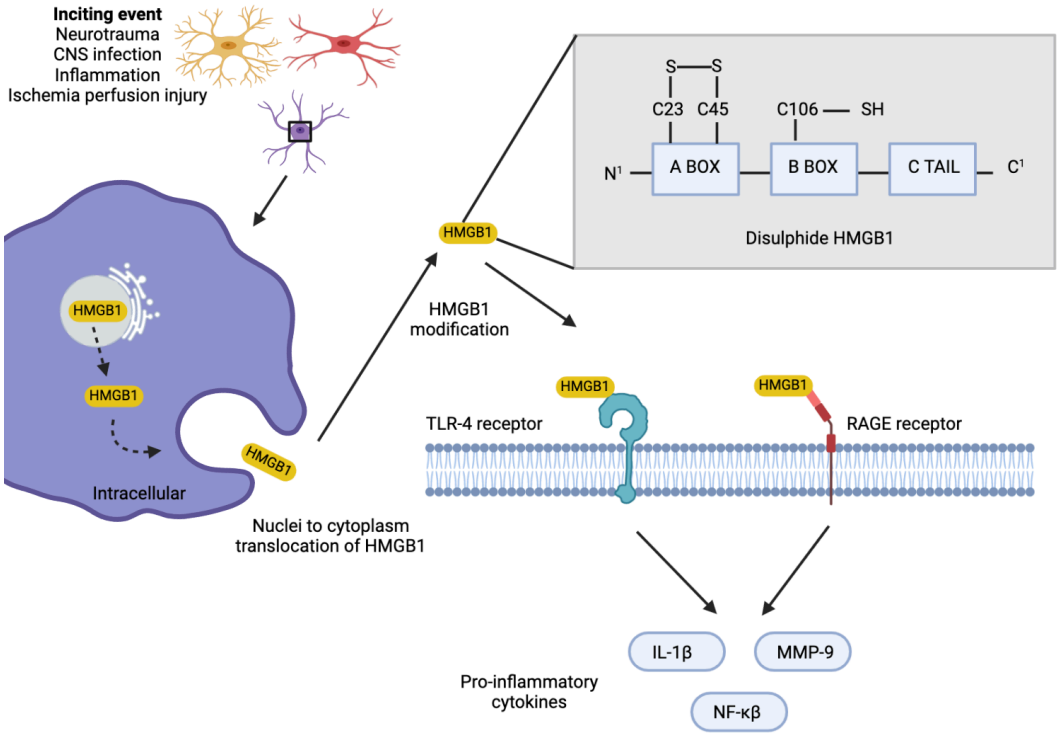

Figure 1.3 HMGB1-TLR4 regulatory axis is activated as a result of epileptogenic insult and further propagates neuroinflammation. HMGB1 undergoes nuclear to cytoplasmic translocation upon a number of inciting events such including neuroinflammation as a result of epileptic insult. Once in the cytoplasm, HMGB1 is oxidised via ROS, resulting in a disulphide isoform of HMGB1 which is functionally able to interact with extracellular TLR-4 and RAGE receptors. Upon binding, a cascade of pro-inflammatory cytokines – including IL-1ß, IL-6 and TNF- α are released from glial cells, macrophages and astrocytes. Neuroinflammation is subsequently exacerbated via activation of the pro-inflammatory NF-κβ pathway alongside activation of matrix metalloproteases, such as MMP-9, which affect BBB permeability allowing for further abnormal neuronal firing (van Vliet, Aronica and Gorter, 2015).

As a result of HMGB1's interaction with TLR-4 and RAGE, a number of inflammatory cytokines are released from glial cells, macrophages, and astrocytes. IL-1ß is one such proinflammatory cytokine which has a well-documented proconvulsant role (Dubé *et al*., 2010), is a potential biomarker for epileptogenesis, and is primarily expressed in activated microglia and astrocytes (Sama *et al*., 2008), particularly following the induction of seizures (Ravizza and Vezzani, 2006). Again, the role of IL-1ß in the propagation of seizure activity has been demonstrated in rodent models (Vezzani *et al*., 1999, 2000; De Simoni *et al*., 2000; Heida and Pittman, 2005). In human studies, brain tissue resected from patients with refractory TLE has shown activation of IL-1ß in glia, astrocytes, and neurons, which was supported by a rodent

model of status epilepticus (SE; Ravizza *et al*., 2008). The authors suggest that this work demonstrates that specific inflammatory pathways are activated during SE and persist in chronic epilepsy tissue. Additionally, a study investigating patients with epilepsy with malformations of cortical development, a positive correlation was found between IL-1ß positive cells and frequency of seizures (Ravizza *et al*., 2006), further highlighting the role of neuroinflammation in the propagation of seizures.

1.4.3.1 Imaging inflammation in epilepsy

Neuroinflammation has been studied extensively using positron emission tomography (PET), specifically using the radioligands (R)-[11C]PK11195 and 18F-PBR111 as measures of translocator protein (TSPO), which is upregulated in the context of activated glial cells (Scott *et al*., 2017). This has been validated in a rat model of TLE – kainic acid-induced SE – where an increase in TSPO expression was associated with increase in activated microglia assessed using immunohistochemistry (Amhaoul *et al*., 2015). In patients with TLE, increases in TSPO have been demonstrated in the hippocampus, parahippocampal gyrus, amgydala, fusiform gyrus, and choroid plexus (Hirvonen *et al*., 2012) and in both ipsi- as well as contra-lateral temporal regions and the thalamus (Gershen *et al*., 2015a). PET is an expensive and scarce tool. Given the supporting evidence that inflammation may have an important role in epilepsy, it is vital to develop a non-invasive, clinically feasible method of detecting inflammation.

Magnetic resonance spectroscopy (MRS; see Chapter 2) has also been used to investigate the role of inflammation in epilepsy. MRS is an MRI technique which can non-invasively measure metabolite values within the brain and, importantly, sequences can be run on a standard MRI scanner. Choline, creatine, and myo-inositol are particularly relevant metabolites to measure when investigating inflammation as they are found primarily in glial cells (Gill *et al*., 1989; Urenjak *et al*., 1993; Soares and Law, 2009). These metabolites are thus expected to be elevated in cases where inflammation is present (Chang *et al*., 2013; Zahr *et al*., 2014). Increases in choline have been found in patients with malformations of cortical development (Simister *et al*., 2007) and hippocampal sclerosis (Meiners *et al*., 2000), while increases in myo-inositol have been seen in patients with cortical dysplasia (Aasly *et al*., 1999) and in the hippocampi of patients with temporal lobe epilepsy (Aydin *et al*., 2012). Similarly,

increases in creatine have been seen in the medial temporal lobes in patients with various epilepsy disorders (Gadian *et al*., 1994) and in patients with refractory temporal lobe epilepsy (Connelly *et al*., 1994). However, there is mixed evidence from MRS metabolites, with some studies showing a reduction in these metabolites where an increase would be expected (Maier *et al*., 2000; Capizzano *et al*., 2002; Doelken *et al*., 2010).

Interestingly, a link between FLAIR signal intensity and levels of several inflammatory mediators has been found in a study of 29 patients with TLE and mesial temporal sclerosis (MTS) following cortico-amygdalo-hippocampectomy. Increases in IL-1ß and tumour necrosis factor-α (TNFα), an additional proinflammatory cytokine, were found in the hippocampi of patients, demonstrating the presence of an inflammatory process. A negative correlation between IL-1ß and FLAIR signal was found, indicating that alterations in FLAIR signal intensity may be a maker of neuroinflammatory processes (Varella *et al*., 2011).

1.4.3.2 Imaging inflammation in other clinical disorders

There are several MR imaging methods which allow an insight into the role of inflammation which are yet to be applied in epilepsy. These include magnetisation transfer imaging (MTI) and advanced diffusion methods. MTI quantifies the transfer of hydrogen nuclei between high-mobility environments (such as free water within the brain) and more restricted environments (such as brain tissue) - where they are bound to macromolecules. This indirectly measures the concentration gradient of macromolecules in an aqueous environment (Sousa, Brito and Magro, 2018). MTI has been applied in patients with schizophrenia, dementia, TBI, tumours, and most commonly, in multiple sclerosis (Symms *et al*., 2004). However only recently has MTI been applied to investigate inflammatory processes. MTI has been demonstrated to show sensitivity to the effects of peripheral inflammation on the brain (Serres *et al*., 2009) in rodents and is sensitive to the effects of inflammation in the brain within regions known to be sensitive to inflammation (Harrison *et al*., 2015) in human populations. Where inflammation is present, an increase in magnetisation transfer from free water to macromolecular-bound protons is seen.

Recently developed two-/multi-compartment models of diffusion imaging (see Chapter 2 for more detailed information) have also shown the ability to image inflammation. Free-water imaging, developed by Pasternak *et al.* (2009), models inflammation by separating out free-water (found extra-cellularly) from hindered water (found intra-cellularly). It is suggested that an increase in extra-cellular free-water is a marker of neuroinflammation (Pasternak *et al.*, 2012). This model has been employed in disorders known to be influenced by inflammation including schizophrenia (Pasternak *et al.*, 2012), Parkinson's disease (Planetta *et al.*, 2016), and in concussion in hockey players (Pasternak *et al.*, 2014).

1.5 Key structures in epilepsy

Epilepsy has traditionally been considered a disorder of grey matter. Evidence for this lies in lesional epilepsy with lesions most commonly seen in grey matter. However, more recent work has led to the acceptance of white matter involvement in the propagation of seizures and in epilepsy as a network disorder (Bernhardt, Bonilha and Gross, 2015; Kreilkamp *et al.*, 2021).

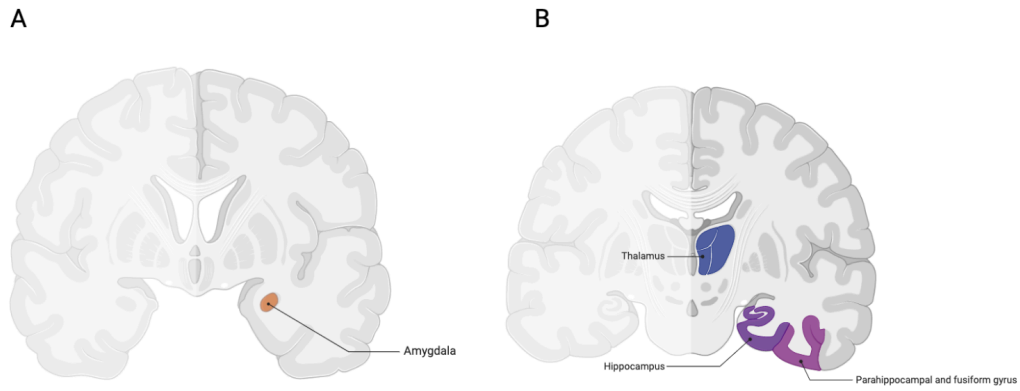

Figure 1.4 Location of (A) Amygdala, and (B) Thalamus, Hippocampus, and Parahippocampal Gyrus on a coronal brain slice - used in subsequent analysis

1.5.1 Thalamus

The thalamus is a mass of nuclei found in the centre of the brain measuring approximately 8cm^3 per hemisphere (Najdenovska *et al.*, 2018). There are two thalami, found bilaterally, with their medial surfaces commonly linked across the third ventricle and their lateral surfaces touching the posterior limb of the internal capsule

(Mtui, Gruener and FitzGerald, 2011) (Figure 1.4). The individual nuclei are connected to each other by association fibres and to other cortical and subcortical brain regions by projection fibres (Kumar *et al*., 2017). The thalamus is connected to almost the whole cortex, and as such, has been considered a primary link for sensory signals (Johansen-Berg *et al*., 2005). Each nucleus is connected to different cortical regions and thus serves a different neurological function. The thalamic nuclei are therefore implicated in a number of neurological and neurodegenerative conditions including Alzheimer's disease (Ryan *et al*., 2013), movement disorders such as dystonia and tremor (Ohye and Shibazaki, 2001), schizophrenia (Alelú-Paz and Giménez-Amaya, 2008), and dyslexia (Díaz *et al*., 2012) along others. Many studies agree on the existence of 14 thalamic nuclei, however these can be further subdivided histologically into more subnuclei and so the number of nuclei often depends on the amount of detail in the atlas or classification used (Morel, 2007; Mai and Paxinos, 2012; Iglesias *et al*., 2018).

1.5.1.1 Role of the thalamus in epilepsy

The thalamus has been demonstrated to play a key role in epilepsy. Malekmohammadi, Elias, & Pouratian (2015) provided evidence that the thalamus is central to regulation of cortical activity through invasive electrophysiological recording of patients with intractable epilepsy. There is a wealth of literature highlighting the positive effects of deep brain stimulation in the thalamus on the frequency of refractory seizures. A meta-analysis of clinical studies found half of all patients experiences a 46-90% reduction in seizure frequency (Li and Cook, 2018), while randomised controls trials have shown a 56% median reduction 2 years (Fisher *et al*., 2010) and 69% reduction 5 years (Salanova *et al*., 2015) following deep brain stimulation of the anterior thalamic nucleus. The anterior thalamic nucleus is able to influence seizure propagation due to its connectivity and functional relationships with the cortex and limbic system (Hodaie *et al*., 2002). Increased metabolic activity in the anterior nucleus has been found in a guinea pig model of seizure (Mirski and Ferrendelli, 1986), and lesioning (Mirski and Ferrendelli, 1987) or high frequency stimulation (Mirski *et al*., 1997) in the anterior nucleus or its afferent pathways has been shown to reduce seizure activity in animal models of epileptogenesis. It has been suggested that low frequency stimulation of the

anterior or intralaminar nuclei synchronises EEG activity leading to a susceptibility to seizures, while more high frequency stimulation desynchronises EEG activity, lowering the susceptibility to seizure activity (Hodaie *et al*., 2002). Additionally, the dorsomedial nucleus of the thalamus has been implicated in the maintenance and propagation of seizures, particularly those involving limbic structures (Bertram *et al*., 1998, 2001). This evidence supporting the ability of stimulation to thalamic nuclei to impact seizure frequency suggests a vital role of the thalamus in the propagation of seizures and the modulation of seizure frequency.

1.5.1.2 Imaging of the thalamus in epilepsy

Neuroimaging studies have also attempted to further understand the role of the thalamus in focal epilepsy. Positron emission tomography (PET) studies have often reported subcortical abnormalities, with those of the thalamus being the most common (Park *et al*., 2018). Glucose uptake has been seen to be abnormal in the thalamus of patients with TLE (Khan *et al*., 1997) and Henry et al. (1990) demonstrated ipsilateral thalamic involvement in the interictal hypometabolism of unilateral TLE. Resting state fMRI (rs-fMRI) has also identified the thalamus as a key region of brain dysfunction in patients with focal epilepsy, despite the heterogeneous nature of focal epilepsy seizure origins (Pedersen *et al*., 2016). Many studies have investigated thalamic atrophy in focal epilepsy using morphometric MR measurements (Keller *et al*., 2002), with a typical finding that patients with TLE show smaller thalamic volumes compared to controls (Dreifuss et al., 2001; Keller, Richardson, Schoene-Bake, et al., 2015). Furthermore, it has been shown that patients with mesial TLE (mTLE) who continued to experience persistent seizures following surgery show more widespread and intense atrophy of the thalamus compared to controls (Keller, Richardson, Schoene-Bake, *et al*., 2015) and have significantly reduced inward surface deflation, which is proxy for atrophy, bilaterally in the thalamus compared to patients rendered seizure free following surgery (Keller, Richardson, O'Muircheartaigh, *et al*., 2015). This suggests that atrophy in the thalamus is able to differentiate between patients rendered seizure free and those who continue to experience persistent seizures following surgery, and that the thalamus may be therefore be involved in driving the persistence of seizures.

1.5.2 The limbic system

The limbic system is made up of the limbic cortex (commonly referred to as the limbic lobe) and its related subcortical nuclei. The cortical regions of the limbic system include the parahippocampal gyrus, hippocampus, cingulate gyrus, and insula, while the subcortical regions include the amygdala, hypothalamus, reticular formation and nucleus accumbens (Mtui, Gruener and FitzGerald, 2011). The limbic system is also known as the circle of Papez (or Papez's circuit) and is thought of as the hub of emotional and behavioural expression in the brain. This section will give a brief overview of the anatomy and functions of regions of the limbic system commonly implicated in epilepsy, namely the hippocampus, amygdala, and parahippocampal gyrus, and their roles in epilepsy research.

1.5.2.1 Hippocampus

The hippocampus (or the hippocampal complex) comprises the subiculum, the hippocampus proper, and the dentate gyrus. It is located in the medial region of the temporal lobe and consists of allocortex arranged in an s-shape along the bottom of the lateral ventricle. The hippocampus is divided into four cornu ammonis (CA) zones (Figure 1.4) based on the pyramidal cells found in the regions. The hippocampus receives afferent and sends efferent connections to a number of cortical and subcortical structures. The largest efferent connection is via the entorhinal cortex to the association regions of the cortex with the larges afferent connection being the performant path, projecting from the entorhinal cortex to the dentate gyrus (Mtui, Gruener and FitzGerald, 2011). The main function of the hippocampus is memory, including short- and long-term memory, working memory, and consolidation of memories (Mtui, Gruener and FitzGerald, 2011).

1.5.2.2 Amygdala

The amygdala is also known as the amygdaloid body or amygdaloid complex and is a group of nuclei sitting above and in front of the temporal horn and lateral ventricle and anterior to the tail of the caudate (Mtui *et al*., 2011) (Figure 1.4). The amygdala is typically associated with emotions, particularly the emotion of fear, however it is also thought to have a role in emotional learning, memory, and attention (Gallagher and Chiba, 1996). Briefly, the amygdala receives information about external stimuli from

the thalamus and sensory cortices. This information is projected in turn to the nuclei of the amygdala before projecting to the orbital prefrontal cortices, midline, hippocampus, and sensory association areas (Janak and Tye, 2015). For a more detailed description of the projections and functions of the amygdala, the reader is referred to Janak and Tye (2015), and Mtui *et al*. (2011).

1.5.2.3 Parahippocampal gyrus

The parahippocampal gyrus comprises the entorhinal, perirhinal, and parahippocampal cortices (Squire, Stark and Clark, 2004) and is found inferior to the hippocampus (Loprinzi, 2019) (Figure 1.4). The allocortical face of the entorhinal cortex connects to the hippocampus, receiving cognitive and sensory information from the cortical association areas and projecting to the hippocampus. Information in then received back from the hippocampus in a consolidated form where it is returned to the association areas (Mtui, Gruener and FitzGerald, 2011). As such, the parahippocampal gyrus also plays a critical role in memory with regions within the parahippocampal gyrus performing information processing (Loprinzi, 2019).

1.5.2.4 The role of the limbic system in epilepsy

The limbic system is largely implicated in epilepsy due to lesions found in the hippocampus. Hippocampal sclerosis (HS) is the most common lesion seen in patients with refractory TLE which in turn, is the most common epilepsy in adults. HS is characterised by a loss of neurons within the hippocampus and is widely associated with focal epilepsy (Walker, 2015). There is evidence of HS in approximately 10% of patients with newly diagnosed focal epilepsy (Van Paesschen *et al*., 1998) and it is the only pathology present in about a third of surgical cases (Blümcke and Spreafico, 2012). HS with additional involvement of the amygdala and parahippocampal gyrus is termed mesial temporal sclerosis (MTS) (RajMohan and Mohandas, 2007).

The amygdala is often implicated in epilepsy, particularly in TLE, with damage found in the amygdala along with the hippocampus in a high proportion of patients (Cendes *et al*., 1993; Saukkonen *et al*., 1994; Pitkänen *et al*., 1998). As such, in some cases, amygdalaectomy rather than hippocampectomy or full temporal lobe resection is enough to eliminate seizures (Rasmussen and Feindel, 1991; Jooma *et al*., 1995;

Wieser, 2000). This indicates that the epileptic focus in TLE is in the hippocampus, amygdala, or both. Additionally, evidence from animal studies has suggested that seizure activity is more often generated in the amygdala than the hippocampus (Goddard, 1967; Kairiss, Racine and Smith, 1984; Racine *et al*., 1988). Further evidence for the role of the amygdala in seizure propagation comes from the effects of nerve agents. The amygdala shows the earliest increase in extracellular glutamate in response to the nerve agent soman (G Lallement *et al*., 1991; Guy Lallement *et al*., 1991) and displays the most extensive damage following soman-induced seizure activity (Shih, Duniho and McDonough, 2003). An extensive review of the role of the amygdala in epilepsy can be found in (Aroniadou-Anderjaska *et al*., 2008).

The parahippocampal gyrus, in particular the entorhinal cortex, has been widely implicated in the propagation of seizures (Miettinen *et al*., 1998; Calcagnotto, Barbarosie and Avoli, 2000; Schwarcz, Eid and Du, 2000; Weissinger *et al*., 2000; Wozny *et al*., 2005), with these studies mostly conducted using animal models. It is suggested that a loss of cells, particularly in layer III of the entorhinal cortex leads to a disruption and overexcitability of information flow to the hippocampus, thus propagating seizure activity (Gloveli, Schmitz and Heinemann, 1998).

The epileptogenic network in TLE primarily involves limbic structures. This is evidenced by the success of seizure freedom following surgical resection of many of these structures. In a recent study of 284 patients who underwent epilepsy surgery, 38% remained seizure free after 10 years. The study found that those patients who underwent amygdalahippocampectomy were less likely to experience seizure freedom than those who had an anterior lobe resection and those who had a temporal lesionectomy (Mohan *et al*., 2018). Similarly, a randomised control trial of patients with temporal-lobe epilepsy found 58% of patients became seizure free following surgery, compared to only 8% in the non-surgical group (Wiebe *et al*., 2001). However, in this study, patients were followed up only one year after surgery and it has been found that the successful outcomes are not always long-lasting (Mohan *et al*., 2018). The updated Cochrane Review of epilepsy surgery outcomes found that out of 16,756 patients, 64% experienced a good outcome following surgery. However, the authors highlighted the poor quality of studies included in the review, with many using

a retrospective design, variable surgical approaches, variable selection criteria for surgery, and outcomes being measured at varying points (West *et al*., 2019).

1.5.2.5 Imaging studies of the limbic system in epilepsy

Imaging studies have allowed an insight into changes occurring in the limbic system in patients with epilepsy. These studies have typically used volumetric analysis (Chapter 2) to measure differences in structure size and shape between patients with epilepsy and control groups. Reductions in the parahippocampal gyrus, hippocampus, and amygdala have all been found in patients with mTLE compared to controls (Keller, Richardson *et al*., 2015; Whelan *et al*., 2018), with a decrease in cortical thickness of the parahippocamapal gyrus also shown in this patient group (Whelan *et al*., 2018). Similarly, in patients with TLE, reductions in volume of the parahippocampal gyrus are widely reported (Bernasconi *et al*., 1999, 2000, 2001; Jutila *et al*., 2001; Bernasconi, Andermann, *et al*., 2003; Bernasconi, Bernasconi, *et al*., 2003), though interestingly, increases have also been found (Keller *et al*., 2002). Additionally, bilateral atrophy of the hippocampus has been found to be related to outcomes of epilepsy surgery in patients with TLE (Keller *et al*., 2007).

1.5.3 White matter pathways

Although epilepsy has been classically considered a grey matter disorder, increasing evidence demonstrates the role of cerebral white matter pathology in focal epilepsy. This evidence typically comes from studies employing advanced diffusion imaging methods (see Chapter 2). Much of this data takes a whole-brain approach, where white matter network alterations are investigated across the entire cerebral cortex, as is the case in this thesis. There are, however, specific white matter pathways which are more commonly studied in focal epilepsy. Both DTI (Chapter 2) and fMRI (previously discussed) are able to quantify white matter connectivity – DTI is able to quantify structural connectivity while fMRI quantifies a proxy of white matter connectivity – the BOLD signal. Both methods have been widely studied in focal epilepsy. To discuss the wealth of literature providing evidence for epilepsy as a network disorder is outside the scope of this thesis, and for a detailed review of this, the reader is referred to (Kramer and Cash, 2012).

1.5.3.1 Thalamocortical connectivity

As the role of the thalamus is widely documented in focal epilepsy, and with the suggestion of epilepsy as a network disorder gaining traction, it is logical to investigate thalamocortical connectivity alterations in patients with focal epilepsy. These fibres connect different thalamic nuclei to the cortex. There is a wealth of literature describing the role of thalamocortical connectivity in the generation and propagation of seizures in patients with generalised epilepsy (Zhang *et al*., 2015) adding to the theory that these connections may also influence seizure activity in focal epilepsy. In a DTI study of paediatric patients with focal cortical dysplasia (FCD), Rezayev *et al*. (2018) found significant reductions in tract volume, length, and count in patients compared to controls. These findings were interpreted by the authors as either a loss of myelin content or abnormal cellular organisation in these fibres (Rezayev *et al*., 2018), and suggest less structural connectivity between the thalamus and cortical areas in these patients. Similarly, in an fMRI study of TLE, patients displayed reduced thalamocortical functional connectivity bilaterally. Interestingly, in patients with purely focal seizures, these changes were limited to the ictal hemisphere, whereas in patients with focal to generalised seizures, changes were more widespread and seen bilaterally (He *et al*., 2015). This suggests that thalamocortical fibres may have a role in the propagation of focal to generalised seizures.

1.5.3.2 Association fibres

Association fibres are also often implicated in focal epilepsy (Law, Smith and Widjaja, 2018). These fibres connect cortical regions within the same cerebral hemisphere. Holt *et al*. (2011) used DTI to investigate the superior longitudinal fasciculus and found significantly reduced FA in this tract in patients relative to controls. However, this was a relatively small study with a sample size of only 12 patients and 12 controls. Campos *et al*. (2015) similarly used DTI to investigate four association fibres (fornix, cingulum, inferior frontal occipital, and uncinate fasciculus) in patients with varying focal epilepsies. Results showed reductions in fractional anisotropy (FA) in all tracts in patients with TLE with HS, bilateral FA decreases in the cingulum only in patients with frontal-lobe epilepsy (FLE) with FCD and no alterations in patients with non-lesional TLE (Campos *et al*., 2015). Changes in FA have also been found in the corpus callosum in patients with TLE which was related to earlier age of seizure onset and

alterations in both FA and MD were found in the left arcuate fasciculus, inferior longitudinal fasciculus, and inferior frontal-occipital fasciculus between patients with focal epilepsy with malformations of cortical development (MCD) who suffered language impairment and those who did not (Riley *et al*., 2010). Together, the literature suggests that these fibres are often implicated, may play a role in the propagation of seizures and in other executive function dysfunction correlated with epilepsy.

1.6 Pharmacoresistance in focal epilepsy

This thesis focuses on patients with a new diagnosis of focal epilepsy, those with a diagnosis of longstanding focal epilepsy who are well controlled by medication, and those who do not achieve seizure freedom with standard AED treatment (refractory focal epilepsy). Approximately 30% of patients with focal epilepsy will not achieve seizure freedom (Kwan and Brodie, 2006). Further, patients with focal epilepsy are less likely to achieve seizure freedom (65%) than those with generalised epilepsy (80%) (Annegers, Hauser and Elveback, 1979). Patients who do not achieve seizure freedom are affected by side effects from multiple drug therapies as well as the negative impact which recurrent seizures have on the brain. Pharmacoresistance is defined by the ILAE as a failure to achieve seizure freedom following trials of two tolerated, appropriately chosen, and used AEDs (Kwan *et al*., 2010).

1.6.1 Adverse effects of AEDs

The adverse effects of AED treatment are multi-faceted. Firstly, they include symptoms related to the known mechanism of action of the drug (Perucca and Gilliam, 2012). Typical symptoms related to this include dizziness, blurred or double vision, memory problems, difficulty concentrating, and depression, and these effects are shared by most AEDs (Perucca and Gilliam, 2012). Up to 48% of patients with epilepsy are affected by cognitive dysfunction including memory problems and difficulty concentrating (Baker *et al*., 1997) and 15-20% of patients experience adverse psychiatric effects including depression and psychosis (Weintraub *et al*., 2007). Secondly, symptoms relating to adverse drug effects can also be due to prolonged exposure (Perucca and Gilliam, 2012) and include changes in body weight (Jallon and Picard, 2001), bone health, sexual dysfunction, and reproductive disorders

(Mintzer, 2010). For example, cumulative exposure to the AED vigabatrin is related to bilateral visual field loss in 14-92% (Wild *et al*., 2007) of patients and is both irreversible (Plant and Sergott, 2011) and can worsen with extended treatment (Hardus *et al*., 2000). Side effects such as these can severely impact patients' quality of life. Finally, prolonged exposure to AEDs has been shown to directly negatively impact quality of life. In a longitudinal study of outcomes of childhood epilepsy, patients in remission who continued to take AEDs reported a worse health-related quality of life compared to patients in remission who no longer took AEDs (Sillanpää, Haataja and Shinnar, 2004). Similarly, in a study of 195 patients who were administered quality of life questionnaires in neurology clinics, AED adverse effects were found to be the strongest predictor of health related quality of life after correction for age, sex, depression and even seizure frequency (Gilliam, 2002).

Along with quality of life issues, prolonged treatment with AEDs is likely to impair brain function and structure. In a study of patients with refractory focal epilepsy, those taking sodium valproate showed decreased whole brain and white matter volumes and decreased cortical thickness of the parietal lobe compared to patients not taking sodium valproate (Pardoe, Berg and Jackson, 2013). Additionally, an MRS study of patients with either generalised or focal to bilateral tonic-clonic seizures showed that patients taking valproate had increased levels of glutamine (Gln) and a non-statistically significant decrease in glutamate (Glu) in the parietal lobe compared to controls. A well-known side effect of valproate is increased serum ammonia which can lead to valproate-induced hyperammonaemiac encephalopathy. Hyperammonaemia stimulates glutamine and inhibits glutaminase and this serious condition caused by AED treatment can lead to death in severe cases (Garcia *et al*., 2009). However, a limitation of this study is the inclusion of only patients taking valproate and controls. There was no control group of patients with epilepsy taking different AEDs and so it cannot be said with confidence that these effects are caused only by valproate and are not an effect of epilepsy itself. Indeed, a reduction in Glu has been seen in patients with refractory mesial temporal lobe epilepsy (mTLE) non-specific to medication type (Bartnik-Olson *et al*., 2017) and the AED lamotrigine has also been shown to affect levels of Glu and Gln (together termed Glx; Choi and Morrell, 2003). Carbamazepine has also been found to alter brain function. In one

study, the extent of fMRI activation in the temporal lobes was found to be negatively correlated to dose of carbamazepine (Jokeit, Okujava and Woermann, 2001). Similarly, in a graph-theory study, the use of carbamazepine was associated with a lower betweenness centrality in brain networks. The authors state that betweenness centrality indicates the presence of hyperconnected nodes which connect distant parts of the brain, and argue that carbamazepine influences this connectivity and affects network changes (Haneef, Levin and Chiang, 2015). Topiramate has also been seen to affect brain networks in an fMRI study of patients with frontal lobe epilepsy. Patients taking topiramate demonstrated a reduction in deactivation of the default mode network (DMN) during tasks. The DMN is the brain network active during rest and is usually deactivated during tasks (Broyd *et al*., 2009). Interestingly these effects were seen in patients taking only topiramate, those taking topiramate as an add-on therapy, and controls after a single dose of topiramate (Yasuda *et al*., 2019). Together these studies suggest that use of AEDs can alter both brain structure and function.

1.6.2 Effects of recurrent seizures

Alongside the adverse effects of prolonged AED treatment, patients who suffer from refractory epilepsy also experience detrimental effects of ongoing seizures. In a study of 146 patients with severe epilepsy, patients were seen to show cognitive decline between an initial cognitive assessment and a follow up ten years later. Frequency of generalised tonic-clonic seizures was the strongest predictor of cognitive decline (Thompson and Duncan, 2005) suggesting that the more severe seizures a person experiences, the greater their cognitive decline. Additionally, a study of patients with generalised epilepsy with only tonic-clonic seizures found that those with poorer seizure control showed reductions of thalamic volumes and fronto-central and limbic cortices (Bernhardt, Rozen, *et al*., 2009). Similarly, a longitudinal study of patients with refractory TLE found cortical atrophy over a mean interval of 2.5 years which was separate from normal ageing. Further, patients with a disease duration over 14 years were found to have more rapid atrophy progression in fronto-central and parietal regions compared to those with a shorter duration (Bernhardt, Worsley, *et al*., 2009). In a study of patients with TLE, hippocampal volume loss over a period of 3.5 years was correlated with the number of generalised seizures between scans (Briellmann *et al*., 2002). This suggests that atrophy is related to seizure frequency. However, a

critique of this study highlighted several limitations in methodology, most notably the lack of control subjects to account for changes due to healthy ageing (Liu *et al*., 2002). Another study of patients with TLE showed that refractory patients had increased atrophy in the ipsilateral hippocampus compared to seizure free patients over a period of 3.4 years (Fuerst *et al*., 2003). Similarly, Coan *et al*. (2009) found that, in patients with medial TLE (mTLE), increased seizure frequency and longer disease duration were associated with increased grey and white matter atrophy. Conversely, in a study of 179 patients with various epilepsy syndromes including TLE, extratemporal parietal epilepsy, and generalised epilepsy, patients with and without volume reduction of the hippocampus, cerebellum, and neocortex were comparable in terms of seizure frequency, AED use, and disease duration (Liu *et al*., 2005). The literature is undecided on whether seizure frequency is linked to increased levels of damage and it must be noted that many studies use disease duration as a proxy for severity. This is not always a reliable measure of epilepsy severity and so increased atrophy or abnormalities may be a function of the epilepsy pathology rather than recurrent seizures. There are few studies investigating the early stages of epilepsy and so it is unclear whether seizures develop due to lesions or vice versa. Regardless, many studies have found correlational links between seizure frequency and increased atrophy, and so routing patients earlier to treatments which are more likely to result in seizure freedom remains advantageous.

1.7 Newly diagnosed focal epilepsy

Studying patients with newly diagnosed focal epilepsy (NDfE) offers the unique potential to understand whether changes seen in imaging studies are a cause or consequence of persistent seizure activity and vice versa. Additionally, studying focal epilepsy at the point of diagnosis may help with the development of a biomarker for treatment response, offering patients earlier treatment stratification and better prognoses. Despite this, NDfE is scarcely investigated using neuroimaging, particularly when compared to longstanding focal epilepsy. What we understand about longstanding focal epilepsy is difficult to translate to those with a new diagnosis due to the chronic effects of seizures and anti-epileptic drugs (AEDs). Early treatment stratification is vital as those who receive appropriate treatment early on have an increased chance of seizure freedom (Marson *et al*., 2005; Kwan and Brodie, 2006),

reducing the effects of persistent seizures and use of multiple AEDs. A non-invasive prognostic biomarker of treatment response would enable those patients unlikely to respond to AEDs to be routed to alternative treatments earlier on in their disease progression.

1.7.1 Imaging NDfE

Though there is limited previous neuroimaging work into NDfE, some studies have been conducted. A longitudinal hippocampal volumetric study found no differences in mean hippocampal volumes between controls and patients with NDfE at the point of diagnosis, or 1, 2 to 3, or 5 years post recruitment (Salmenperä *et al*., 2005). A recent functional connectivity study into NDfE found reduced connectivity in patients between the fronto-parietal attention network and frontal and temporal cortical regions relative to controls. However, no difference was found between patients who were seizure free and those still experiencing seizures at one-year follow-up (Alonazi *et al*., 2019). Additionally, in a study which compared predicted brain age and chronological brain age based on T1w MRI, only patients with longstanding medically refractory focal epilepsy demonstrated changes which resembled premature brain ageing; patients with NDfE displayed no differences between predicted and chronological brain age (Pardoe *et al*., 2017). Clearly more work is needed in patients with NDfE to fully understand the mechanisms driving seizure persistence.

1.8 Biomarkers of pharmacoresistance

The reasons why patients with refractory epilepsy do not achieve seizure freedom are poorly understood and there is currently no definitive biomarker for treatment response.

1.8.1 Clinical biomarkers

There are some clinical predictors of treatment response, however these are not always reliable. It is well known that the earlier in their treatment timeline a patient responds to AEDs, the better their outcome usually is. This was found in a longitudinal study of over 1000 patients with newly diagnosed epilepsy, where patients had a higher probability of seizure freedom if taking one compared to two drug regimens, and if taking two compared to three drug regimens. It was found that less than 2% of patients

became seizure free on regimens following this, however importantly, some patients did become seizure free on their sixth or seventh (Brodie *et al*., 2012). In patients with mTLE, the presence of hippocampal sclerosis has often been thought of as a predictor of poor treatment outcome (Yasuda and Cendes, 2012). This was supported in Varoglu *et al*. (2009), however other risk factors were also identified including sex, age at seizure onset and of head trauma, and cognitive disability. A review by Mohanraj and Brodie (2013) of early predictors of pharmacoresistance in newly diagnosed epilepsy demonstrated that risk factors for poorer prognosis included: seizure type (Annegers *et al*., 1996), with those presenting with multiple seizure types at a higher risk (Goodridge and Shorvon, 1983; Beghi and Tognoni, 1988; Collaborative Group for the Study of Epilepsy, 1992); the presence of a structural brain abnormality (Sillanpää, 1993; Hauser *et al*., 1996; Äikiä *et al*., 1999; Casetta *et al*., 1999; Ko and Holmes, 1999; Berg *et al*., 2001); age of onset, with studies demonstrating that those diagnosed before 12 months have poorer outcomes on average (Camfield *et al*., 1993; Casetta Granieri *et al*., 1999; Ko and Holmes, 1999), and those diagnosed after 65 years having better outcomes (Stephen *et al*., 2006); the presence of a co-morbidity, including psychiatric problems (Hitiris *et al*., 2007) and neurological deficits (Brorson and Wranne, 1987; Hauser *et al*., 1996; Arts *et al*., 1999; Shinnar, *et al*., 2001), though some studies have found no evidence of a link between neurological deficits and poorer prognosis (MacDonald *et al*., 2000; Hitiris *et al*., 2007); febrile seizures in early infancy (Hitiris *et al*., 2007; Geerts *et al*., 2010). Together, these studies suggest that while these clinical factors may be indicators of pharmacoresistance, they cannot be seen as a reliable predictor for all patients.

1.8.2 Imaging biomarkers

Research studies have attempted to identify biomarkers of treatment response in patients with refractory focal epilepsy, however insights gained from these studies remain limited. Volumetric studies have demonstrated a reduction in volume of the corpus callosum (Kim *et al*., 2017), and in the bilateral periorbital frontal, cingulum, and temporal lobe contralateral to epileptic focus (Bilevicius *et al*., 2010) in refractory compared to non-refractory patients with mTLE. Additionally, fMRI with patients with mTLE has shown differences in thalamo-hippocampal functional connectivity between patient groups, with refractory patients showing a decrease bilaterally (Pressl

et al., 2019). In a study of newly diagnosed TLE, patients were categorised according to their response to first AED. Neuronal and axonal dysfunction and damage were assessed using MRS of N-acetylaspartate (NAA) specifically in the bilateral hippocampi. Patients who responded poorly to their first AED demonstrated reduced NAA compared to both controls, and those who responded well to the first AED. This is suggestive of increased neuronal damage/dysfunction in those who do not respond well to their first AED (Campos *et al*., 2010). Imaging of inflammatory markers is another potential route to development of a biomarker of pharmacoresistance, though this has been studied mostly in animal models. In a kainic acid model rat model of epilepsy, increased TSPO expression was found to be correlated with spontaneous seizures (Amhaoul *et al*., 2015). Similarly, in rats with electrically induced SE, in those who continued to experience seizures following treatment with phenobarbital there was increased uptake of (R)-[11C]PK11195 compared to rats who responded well to treatment (Bogdanović et al., 2014). Using MRS, Pascente *et al*. (2016) found, in a pilocarpine model of SE in rats, that an increase in myo-inositol in the hippocampus 72 days post-SE was a predictor of epileptogenesis. In patients with NDfE, a recent volumetric study of the corpus callosum (CC) found differences between patients with NDfE and controls, with patients demonstrating lower CC volume than controls. Furthermore, patients who went on to respond well to AED treatment showed lower CC volumes compared to non-responders. However, non-responders were diagnosed on average 18 months later than responders, experienced an average of two additional seizures, and follow-up of these patients was relatively short (Kim *et al*., 2017).These early biomarkers show some potential in their predictive power, but clearly, more work is needed to develop a reliable, non-invasive biomarker of treatment response in patients.

1.9 Aims of this thesis

The development of a non-invasive, clinically feasible biomarker for AED treatment outcome would allow for those patients who are likely to respond poorly to AEDs to be routed earlier to alternative or adjunctive treatments such as surgery or stimulation treatments. Such a biomarker would lead to more personalised treatment pathways, a better prognosis, and improved quality of life for patients with refractory focal epilepsy. Broadly, this thesis aims to use advanced imaging methods in order to

develop a non-invasive biomarker for AED treatment response in patients with focal epilepsy. A series of advanced diffusion, morphometric, MRS, and supplementary blood analyses in two cohorts; one with patients with newly diagnosed focal epilepsy; one with patients with longstanding focal epilepsy, will be performed. In both cohorts, the goal of these analyses is to investigate the correlates of pharmacoresistance in patients with focal epilepsy.

2 Relevant advanced MRI techniques

2.1 Background

This chapter provides brief background information regarding advanced MRI techniques used in this thesis and their relation to epilepsy. It is not intended to be a detailed review of MR physics or provide a detailed description of the principles underlying MR acquisition as this is beyond the scope of this thesis. For this information the reader is directed to relevant literature throughout this chapter.

2.2 Volume T1-weighted imaging

2.2.1 Structural scans

T1-weighted (T1-w) are structural scans commonly used in clinical and research environments. MR imaging relies on the principle that electrically charged protons within atoms precess (i.e. spin around their axis) when in a magnetic field. A radio-frequency pulse is then applied by the MR scanner, changing the orientation of the spins. The MR scanner can then measure the response of the protons to this radio-frequency pulse, generating an image. For an extensive description of the principles of MR imaging, the reader is referred to (Johnson, Kuzniecky and Pell, 2005).

T1-w images are based on spin-lattice relaxation of hydrogen protons within atoms in the brain (Johnson, Kuzniecky and Pell, 2005). Energy is transferred to protons through the application of a radio-frequency pulse which projects them into the transverse plane. As this energy wears off, the proton spins return to the plane of the magnetic field (Johnson, Kuzniecky and Pell, 2005).T1 relaxation is defined as the time taken for protons to reach 63% of their original magnetisation orientation.

Relaxation times differ across magnetic field strength and tissue type. On a T1-w image, fat appears brightest with the shortest T1, WM is bright with a slightly longer T1, while GM is darker with a longer T1 and CSF even darker with the longest T1 (MacIntosh and Graham, 2013) (Figure 2.1).

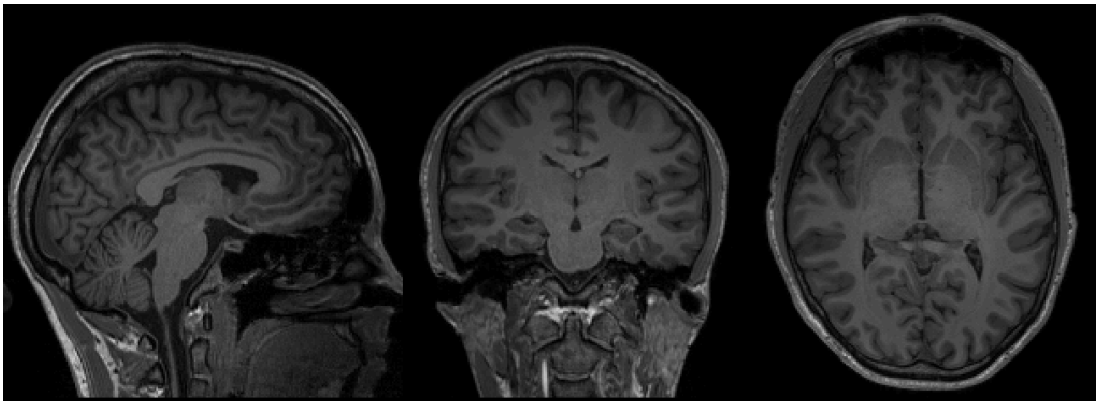

Figure 2.1 Example T1 image. Note the bright WM, dark GM, and darker CSF

Due to the different signal intensities of T1-w images, they can be segmented into grey matter, white matter, and CSF using automated software such as Freesurfer (Fischl, 2012), as used in this thesis. Freesurfer allows further segmentation of cortical and subcortical regions into predetermined parcellated regions of interest (Figure 2.2). Particular subcortical regions, including the hippocampus, amygdala, and the thalamus, can be further segmented into their respective subfields and nuclei. This provides quantitative information regarding volume changes in specific regions of interest.

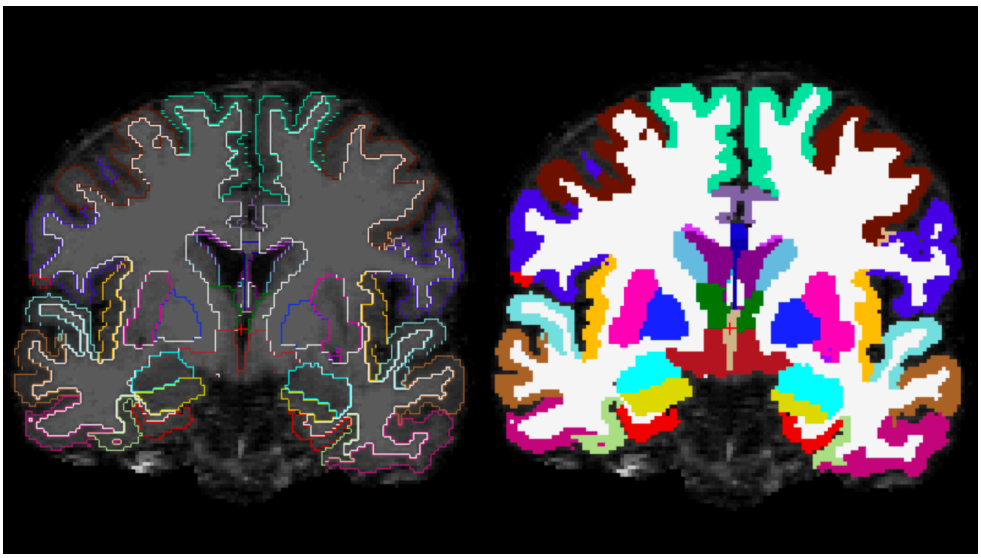

Figure 2.2 Automatic parcellation and segmentation of cortical and subcortical regions of interest by Freesurfer software

2.2.2 Volume changes in epilepsy

As discussed in Chapter 1, volume changes have been widely investigated in focal epilepsy. Alterations have been seen in the thalamus (Dreifuss *et al*., 2001; Keller, Richardson, Schoene-Bake, *et al*., 2015), hippocampus, amygdala, parahippocampal gyrus (Keller, Richardson, Schoene-Bake, *et al*., 2015; Whelan *et al*., 2018), and many white matter tracts implicated in the progression of epilepsy (Campos *et al*., 2015; Rezayev *et al*., 2018). In patients with TLE, atrophy is often seen in temporal lobe structures (Bonilha and Keller, 2015). Additionally, volume changes have been found to relate to outcomes of epilepsy surgery (Keller, Richardson, O'Muircheartaigh, *et al*., 2015), and in patients with NDfE at the point of diagnosis (Leek *et al*., 2020).

2.3 Diffusion imaging

Diffusion weighed imaging (DWI) is a variation of MRI which measures the rate of water diffusion within tissue. It is based on the theory of Brownian motion, that is, that water diffusing freely does so randomly (Soares *et al*., 2013). Within the brain, there are restrictions to free diffusion – brain tissue - and these restrictions are higher when diffusion is occurring perpendicular to structures. This means that, by measuring the movement of water within the brain, we can see changes in brain tissue architecture (Basser, Mattiello and Lebihan, 1994). Further, by measuring in which direction water is moving fastest we can reconstruct white matter pathways, as water will move the quickest alongside these pathways. For detailed information on the principles of DWI,

the reader is referred to Merboldt, Hanicke and Frahm (1985, Taylor and Bushell (1985), and Le Bihan *et al*. (1986).

2.3.1 Diffusion tensor imaging

The tensor model was proposed in order to quantify diffusion anisotropy from DWI (Basser, Mattiello and LeBihan, 1994). The tensor is a six by six matrix which describes the diffusion environment in three different directions, x, y, and z. It is therefore necessary to acquire a minimum of six DWIs and an image without diffusion weighting (b0 image) to complete the nine elements of the tensor.

$$\begin{bmatrix} D_{xx} & D_{xy} & D_{xz} \\ D_{yx} & D_{yy} & D_{yz} \\ D_{zx} & D_{zy} & D_{zz} \end{bmatrix} \xrightarrow{\text{Diagonalisation}} \begin{bmatrix} \lambda_1 & 0 & 0 \\ 0 & \lambda_2 & 0 \\ 0 & 0 & \lambda_3 \end{bmatrix}$$

A matrix is then calculated for each voxel in the DWI and then diagonialised – where all non-diagonal elements are zeroed, and diagonal elements are transformed to match with the principle direction of diffusion in the voxel. These new diagonal elements are the three eigenvectors $(\varepsilon_1, \varepsilon_2, \varepsilon_3)$ of diffusion with their eigenvalues $(\lambda_1, \lambda_2, \lambda_3)$. These represent the main direction of diffusion in the voxel and are arranged according to their magnitude (da Costa Leite and Castillo, 2016; Rajagopalan *et al*., 2017). This concept is often visualised using the ellipsoid model (Figure 2.3). For detailed information on how to calculate the diffusion tensor see Soares *et al*. (2013).

2.3.1.1 DTI parameters

The most commonly used parameters in DTI experiments are fractional anisotropy (FA) and mean diffusivity (MD) (Soares *et al*., 2013). Further, both axial (AD) and radial (RD) diffusivity are also easily calculated and can offer further valuable information. FA measures the fraction of diffusion which is anisotropic. FA can thus range from 0 (complete isotropic diffusion) to 1 (complete anisotropic diffusion) and provides no information on orientation. Rather, a decrease in FA implies a loss of tract

coherence in the main diffusion direction (Soares *et al.*, 2013). MD provides

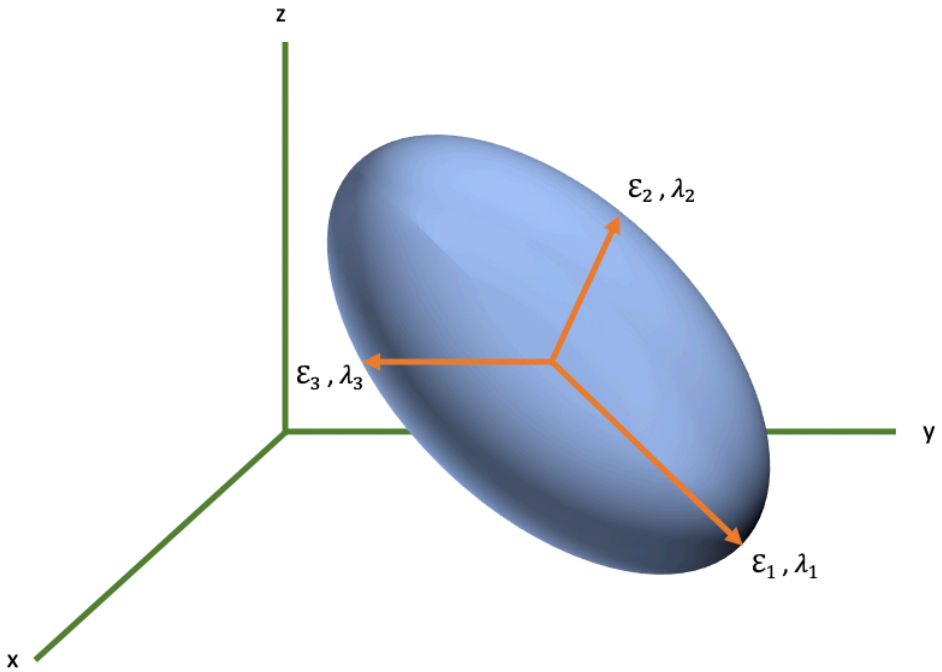

Figure 2.3 The diffusion ellipsoid model demonstrating the three directions (x,y,z), three unit vectors ($\varepsilon_1, \varepsilon_2, \varepsilon_3$), and their corresponding lengths ($\lambda_1, \lambda_2, \lambda_3$), the eigenvalues. In perfect isotropic diffusion, the ellipsoid becomes a sphere with $\lambda_1 = \lambda_2 = \lambda_3$.

information on the overall diffusion as an average of all three eigenvalues, and is often increased in damaged tissue due to an increase in free diffusion (Soares *et al.*, 2013). RD is calculated from the first eigenvector while AD is calculated from the average of the second and third eigenvectors (Chanraud *et al.*, 2010; Basser and Pierpaoli, 2011). RD therefore offers information on the diffusion perpendicular to the principle direction of diffusion and has been thought to represent myelin integrity (da Costa Leite and Castillo, 2016). AD, on the other hand, measures diffusion along the length of the principle direction of diffusivity and can be considered a measure of fibre integrity and number (da Costa Leite and Castillo, 2016).

2.3.1.2 DTI in epilepsy

DTI has become one of the most common research imaging methods for investigation in epilepsy. Typically, studies of DTI in epilepsy demonstrate a profile of reduced FA and increased MD in the white matter of patient groups compared to healthy controls. In patients with TLE, widespread reduction of FA has been consistently identified in a number of WM tracts, including the corpus callosum, external capsule (Gross, Concha and Beaulieu, 2006; Concha *et al.*, 2009), fornix, cingulum (Ahmadi *et al.*,

2009; Concha *et al*., 2009), parahippocampal fibres (McDonald *et al*., 2008; Ahmadi *et al*., 2009), uncinate fasciculus (McDonald *et al*., 2008), and the inferior and superior longitudinal fascicles (McDonald *et al*., 2008; Ahmadi *et al*., 2009). Increases in MD in patients with TLE have been found in the uncinate fasciculus, parahippocampal fibres, inferior longitudinal fasciculus (McDonald *et al*., 2008), fornix, cingulum, external capsule, and the corpus callosum (Concha *et al*., 2009). Investigations using DTI into AED treatment response are sparse, however one recent study has found, albeit with a small sample size of only seven drug-refractory patients, that widespread bilateral changes were more pronounced in patients with refractory compared to non-refractory genetic generalised epilepsy (GGE; Jiang et al., 2017).

2.3.2 Diffusion kurtosis imaging

A major limitation of DTI is the assumption of a Gaussian distribution of water diffusion in the brain. However, within the brain there are several barriers to diffusion, including cell membranes and different compartments (i.e. intra- and extra- cellular water) which alters water diffusion meaning it is no longer Gaussian (non-Gaussian) (Jensen and Helpern, 2010). DTI therefore cannot provide an accurate description of water diffusion in biological tissues such as the brain. Diffusion kurtosis imaging is an extension of DTI which provides information on the kurtosis (skew) of water diffusion. Thus, DKI is able to characterise the non-Gaussianity of water diffusion, providing a more complete picture of tissue structures (barriers to diffusion) within the brain (Jensen and Helpern, 2010).

Similarly, DTI parameters rely on the diffusion environment being anisotropic; FA measures the degree of anisotropy, while MD, AD, and RD quantify diffusion in certain directions according to the diffusion tensor. DTI is therefore ill-equipped to define diffusion in environments with isotropic diffusion, such as grey matter (Jensen and Helpern, 2010). DKI, on the other hand, measures the non-Gaussianity of diffusion and thus, is better placed to quantify diffusion in isotropic environments, such as grey matter (Arab, Wojna-Pelczar, Khairnar, Szabó, & Ruda-Kucerova, 2018, Gao et al., 2012). Additionally, it has been shown that, by measuring this non-Gaussianity of diffusion, DKI is able to provide information on voxels with crossing fibres (Lazar *et al*., 2008), previously not possible with DTI.

2.3.2.1 DKI parameters

The additional parameters gained with the use of DKI include mean kurtosis (MK), axial kurtosis (AK), and radial kurtosis (RK). An increase in kurtosis values is indicative of a greater deviation from a Gaussian distribution, meaning a more restricted and complex diffusion environment (Hui *et al*., 2008). This has been suggested to be due to an increase of protein accumulation or iron deposition (Arab *et al*., 2018), an increase in cell-density, myelination, or increased activity of glial cells (Zhuo *et al*., 2012). A decrease in kurtosis measures can be related to cell loss (Arab *et al*., 2018) or an increase in extracellular space (Gong *et al*., 2013). DKI has been shown in clinical samples to be sensitive to microstructural changes in GM in patients with schizophrenia (McKenna *et al*., 2019), traumatic brain injury (Zhuo *et al*., 2012), stroke (Weber *et al*., 2015), and multiple neurodegenerative disorders (Arab *et al*., 2018).

2.3.2.2 DKI in epilepsy

In studies of epilepsy, DKI findings tend to be more widespread than DTI. This has been seen in patients with GGE (Zhang *et al*., 2013, 2016), and in patients with TLE (Gao *et al*., 2012; Bonilha *et al*., 2015; Glenn *et al*., 2016). Using a voxel-based approach, a more widespread pattern of alterations in MK and RK in the left temporal, bilateral orbitofrontal, and frontoparietal regions were observed in patients with TLE compared to standard DTI metrics (Bonilha *et al*., 2015). A WM atlas region of interest analysis found widespread reductions in MK and RK in later myelinating tracts in patients with TLE, with MK and RK being more sensitive to changes than FA (Lee *et al*., 2013). These findings were consistent with a later study that also demonstrated significantly reduced MK along the length of ipsilateral and contralateral WM tracts in patients with TLE (Glenn et al., 2016). In GGE, tract-based spatial statistics analysis has shown that reduced MK and RK were more widespread in patients compared to DTI metrics, although kurtosis-based changes did not necessarily overlap with changes seen in DTI metrics (Lee *et al*., 2014). This suggests that while DKI is seen as an extension of DTI, kurtosis- and tensor-based metrics are potentially measuring different biological characteristics.

DKI has also been used to investigate GM structural changes in epilepsy, though not as widely as it has been used to investigate WM. Bonilha et al. (2015) performed a whole-brain voxel-wise analysis in patients with TLE using both DTI and DKI parameters, and found multiple cortical areas showing a decrease in kurtosis measures in patients. Interestingly, the pattern of changes seen, in both grey and white matter, was more diffuse with DKI rather than DTI metrics. The authors suggested that DKI may provide a sensitive and specific biomarker of TLE and is more sensitive than DTI at detecting microstructural abnormalities in patients with TLE. This study supported earlier work by Gao et al. (2012) who found a more widespread pattern of DKI changes in children with TLE and suggested DKI to be more accurate and sensitive to microstructural changes in the temporal lobe. This previous literature suggests that DKI parameters are able to offer further insight into the microstructural environment of GM as well as in WM. The additional parameters provided by DKI offering a more detailed and sensitive description of the microstructural environment within the brain allows for the potential to detect changes in patients with refractory focal epilepsy compared to those who are non-refractory.

2.3.3 Two-compartment models

While both DTI and DKI are reasonably sensitive to changes in white matter microstructure, these parameters are purely diffusional; they only describe the tissue environment in terms of diffusional, rather than biological, parameters. They therefore have limited ability to biologically describe tissue microstructure (Fieremans, Jensen and Helpern, 2011). In order for alternative diffusion methods to be more biologically interpretable, a diffusion model having parameters with realistic biological meaning is needed (Winston, 2015). Because of this need, there has been an increase in the development of new diffusion methods which attempt to model the diffusion environment in a more biophysical manner. The simplest of such models are based on the assumption that there are two non-exchanging water compartments within the brain: a fast (which measures less hindered extra-axonal water) and a slow (which models more restricted intra-axonal water) diffusion compartment (Assaf *et al*., 2004; Fieremans, Jensen and Helpern, 2011; Kleban *et al*., 2020) (Figure 2.3).

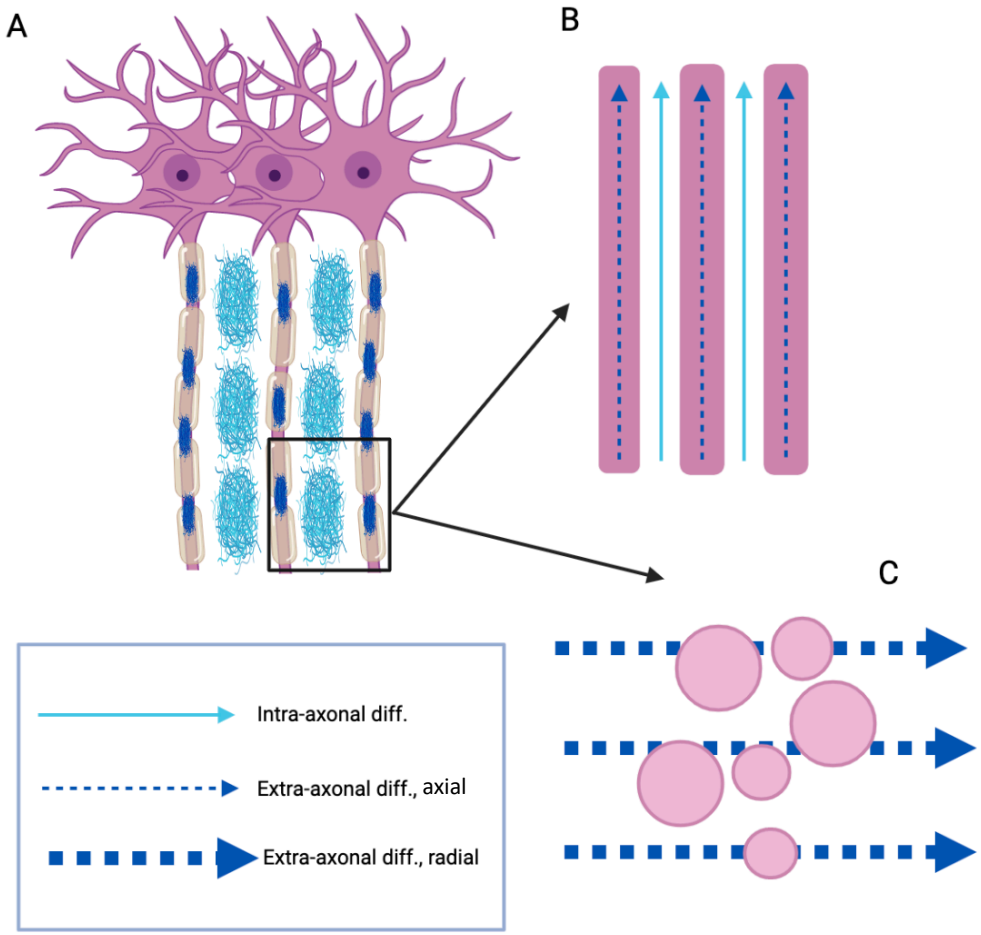

Figure 2.4 Schematic showing intra- and extra- axonal diffusion in the brain. (A) highlights flow of water within (intra-) and between (extra-) axons. (B) demonstrates intra-axonal and axial extra-axonal diffusion. (C) shows radial extra-axonal diffusion.

dMRI techniques employing a two-/multi-compartment model, including free-water imaging (FWI; Pasternak, Sochen, Gur, Intrator, & Assaf, 2009), composite hindered and restricted model of diffusion (CHARMED; Assaf & Basser, 2005), and neurite orientation dispersion and density imaging (NODDI; Zhang *et al*, 2012) have been used to study patient cohorts and have demonstrated that it is possible to characterise white matter microstructure in a way which is biologically meaningful. NODDI has been used in patients with focal cortical dysplasia (FCD) and epilepsy and has indicated that areas of reduced intracellular volume fraction (ICVF), a marker of neurite density, were located in the same areas as the FCD (Zhang *et al*., 2012). In one patient, structural imaging was initially reported as normal but a clear reduction in ICVF assisted the detection FCD on review (Winston *et al*., 2014). Rostampour,

Hashemi, Najibi, & Oghabian (2018) used NODDI to investigate whether the method was able to detect structural abnormalities in patients with MRI-negative focal epilepsy. They found that cortical abnormalities could be detected on orientation dispersion index (ODI) maps and that subcortical changes including a decrease of FA and neurite density (ND) and increase of ODI was seen in patients (Rostampour *et al*., 2018). Recent work by Winston *et al*. (2020) investigated microstructural changes in patients with TLE using two multi-compartment models; NODDI and Multi-Compartment Driven Equilibrium Single Pulse Observation of T1/T2 (mcDESPOT). Findings showed that patients had reduced ND and increased MD in intracortical grey matter, and reduced FA, ND, and myelin water fraction (MWF), and increased RD in subcortical white matter compared to controls. Additionally, the reduction in FA and increase in RD was related to a reduction in ND in both GM and WM, with an additional relationship with MWF in WM only. The authors concluded that diffusivity changes seen with standard DTI are related to both ND and MWF, and that multi-compartment models are better able to understand the biological processes driving changes in diffusion parameters (Winston *et al*., 2020). By modelling diffusion with two-compartment models, evidence suggests that improved detection of focal abnormalities and further insights into the underlying microstructure of the brain is possible.

2.3.3.1 Fiber Ball Imaging

Fiber ball imaging (FBI) is a recently developed two-compartment method of diffusion (Jensen, Russell Glenn and Helpern, 2016) which offers the ability to probe increasingly into the cerebral microscopic environment. This offers the potential to discriminate between multiple biological characteristics. Given that extra-axonal water in the brain is more mobile than intra-axonal water in several directions – as intra-axonal water is restricted by tissue membranes such as myelin – the signal from this compartment drops off with increased b-value. By using b-values greater than 4000 FBI is able to model the signal from only the intra-axonal compartment, allowing the estimation of microstructural properties associated with axonal fibre bundles, including the FA of the intra-axonal space (FAA) and zeta (a property related to the axonal water fraction; AWF, and the intra-axonal diffusivity (D_a)). One major advantage of FBI compared to other two-compartment models is that it requires a

tissue model only for the intra-axonal and not the extra-axonal compartment, which has proven to be more difficult. FBI models the intra-axonal space using the "stick model" which has been validated by two independent groups (McKinnon *et al*., 2017; Veraart, Fieremans and Novikov, 2019). Highly diffusion weighted MRI (b>>4000) is used to model the fibre orientation distribution function (fODF) of white matter fibre bundles. Fiber Ball White Matter Modelling (FBWM; (McKinnon, Helpern and Jensen, 2018)) builds upon the principles of FBI and uses both high and low diffusion weightings to model the extra-axonal space as well as the intra-axonal space. FBWM therefore allows the estimation of additional microstructural parameters including the intrinsic intra-axonal diffusivity (D_a), the mean extra-axonal diffusivity (MD_e), along with radial ($De,_\perp$) and axial ($De_{,\parallel}$) extra-axonal diffusivity, the FA of the extra-axonal space (FAE), and AWF.

2.3.3.2 Advantages of FBI over other two-/multi-compartment models

While FBI/FBWM have yet to be applied to patient cohorts, they offer a significant advantage over other two-/multi-compartment models. Many other dMRI tissue models are based on nonlinear fitting algorithms, which can lead to problems with increased computational times, sensitivity to noise and imaging artefact, and issues related to the accuracy of underlying idealisations (Novikov, Kiselev and Jespersen, 2018). FBWM on the other hand, is based on well-supported assumptions and a simple computational scheme involving straightforward linear transformation of the dMRI signal, together with a one-dimensional numerical optimisation. Further, FBWM should more accurately model regions with crossing fibres due to its use of the FODF from FBI, which, unlike other models such as the White Matter Tract Integrity (WMTI) method (Fieremans, Jensen and Helpern, 2011), does not assume that all axons in a given voxel are approximately oriented in the same direction.

Tractography

Diffusion imaging allows for the use of tractography – a method which tracks WM fibre tracts within the brain (see Figure 2.4 for an example of tractography [TractSeg]). There are an increasing number of manual and automated fibre tractography techniques. Manual methods require the investigator to manually trace WM fibres using diffusion data whereas recently introduced automated tractography methods use

computerised algorithms to automatically reconstruct WM fibre tract bundles based on either deterministic or probabilistic tractography. Deterministic tractography is based on streamlines. A region of interest is located (seed) and adjacent voxels are included in the streamline as long as their principle eigenvectors are parallel, or the angle does not differ too extremely. An issue with deterministic tractography is that of 'crossing fibres'. This is due to the resolution of DTI typically being ~2mm, which is too low to identify the orientation of individual fibres. If one voxel has multiple crossing fibres, then the angle of the eigenvector will differ significantly from the previous voxel and so the streamline will end. Probabilistic tractography is better able to handle this issue as this uncertainty is calculated for each voxel. The most likely WM pathways which connect two regions are then reconstructed (da Costa Leite and Castillo, 2016).

Manual tractography has long been considered as gold standard given the necessity of expert human delineation of tracts. However, the approach is time consuming and resource-intensive, given the reliance on highly trained researchers (Hagler Jr. *et al*., 2009). Kreilkamp et al. (2019) investigated the relationship between manually and automatically delineated tracts using Automated Fiber Quantification (AFQ; Yeatman *et al*., 2012) in patients with TLE. While the manual approach was found to be more sensitive to pathologic diffusion alterations, there was moderate to good Dice coefficient and a strong correlation between whole and along-tract manual and automated measures.

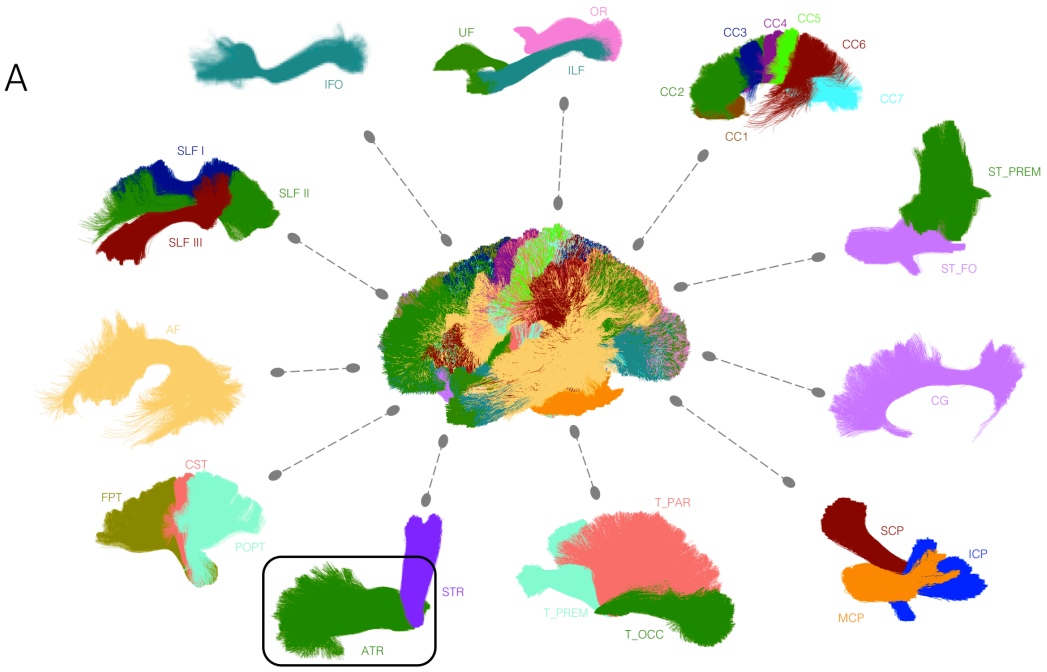

Figure 2.5 (A) White matter tracts automatically segmented using TractSeg included in this thesis. See Table 3.2 for definition of abbreviations.

2.3.3.3 Tractography in epilepsy

Along-tract automated tractography using TRActs Constrained by UnderLying Anatomy (TRACULA; Yendiki et al., 2011) in TLE has revealed regionally reduced FA in the uncinate fasciculus, inferior longitudinal fasciculus and cingulate anterior bundle ipsilateral to seizure onset, with a more widespread pattern of increased MD in patients compared to controls (Kreilkamp et al., 2017). Using AFQ (Yeatman et al., 2012), significantly reduced FA was found regionally in the right uncinate of patients with right TLE, and significantly increased MD regionally in the left and right uncinate fasciculi in patients with left TLE. Additionally, altered diffusion characteristics were correlated with a number of clinical features including age of onset, seizure burden, and longer disease duration (Kreilkamp et al., 2019). AFQ has also been used to attempt prediction response to epilepsy surgery in patients with TLE, where it was found that only patients with persistent postoperative seizures had significant preoperative regional diffusion alterations of the ipsilateral dorsal fornix and contralateral parahippocampal WM (Keller et al., 2017). Preoperative diffusion characteristics were able to predict postoperative outcome with 84% sensitivity and 89% specificity (Keller et al., 2017). However, recent work has highlighted the need to move beyond standard DTI for tractography. Farquharson et al. (2013) found that

DTI based tractography underestimated the extent of tracts connecting to the sensorimotor cortex in a control group. A more advanced method of tractography, constrained spherical deconvolution (CSD), which is better able to model crossing fibres (Tournier, Calamante and Connelly, 2007), was found to consistently produce more biologically feasible tracts (Farquharson et al., 2013). This demonstrates the need for better models of diffusion to more accurately reconstruct biologically realistic fibre tracts. Along-tract AFQ tractography has also been used with DKI metrics, with patients showing changes in regions of the fimbria-fornix, parahippocampal WM, uncinate fasciculus, arcuate fasciculus and the inferior longitudinal fasciculus (Glenn et al., 2016). Along-tract methods potentially offer more sensitive measures of WM changes than whole-tract techniques. Tissue characteristics may vary along the length of tracts (Johnson et al., 2014) and so it is likely that tissue abnormalities in focal epilepsies also vary along tracts. Along-tract tractography offers the ability to visualise these changes along the length of tracts, rather than averaged across the whole tract. Figure 2.5 demonstrates the differences in sensitivities of these methods to MD.

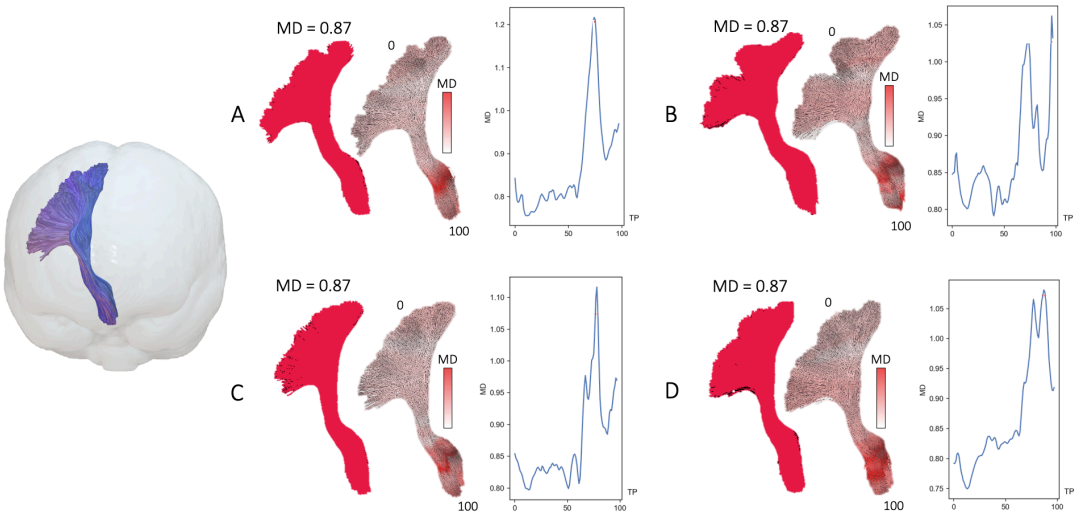

Figure 2.6 The advantage of assessing along-tract diffusion metrics over whole tract averaging. (a–d) The left corticospinal tract (shown on the left in a glass-brain projection for reference) of four subjects. Averaging a diffusion metric over the entire tract yields the same mean diffusivity (MD) value (0.87 μm2/ms) for each subject (full red tract). Analysis of MD at 100 points along the length of the corticospinal tract demonstrates considerable variability in regional MD within and between tracts. TP = tract points

2.4 Magnetic resonance spectroscopy

MRS quantitively measures the metabolic environment of the brain in vivo (Tschampa *et al.*, 2015). These measurements can provide information on neuronal integrity, energy-metabolism, and membrane turnover (Benarroch, 2008; Mountford *et al.*,

2010; Zhu and Barker, 2010). While standard MRI produces images with thousands of voxels whose signal reflect bulk magnetic properties (T1, T2, etc), MRS analyses the chemical composition of tissues in a very small number of much larger voxels. Only some nuclei demonstrate magnetic resonance: Hydrogen-1 (^{1}H), Phosphorus-13 (^{31}P), Carbon-13 (^{13}C), Flourine-19 (^{19}F), and Sodium-23 (^{23}NA), with ^{1}H and ^{31}P being the most common (Ross and Sachdev, 2004). Further, these nuclei are present in compounds of clinical interest in sufficient concentrations that they can be measured using MRS. The sensitivity of ^{1}H (also termed proton MRS due to the nucleus only containing a single proton) is much greater than ^{31}P and so can be used for much smaller volumes of tissue (Duncan, 1996). Water and fat are suppressed from the signal to allow the detection of small metabolites existing in millimolar concentrations. Metabolites can be differentiated because they resonate at different frequencies based on their local chemical environments. This difference in resonance frequencies is called chemical shift and is denoted by δ and measured in parts per million (ppm), relative to the frequency of a reference compound, typically tri-methyl silane (TMS) (McLean and Cross, 2009). Each metabolite has a constant number, location, and relative size on the spectra, and thus, analysis of the spectra can show which metabolites are present and their concentrations (McLean and Cross, 2009). There are two main approaches to defining the location of the region of interest in the brain: single voxel, in which data is acquired from a single volume of interest; and chemical shift imaging (CSI; or magnetic resonance spectroscopic imaging), where data is collected from a number of voxels simultaneously, usually a 16x16 grid (Duncan, 1996; McLean and Cross, 2009). Both methods have advantages and disadvantages, with the main difference being acquisition time, which is much faster for single voxel, and signal to noise which is again greater for single voxel, however it has poor spatial resolution and there is issues with lesion heterogeneity (Ramli *et al*., 2015). An obvious advantage of CSI is the ability to gather data from a much greater volume of interest, along with the advantage of increased spatial resolution allowing for consideration of lesion heterogeneity (Ramli *et al*., 2015). Proton MRS is the most commonly used nucleus and is widely available on clinical MRI scanners (McLean and Cross, 2009).

Metabolites which are reliably identified with proton MRS include N-acetlaspartate (NAA), the tallest peak in the spectrum found at $\delta = 2.0$; choline (Cho), the third tallest peak found at $\delta = 3.2$; creatine (Cr), which shows two peaks at $\delta = 3.0$ and 3.9; myo-inositol (mIns), which has several multiplet peaks with the largest near $\delta = 3.6$l and Glx (glutamate and glutamine), which resonate closely together, their summed peak seen at $\delta = 2.3$ (Ross and Sachdev, 2004). See Figure 2.6 for an example MRS spectra.

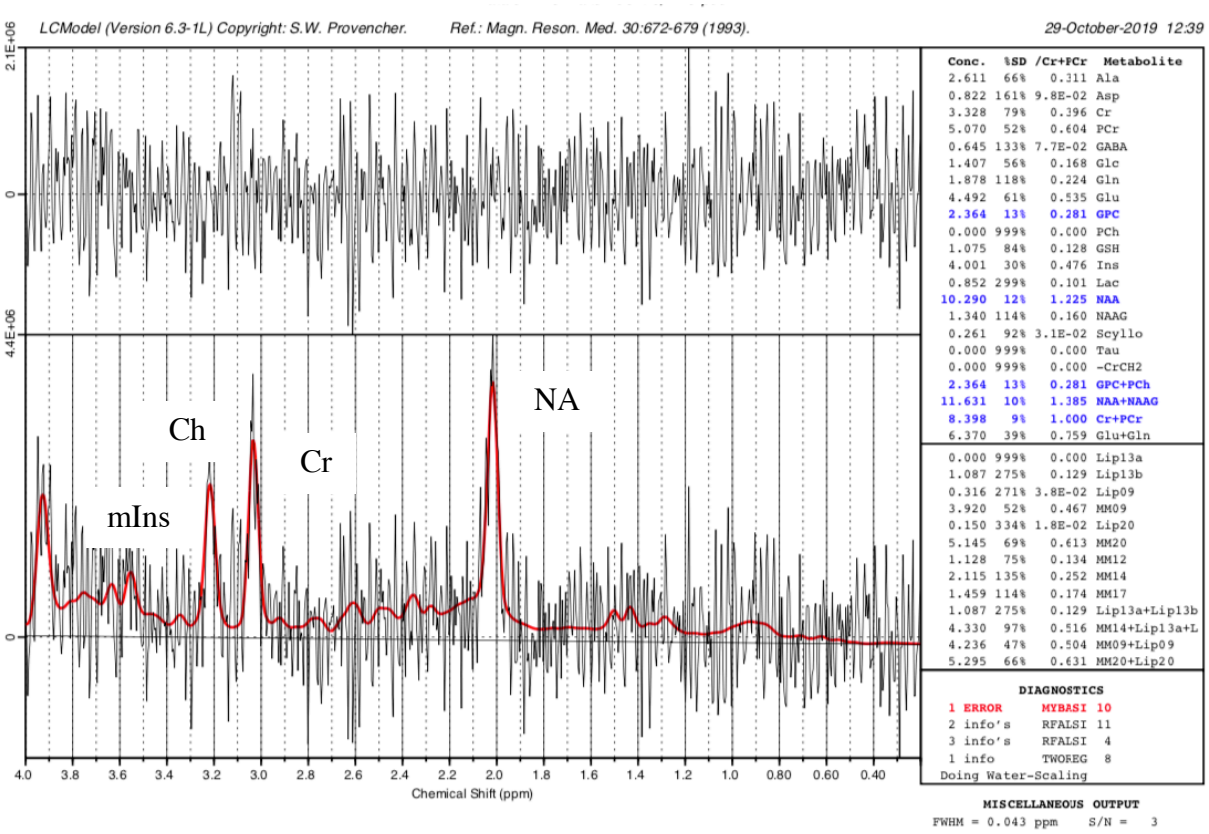

Figure 2.7 Example MRS spectra following analysis with LCModel – a common software package for analysing MRS data

2.4.1 MRS in clinical populations including epilepsy

NAA has been suggested as a marker of neuronal health or dysfunction, as it is located solely in neurons (Cendes *et al*., 1997) and is consistently found to be reduced in studies of diseases known to involve neuronal loss such as tumour and multiple sclerosis (MS; Barker & Lin, 2006; Soares & Law, 2009). Additionally, links have been seen between levels of NAA and measures of disability in MS, suggesting that higher levels of NAA are related to better neuronal health (Barker and Lin, 2006). NAA is thought to be a marker of neuronal dysfunction, rather than of neuronal loss,

due to the ability for NAA deficits to reverse, which has been seen in temporal lobe epilepsy following surgery (Cendes *et al*., 1997). A statistically significant 12% decrease in mean global NAA, as measured by whole-brain MRS, has been demonstrated in patients with temporal lobe epilepsy (Kirov *et al*., 2018). Decreases in NAA have also been seen in the temporal lobes of patients with various epilepsies (Gadian *et al*., 1994) and in those with refractory TLE (Connelly *et al*., 1994).

The Cho peak in MRS is made up of phosphocholine, glycerophosphocholine and free choline (Barker and Lin, 2006) and has been noted to be in high levels in glial cells (Gill *et al*., 1989). The presence of elevated Cho levels due to inflammation has been supported by histological findings in patients with encephalomyelitis (Brenner *et al*., 1993). Investigation of Cho levels in focal epilepsy are far from conclusive, with studies demonstrating both an increase (Meiners *et al*., 2000; Simister *et al*., 2007; Chernov *et al*., 2009) and decrease (Maier *et al*., 2000; Capizzano *et al*., 2002; Doelken *et al*., 2010) in Cho in patients compared to control groups.

Cr consists of both creatine and phosphocreatine and again, is found in much higher concentrations in glial cells than neurons (Urenjak *et al*., 1993), indicating its ability to detect inflammation. Increases in Cr have been seen in the medial temporal lobes of patients with a variety of epilepsies (Gadian *et al*., 1994) and in patients with refractory temporal lobe epilepsy (Connelly *et al*., 1994).

mIns is not present at all in neurons and is found primarily in astrocytes (Soares and Law, 2009). It is elevated in environments where there is inflammation, particularly gliosis and astrocytosis and is considered a glial marker. The literature on mIns in focal epilepsy is similar to that of Cho, with studies showing both an increase (Aasly *et al*., 1999; Aydin *et al*., 2012; Zahr *et al*., 2014) and decrease (Doelken *et al*., 2010) in patients. Further work is clearly needed to elucidate the true picture of these metabolites in epilepsy.

Both glutamine and glutamate are key in brain metabolism, with glutamate being released during neuronal excitation. Glutamate is converted to glutamine in astrocytes where it is released and taken up by neurons (Barker and Lin, 2006). Glutamate and

glutamine are difficult to separate and so are often reported together. Increases in Glx have been seen in patients with MRI-negative TLE (Doelken *et al*., 2008) though findings did not reach statistical significance.

Together, MRS studies into epilepsy imply a loss, or more likely dysfunction of neurons, and a possibility of gliosis and neuroinflammation. Despite some contradictions in epilepsy research using MRS, brain metabolite values are able to give a fairly complete picture of the microstructural environment and should be able to offer complementary information to diffusion MRI findings.

3 Methods and Materials

3.1 Participants

3.1.1 Cohort 1

Patients with newly diagnosed focal epilepsy (NDfE) were recruited from The Walton Centre NHS Foundation Trust in Liverpool, UK. Patients diagnosed six months or less prior to inclusion in the study were considered newly diagnosed. All patients and controls gave informed consent and ethical approval was given by the Health Research Authority (reference 14/NW/0332). Focal epilepsy was diagnosed by expert epileptologists according to seizure semiology. Patients with primary generalised seizures, provoked seizures, acute symptomatic seizures, or known progressive neurological disease were excluded.

27 patients with NDfE (mean age=33, SD=11, 12 female) and 36 healthy controls (mean age=34, SD=12, 22 female) were recruited into the study. See table 3.1 for demographic data including clinical scan reporting for patients. Treatment outcome data was collected up to 36 months for all patients (mean outcome=30.7 months, SD=8.4 months). 12 patients were classified as refractory and 15 patients were classified as non-refractory based on their latest available outcome data. A patient was

classified as refractory if they had experienced a seizure within the last six months prior to treatment outcome collection. If a patient had experienced no seizures in the six months prior to treatment outcome collection, they were classified as non-refractory. See table 3.2 for demographic data including clinical scan reporting for patients. All scans were reported for incidental findings at The Walton Centre by expert neuroradiologists.

ID	Age	12 month outcome	24 month outcome	Sex	DOB	Handedness	IQ Test Result	Date Of scan	EEG	MRI Report	Medication	Dx > fMRI	Seizures between Dx & MRI	seizures betw dx+mri, normalized for mths	Neurological History
1	18	PS	PS	M	29/09/1997	50	127	28/10/2014	rTL	FCD & Hipp R<L, signal change in right fusiform and parahippocampal gyrus (FCD), volume loss in right hippocampus (rHS)	LMT 400mgs	6	Multiple FSIA	nan	No neurological history
2	37	SF	SF	F	01/11/1977	85	94	29/10/2014	N	Normal	LMT 1000mgs	2	FTBTC	0.5	Syncope followed by concussive seizure
3	39	SF	SF	M	13/02/1975	95	127	13/11/2014	N	Frontal focal gliosis, gyrus rectus (left+right) and orbital gyrus and temporal pole (both only left)	LMT 100mgs	7	No Seizures	0	2 FTBTC & brain injury age of 15
4	57	SF	SF	M	19/12/1957	-60	86	17/11/2014	N	FCD in left middle frontal gyrus	LEV1000mgs	8	FSIA	0.125	FTBTC & pituitary cyst
5	43	PS	PS	F	30/07/1971	25	54	17/11/2014	N	Normal	LEV 1000mgs	1	FSIA	1	Headaches & previous seizures
6	30	SF	SF	M	11/03/1983	80	91	18/11/2014	N	Normal	LAM 150mgs	7	Single FSIA	0.142857143	No neurological history
7	28	PS	PS	F	01/05/1985	70	91	19/11/2014	N	Normal	LEV 1000mgs	5	No Seizures	0	FSIA & FTBTC
8	37	PS	PS	M	25/02/1977	75	91	24/11/2014	A	Normal	ZNS 200mgs	8	2 FSIA	0.25	FSIA & FTBTC
9	30	PS	PS	M	20/02/1984	70	105	25/11/2014	N	Hippo L<R	LMT 500 mgs	8	FSIA	0.125	Von Willebrand disease
10	22	**PS**	SF	M	09/05/1992	70	86	27/11/2014	N	Normal	ZNS 150mgs	1	No Seizures	0	FTBTC
11	37	SF	SF	M	18/10/1977	100	83	27/11/2014	N	Normal	LMT 150mgs	2	No Seizures	0	History of FC
12	38	PS	PS	F	20/04/1976	85	89	27/11/2014	N	Large ventricles, Multiple WM hypointensity; haemosiderin and suggestive of previous microhaemorrhages	ZNS 250mgs	5	FSIA & FTBTC	0.4	Previous hypoxic brain injury
13	37	**PS**	SF	F	30/12/1977	70	113	02/12/2014	N	Normal, Large ventricles	ZNS 500mgs	1	No Seizures	0	FSA
14	18	PS	PS	F	17/11/1996	40	89	02/12/2014	N	Normal	LMT 150mgs	11	4 FSIA & FTBTC	0.454545455	No neurological history
15	54	PS	SF	F	25/03/1960	95	79	08/12/2014	N	Normal	LMT 100mgs	1	6 FSIA	6	FTBTC and history of FC
16	41	PS	PS	F	16/11/1975	70	109	22/01/2015	A	Normal	LEV 500mgs	5	FSIA & FTBTC	0.4	FTBTC
17	25	SF	SF	F	30/11/1989	100	113	11/02/2015	N	Normal	LMT 200mgs	3	FSIA	0.333333333	No neurological history
18	18	PS	PS	M	02/10/1997	85	103	18/02/2015	A	Normal, processing – poor TL coverage	LMT 50mgs	2	FSIA	0.5	FTBTC
19	56	PS	PS	M	03/07/1958	100	91	23/02/2015	N	Normal	LMT 150mgs	1	No Seizures	0	FSA & FTBTC
20	41	PS	not known	F	05/11/1971	100	70	04/03/2015	N	Normal	LMT 300mgs	2	No Seizures	0	FSIA & FTBTC
21	22	PS	SF	M	22/10/1992	50	142	13/03/2015	N	R hippo change*	LMT 50mgs	3	No Seizures	0	FTBTC
22	23	SF	not known	M	08/06/1991	100	88	26/06/2015	N	Normal	LMT l50mgs	3	No Seizures	0	FTBTC
23	20	PS	PS	F	01/06/1995	-25	102	15/09/2015	N	Normal	LMT 100mgs	1	No Seizures	0	No neurological history
24	32	SF	SF	M	11/10/1983	100	88	17/09/2015	N	Right FL gliosis, encephalomalacia & CC atrophy; left posterior gliosis	LEV 1000mgs	1	No Seizures	0	FTBS & previous brain injury

25	38	PS	PS	F	23/08/1978	80	87	24/09/2015	N	Normal	LEV 1000mgs	2	No Seizures	0	FTBTC
26	28	**PS**	SF	M	21/09/1987	60	NA	13/10/2015	N	Normal	LMT 150 mgs	1	No Seizures	0	2 FTBTC
27	24	SF	not known	M	21/06/1991	55	106	23/10/2015	N	Normal	Unknown	2	No Seizures	0	No neurological history

Table 3.1 Patient characteristics cohort 1. Abbreviations: BC, birth complications; CF, complex focal seizures; CFTB, complex focal to bilateral seizures; Dur, duration of epilepsy; F, focal seizures (unknown whether simple or complex); FC, febrile seizures; FH, family history of epilepsy; Fr, frontal; L, left; Lat, lateralisation (left / right); Loc, localisation (lobar); N, no; nRe, non-refractory; Re, refractory; R, right; SF, simple focal seizures; SFree, number of years seizure free; SFreq, seizure frequency; SFTB, simple focal to bilateral seizures; T, temporal; U, unresolved; Y, yes.

Patient ID	Most recent outcome	Most recent outcome months	Date of scan	12 month date	12 month outcome	24 month date	24 month outcome	36 month date	36 month outcome
1	PS	36	28/10/2014	28/10/2015	PS	28/10/2016	PS	28/10/2017	PS
2	SF	36	29/10/2014	29/10/2015	SF	29/10/2016	SF	29/10/2017	SF
3	SF	36	13/11/2014	13/11/2015	SF	13/11/2016	SF	13/11/2017	SF
4	SF	24	17/11/2014	17/11/2015	SF	17/11/2016	SF	17/11/2017	not known
5	PS	24	17/11/2014	17/11/2015	PS	17/11/2016	PS	17/11/2017	not known
6	PS	36	18/11/2014	18/11/2015	SF	18/11/2016	SF	18/11/2017	PS
7	PS	36	19/11/2014	19/11/2015	PS	19/11/2016	PS	19/11/2017	PS
8	PS	36	24/11/2014	24/11/2015	PS	24/11/2016	PS	24/11/2017	PS
9	SF	36	25/11/2014	25/11/2015	PS	25/11/2016	PS	25/11/2017	SF
10	SF	36	27/11/2014	27/11/2015	PS	27/11/2016	SF	27/11/2017	SF
11	SF	24	27/11/2014	27/11/2015	SF	27/11/2016	SF	27/11/2017	not known
12	PS	36	27/11/2014	27/11/2015	PS	27/11/2016	PS	27/11/2017	PS
13	SF	24	02/12/2014	02/12/2015	PS	02/12/2016	SF	02/12/2017	not known
14	PS	36	02/12/2014	02/12/2015	PS	02/12/2016	PS	02/12/2017	PS
15	SF	36	08/12/2014	08/12/2015	PS	08/12/2016	SF	08/12/2017	SF
16	PS	36	22/01/2015	22/01/2016	PS	22/01/2017	PS	22/01/2018	PS
17	SF	36	11/02/2015	11/02/2016	SF	11/02/2017	SF	11/02/2018	SF
18	SF	36	18/02/2015	18/02/2016	PS	18/02/2017	PS	18/02/2018	SF
19	SF	36	23/02/2015	23/02/2016	PS	23/02/2017	PS	23/02/2018	SF
20	PS	12	04/03/2015	04/03/2016	PS	04/03/2017	not known	04/03/2018	not known
21	SF	36	13/03/2015	13/03/2016	PS	13/03/2017	SF	13/03/2018	SF
22	PS	12	26/06/2015	26/06/2016	PS	26/06/2017	not known	26/06/2018	not known
23	PS	36	15/09/2015	15/09/2016	PS	15/09/2017	PS	15/09/2018	PS
24	SF	24	17/09/2015	17/09/2016	SF	17/09/2017	SF	17/09/2018	not known
25	PS	36	24/09/2015	24/09/2016	PS	24/09/2017	PS	24/09/2018	PS
26	PS	36	13/10/2015	13/10/2016	PS	13/10/2017	SF	13/10/2018	PS
27	SF	12	23/10/2015	23/10/2016	SF	23/10/2017	not known	23/10/2018	not known

Table 3.2 Cohort 1 patient outcomes. Abbreviations: PS = persistent seizures, SF = seizure free

3.1.2 Cohort 2

Patients with focal epilepsy were recruited from outpatient clinics and clinical databases from The Walton Centre NHS Foundation Trust in Liverpool, UK. All patients and controls gave informed consent and ethical approval was given by the Health Research Authority (reference 17/NW/0342). Focal epilepsy was diagnosed by expert epileptologists based on seizure semiology. Non-refractory patients had experienced no seizures for at least six months prior to recruitment into the study. Refractory patients were experiencing persistent seizures prior to recruitment. Patients

with primary generalised seizures, non-epileptic seizures, previous neurosurgery or known progressive neurological disease were excluded. Two refractory patients (FBIP01 and FBIP23) withdrew from the study following ending their scans early due to anxiety and claustrophobia. All scans were reported for incidental findings at The Walton Centre by expert neuroradiologists. See Table 3.3 for demographic data including clinical scan reporting for patients.

16 adults with non-refractory focal epilepsy (mean age=41, SD=12, 8 female), 15 adults with refractory focal epilepsy (mean age=38, SD=12, 8 female), and 15 controls (mean age=38, SD=13, 7 female) were studied. One non-refractory patient (FBIP33) was removed from DKI, FBI/FBWM and MRS analysis after scanning as large areas of volume loss affected preprocessing with standard pipelines. Additionally, for MRS analysis, subjects were removed if there was excess noise in the spectra. In total, eight subjects (3 controls, 1 refractory, 4 non-refractory) right thalamic values were removed, and three subjects (1 refractory, 2 non-refractory) left thalamic values were removed due to poor quality spectra. Finally, human error meant that 3 patients (1 refractory, 2 non-refractory) and 1 control subject were excluded from HMGB1 analysis.

Study ID	Group	Age	Sex	Sfree	Type	Lat	Loc	Sfreq	Onset	Dur	FH	BC	FC	Known neuro issues	Radiological MRI findings
FBIP02	Re	32	M		CFTB	R	T	Frequent	0	32	N	N	Y	Meningitis when baby	None.
FBIP03	Re	33	M		SFTB	L	F	2/m	16	17	N	N	N		None.
FBIP04	Re	21	F		F	R	F	20/m	1.5	19.5	N	Emergency c-section	Y		None.
FBIP05	Re	34	M		F	U	F	1/2m	13	21	N	N	N		Fluid effusion seen in the mastoid air cells, more on the right side.
FBIP06	Re	18	M		CF	L	F	6/m	10	8	N	N	N		Scattered T2 white matter focal hyperintensities, seen mainly in the subcortical white matter of the frontal lobes bilaterally.
FBIP07	Re	51	M		F	U	T	12/m	14	37	N	N	Y	Encephalitis when infant	Increased T2 signal with loss of volume of the body and tail of the hippocampi bilaterally. Likely bilateral mesial temporal sclerosis.
FBIP08	nRe	26	M	2	SFTB	U	U	1-2/m	24	2	N	N	N		None
FBIP09	nRe	48	F	3	SFTB	R	T		12	36	N	N	N		Pineal cyst measuring about 1.2 cm in maximum dimension, a few scattered tiny foci of T2 hyperintensity seen in the subcortical and deep white matter of the frontal lobes bilaterally. Mega cisterna magna (incidental).
FBIP10	Re	50	F		CFTB	U	U	3-6/m	18	32	N	N	N		Slight upward convexity of the upper margin of the pituitary (incidental).
FBIP11	Re	32	M		CFTB	R	T	1-2/m	23	9	N	N	N		Quadrigeminal plate lipoma, mega cisterna magna (incidental).
FBIP12	Re	51	F		CF	R	T	14/m	11	40	Y	N	N		Slightly increased T2 hyperintensity in right hippocampus, subtle hippocampal volume asymmetry. Suspicion of right mesial temporal sclerosis.
FBIP13	nRe	24	F	3		R	T		21	3	N	N	N		Temporal horn of the right lateral ventricle slightly more prominent compared to the left; no evidence of mesial temporal sclerosis.
FBIP14	Re	36	F		CFTB	U	U	15/M	20	16	N	N	N		Borderline loss of cerebellar volume.
FBIP15	Re	38	F		CFTB	L	F	16-20/m	17	21	Y	N	N		Lesion seen at the posterior aspect of the left frontal lobe; mild generalised loss of cerebellar volume.
FBIP16	Re	48	F		CFTB	U	T	20/day	10	38	N	N	N		None.
FBIP17	Re	41	F		CFTB	U	U	10-16/day	27	14	N	Premature	N		Focal encephalomalacia/gliosis seen in the left lateral orbital gyrus, anterior aspect of the left temporal lobe; borderline loss of cerebellar volume.
FBIP18	nRe	33	M	1	CFTB	U	U		29	4	N	N	N		10 mm × 6 mm dural based structure seen at the left posterior temporal/occipitotemporal region; appearances compatible with meningioma.
FBIP19	Re	28	M			R	T	1/m	13	15	N	N	N		Right hippocampus sclerosis.
FBIP20	nRe	46	F	1.5	CFTB	U	U	cps 4/6m, sps 2/3m	22	24	N	N	N		Upward convexity of the upper margin of the pituitary (incidental).
FBIP21	nRe	60	M	1	SFTB	U	R	1 total	56	4	Y	N	N		None.
FBIP22	nRe	38	F	5	SFTB	R	T		30	8	U	U	N/K	Poss encephalitis - not confirmed	None.
FBIP24	Re	58	F		SFTB	U	U	10-15/day	11	47	N	U	N		Right-sided subependymal grey matter heterotopia along ventricular trigone and temporal and occipital horns of lateral ventricle. Polymicrogyria extending from the periventricular heterotopic grey matter. Additional closed lip schizencephaly and dysplasia. Right sided cerebellar volume loss. Cerebellar atrophy.

FBIP25	nRe	44	M	5	SFTB	R	T		39	5	N	N	N	Car accident when 15, brain injury	Encephalomalacia/gliosis in the left gyrus rectus and medial orbital gyrus. Focal damage in right temporal pole. Small focus of gliosis/encephalomalacia is close to left temporal bone. Mild periventricular T2 hyperintensity adjacent to the left ventricular trigone/supratrigonal white matter.
FBIP26	nRe	26	M	2	CFTB	U	T		21	5	Y	N	N		Right hippocampus marginally smaller than the left.
FBIP27	nRe	29	F	3	CF	U	U		22	7	N	N	N		None.
FBIP28	nRe	35	M	2	CFTB	R	F		31	4	N	N	N	Accident when 11, brain injury	Encephalomalacia/gliotic changes in right frontal lobe extending to left frontal lobe. Some anterior corpus callosum volume loss. Gliotic/encephalomalacia changes in the left parietal lobe. Subtle volume loss of right temporal pole.
FBIP29	nRe	59	F	4.5	SFTB	U	U	1 total	54	5	N	3 months premature	Y		Mild to moderate small vessel ischaemia.
FBIP30	nRe	54	M	11	SFTB	L	T	2 total	43	11	N	Spina bifida, hydocephalus	Y	Hydrocephalus when born	Right-sided frontal porencephalic cyst with surrounding gliotic changes. Smaller porencephalic cyst in the left frontal lobe. Atrophy of the anterior aspect of the body of the corpus callosum. Mild enlargement of the lateral and third ventricles secondary white matter volume loss.
FBIP31	nRe	51	F	3	SFTB	L	F	3 total	48	3	U	U	N		Gliosis of anterior left superior frontal gyrus. Mild generalised brain volume loss. Mild small vessel type ischaemic changes in white matter adjacent to anterior aspect of right lateral ventricle.
FBIP32	nRe	38	F	0.75	CFTB	U	U	2 total	36	2.5	Y	N	N	Enlarged ventricles	Heterotopic subependymal grey matter nodules seen along the body of the right lateral ventricle.

Table 3.3 Patient characteristics cohort 2. Abbreviations: BC, birth complications; CF, complex focal seizures; CFTB, complex focal to bilateral seizures; Dur, duration of epilepsy; F, focal seizures (unknown whether simple or complex); FC, febrile seizures; FH, family history of epilepsy; Fr, frontal; L, left; Lat, lateralisation (left / right); Loc, localisation (lobar); N, no; nRe, non-refractory; Re, refractory; R, right; SF, simple focal seizures; SFree, number of years seizure free; SFreq, seizure frequency; SFTB, simple focal to bilateral seizures; T, temporal; U, unresolved; Y, yes.

3.2 Applied MR Acquisition

3.2.1 Cohort 1

All patients and controls were scanned at the Liverpool Magnetic Resonance Imaging Centre (LiMRIC) on a 3T Siemens Trio MR scanner. Patients were scanned an average of 3.7 months after diagnosis (SD 2.9, range 1-11 months).

A T1w magnetisation-prepared rapid acquisition gradient echo (MPRAGE) was acquired (176 slices, repetition time [TR] = 2040 ms, inversion time [TI] = 1100 ms, echo time [TE] = 5.57 ms, resolution = 1.0 x 1.0 x.1.0 mm, flip angle = 8°).

A T2w Turbo Spin Echo sequence was also acquired (160 slices, TR = 3000ms, TE = 355 ms, resolution = 1.0 x 1.0 x 1.0 mm).

Finally, a diffusion weighted sequence was performed (72 slices, TR = 5.7 ms, TE = 104 ms, resolution = 3.1 x 3.1 x 3.1 mm, b-values = 0, 1000, 2000, 60 directions).

3.2.2 Cohort 2

All patients and controls were scanned at the LiMRIC on a 3T Siemens Prisma MR scanner.

A T1w MPRAGE (192 slices, TR = 2,000ms, TI = 912ms, TE = 2.25ms, resolution = 1.0 x 1.0 x 1.0 mm, flip angle = 8°) was first performed.

A standard diffusion weighted scan was performed (TR = 3200 ms, TE = 90 ms, 50 axial slices, resolution = 2.5 x 2.5 x 2.5 mm, b-values = 0, 1000, 2000, 64 directions).

FBI requires two diffusion weighted scans in order to calculate all parameters: (i) an FBI sequence (TR = 4400ms, TE = 100ms, 46 axial slices, resolution = 2.7 x 2.7 x 2.7 mm, b-values = 0, 5000, 128 directions; (ii) a DKI sequence which was parameter-matched to the FBI scan (b-values = 0, 1000, 2000, 30 directions).

MRS was performed using single voxel, point-resolved spectroscopy (PRESS) sequence in the transversal orientation (conventional spin echo sequence (TE / TR = 30ms/1700ms), NEX = 1, flip angle 90°, slice thickness = 20mm, field of view (FOV) 10 x 10 x 10 mm3, acquisition time = 853ms). Two acquisitions were performed to cover the left and right thalamus, along with two additional non-water suppressed sequences for each thalamus. See Figure 3.1 for voxel placement. For each main sequence, manual shimming was performed to corrected for field inhomogeneities.

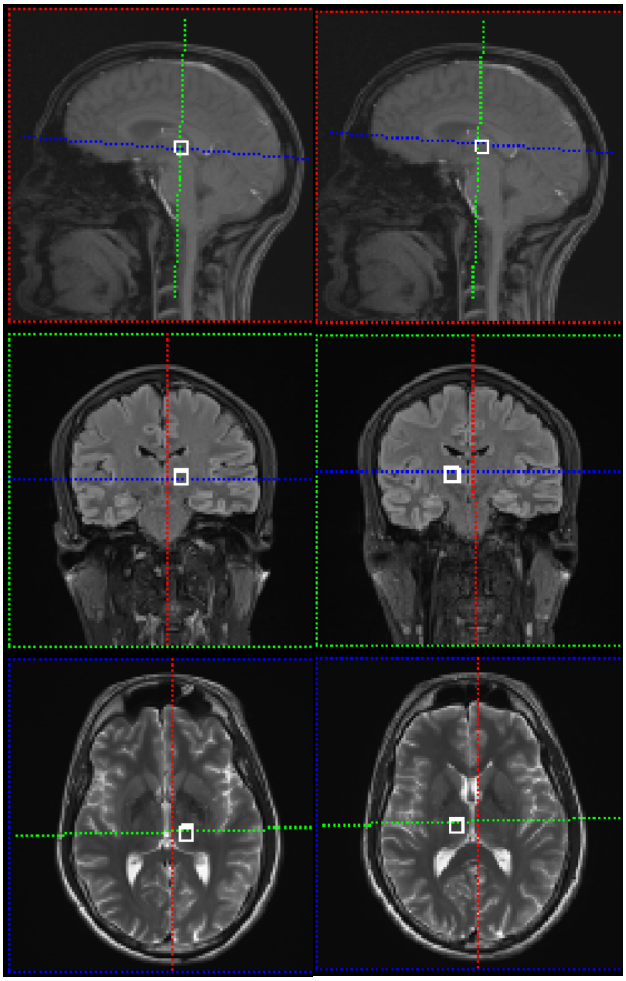

Figure 3.1 Voxel placement for MRS metabolite measurement. Two MRS sequences were performed, one for the left thalamus, one for the right thalamus

3.3 MR image processing

3.3.1 Preprocessing

3.3.1.1 Freesurfer segmentation

For generation of grey matter segmentations, T1-w data was preprocessed using Freesurfer version 6 (Fischl, 2012) to automatically segment and parcellate the data.

Freesurfer is a collection of tools which allow automatic analysis of the human brain. This includes parcellation of the cortex and subcortical regions, further segmentation of hippocampal subfields, mapping of the thickness of cortical grey matter, and thalamic nuclei segmentation. For a detailed description of Freesurfer, the reader is referred to Fischl (2012). The standard "recon-all" processing pipeline was used, which segments both grey and white matter and provides surface and morphometry data for each subject. Standard segmentation was used to generate hippocampus, amygdala, and parahippocampal gyrus. Additional steps to segment thalamic nuclei were performed using Freesurfer development version 092018 using the segmentation of thalamic nuclei pipeline as described in Iglesias et al., 2018[2] using a probabilistic atlas build with histological data. This pipeline gives volumes for 26 thalamic nuclei for each hemisphere along with left and right whole thalamic volumes. The 26 thalamic nuclei were then grouped into nine larger groups by function for analysis. See Figure 3.2 for segmented thalamus and Table 3.1 for nuclei included in each group. (Note: five nuclei were not reliably segmented in all subjects either hemisphere so were removed from further analysis).

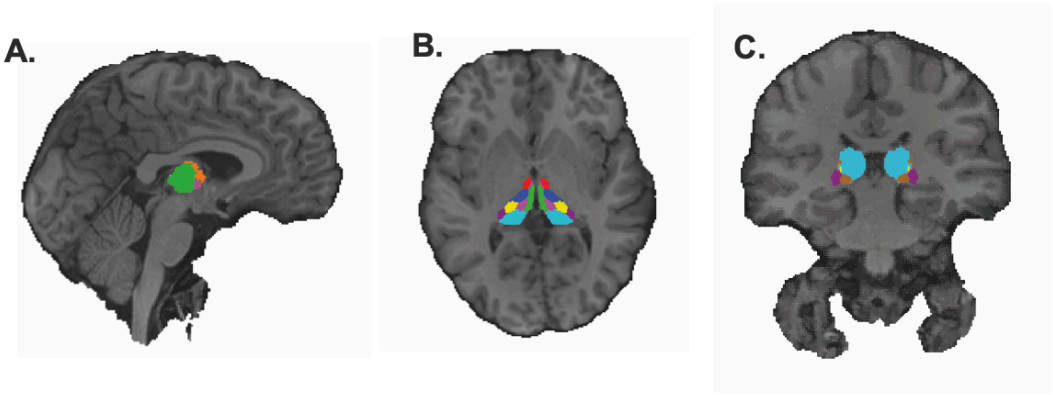

Figure 3.2 (A) Sagittal, (B) Axial, and (C) Coronal T1 slices showing segmented thalamic nuclei grouped functionally using Freesurfer development version 092018. Key: Orange = Anterior, Pink = Intralaminar, Cyan = Lateral geniculate, Brown = Medial geniculate, Red = Ventral anterior, Blue = Ventral lateral, Yellow = Ventral postero lateral

[2] http://freesurfer.net/fswiki/ThalamicNuclei

Thalamic group	Thalamic nuclei included	Main functions
Anterior	Antero-ventral Latero-dorsal	Head direction and spatial navigation (Child and Benarroch, 2013) Episodic memory (Kosif, 2016) Emotional and executive functions (Child and Benarroch, 2013)
Intralaminar	Central medial Central lateral Centro-median Parafascicular Paracentral	Modulation of memory networks (Lambert *et al*., 2017) Attention and arousal (Kinomura *et al*., 1996) Support of awareness processes (Steriade, 1997)
Lateral geniculate	Lateral geniculate	Visual relay (Bürgel *et al*., 1999)
Pulvinar	Latero-posterior Pulvinar anterior Pulvinar inferior Pulvinar lateral Pulvinar medial	Integration of somatosensory and visual information (Schmahmann, 2003) Visual perception and eye movements (Swenson, 2006)
Medial geniculate	Limitans (suprageniculate) Medial geniculate	Auditory relay (Winer, 1992)
Medial	Medio-dorsal lateral parvocellular	Maintaining and modulating working

	Medio-dorsal medial magnocellular Paratenial Reuniens	memory (Watanabe and Funahashi, 2012)
Reticular	Reticular	Sleep/wake cycles (Swenson, 2006) Attention (Kosif, 2016)
Ventral anterior	Ventral anterior Ventral anterior magnocellular	Modulation of basal-ganglia motor activity (Schmahmann, 2003) and speech (Barbas, García-Cabezas and Zikopoulos, 2013) Planning and initiating movements (Swenson, 2006)
Ventral lateral	Ventral lateral anterior Ventral lateral posterior	Verbal fluency and speech (Schmahmann, 2003)
Ventro-medial	Ventro-medial	
Ventral postero-lateral	Ventral poster-lateral	Major sensory nuclei (Behrens *et al*., 2003)

Table 4 Thalamic nuclei groups and their key functions

3.3.1.2 dMRI preprocessing for diffusion map generation

Preprocessing of dMRI data included MRtrix3 denoising and Gibbs ringing removal (Tournier, Calamante and Connelly, 2007), and Rician noise removal using Matlab Version R2016b. FMRIB Software Library (FSL; Smith et al., 2004; version 6[3]) was used to extract and skull-strip a non-diffusion weighted b0 image to generate a b0 mask. The b0 mask is binarised and used in FSL eddy current correction to mitigate effects of image artefacts (Andersson and Sotiropoulos, 2016). DTI (FA & MD) and DKI (MK, AK, & RK) parameter maps were generated using Diffusional Kurtosis

[3] http://fsl.fmrib.ox.ac.uk/fsl/fslwiki/FSL

Estimator (DKE[4]; Tabesh *et al*, 2011) from the standard DKI scan. FBI (FAA & zeta) and FBWM (AWF, Da, De-mean, De-rad, De-par, & De-fa) maps were generated using DKE as previously described in McKinnon et al. (2018[5]) using the FBI and FBI-matched DKI scans.

3.3.1.3 dMRI preprocessing for tractography

To prepare data for TractSeg white matter fibre tract segmentation, eddy corrected diffusion images, b0 masks, and b-value and b-vector files were all normalised to standard Montreal Neurological Institute (MNI) space using FSL FLIRT (Jenkinson and Smith, 2001; Jenkinson *et al*., 2002; Greve and Fischl, 2009) and the MNI FA template available in FSL.

3.3.2 Generation of dMRI values for grey matter segmentations

Diffusion maps were registered into T1 space using FSL FLIRT (Jenkinson and Smith, 2001; Jenkinson *et al*., 2002; Greve and Fischl, 2009). Diffusion maps were then masked with previously generated T1 thalamic nuclei, amygdala, hippocampus, and parahippocampal gyrus regions of interest using FSL "fslstats" to generate mean diffusion values for each region.

3.3.3 White matter fibre tract segmentation

WM tracts were generated using TractSeg (Wasserthal, Neher, Hirjak, & Maier-Hein, 2019; Wasserthal, Neher, & Maier-Hein, 2018a; Wasserthal et al., 2018b[6]). TractSeg is a recently developed method for WM tract segmentation, which shortens typical tractography pipelines by using a fully convolutional neural network. This method directly segments white matter tracts using fODF peaks and is shown to be faster and more accurate in tract segmentation than six other reference methods of tractography and tract segmentation (Wasserthal, P. Neher and Maier-Hein, 2018). Tractometry, the final part of the TractSeg pipeline, outputs diffusion parameter values for 100 points along each segmented WM fibre tract which we compared for along-tract analysis. The 100 points for each tract are standardised across patients meaning that direct comparisons can be made between groups.

[4] https://www.nitric.org/projects.dke/)
[5] https://github.com/m-ama/FBWM/)
[6] https://github.com/MIC-DKFZ/TractSeg/

AF	Arcuate fascicle
ATR	Anterior thalamic radiation
CC1	Corpus callosum: rostrum
CC2	Corpus callosum: genu
CC3	Corpus callosum: rostral body, premotor
CC4	Corpus callosum: anterior midbody, primary motor
CC5	Corpus callosum: posterior midbody, primary somatosensory
CC6	Corpus callosum: isthmus
CC7	Corpus callosum: splenium
CG	Cingulum
CST	Corticospinal tract
FPT	Frontopontine tract
ICP	Inferior cerebellar peduncle
IFO	Inferior occipitofrontal fascicle
ILF	Inferior longitudinal fascicle
MCP	Middle cerebellar peduncle
OR	Optic radiation
POPT	Parieto-occipital pontine
SCP	Superior cerebellar peduncle
SLFI	Superior longitudinal fascicle segment I
SFLII	Superior longitudinal fascicle segment II
SLFIII	Superior longitudinal fascicle segment III
STR	Superior thalamic radiations
ST_FO	Striatofrontal orbital
ST_PREM	Striatoprefrontal
T_PAR	Thalamoparietal
T_PREM	Thalamopremotor
T_OCC	Thalamo-occipital
UF	Uncinate fascicle

Table 5 White matter tracts analysed in the present study. See Figure 2.4

3.3.4 MRS spectra analysis

MRS spectra was automatically quantified using LCModel version 6.3-1N (Provencher, 1993), according to Chapter 6 of the LCModel User Manual (Provencher, 2019) to include eddy-current correction and water-scaling for each spectra. Metabolite concentrations with a %SD>25 (Cramer-Rao lower bounds) were removed from the dataset as according to the manual. A %SD over this indicates that the metabolite is undetectable from the data. Metabolite concentrations analysed included mIns, Cr (creatine+phosphocreatine), Cho (choline+phosphocreatine), Glx (glutamine+glutamate), and NAA (N-acetylaspartate) for both the left and right thalamus. Concentration sums were used for Cr, Cho, Glx as individual metabolite concentrations are difficult to resolve from each other. All spectra were manually checked for quality following LCModel. Metabolite concentrations were used as a non-water suppressed scan was collected, allowing for water scaling during analysis

with LCModel, giving more accurate concentrations. Typically, if a non-water suppressed scan is not collected, metabolite ratios with Cr+PCr are more accurate.

3.4 Serum acquisition and processing

3.4.1 Serum acquisition

Blood samples for serums were collected from all patients and controls. Samples were collected in 9ml plain tubes, which were centrifuged within 15 minutes, or stored at 4°C, and centrifuged on the same day as withdrawal of blood. Serum was stored at -85°C prior to analysis.

3.4.2 HMGB1 analysis

A two-step sandwich ELISA assay kit (Shino-Test Corp, Japan. Ref. ST51011) was used to quantify HMGB1 serum concentrations according to the manufacturer's protocol (IBL International, 2017). Samples were thawed on ice 2 hours prior and components, including standard serial dilutions, prepared in advance according to the protocol. An 8-channel micro pipettor was used to pipette 50µl of diluent buffer into each well of a 96-well microtiter plate pre-coated with polyclonal antibody specific to HMGB1. 50µl of each standard solution, positive control and serum sample were pipetted in duplicate into their respective wells. The plate was sealed with adhesive foil, shaken for 30 seconds and incubated at +37°C for 24 hours. The incubation solution was discarded, and the plate washed 5 times with diluted wash buffer (400µl/well). 100µl of enzyme conjugate was pipetted into each well and the plate incubated for 2 hours at +25°C. The incubation solution was discarded, and the plate washed. Colour reagents A and B were added together (1:1 ratio) immediately before pipetting 100µl of solution into each well at equal time intervals and incubating at room temperature for 30 minutes. 100µl of stop solution was added, and the plate shaken gently. The optical density was measured at 450nm using a photometer.

3.4.3 Il-1B analysis

A high sensitivity (HS) solid phase human IL-1ß ELISA assay (R&D Systems, USA. Ref. HSLB00D) was performed to quantify absolute IL-1ß serum concentration in both refractory and seizure free patients alongside controls, according to the manufacturer's protocol (R&D Systems Inc, 2017). 50µl of Assay Diluent RD1-63

was pipetted into each well of a 96-well polystyrene microtiter plate pre-coated with monoclonal antibody specific for human IL-1ß followed by 100µl of each standard, positive control and serum sample into their respective wells. Whilst most samples were pipetted in duplicate, some were performed in singular due to plate restrictions. Due to human error during the protocol, the standard curve from the manufacturer's protocol was used.

3.5 Statistics

Statistical testing was performed using SPSS statistics and results were considered significant at $p<0.05$.

3.5.1 Chapter 4 & 5 specific statistics

Group comparisons were performed firstly between controls and all patients, and secondly between controls, refractory patients, and non-refractory patients. Group comparisons were performed for DKI values (MK, AK, and RK) of each thalamic nuclei, hippocampi, amygdalae, and parahippocampal gyri using multivariate analysis of variance (MANOVA) with age and sex as covariates. Where significant effects were revealed, Bonferroni posthoc comparisons were applied. These posthoc analysis were used to correct for multiple comparisons.

3.5.2 Chapter 6 specific statistics

All group comparisons were performed between first controls and all patients, and secondly between controls, refractory patients, and non-refractory patients. Group comparisons were performed for right and left thalamic volumes and all DKI thalamic values using MANOVA with age, sex, intracranial volume (which was estimated by Freesurfer v6) as covariates with posthoc Bonferroni analysis providing further investigation and correction for multiple comparisons. For spectroscopy and HMGB1 analysis, due to missing values, group comparisons were first performed using one-way ANOVA – this was performed for all metabolite values, HMGB1 levels, and IL-1ß values. For possibly significant effects, group comparisons were then investigated separately using univariate analysis of variance and corrected for age, sex, and multiple comparisons using Bonferroni correction.

3.5.3 WM along-tract statistics (Chapters 4, 5, & 7)

Fifty white matter tracts were generated using TractSeg[7] (Wasserthal, P. Neher and Maier-Hein, 2018; Wasserthal *et al*., 2019) (Figure 2.4, Table 3.2). TractSeg is a recently developed method for WM tract segmentation, which shortens typical tractography pipelines by using a fully convolutional neural network. This method directly segments white matter tracts in fields of fODF peaks via a fully convolutional neural network and has been demonstrated to yield more accurate tract segmentation compared to six other reference methods of tractography and tract segmentation (Wasserthal, P. Neher and Maier-Hein, 2018). Tractometry, the final part of the TractSeg pipeline, outputs diffusion parameter values for 100 points along each segmented white matter fibre tract which we used for along-tract analysis. The 100 points for each tract were standardised across participants so that direct comparisons for each FBI and FBWM map could be made between groups (Figure 3.3 B-D).

TractSeg permits statistical analysis along the 100 points of each tract in order to investigate differences in diffusion parameter values along the entire tract. Statistical analysis in this way was performed as per the tractometry documentation available online12, which is based on statistical analysis from Yeatman *et al.,* (2012). We adopted this approach and corrected for age, sex, and multiple comparisons using Family Wise Error correction. Results were considered significant if the minimal p-value for each along-tract point was lower than the alpha value corrected for multiple comparison.

[7] https://github.com/MIC-DKFZ/TractSeg/

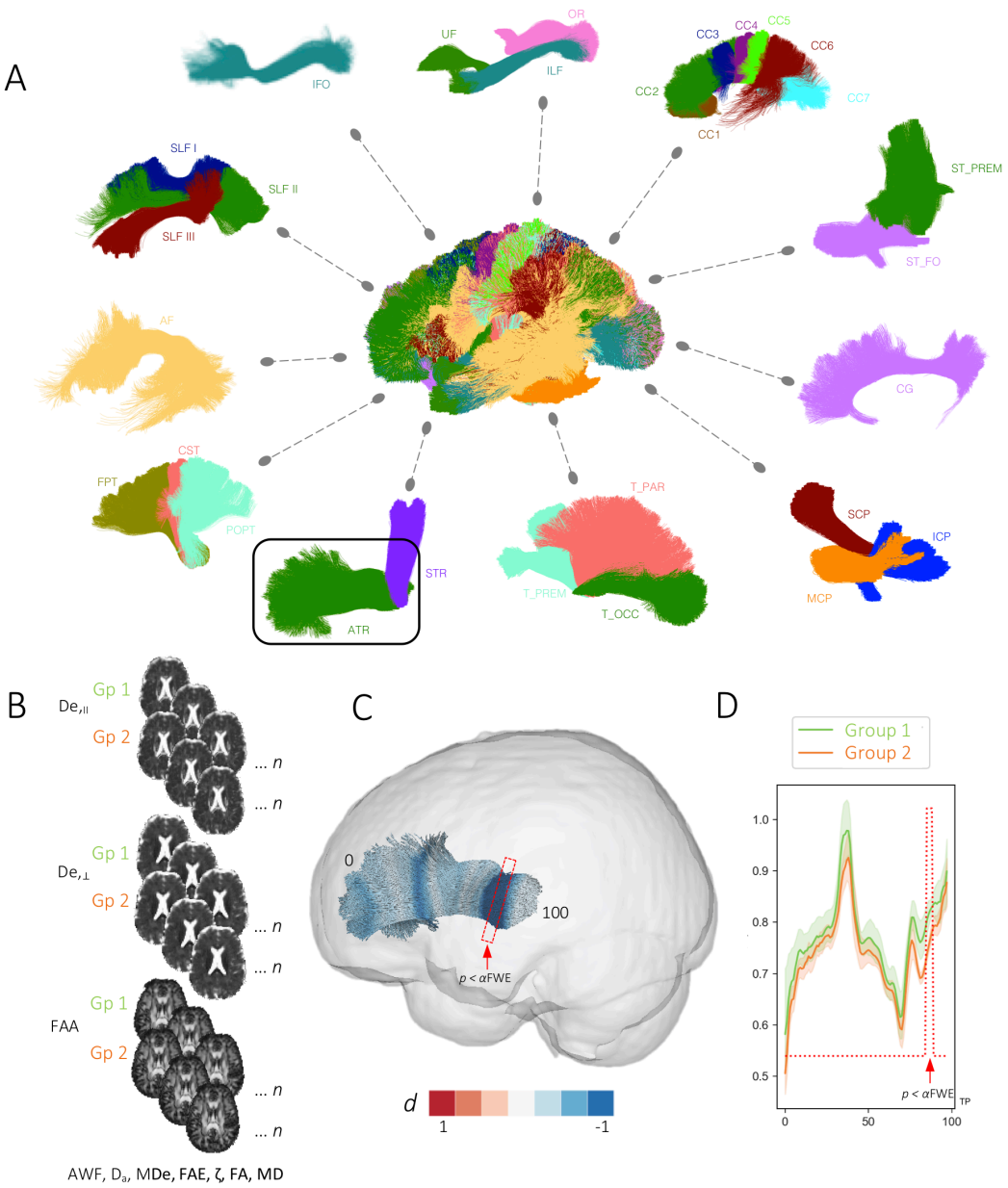

Figure 3.3 (a) White matter tracts automatically segmented using TractSeg included in this thesis. See Table 3.2 for definition of abbreviations. (b) Illustration of group comparisons of FBWM maps for along-tract analyses. (c) Visualization of Cohen's d effect sizes computed along the length of an exemplar tract (ATR; see a) that is significantly different between two groups. (d) Mean (±SEM) diffusion values are plotted for each point along the tract. P < αFWE: region along the tract where the p value is smaller than the αFWE and considered statistically significant. TP = tract points

4 Diffusion kurtosis imaging of grey and white matter in newly diagnosed focal epilepsy

4.1 Introduction

Although there is a wealth of literature demonstrating multiple brain abnormalities in patients with epilepsy, it remains unclear whether these changes are a cause or consequence of seizures and long-term use of AEDs (Pohlmann-Eden, 2011). In order to investigate this, it is necessary to study patients at the earliest possible time point, the point of diagnosis. Identifying abnormalities present at the point of diagnosis may provide insights into possible biomarkers of pharmacoresistance. This would allow for earlier treatment stratification and potentially better prognoses for patients. Early treatment stratification is vital as those who receive appropriate treatment early on have an increased chance of seizure freedom (Kwan and Brodie, 2006). Despite this, there are few sophisticated neuroimaging studies with patients with newly diagnosed focal epilepsy (NDfE).

The few imaging studies which have investigated NDfE have tended to be volumetric and have failed to elucidate a potential biomarker of pharmacoresistance. A longitudinal hippocampal volumetric study found no differences in mean hippocampal volumes between controls and patients with NDfE at the point of diagnosis, or 1, 2 to 3, or 5 years post recruitment (Salmenperä *et al*., 2005). In a volumetric study of the corpus callosum (CC) differences were found between patients with NDfE and controls, with patients demonstrating lower CC volume than controls. Furthermore, patients who went on to respond well to AED treatment showed lower CC volumes compared to non-responders. However, non-responders were diagnosed on average 18

months later than responders, experienced an average of two additional seizures, and follow-up of these patients was relatively short (Kim *et al*., 2017), casting doubt on the reliability of these findings. Similarly, in a more recent volumetric study, patients with NDfE demonstrated increased atrophy in the left hippocampus and left and right thalami compared to controls, though no relationship was found between these changes and future seizure control (Leek *et al*., 2020). Further, even using more sophisticated imaging techniques, it has proven difficult to show differences at diagnosis between patients who go on to become seizure free and those who become pharmacoresistant. For example, a functional connectivity study found reduced connectivity in patients between the fronto-parietal attention network and frontal and temporal cortical regions relative to controls. However, no difference was found between patients who were seizure free and those still experiencing seizures at one-year follow-up (Alonazi *et al*., 2019). A more recent study into NDfE using advanced diffusion and connectomes was able to demonstrate differences at the point of diagnosis between patients who went on to become seizure free and those who became pharmacoresistant (Kreilkamp *et al*., 2021). This included decreased FA in both regions of interest and connectivity metrics. Patients who went on to become non-refractory demonstrated decreased anisotropy and increased diffusivity compared to those who went on to become non-refractory. These findings demonstrate the importance of using more advanced, sophisticated neuroimaging techniques when studying patients with NDfE. Differences found at the point of diagnosis between patients who go on to become pharmacoresistant and those who do not are likely to be subtle, and as such, require sensitive methods to elucidate.

Epilepsy has long been considered a disorder of GM (Chapter 1), with many volumetric abnormalities consistently found (Simon S. Keller *et al*., 2002; Keller and Roberts, 2008; O'Dwyer *et al*., 2010; Centeno *et al*., 2014; Colnaghi *et al*., 2017). However more recent work has demonstrated the role of WM (Chapter 1) and epilepsy is now considered a network disorder (Keller, Richardson, Schoene-Bake, *et al*., 2015; Glenn *et al*., 2016; De Bézenac *et al*., 2019; Kreilkamp *et al*., 2021) with abnormalities which can lie far from the seizure focus. Networks are typically made up of brain regions and the connections between those regions, which can be made up from a number of data types.

WM pathologies commonly found include oligodendroglial hyperplasia (Schurr *et al*., 2017), and an increase of WM neurons (Liu *et al*., 2014). It is therefore important to fully investigate both GM *and* WM when searching for a potential biomarker for pharmacoresistance. In the present study, we have used DKI to examine differences in WM along tracts using diffusion tractography (TractSeg; (Wasserthal, Neher and Maier-Hein [2018]; Chapter 2). This approach offers analysis of diffusion characteristics along the length of tracts to investigate regionally specific alterations, which may be more sensitive than averaging diffusion characteristics over the whole tract (Figure 2.5). Measuring DKI metrics along tracts in this way has been implemented previously in patients with TLE where alterations were found in both extrahippocampal and extratemporal WM tracts (Glenn *et al*., 2016). Further, we investigated diffusion alterations in subcortical grey matter using Freesurfer (Fischl, 2012). DTI is known to be less sensitive to changes in GM than DKI (Gao *et al*., 2012; Bonilha *et al*., 2015), and there are questions surrounding the ability of DTI to measure changes in GM (Chapter 2), highlighting our reasoning for using only DKI to examine grey matter changes. There is a scarcity of literature employing DKI in this way, however, both Gao *et al*. (2012) and Bonilha *et al*. (2015) demonstrated reduced kurtosis values in patients with TLE and suggested the potential of DKI to differentiate between refractory and non-refractory patients.

The objective of this study was to characterise microstructural alterations in GM and WM using DKI in patients with NDfE. We explored differences in these parameters in patients who went on to become refractory or non-refractory up to 36 months post inclusion into the study. dMRI has not been used to study NDfE this extensively before and we expected to show that alterations commonly seen in longstanding focal epilepsy are present at diagnosis. Further, we expected to find differences between patient groups at the point of diagnosis which we anticipate will assist with the development of a biomarker for pharmacoresistance in focal epilepsy.

4.2 Methods

3.1.1 Participants

3.1.2 MRI acquisition

4.3 Results

4.3.1 Grey matter changes

In order to investigate changes in subcortical grey matter at the point of diagnosis in patients with NDfE, we compared DKI measures in the thalamic nuclei, hippocampus, amygdala, and parahippocampal gyrus of patients who went on to continue to experience persistent seizures and those who went on to become seizure free relative to controls (Table 4.1). No significant differences were observed between patients who went on to become refractory and those who went on to become seizure free. Significant changes were seen between both patient groups and controls, which were restricted to thalamic nuclei.

Parameter	Segmentation	Controls		Refractory		p-value	F-value
KFA	R ventral anterior	0.68	(0.06)	0.63	(0.10)	0.039	3.441
AK	R ventral lateral	1.18	(0.11)	1.06	(0.17)	0.016	5.579
	R ventral postero-lateral	1.14	(0.10)	1.03	(0.16)	0.022	3.884
		Controls		Non-refractory			
KFA	L anterior	0.62	(0.05)	0.67	(0.04)	0.012	4.683
	L ventral postero-lateral	0.66	(0.08)	0.58	(0.10)	0.041	3.788
MK	R medial geniculate	0.63	(0.48)	0.67	(0.05)	0.048	3.264
AK	L ventral postero-lateral	0.97	(0.12)	0.86	(0.13)	0.025	3.769
	R ventral anterior	1.13	(0.16)	0.99	(0.17)	0.022	4.830

Table 6 DKI and DTI significant GM segmentation differences between patients with refractory epilepsy, patients with non-refractory epilepsy, and controls. The mean (standard deviation) of the individual diffusion parameter, p-value, and F statistic (from tests of between-subjects effects) for each significant region are provided.

4.3.1.1 Controls vs refractory patients

Relative to controls, refractory patients demonstrated significant changes in the thalamus. Reductions in KFA in the right ventral anterior nucleus (p = 0.039) and AK in the right ventral lateral (p = 0.016) and right ventral postero-lateral (p= 0.022) nuclei were observed (Figure 4.1).

4.3.1.2 Controls vs non-refractory patients

Significant changes in the thalamus were also seen in non-refractory patients relative to controls. Significant increases were found in KFA in the left anterior nucleus (p = 0.012) and MK in the right medial geniculate nucleus (p = 0.048). Significant reductions were found in KFA in the left ventral postero-lateral nucleus (p = 0.041) and in AK in the left ventral postero-lateral (p = 0.025) and right ventral anterior (p = 0.022) nuclei (Figure 4.1).

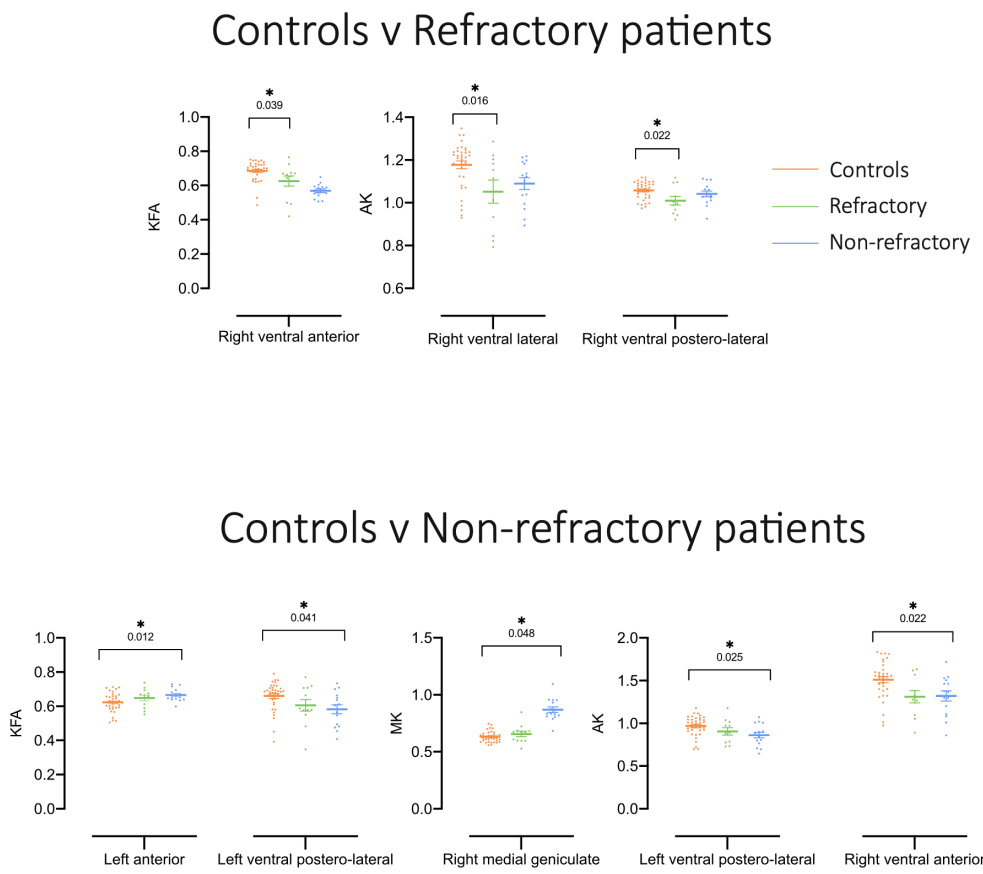

Figure 4.1 Statistically significant differences in GM regions of interest between controls vs refractory patients and controls vs non-refractory patients

4.3.2 White matter changes

In order to investigate changes in white matter at the point of diagnosis in patients with NDfe, we compared DKI and DTI measures in 50 white matter tracts (Figure 2.4, Table 3.2) in patients who went on to continue to experience persistent seizures and those who went on to become seizure free relative to controls (Table 4.2).

Parameter	Tract	Controls		Refractory		αFWE	Min p-value	t-value	Cohen's d
KFA	CC 6	0.70	(0.02)	0.68	(0.02)	0.000289	0.000137	4.17	-1.37
	L SLF I	0.66	(0.03)	0.63	(0.03)	0.000275	0.000275	3.95	-1.30
	R SLF II	0.68	(0.02)	0.65	(0.02)	0.000326	5.50E-05	4.46	-1.47
AK	L ICP	1.15	(0.11)	0.88	(0.42)	0.001633	0.000577	3.71	-1.24
	R T PAR	1.19	(0.10)	1.05	(0.13)	0.000309	0.00023	4.00	-1.32
	R T OCC	1.19	(0.08)	0.97	(0.33)	0.000613	0.000583	3.70	-1.24
MK	L ICP	0.82	(0.09)	0.62	(0.31)	0.001666	0.001001	3.52	-1.18
	R IFO	0.77	(0.04)	0.72	(0.04)	0.000302	0.000269	3.96	-1.30
	R ILF	0.84	(0.05)	0.77	(0.06)	0.000441	6.60E-05	4.40	-1.45
	L ST PREM	0.91	(0.03)	0.85	(0.05)	0.000442	0.000351	3.87	-1.28
RK	L ST PREM	0.73	(0.06)	0.65	(0.08)	0.000523	0.000323	3.90	-1.28
FA	L ICP	0.13	(0.02)	0.10	(0.05)	0.001039	0.000873	3.57	-1.19
	R UF	0.15	(0.01)	0.17	(0.02)	0.000242	2.50E-05	-4.70	1.55
AD	R CG	0.89	(0.04)	0.95	(0.05)	0.000367	0.000269	-3.96	1.30
	L SLF II	0.90	(0.04)	0.95	(0.05)	0.000412	0.000224	-4.01	1.32
MD	CC 7	1.05	(0.27)	1.45	(0.49)	0.000241	0.000211	-4.03	1.34
	R CG	0.77	(0.03)	0.82	(0.04)	0.000242	6.00E-05	-4.43	1.46
RD	CC 7	0.96	(0.26)	1.36	(0.47)	2.00E-04	0.00015	-4.14	1.37
	R CG	0.71	(0.03)	0.75	(0.04)	0.00031	5.30E-05	-4.47	1.48
		Controls		Non-refractory					
KFA	L AF	0.72	(0.02)	0.70	(0.03)	0.000186	0.000127	4.17	-1.27
	R ATR	0.67	(0.02)	0.63	(0.06)	0.000334	8.70E-05	4.29	-1.31
	CC 6	0.70	(0.01)	0.68	(0.02)	0.000257	3.10E-05	4.60	-1.40
	L CG	0.72	(0.03)	0.69	(0.03)	0.000304	4.50E-05	4.49	-1.37
	R CG	0.74	(0.03)	0.70	(0.04)	0.000405	4.80E-05	4.47	-1.36
	L IFO	0.70	(0.02)	0.66	(0.04)	0.000299	6.30E-05	4.39	-1.34
	MCP	0.72	(0.05)	0.66	(0.06)	0.000273	0.000191	4.04	-1.23
	L SCP	0.68	(0.04)	0.63	(0.06)	0.000403	0.000113	4.21	-1.28
	R SCP	0.71	(0.03)	0.67	(0.05)	4.00E-04	5.00E-05	4.46	-1.36
AK	R ATR	1.06	(0.07)	0.95	(0.09	0.000372	4.20E-05	4.51	-1.37
	CC 4	0.65	(0.17)	0.81	(0.17)	0.00021	0.000126	-4.17	1.27
	R STR	1.25	(0.07)	1.17	(0.08)	0.000298	0.000103	4.24	-1.29
MK	CC 6	0.84	(0.03)	0.79	(0.05)	0.000499	0.000215	4.01	-1.22
RK	CC 6	0.68	(0.06)	0.61	(0.05)	0.000315	0.000159	4.10	-1.24

	L IFO	0.60	(0.05)	0.53	(0.07)	0.000317	0.000122	4.18	-1.28
	R POPT	0.79	(0.07)	0.69	(0.07)	0.000278	1.00E-05	4.93	-1.50
	R T PAR	0.76	(0.05)	0.70	(0.05)	0.000413	3.00E-04	3.90	-1.18
FA	CC 6	0.17	(0.01)	0.16	(0.01)	0.000392	0.000344	3.86	-1.17
	MCP	0.18	(0.02)	0.21	(0.02)	0.000234	0.000126	-4.17	1.27
	R POPT	0.16	(0.02)	0.14	(0.01)	0.000261	0.000208	4.01	-1.22
	L SCP	0.16	(0.01)	0.15	(0.02)	0.000291	4.10E-05	4.52	-1.37
	L TPREM	0.16	(0.01)	0.14	(0.01)	0.000311	1.90E-05	4.74	-1.44
AD	CC 6	1.23	(0.12)	1.46	(0.22)	0.00034	2.90E-05	-4.62	1.41
	L CST	0.90	(0.04)	0.96	(0.07)	0.000377	0.000177	-4.07	1.24
	L IFO	1.05	(0.09)	1.26	(0.26)	0.000339	9.80E-05	-4.25	1.30
	L ILF	0.96	(0.18)	1.14	(0.20)	0.003661	0.000859	-3.56	1.08
	R ILF	0.95	(0.06)	1.03	(0.13)	0.000613	0.000136	-4.15	1.27
	R POPT	0.94	(0.04)	1.01	(0.08)	0.000339	0.000312	-3.89	1.19
	R SCP	0.96	(0.06)	1.06	(0.10)	0.000427	0.000251	-3.96	1.21
MD	CC 6	0.84	(0.04)	0.91	(0.08)	0.000533	1.90E-05	-4.74	1.45
	L IFO	0.89	(0.09)	1.08	(0.25)	0.00034	0.000182	-4.06	1.24
	L ILF	0.82	(0.16)	0.99	(0.22)	0.003233	0.00096	-3.52	1.07
	R ILF	0.80	(0.05)	0.88	(0.13)	0.000463	0.000208	-4.02	1.23
	R POPT	0.82	(0.04)	0.89	(0.07)	0.000456	7.90E-05	-4.32	1.32
	R SCP	0.80	(0.06)	0.90	(0.10)	0.000286	0.000179	-4.06	1.24
	L ST PREM	0.86	(0.05)	0.90	(0.05)	0.00049	0.00032	-3.88	1.18
RD	CC 6	0.77	(0.04)	0.84	(0.07)	0.000521	1.00E-05	-4.92	1.50
	L CG	0.73	(0.03)	0.77	(0.05)	0.000334	0.000211	-4.01	1.22
	L IFO	0.81	(0.09)	0.99	(0.24)	0.000445	0.000272	-3.93	1.21
	L ILF	0.75	(0.15)	0.91	(0.21)	0.003013	0.000981	-3.51	1.07
	R ILF	0.72	(0.05)	0.80	(0.12)	0.000626	0.000279	-3.92	1.20
	R POPT	0.76	(0.04)	0.83	(0.07)	0.00031	4.60E-05	-4.48	1.37
	R SCP	0.72	(0.06)	0.82	(0.10)	0.00045	0.000187	-4.05	1.24
	L UF	0.79	(0.15)	0.87	(0.09)	0.005644	0.005209	-2.93	0.89
	L ST PREM	0.78	(0.04)	0.83	(0.05)	0.000606	0.00012	-4.19	1.28
		Refractory		Non-refractory					
AK	L CG	0.93	(0.06)	1.05	(0.08)	0.000212	1.50E-05	-5.35	2.01
	R ST PREM	0.99	(0.10)	1.10	(0.10)	0.000411	0.000245	-4.27	1.61
FA	L SCP	0.17	(0.02)	0.16	(0.01)	0.000281	0.000255	4.26	-1.60

Table 7 DKI and DTI significant WM tract differences between patients with refractory epilepsy, patients with non-refractory epilepsy, and controls. The mean (standard deviation) of the individual diffusion parameter, minimum p-value and its corresponding α value, t statistic, and Cohen's d for the peak of each significant tract are provided. Abbreviations for tracts are provided in Table 3.2.

4.3.2.1 Controls vs refractory patients

Relative to controls, significant differences and large effect sizes were found in refractory patients for all DKI metrics across 9 tracts ($p<0.05$; large $d = \pm 0.8$). Significant differences in DKI metrics between patients with refractory epilepsy and controls are illustrated in Figure 4.2. Significant reductions were seen in KFA in circumscribed regions of the isthmus of the corpus callosum (CC6), the left superior longitudinal fascicle segment I (SLF I), and right SLF segment III (SLF III). Significant MK reductions were also seen in refractory patients relative to controls in regions of the left inferior cerebellar peduncle (ICP), right and left inferior longitudinal fascicles (ILF), and the left striatoprefrontal (ST PREM) tract. Furthermore, reductions in AK were found in regions of the left ICP, left thalamo-occipital (T OCC), and right thalamoparietal (T PAR) tracts, and reduction in RK was found in one region of the left ST PREM tract.

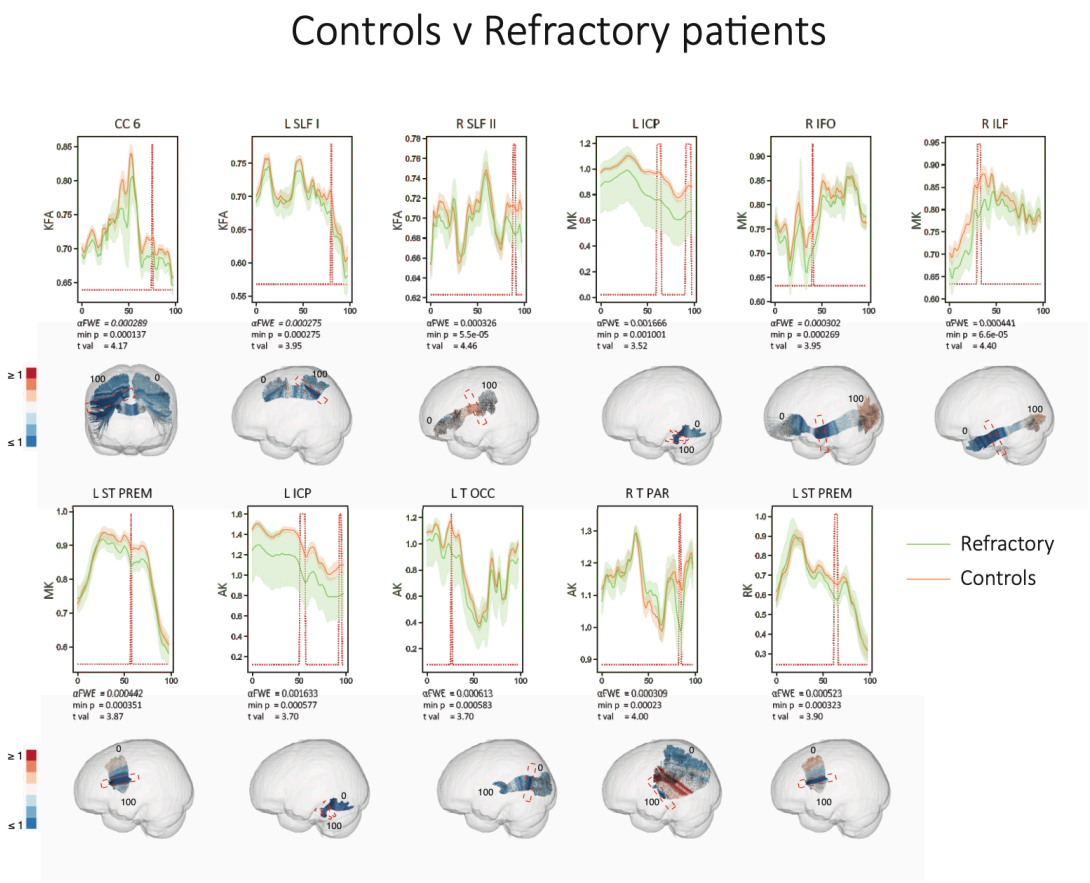

Figure 4.2 Statistically significant (red peaks) along-tract differences in DKI diffusion properties in refractory patients compared to controls. 3D plots show Cohen's d values projected onto the relevant tracts with significant region highlighted by red boxes. Effect sizes greater than and equal to 1 are shown in dark red, with those less than and equal to −1 shown in dark blue.

Further, significant differences were found for all DTI metrics across five tracts between refractory patients and controls. Significant differences in DTI metrics between patients with refractory epilepsy and controls are illustrated in Figure 4.3. A

significant reduction in FA in a region of the left ICP and a significant increase in FA in a region of the right uncinate fascicle (UF) was found in refractory patients relative to controls. Significant increases in MD and RD were seen in regions of the splenium of the corpus callosum (CC7) and the right cingulum (CG) in refractory patients compared to controls. Significant increases were also seen in AD in regions of the right CG and left SLF III in refractory patients.

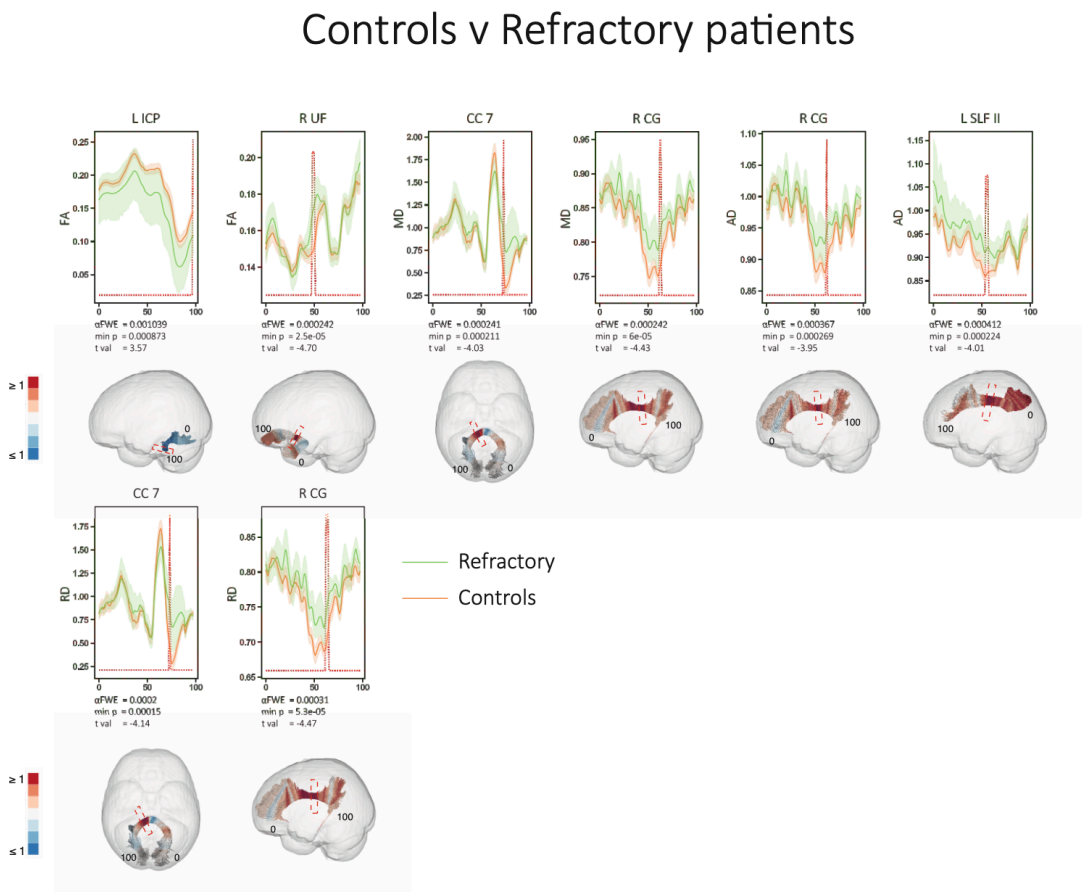

Figure 4.3 Statistically significant (red peaks) along-tract differences in DTI diffusion properties in refractory patients compared to controls. 3D plots show Cohen's d values projected onto the relevant tracts with significant region highlighted by red boxes. Effect sizes greater than and equal to 1 are shown in dark red, with those less than and equal to −1 shown in dark blue.

4.3.2.2 Controls vs non-refractory patients

Significant alterations and large effect sizes ($p<0.05$; $d = \pm 0.8$) across all DKI metrics and 13 tracts were found for non-refractory patients relative to controls. Significant differences between non-refractory patients and controls are illustrated in Figure 4.4. Significant reductions were found in non-refractory patients in regions of the left arcuate fascicle (AF), right anterior thalamic radiation (ATR), CC6, left and right CG,

left IFO, middle cerebellar peduncle (MCP), and left and right superior cerebellar peduncles (SCP). A reduction in MK was also seen in non-refractory patients in a region of the CC6 and reductions in AK were found in regions of the right ATR and right STR. An increase in AK in non-refractory patients was found in the anterior midbody of the corpus callosum (CC4). In non-refractory patients, decreases in RK were found in regions of the CC6, left IFO, right parieto-occipital pontine (POPT) and right T PAR tracts.

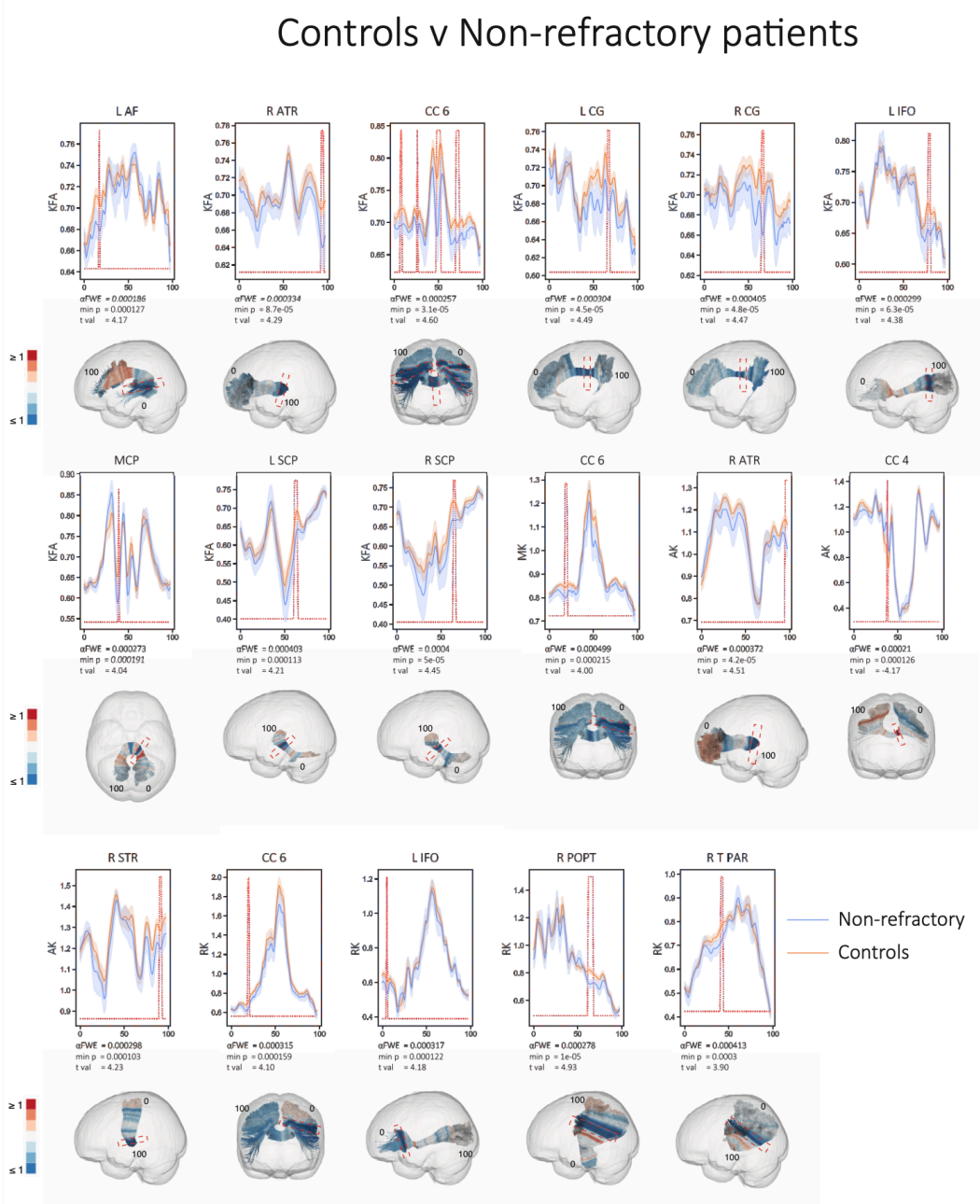

Figure 4.4 Statistically significant (red peaks) along-tract differences in DKI diffusion properties in non-refractory patients compared to controls. 3D plots show Cohen's d values projected onto the relevant tracts with significant region highlighted by red boxes. Effect sizes greater than and equal to 1 are shown in dark red, with those less than and equal to −1 shown in dark blue.

Differences were also seen for all DTI metrics across 13 tracts between non-refractory patients and controls (Figure 4.5). Reductions in FA were seen in non-refractory patients in regions of the CC6, right POPT, left SCP, and left T PREM tract, while an increase in FA was found in a region of the MCP relative to controls. Increases in AD, MD, and RD were also found in non-refractory patients in regions of the CC6, left IFO, left and right ILF, right POPT, and right SCP. Further increases were found in AD in a region of the left corticospinal tract (CST), in MD and RD in regions of the left ST PREM tract, and in RD only in regions of the left CG and left UF.

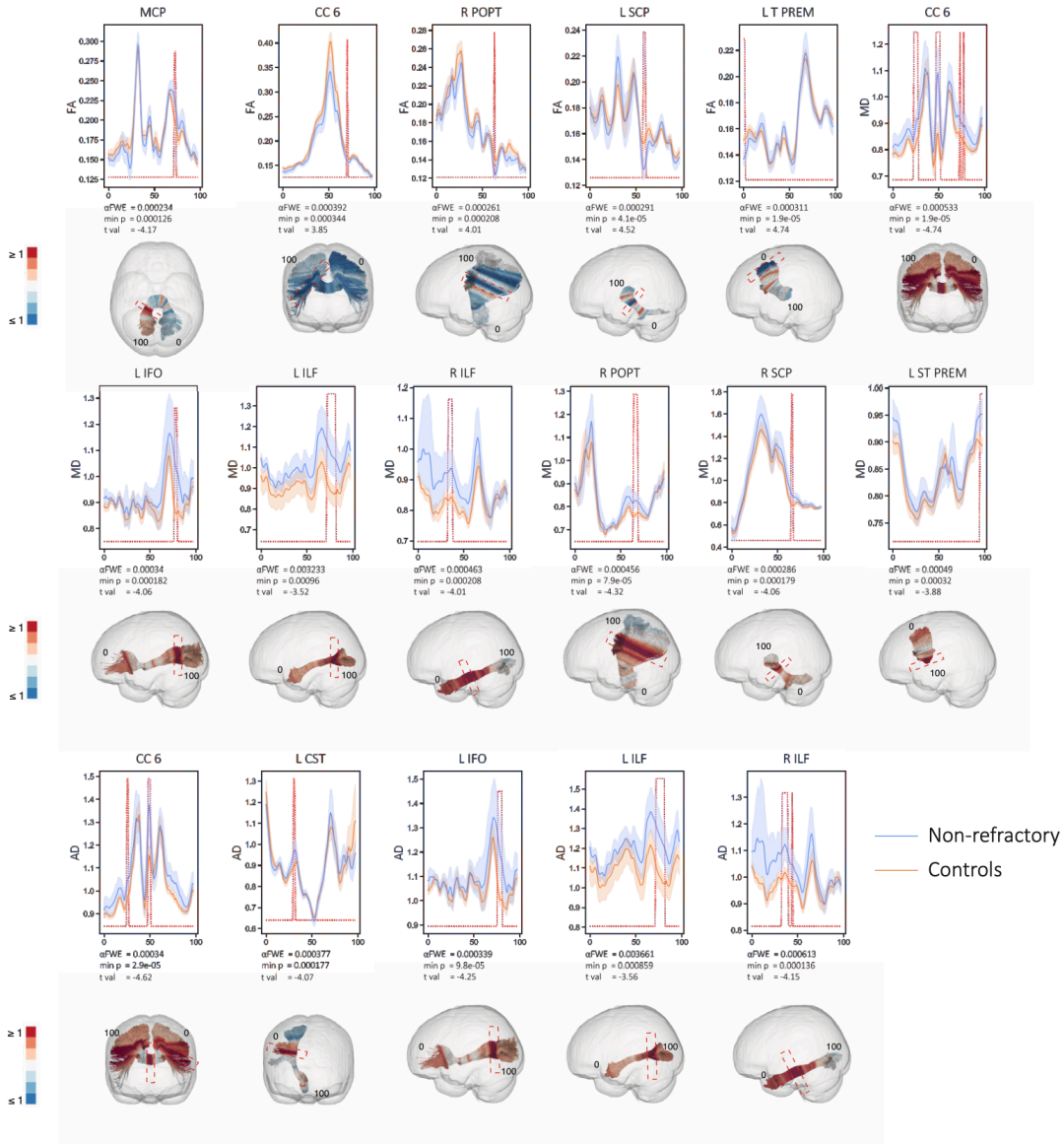

Figure 4.5 Statistically significant (red peaks) along-tract differences in DTI diffusion properties in non-refractory patients compared to controls. 3D plots show Cohen's d values projected onto the relevant tracts with significant region highlighted by red boxes. Effect sizes greater than and equal to 1 are shown in dark red, with those less than and equal to −1 shown in dark blue.

4.3.2.3 Refractory vs non-refractory patients

In comparisons between patients who went on to become refractory (experienced at least one seizure in the six months prior to last outcome measurement) and those who went on to become non-refractory (no seizures in six months prior to last outcome measurement), significant differences were found in AK and FA only across three tracts. Effect sizes for significant regions were large (d = ± 0.8) and significant differences between refractory and non-refractory patients are illustrated in Figure 4.6.

Significant differences were seen in AK in regions of the left CG and right ST PREM and in FA in a region of the left SCP. Patients with refractory epilepsy showed lower AK values and increased FA values in these regions relative to those with non-refractory epilepsy.

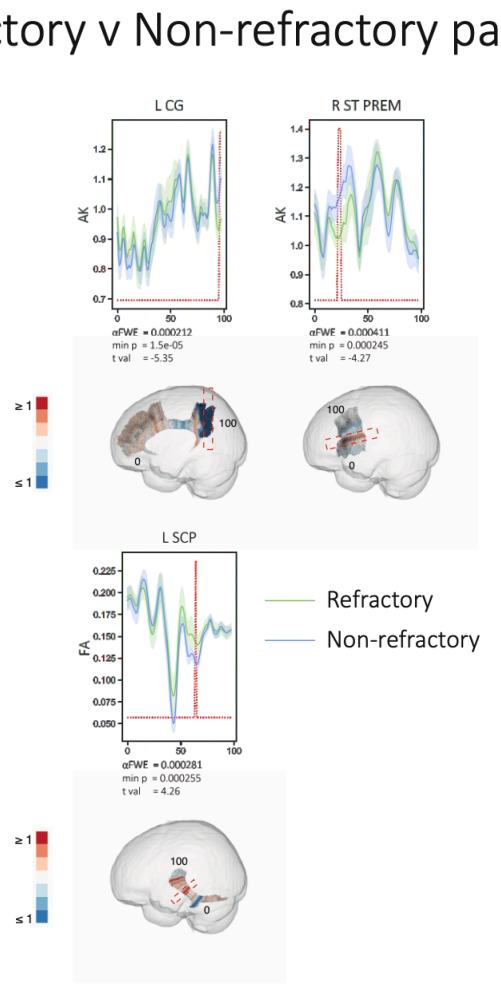

Figure 4.6 Statistically significant (red peaks) along-tract differences in DKI and DTI diffusion properties in non-refractory patients compared to refractory. 3D plots show Cohen's d values projected onto the relevant tracts with significant region highlighted by red boxes. Effect sizes greater than and equal to 1 are shown in dark red, with those less than and equal to –1 shown in dark blue.

4.4 Discussion

In the present study, we sought to determine whether diffusion changes commonly seen in patients with longstanding focal epilepsy are present at the point of diagnosis. We report significant changes in diffusion parameters in both grey and white matter in patients with NDfE. Further, we aimed to explore whether there were differences, at the point of diagnosis, between patients who went on to become refractory, and those who became seizure free 30.7 months post inclusion in the study. We

demonstrated that there are differences between these patient groups, potentially offering a non-invasive biomarker of pharmacoresistance.

4.4.1 Biological/clinical implications

This is the first study to use DKI to investigate NDfE, and there is a lack of research using this method even in longstanding focal epilepsy. We report changes at the point of diagnosis in several diffusion parameters in both white (KFA, AK, MK, RK) and grey (AK, MK, KFA) matter. In longstanding epilepsy, AK has been suggested to be indicative of intra-axonal alterations rather than extra (Hui *et al*., 2008), thus providing information on axonal damage or loss. MK has been suggested to be associated with increased glial activity (Zhuo *et al*., 2012), which could indicate its utility as a marker of neuroinflammation. KFA is the kurtosis equivalent of standard FA which is better able to model GM (Hansen and Jespersen, 2016)(Chapter 2), and again is a marker of neuronal loss or damage. Overall, a decrease in diffusion parameters is linked to a less restricted diffusion environment and thus a potential loss of axons or increase in inflammation (Hui *et al*., 2008). Decreases in AK and MK have been seen in clinical populations (Falangola *et al*., 2008; Hui *et al*., 2008; Gong *et al*., 2017; Zhou *et al*., 2019) and in TLE previously (Gao *et al*., 2012; Bonilha *et al*., 2015) and our work is in line with those findings. Further, we suggest that several key biological changes begin to happen at the point of diagnosis which is vital for understanding the progression of epilepsy as a disorder.

We report a widespread pattern of changes in white matter, with a more restricted pattern of grey matter changes, localised to the thalamic nuclei. These widespread white matter changes are in line with recent work demonstrating network alterations in patients with NDfE (Kreilkamp *et al*., 2021). We found that DKI of white matter tracts was able to show changes at the point of diagnosis between patients who went on to experience persistent seizures and those who became seizure free. This is in line with literature suggesting epilepsy as a network disorder (Keller, Richardson, Schoene-Bake, *et al*., 2015; Glenn *et al*., 2016) and suggests these network changes begin to happen early on in the disease progression. Further, previous work has shown that changes in white matter connectivity are linked to post-surgical outcome which may suggest the presence of a wider epileptogenic network in those with postoperative

seizures (Bonilha *et al*., 2013; Keller, Richardson, Schoene-Bake, *et al*., 2015). Our work supports this theory, as white matter alterations were seen at diagnosis. It is possible that this is the beginning of a wider epileptogenic network, leading to pharmacoresistance later in the disorder.

In the present study, we found diffusion changes in grey matter restricted to the thalamus in both patient groups. The thalamus is known to play a key role in focal epilepsy (Malekmohammadi, Elias and Pouratian, 2015)(Chapter 2). Deep brain stimulation of the thalamus has been shown to reduce seizure frequency (Fisher *et al*., 2010; Salanova *et al*., 2015; Li and Cook, 2018) and imaging studies have demonstrated abnormalities in volume (Dreifuss *et al*., 2001; Keller, Richardson, Schoene-Bake, *et al*., 2015), glucose uptake (Khan *et al*., 1997), and functional dysfunction (Pedersen *et al*., 2016) in the thalamus. Particularly relevant to the present study is the work by Leek *et al*. (2020) which demonstrated reduced thalamic volume in patients with NDfE compared to controls. However, this study also found volumetric changes in the hippocampus (Leek *et al*., 2020), where we found no changes in diffusion measures outside of the thalamus. It is however important to note the differences between gross volumetric studies and those using more advanced imaging techniques. Although volumetric studies can detect changes in gross volume size in various structures within the brain, they are unable to infer a cause of these changes or any biological processes underlying them. Further, many brain changes which result from epileptogenic activity may not be detectable with volumetric methods (Kreilkamp *et al*., 2021). Thus, it remains important to explore brain abnormalities in patients with NDfE with more sophisticated and advanced imaging techniques (Pohlmann-Eden, 2011; De Bézenac *et al*., 2019), as in the present study.

4.4.2 Conclusions

In this novel DKI investigation of NDfE, we have demonstrated diffusional changes in the thalamus and widespread white matter tracts in patients with NDfE. Further, we have shown that white matter changes differ between patients who go on to experience persistent seizures and those who become seizure free. It is vital that we use advanced imaging to allow the microstructural investigation of biological processes happening

at the onset of the disorder. We suggest that a disordered white matter network may be a driver of pharmacoresistance from the onset of focal epilepsy.

5 Diffusion kurtosis imaging of grey and white matter in longstanding focal epilepsy

5.1 Introduction

Approximately 30% of people with focal epilepsy will not achieve seizure freedom from anti-epileptic drug (AED) treatment. Experiencing continued seizures despite available drug treatments greatly affects quality of life and leads to greater adverse effects from the use of prolonged ineffective AED treatment (Baker *et al*., 1997; Perucca and Gilliam, 2012). Likewise, ongoing seizures have been shown to lead to an increase in cognitive decline (Thompson and Duncan, 2005) and cause increased inflammation and microstructural damage to the brain (Pardoe, Berg and Jackson, 2013). The consequences of pharmacoresistance in focal epilepsy are further discussed Chapter 1. The use of neuroimaging to study patients with pharmacoresistant epilepsy has the potential to identify clinical or imaging biomarkers of treatment outcome, leading to the earlier stratification of patients and therefore more appropriate treatment regimes.

In the present study, we have used Diffusion Tensor Imaging (DTI) to investigate white matter (WM) and grey matter (GM) changes, and Diffusion Kurtosis Imaging (DKI) to investigate GM changes in patients with refractory and non-refractory longstanding focal epilepsy. As discussed in Chapter 2, there are few studies using DKI to investigate GM in focal epilepsy, though epilepsy has long been considered a disorder of GM. Studies commonly focus on volumetric changes, typically reporting reductions in various GM regions (Keller and Roberts, 2008; O'Dwyer *et al*., 2010; Colnaghi *et al*., 2017) though increases have been seen (S S Keller *et al*., 2002). There

is a move toward the consideration of epilepsy as a network disorder (Bernhardt, Bonilha and Gross, 2015; Kreilkamp *et al*., 2021) with WM pathologies also found, including focal cortical dysplasia and cortical tubers (Blümcke *et al*., 2011), oligodendroglial hyperplasia (Schurr *et al*., 2017), and an increase of WM neurons (Liu *et al*., 2014). Further, studies of along-tract measures in those with focal epilepsy have demonstrated alterations in extrahippocampal and extratemporal WM tracts (Glenn *et al*., 2016). It is clear there is a role of abnormalities in both GM *and* WM in focal epilepsy and thus it is important to investigate both in order to elucidate a biomarker of pharmacoresistance.

By utilising DKI in this study, we are able to further investigate microstructural changes in patients with longstanding focal epilepsy. DTI has widely been used to investigate alterations in WM in those with epilepsy, however this method is not reliable in the study of GM. DKI offers the ability over standard DTI to explore changes in anisotropic environments (such as GM) as the method does not assume an anisotropic diffusion environment (Jensen and Helpern, 2010) (see Chapter 3 for more detailed discussion). When DKI is used, typically, it is able to identify more widespread changes in both WM and GM (Gao *et al*., 2012; Bonilha *et al*., 2015), and shows increased sensitivity to structural alterations (Lee *et al*., 2013) when compared with DTI, suggesting that DKI may be a superior method compared with DTI to detect microstructural abnormalities. Further, we have used along-tract methods (Tractseg; Wasserthal, P. Neher and Maier-Hein [2018]; Chapter 2), allowing for investigation of regionally specific alterations (Figure 2.5). Combining along-tract measures and DKI gives a deeper insight into microstructural changes in patients with longstanding focal epilepsy.

In the present study, we aimed to characterise microstructural alterations in both GM and WM using dMRI (DTI and DKI) in patients with longstanding focal epilepsy. By comparing directly between patients experiencing ongoing seizures (refractory patients) and those not currently experiencing seizures (non-refractory patients), we aimed to identify an imaging biomarker of treatment outcome in focal epilepsy. To our knowledge, ours is the first study to explore in depth dMRI alterations in both GM and WM in patients with refractory and non-refractory longstanding focal epilepsy.

We expected to find differences between patients with refractory and non-refractory epilepsy in regions of both GM and WM.

5.2 Methods

3.1.2 Participants

3.2.2 MR acquisition

3.3 MR image processing

3.3.1.1 Freesurfer segmentation of T1 images

3.3.1.2 dMRI preprocessing for diffusion map generation

3.3.1.3 dMRI preprocessing for tractography

3.3.2 Generation of dMRI values for grey matter segmentations

3.3.3 White matter fibre tract segmentation

3.5 Statistics

3.5.1 GM statistics

3.5.3 WM along-tract statistics

5.3 Results

5.3.1 GM segmentations

All significant differences in DKI and DTI parameters between patients with refractory epilepsy, non-refractory epilepsy, and controls are shown in Table 5.1. Significant differences were seen between controls and non-refractory patients and between refractory and non-refractory patients. No significant differences were found between controls and refractory patients. Comparisons between controls and non-refractory patients demonstrated differences in AK and MK, restricted to the bilateral thalamic nuclei and the right parahippocampal gyrus. Between refractory and non-refractory patients, differences were seen in AK and were found bilaterally in the thalamic nuclei, and right amygdala and parahippocampal gyrus.

Parameter	Segmentation	Controls		Non-refractory		p-value	F-value
AK	L ventral postero-lateral	0.68	(0.03)	0.63	(0.05)	0.019	4.409
	R intralaminar	0.65	(0.03)	0.61	(0.04)	0.040	4.855
	R parahippocampal	0.53	(0.05)	0.50	(0.07)	0.006	7.293
MK	R parahippocampal	0.56	(0.05)	0.51	(0.07)	0.027	4.470
AD	L ventral-postero lateral	1.15	(0.05)	1.12	(0.06)	0.021	4.957
	R pulvinar	1.30	(0.07)	1.40	(0.15)	0.048	3.677
		Refractory		Non-refractory			
AK	L lateral geniculate	0.56	(0.06)	0.50	(0.07)	0.035	3.996
	R amygdala	0.54	(0.03)	0.49	(0.07)	0.020	4.150
	R ventral lateral	0.70	(0.03)	0.66	(0.04)	0.013	4.737
	R intralaminar	0.66	(0.05)	0.61	(0.04)	0.024	4.855
	R parahippocampal	0.55	(0.04)	0.49	(0.07)	0.006	7.293
AD	L ventral-postero lateral	1.15	(0.03)	1.20	(0.06)	0.039	4.957
	R ventral lateral	1.20	(0.03)	1.25	(0.06)	0.030	3.988
	R parahippocampal	1.67	(0.18)	1.47	(0.22)	0.018	4.253
MD	R parahippocampal	1.47	(0.16)	1.29	(0.19)	0.017	4.331
RD	R parahippocampal	1.37	(0.15)	1.21	(0.18)	0.017	4.305

Table 8 DKI and DTI significant GM segmentation differences between patients with refractory epilepsy, patients with non-refractory epilepsy, and controls. The mean (standard deviation) of the individual diffusion parameter, p-value, and F statistic (from tests of between-subjects effects) for each significant region are provided.

5.3.1.1 Controls vs non-refractory patients

Relative to controls, non-refractory patients demonstrated reductions in AK in the left ventral postero-lateral ($p = 0.019$) and right intralaminar ($p = 0.04$) thalamic nuclei and in AK ($p = 0.006$) and MK ($p=0.027$) in the right parahippocampal gyrus (Figure 5.1).

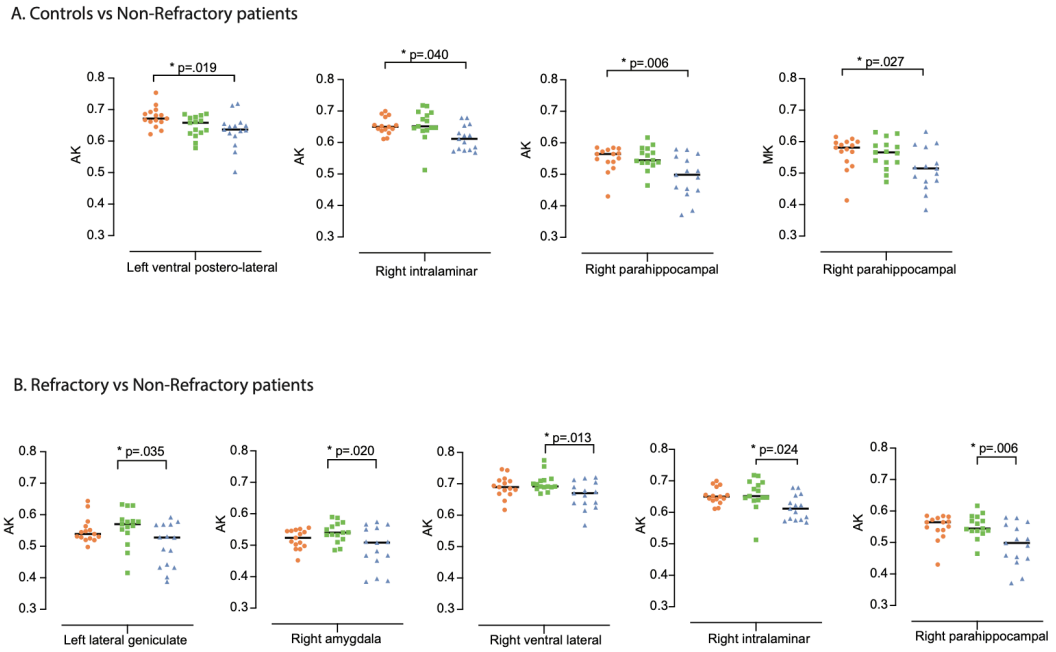

Figure 5.1 Statistically significant differences DKI metrics in grey matter regions of interest between A: controls and non-refractory patients; and B: refractory and non-refractory patients

5.3.1.2 Refractory vs non-refractory patients

In direct patient comparisons, non-refractory patients were found to have lower AK values compared to refractory patients in the left lateral geniculate ($p = 0.035$), right ventral lateral ($p = 0.013$) and right intralaminar ($p = 0.024$) thalamic nuclei and in the right amygdala ($p = 0.02$) and right parahippocampal gyrus ($p = 0.006$) (Figure 5.l).

5.3.2 WM tractography

All significant differences in DKI and DTI parameters of WM tractography between patients with refractory epilepsy, non-refractory epilepsy, and controls are shown in Table 5.2.

Parameter	Tract	Controls		Refractory		αFWE	Min p-value	t-value	Cohen's d
AK	R CST	0.65	(0.03)	0.59	(0.03)	0.000171	4.10E-05	4.86	-1.73
	L POPT	0.59	(0.03)	0.55	(0.03)	0.000211	0.000111	4.49	-1.60
	L SCP	0.70	(0.03)	0.64	(0.04)	0.000347	0.000165	4.35	-1.54
	L STR	0.69	(0.04)	0.64	(0.04)	0.000313	0.000312	4.11	-1.46
MK	CC 3	0.94	(0.08)	0.82	(0.11)	0.001054	0.000974	3.68	-1.31
	CC 4	0.97	(0.08)	0.84	(0.11)	0.000464	0.000262	4.18	-1.48

RK	R IFO	1.22	(0.22)	1.03	(0.17)	0.003192	0.003132	3.23	-1.15
	L SLF III	1.61	(0.15)	1.37	(0.17)	0.000475	0.000327	4.09	-1.45
	R SLF III	1.38	(0.07)	1.23	(0.13)	0.000733	8.10E-05	4.61	-1.64
	L ST FO	1.18	(0.12)	1.03	(0.11)	0.000802	0.000699	3.81	-1.35
	R ST FO	1.35	(0.12)	1.19	(0.11)	0.00066	0.000562	3.89	-1.38
MD	R FPT	0.95	(0.03)	1.02	(0.06)	0.000338	0.000281	-4.15	1.47
	R ICP	0.48	(0.54)	1.00	(0.44)	0.00491	0.004721	-3.07	1.09
RD	R CST	0.62	(0.06)	0.73	(0.08)	0.000283	0.000274	-4.16	1.48
	R FPT	0.64	(0.04)	0.71	(0.05)	0.00026	0.000161	-4.36	1.55
	R ICP	0.35	(0.4)	0.78	(0.36)	0.003698	0.002477	-3.33	1.18
		Controls		Non-refractory					
KFA	L CST	0.58	(0.03)	0.63	(0.04)	0.000375	8.30E-05	-4.60	1.64
	R OR	0.45	(0.03)	0.51	(0.05)	0.000457	0.000256	-4.18	1.49
AK	L CST	0.95	(0.05)	0.84	(0.07)	0.000319	5.30E-05	4.76	-1.69
	R OR	0.60	(0.04)	0.53	(0.06)	0.000594	0.000575	3.88	-1.38
	L STR	0.76	(0.03)	0.69	(0.05)	0.000355	0.00015	4.38	-1.56
	L T PAR	0.63	(0.04)	0.58	(0.05)	0.001252	0.001165	3.62	-1.29
MK	L CST	1.19	(0.06)	1.09	(0.1)	4.00E-04	0.000221	4.24	-1.51
FA	CC 1	0.37	(0.04)	0.31	(0.05)	0.002202	0.000699	3.81	-1.35
	R UF	0.37	(0.04)	0.29	(0.1)	0.004744	0.004323	3.11	-1.10
AD	L STR	1.40	(0.07)	1.55	(0.12)	0.000818	0.000263	-4.17	1.48
	L UF	1.20	(0.06)	1.29	(0.05)	0.000307	0.000149	-4.38	1.56
	L T PAR	1.50	(0.1)	1.68	(0.16)	0.000841	0.000611	-3.86	1.37
	R T PAR	1.33	(0.04)	1.40	(0.06)	0.000844	0.00055	-3.90	1.39
MD	L ATR	0.91	(0.05)	0.98	(0.04)	0.000658	0.000113	-4.48	1.59
RD	L ATR	0.70	(0.04)	0.76	(0.05)	0.000699	8.20E-05	-4.60	1.64
		Refractory		Non-refractory					
KFA	R ICP	0.49	(0.21)	0.23	(0.29)	0.003482	0.00271	3.29	-1.17
AK	R ICP	0.66	(0.28)	0.31	(0.35)	0.004549	0.002259	3.36	-1.19
	L SCP	0.71	(0.09)	0.57	(0.2)	0.0046	0.00431	3.11	-1.10
	R SCP	0.69	(0.11)	0.51	(0.18)	0.003849	0.000327	4.09	-1.45
MK	R ICP	0.83	(0.35)	0.43	(0.48)	0.005753	0.004638	3.08	-1.09
RK	MCP	1.40	(0.19)	0.94	(0.48)	0.002455	0.001136	3.63	-1.29
FA	R SCP	0.44	(0.05)	0.34	(0.11)	0.003379	0.001382	3.55	-1.26
AD	R AF	1.24	(0.06)	1.33	(0.06)	0.000416	0.000351	-4.07	1.45
	R ATR	1.44	(0.1)	1.57	(0.11)	0.000797	0.000782	-3.77	1.34
	R SCP	1.95	(0.24)	1.53	(0.52)	0.003635	0.001288	3.58	-1.27
MD	R CST	1.14	(0.08)	1.01	(0.08)	0.000621	1.10E-05	5.33	-1.89
	L FPT	1.04	(0.08)	0.93	(0.05)	0.000442	1.90E-05	5.15	-1.83
	R ICP	0.98	(0.42)	0.49	(0.54)	0.005289	0.002445	3.33	-1.18
	L POPT	1.08	(0.08)	0.96	(0.08)	0.000546	0.00013	4.43	-1.58
	R POPT	1.22	(0.13)	1.05	(0.1)	0.00062	8.40E-05	4.59	-1.63
RD	R CST	0.73	(0.08)	0.60	(0.07)	0.000405	9.00E-06	5.39	-1.92

L FPT	0.74	(0.08)	0.64	(0.06)	0.000596	1.40E-05	5.24	-1.86
R ICP	0.73	(0.33)	0.34	(0.39)	0.002663	0.001238	3.59	-1.28
L POPT	0.75	(0.1)	0.61	(0.1)	0.00053	0.000187	4.30	-1.53
R POPT	0.87	(0.12)	0.69	(0.13)	0.000604	5.20E-05	4.77	-1.69

Table 9 DKI and DTI significant WM tract differences between patients with refractory epilepsy, patients with non-refractory epilepsy, and controls. The mean (standard deviation) of the individual diffusion parameter, minimum p-value and its corresponding α value, t statistic, and Cohen's d for the peak of each significant tract are provided. Abbreviations for tracts are provided in Table 3.2.

5.3.2.1 Controls vs refractory patients

Relative to controls, significant differences were found in refractory patients in three DKI metrics (MK, AK, RK) across 11 tracts and effect sizes for significant regions were large (d = ± 0.8). Significant differences in DKI parameters between patients with refractory epilepsy and controls are displayed in Figure 5.2. Significant reductions in MK were found in patients with refractory epilepsy in regions of the rostral body (CC3) and the anterior midbody (CC4) of the corpus callosum compared to controls. Further reductions were seen in AK in regions of the right corticospinal tract (CST), left parieto-occipital tract (POPT), left superior cerebellar peduncle (SCP) and left superior thalamic radiation (STR) in patients compared to controls. A decrease in RK in patients was also found in regions of the right inferior occipitofrontal peduncle (IFO), left superior longitudinal fascicle segment III (SLF III), and left and right striatofrontal orbital tracts (ST FO) compared to controls.

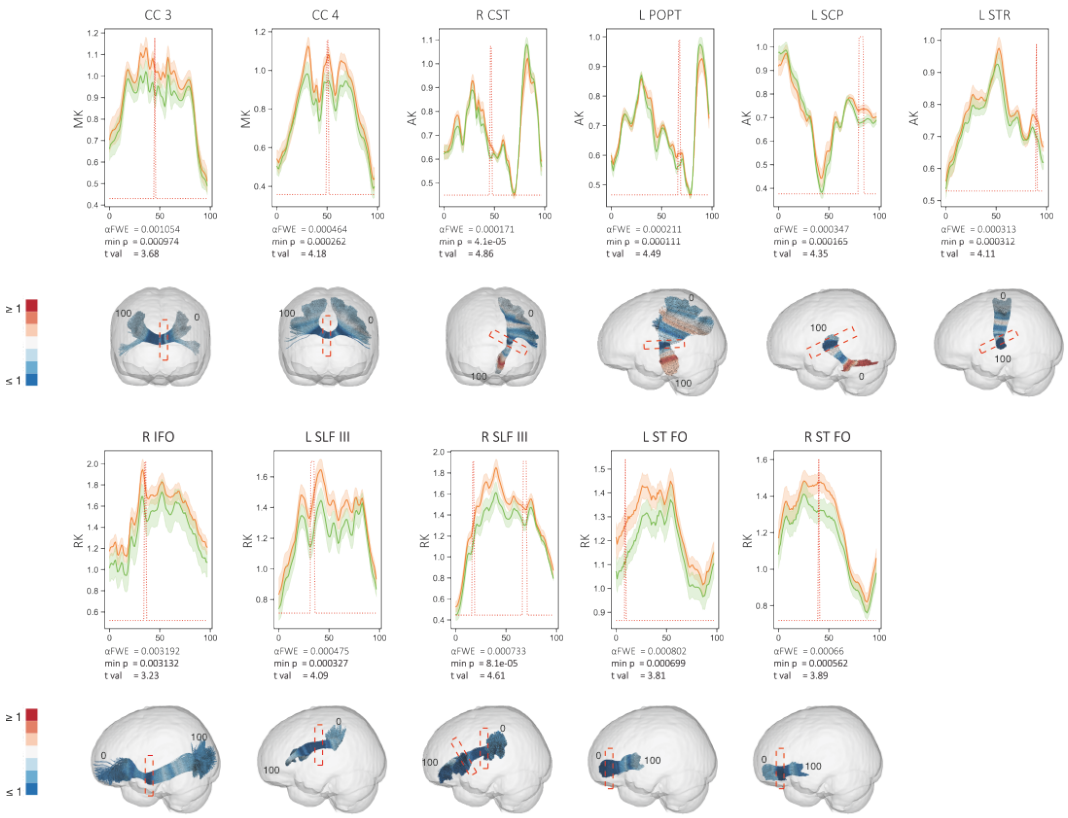

Figure 5.2 Statistically significant (red peaks) along-tract differences in DKI diffusion metrics in refractory patients (green) relative to controls (orange). 3D plots show Cohen's d values projected onto the relevant tracts with significant regions highlighted by red boxes. Effect sizes greater than and equal to 1 are shown in dark red, with those less than and equal to -1 shown in dark blue.

Further differences were found in two DTI metrics (MD, RD) across three tracts, again showing large effect sizes (d = ± 0.8). Significant differences in DTI parameters between patients with refractory epilepsy and controls are illustrated in Figure 5.3. Significant increases in MD were seen in patients with refractory epilepsy in regions of the right frontopontine tract (FPT) and right inferior cerebellar peduncle (ICP) compared to controls. Increases were also found RD in patients in regions of the right CST, right FPT, and right ICP compared to controls.

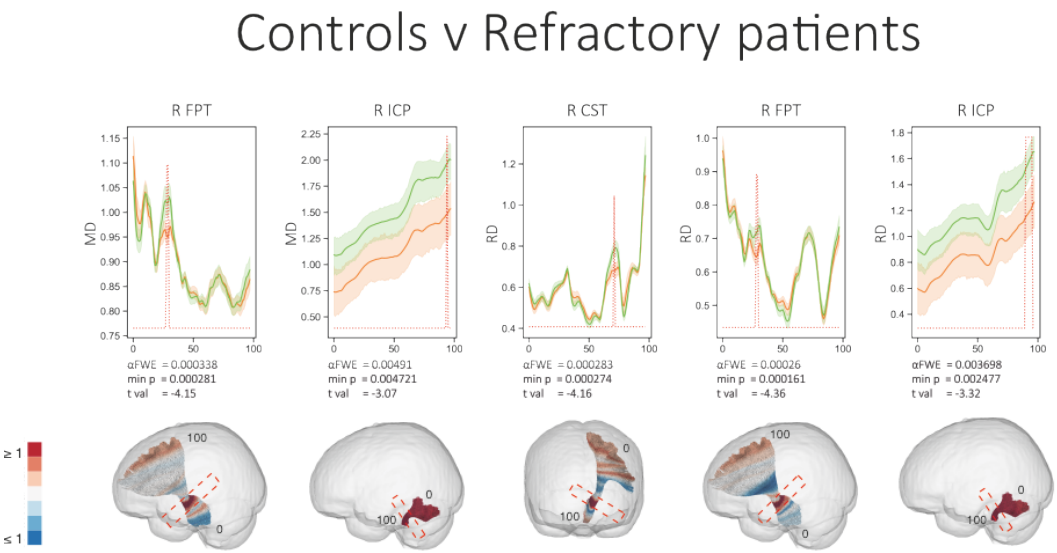

Figure 5.3 Statistically significant (red peaks) along-tract differenes in DTI diffusion metrics in refractory patients (green) relative to controls (orange). 3D plots show Cohen's d values projected onto the relevant tracts with significant regions highlighted by red boxes. Effect sizes greaater than and equal to 1 are shown in dark red, with those less than and equal to -1 shown in dark blue.

5.3.2.2 Controls vs non-refractory patients

Relative to controls, significant differences were found in non-refractory patients in three DKI metrics (KFA, MK, AK) across four tracts with large effect sizes (d = ± 0.8). Significant differences in DKI metrics between non-refractory patients and controls are shown in Figure 5.4. Increases in KFA were found in patients with non-refractory epilepsy in regions of the left CST and right optic radiation (OR) compared to controls. Reductions were found in patients in MK in a region of the left CST and in AK in regions of the left CST, right OR, left STR, and left thalamoparietal tract (T PAR) compared to controls.

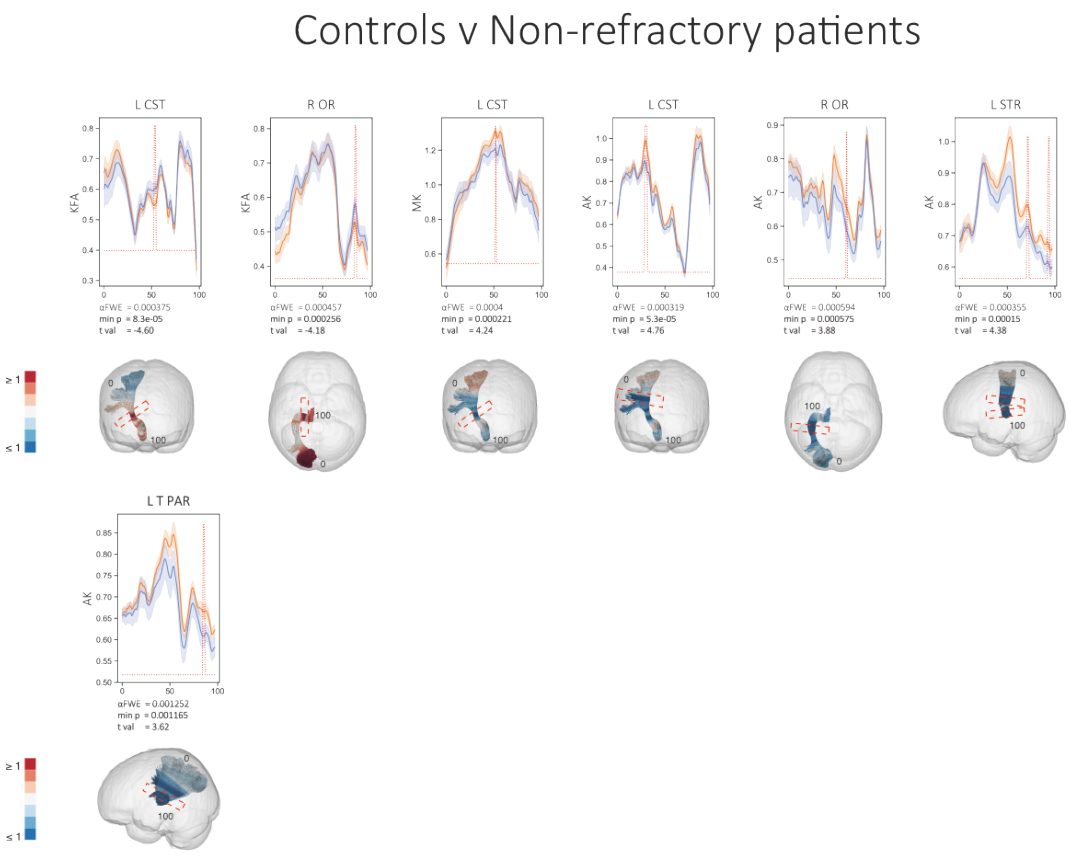

Figure 5.4 Statistically significant (red peaks) along-tract differenes in DKI diffusion metrics in non-refractory (blue) patients relative to controls (orange). 3D plots show Cohen's d values projected onto the relevant tracts with significant regions highlighted by red boxes. Effect sizes greaater than and equal to 1 are shown in dark red, with those less than and equal to -1 shown in dark blue.

Differences between non-refractory patients and controls were also found across all DTI metrics (FA, MD, AD, RD) in seven tracts with significant regions showing large effect sizes (d = ± 0.8). Significant differences in DTI metrics between non-refractory patients and controls are displayed in Figure 5.5. Significant reductions in FA were found in patients with non-refractory epilepsy in regions of the rostrum of the corpus callosum (CC1) and the right uncinate fasciculus (UF) compared to controls. Increases were found in patients in MD in a region of the left anterior thalamic radiation (ATR), in AD in regions of the left STR, left and right T PAR, and left UF, and in RD in the left ATR compared to controls.

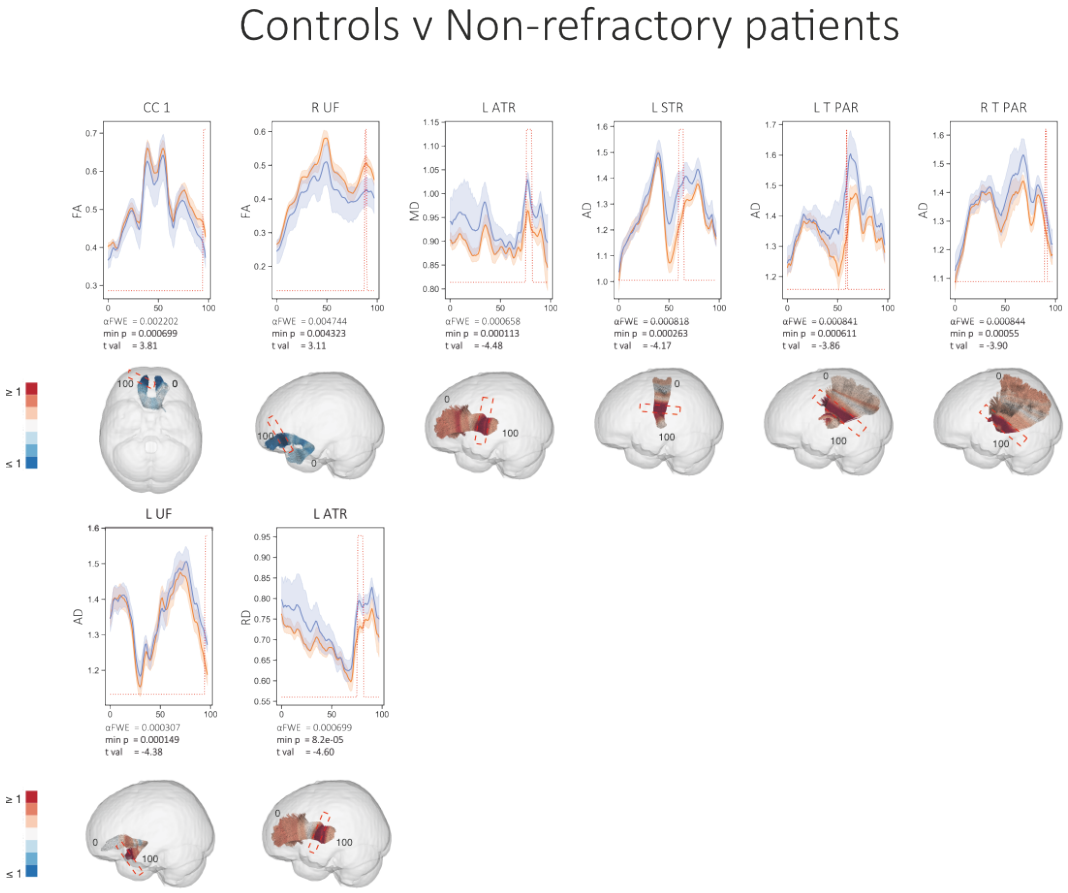

Figure 5.5 Statistically significant (red peaks) along-tract differences in DTI diffusion metrics in non-refractory patients (blue) relative to controls (orange). 3D plots show Cohen's d values projected onto the relevant tracts with significant regions highlighted by red boxes. Effect sizes greater than and equal to 1 are shown in dark red, with those less than and equal to -1 shown in dark blue.

5.3.2.3 Refractory vs non-refractory patients

In direct comparisons between patient groups, significant differences were found across all DKI metrics (KFA, MK, AK, RK) in three tracts, with significant regions showing large effect sizes (d = ± 0.8). Differences in DKI metrics between patient groups can be seen in Figure 5.6. Across all metrics, patients with refractory epilepsy showed higher values compared to those with non-refractory epilepsy. These differences were seen in KFA, MK and AK in regions of the right ICP and, in AK in regions of the left and right SCP, and in RK in a region of the middle cerebellar peduncle (MCP).

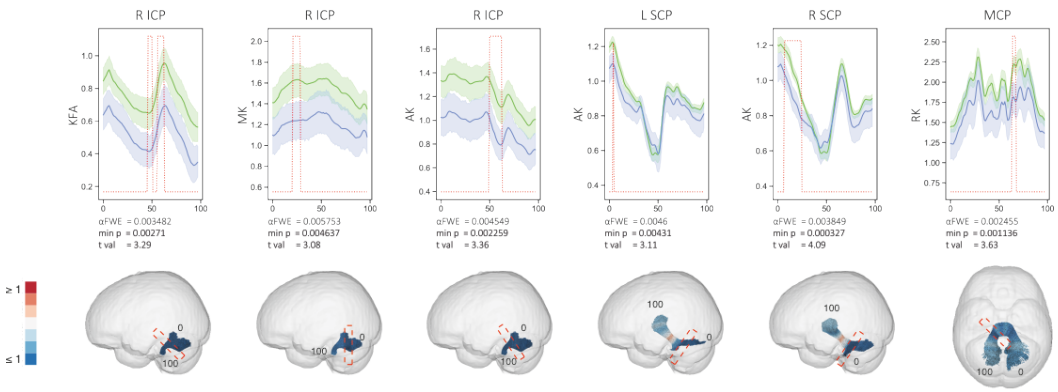

Figure 5.6 Statistically significant (red peaks) along-tract differenes in DKI diffusion metrics in refractory patients (green) relative to non-refractory patients (blue). 3D plots show Cohen's d values projected onto the relevant tracts with significant regions highlighted by red boxes. Effect sizes greaater than and equal to 1 are shown in dark red, with those less than and equal to -1 shown in dark blue.

More widespread differences were seen between refractory and non-refractory patients in DTI metrics, with differences in all four DTI metrics (FA, MD, AD, RD) across eight tracts, again showing large effect sizes (d = ± 0.8). Differences in DTI metrics between patient groups can be seen in Figure 5.7. Patients with refractory epilepsy showed higher FA in a region of the right SCP, MD in regions of the right CST, left FPT, right ICP, and left and right POPT, AD in a region of the right SCP, and RD in regions of the right CST, left FPT, right ICP, and left and right POPT compared to non-refractory patients. In regions of the right arcuate fascicle (AF) and right ATR, patients with refractory epilepsy had lower AD values compared to non-refractory patients.

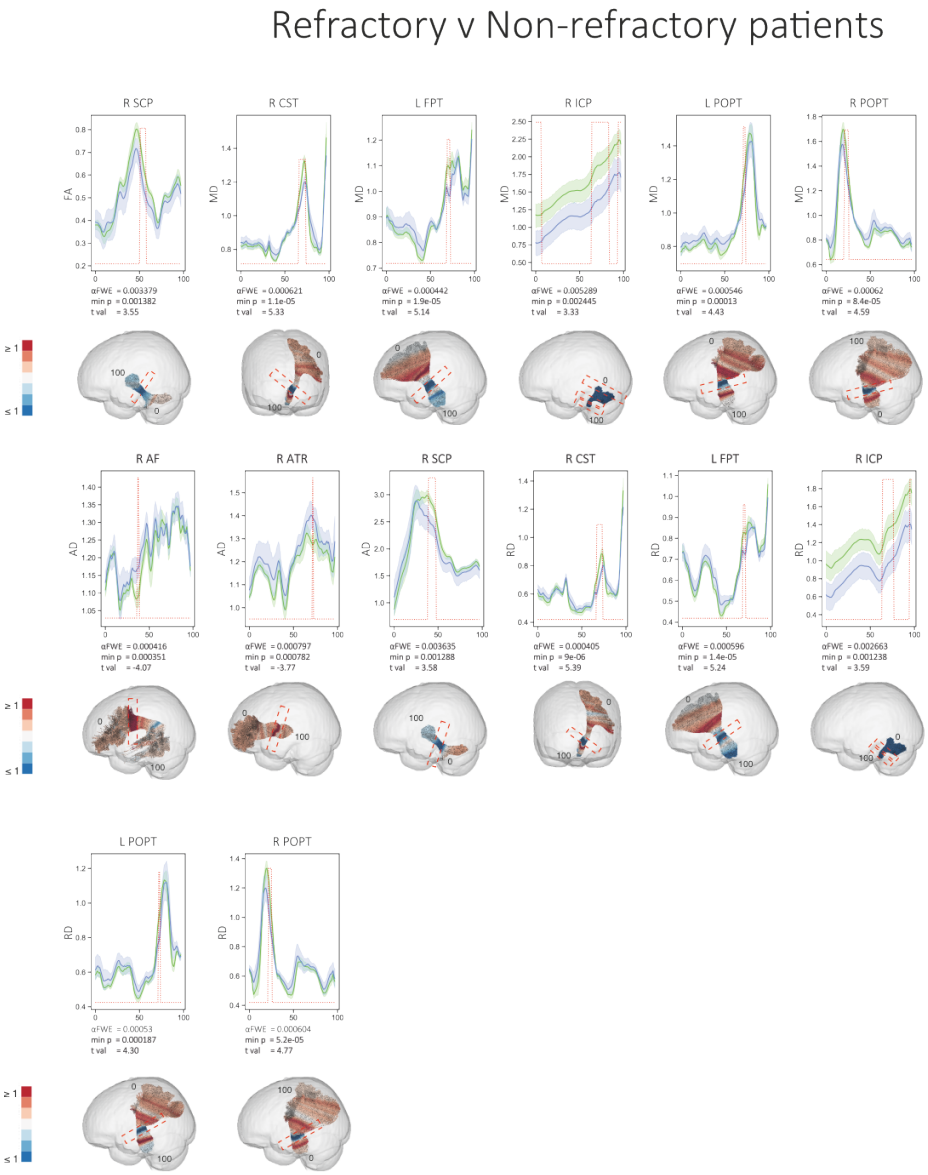

Figure 5.7 Statistically significant (red peaks) along-tract differences in DTI diffusion metrics in refractory patients (green) relative to non-refractory patients (blue). 3D plots show Cohen's d values projected onto the relevant tracts with significant regions highlighted by red boxes. Effect sizes greater than and equal to 1 are shown in dark red, with those less than and equal to -1 shown in dark blue.

5.4 Discussion

In the present study, we sought to characterise microstructural abnormalities in grey and white matter in patients with longstanding focal epilepsy using DTI and DKI. We report significant changes in WM in both patient groups relative to controls, and in GM in non-refractory patients relative to controls. Additionally, significant changes were found between patient groups using both DKI and DTI. In refractory patients, DKI changes were more widespread relative to controls, while in non-refractory

patients, it was DTI changes which showed a larger pattern. In direct patient comparisons, DTI alterations were more widespread than DKI changes.

5.4.1 Biological/clinical implications

Although DKI as a method is well suited to the study of epilepsy, there is a lack of literature in this area (Winston, 2015). Across patient groups, we report changes in several diffusion parameters in both WM (KFA, MK, AK, RK) and GM (MK, AK). In general, a decrease in DKI parameters is linked to a less restricted diffusion environment, suggestive of a loss of axons (Hui *et al*., 2008). In the present study, we report a general decrease in MK, AK, and RK in patient groups relative to controls. This is suggestive of a less restrictive diffusion environment in patients. Additionally, AK has been suggested to be linked to intra-axonal changes, rather than extra-axonal (Hui *et al*., 2008), while MK has been suggested as a marker of neuroinflammation (Zhuo *et al*., 2012). Decreases in these diffusion measures have previously been seen in clinical populations (Falangola *et al*., 2008; Hui *et al*., 2008; Gong *et al*., 2017; Zhou *et al*., 2019) and in patients with TLE (Gao *et al*., 2012; Bonilha and Keller, 2015). Our work supports this previous literature. Conversely to expectations, lower kurtosis values were found in patients with non-refractory epilepsy. We would expect patients with refractory epilepsy to demonstrate these findings due to an increase in a change in the diffusion environment – tentatively linked to cell loss or inflammation (Hui *et al*., 2008), however that is questionable when found in patients responding well to treatment and may be a product of small sample size, or of the method not entirely demonstrating clear biological processes (further discussed in Chapter 8).

Epilepsy is increasingly being considered a network disorder (Bernhardt, Bonilha and Gross, 2015; Kreilkamp *et al*., 2021), with white matter abnormalities thought to drive seizure propagation. In a large study of multiple epilepsy syndromes, white matter abnormalities were seen in patients with hippocampal sclerosis, extratemporal epilepsies, and those with temporal lobe epilepsy (Hatton *et al*., 2020). Similarly, using along-tract methodology, Glenn *et al*. (2016) were able to reveal alterations in patients with TLE in several key white matter tracts. Here, we report significant changes in diffusion parameters in several white matter tracts across patient groups, demonstrating the importance of white matter tracts in focal epilepsy and supporting

this suggestion of epilepsy as a network disorder. Changes in white matter architecture have also shown to be related to post-surgical outcome (Bonilha *et al*., 2013; Keller, Richardson, O'Muircheartaigh, *et al*., 2015), demonstrating the importance of white matter to treatment outcome. In the present study, we revealed diffusional white matter changes between patients with refractory and non-refractory epilepsy. This supports previous literature.

In the present study, we revealed changes in several regions of grey matter including thalamic nuclei, the parahippocampal gyrus, and the amygdala. The thalamus is well known to play a key role in epilepsy (Malekmohammadi, Elias and Pouratian, 2015), with deep brain stimulation of the thalamus shown to reduce seizure frequency (Fisher *et al*., 2010; Salanova *et al*., 2015; Li and Cook, 2018), and volumetric abnormalities often found (Dreifuss *et al*., 2001; Keller, Richardson, Schoene-Bake, *et al*., 2015). The amygdala has been suggested to generate seizure activity (Goddard, 1967; Kairiss, Racine and Smith, 1984; Racine *et al*., 1988), and amygdalaectomy alone has been shown to eliminate seizures (Rasmussen and Feindel, 1991; Jooma *et al*., 1995; Wieser, 2000). Similarly, the parahippocampal gyrus has been implicated in the propagation of seizures (Miettinen *et al*., 1998; Calcagnotto, Barbarosie and Avoli, 2000; Schwarcz, Eid and Du, 2000; Weissinger *et al*., 2000; Wozny *et al*., 2005), with the suggestion that a loss of cells in the parahippocampal gyrus leads to a disruption of information flow to the hippocampus (Gloveli, Schmitz and Heinemann, 1998). These regions appear to be largely implicated in the propagation of seizures and our findings support this. The use of DKI further allows us to build on this previous literature, which was largely conducted using animal models. Changes in DKI parameters allow us to infer that these changes may be due to an increase in diffusional space, and we can begin to attribute this to neuronal loss or neuroinflammation.

5.4.2 Conclusions

In this investigation of diffusional changes in patients with longstanding focal epilepsy, we revealed changes in both white and grey matter regions. We were further able to find differences between refractory and non-refractory patients. The use of DKI in this study has allowed us to demonstrate more changes than previously possible with simply DTI, and we suggest a utility including this method in future work.

6 Investigation into thalamic changes in longstanding focal epilepsy using advanced imaging methods

6.1 Introduction

Approximately 30% of people with focal epilepsy will not achieve seizure freedom through the use of anti-epileptic drugs (AEDs; Kwan & Brodie, 2006). The reasons for this remain largely unknown as the mechanisms behind seizure generation are poorly understood. Understanding these mechanisms offers the potential for better drug development and treatment options, leading to earlier treatment stratification and a better prognosis for patients. In this study, we have investigated the role of the thalamus in refractory focal epilepsy using diffusion kurtosis imaging (DKI), magnetic resonance spectroscopy (MRS), and serum marker (high mobility box group 1; HMGB1, and interleukin 1-beta; IL-1ß) levels.

The thalamus has been demonstrated to play a key role in epilepsy (see Chapter 1). Evidence has shown the role of the thalamus in the regulation of cortical activity (Malekmohammadi, Elias and Pouratian, 2015). Deep brain stimulation of the thalamus has been widely shown to reduce seizure frequency (Fisher *et al*., 2010; Salanova *et al*., 2015; Li and Cook, 2018) with studies indicating specific thalamic nuclei including the anterior and intralaminar (Hodaie *et al*., 2002) and the dorsomedial (Bertram *et al*., 1998, 2001) nuclei. These nuclei have been suggested to

be involved in increasing susceptibility to seizures and the propagation of seizure activity (Mirski and Ferrendelli, 1986, 1987; Mirski *et al*., 1997; Hodaie *et al*., 2002). Neuroimaging studies have further outlined the role of the thalamus in epilepsy with PET (Henry *et al*., 1990; Khan *et al*., 1997; Park *et al*., 2018), rs-fMRI (Pedersen *et al*., 2016), and structural imaging (Dreifuss *et al*., 2001; Keller, Richardson, O'Muircheartaigh, *et al*., 2015; Keller, Richardson, Schoene-Bake, *et al*., 2015) showing abnormalities of the thalamus in patients with focal epilepsy. Further, structural differences in the thalamus have demonstrated the ability to differentiate between patients who go on to become non-refractory and those who continue to experience persistent seizures following surgery (Keller, Richardson, O'Muircheartaigh, *et al*., 2015). Taken together, this evidence suggests that understanding the role of the thalamus may be vital to understanding differences in seizure control and propagation of seizures, however, more advanced methods are needed to fully understand this role.

In the present study, we have attempted to characterise changes in the thalamus in patients with refractory focal epilepsy by looking at not only thalamic volumes, but also diffusional kurtosis metrics of the thalamus. DKI is an extension of standard DTI (see Chapter 2 for detailed description) which allows investigation of grey matter (GM). DKI offers the ability to gain unique insight into the microstructural environment of GM, allowing for a more specific understanding of cellular changes. This is because DKI does not assume a Gaussian water diffusion, which DTI does (Jensen and Helpern, 2010). However, there are issues with the biological meaning of DKI metrics, and the parameters have been said to be purely diffusional (Fieremans, Jensen and Helpern, 2011), making biological interpretation difficult. This is demonstrated by the suggestion that an increase in kurtosis could be linked to glial activity, while a decrease is linked to increased extracellular space (Zhuo *et al*., 2012; Gong *et al*., 2013). Both these processes are related to inflammation, making it difficult to tell if an increase or decrease in kurtosis is caused by inflammation, or another factor such as cell loss. In this study, we have attempted to further understand the biological meaning of DKI parameters by relating these to both MRS metabolite levels and peripheral markers of cell loss and inflammation – serum HMGB1 and IL-1ß.

MRS allows for quantification of metabolites within the brain (Chapter 2). Metabolite values can provide information on processes such as neuronal integrity, metabolism, and membrane turnover (Benarroch, 2008; Mountford *et al*., 2010; Zhu and Barker, 2010). Metabolites commonly implicated in epilepsy include NAA, a marker of neuronal dysfunction, which is often decreased in patients with epilepsy (Connelly *et al*., 1994; Gadian *et al*., 1994; Kirov *et al*., 2018); Cr is a marker of inflammation which is reliably increased in patients with epilepsy (Connelly *et al*., 1994; Gadian *et al*., 1994) while Cho and mIns are also markers of inflammation which have both been found to increase and decrease in epilepsy; Glx is key in brain metabolism and has often been seen to increase in those with epilepsy (Doelken *et al*., 2008). MRS can offer a deeper insight into brain changes in epilepsy and may provide further information alongside structural and diffusion imaging.

HMGB1 (see Chapter 1 for detailed description) is released by glial cells and neurons due to epileptogenic insult (Paudel *et al*., 2018). Increases in neuronal HMGB1 have been shown in both mice and human studies to contribute to spontaneous epileptic discharges (Maroso *et al*., 2010; Fu *et al*., 2017; Zhao *et al*., 2017). Additionally, changes in neuronal HMGB1 translate to changes in serum HMGB1 levels (Ravizza *et al*., 2018), allowing for the potential of serum HMGB1 as a peripheral marker of neuroinflammation. HMGB1 interacts with Toll-like receptor 4 (TLR-4) and the receptor for advanced glycation endproducts (RAGE), both of which have been shown to be upregulated due to seizure activity (Maroso *et al*., 2010; Zurolo *et al*., 2011; Iori *et al*., 2013). Because of this interaction, a number of inflammatory cytokines are released from glial cells, macrophages, and astrocytes, including IL-1ß. IL-1ß has been implicated in epilepsy previously, with activation seen in the resected brain tissue of patients with refractory TLE (Ravizza *et al*., 2008) and positive correlations between IL-1ß and frequency of seizures was found in patients with epilepsy with malformations of cortical development (Ravizza *et al*., 2006). Together, serum levels of HMGB1 and IL-1ß may offer the ability to non-invasively measure peripheral inflammation in patients with refractory epilepsy which may help to elucidate the biological processes underlying changes in diffusional imaging parameters.

In the present study, we have attempted to investigate thalamic changes in patients with refractory focal epilepsy using thalamic volumes, DKI values, and MRS metabolite concentrations. We have also investigated serum levels of HMGB1 and IL-1ß peripherally. We hypothesised that refractory patients would show volumetric, DKI, and metabolite changes in the thalamus, along with an increase in peripheral inflammatory markers compared to controls and non-refractory patients. We expect that inclusion of these measures to increase our understanding of the biological meaning behind DKI parameters.

6.2 Methods

3.1.2 Participants

3.2.2 MR acquisition

3.4.1 Serum acquisition

3.3 Preprocessing of MR data

3.3.1.1 DKI thalamic analysis

3.3.4 MRS spectra analysis

3.4.2 HMGB1 serum analysis

3.4.2 IL-1β serum analysis

3.5.2 Statistics

6.3 Results

6.3.1 Group comparisons

6.3.1.1 Thalamic volumes (Figure 6.1)

No significant differences were seen between left and right thalamic volumes for any patient groups.

6.3.1.2 DKI values (Figure 6.2)

Analysis of DKI values revealed a significant reduction in right AK in non-refractory patients compared to refractory patients (p=.008). No significant differences were seen between any other patient groups or for any other metrics.

6.3.1.3 MRS values (Figure 6.3)

Analysis of MRS metabolite values revealed a significant reduction in left Glx in patients compared to controls (p=.039). No other significant differences were seen between any other patient groups or metabolites.

6.3.1.4 Serum marker values (Figure 6.4)

No significant differences were seen in serum HMGB1 for any patient groups. A significant reduction in IL-1ß was seen in patients compared to controls (p<.001), and between controls and refractory (p<.001) and non-refractory patients (p<.001). No difference was seen between refractory and non-refractory patients in direct patient comparisons.

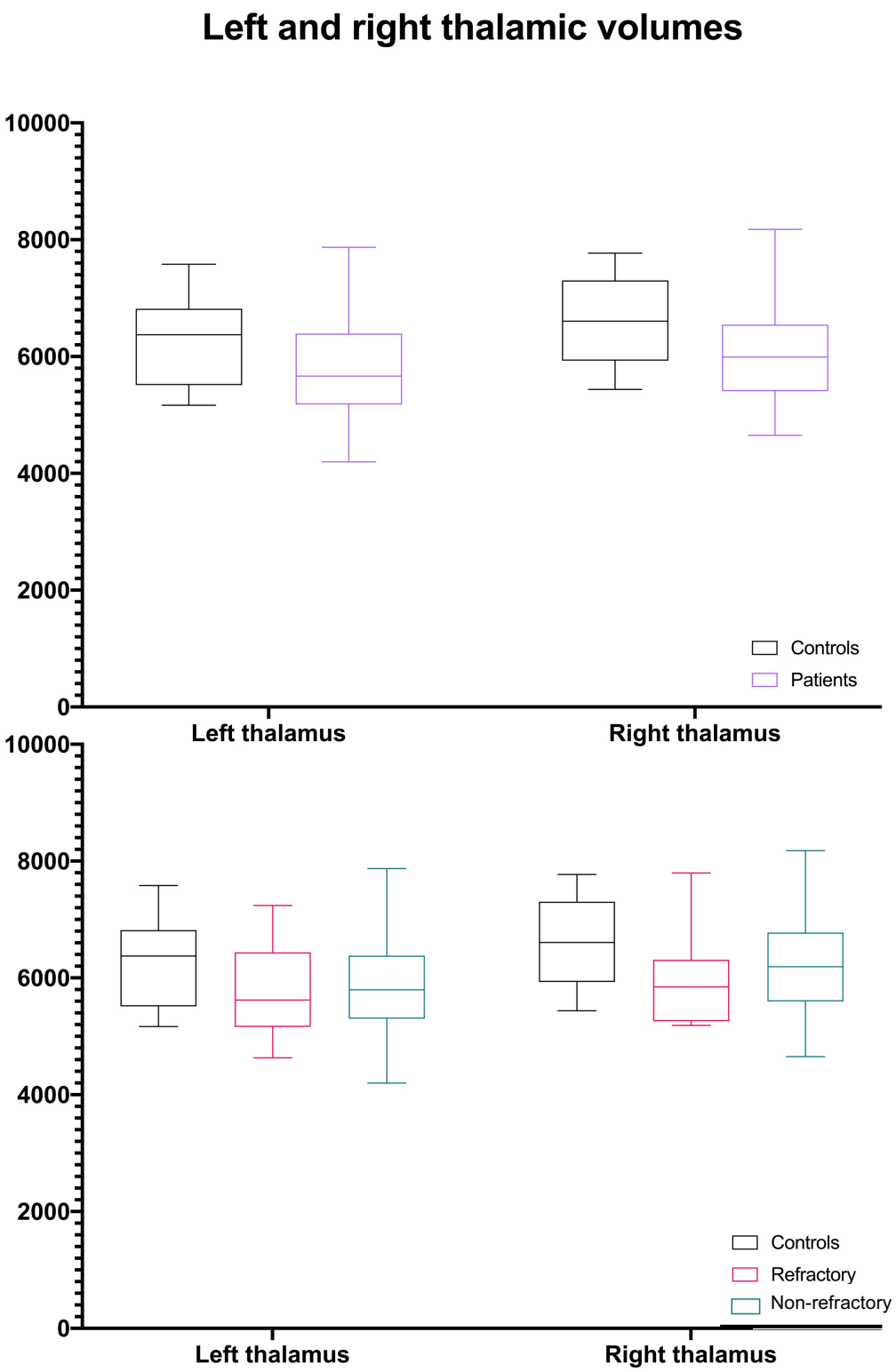

Figure 6.1 Group comparisons of right and left thalamic volumes for controls vs patients (top), and controls vs refractory vs non-refractory patients (bottom)

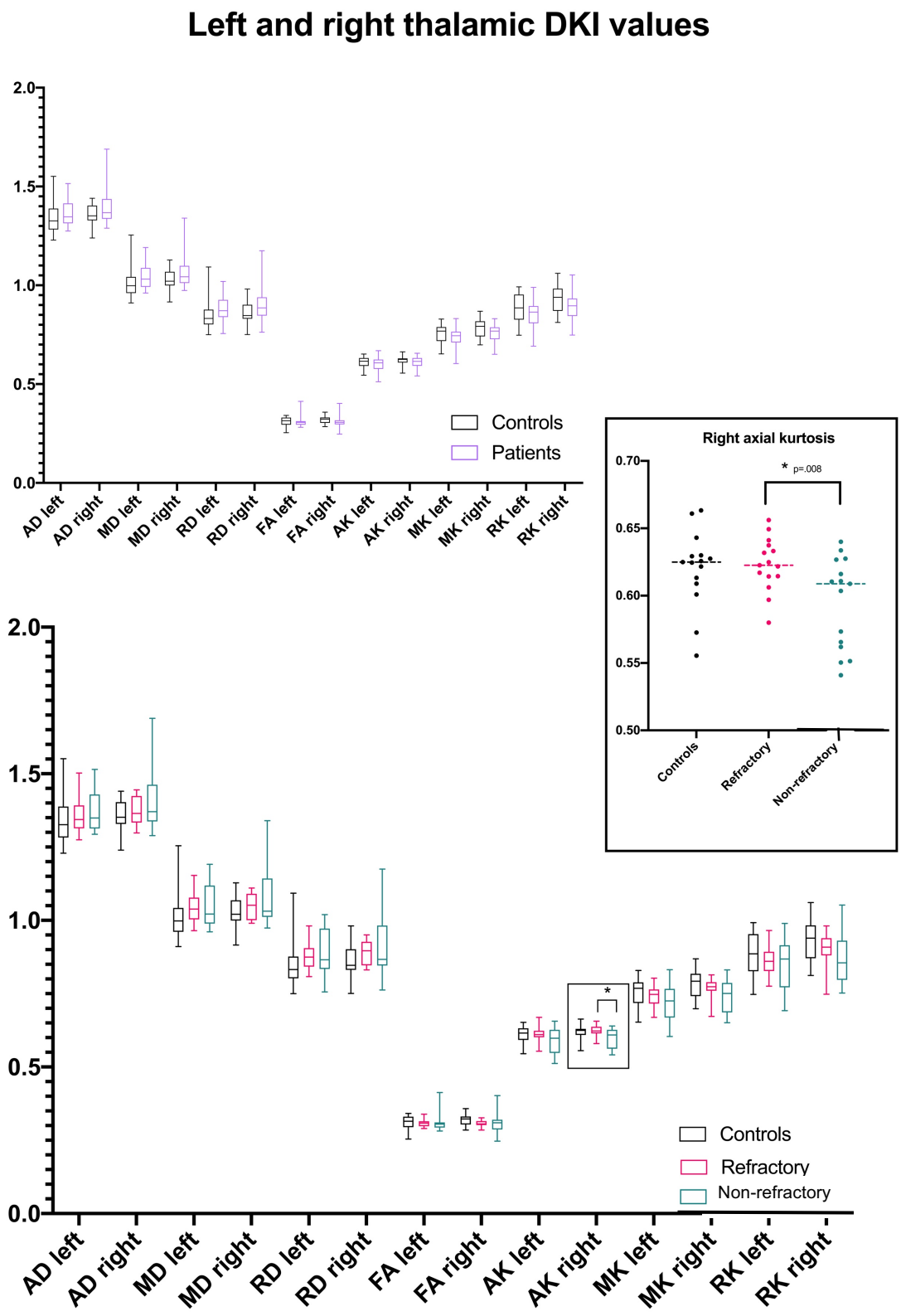

Figure 6.2 Group comparisons of left and right DTI and DKI values for controls vs patients (top) and controls vs refractory vs non-refractory patients (bottom). Highlighted is individual values for right axial kurtosis, showing significance between refractory and non-refractory patients

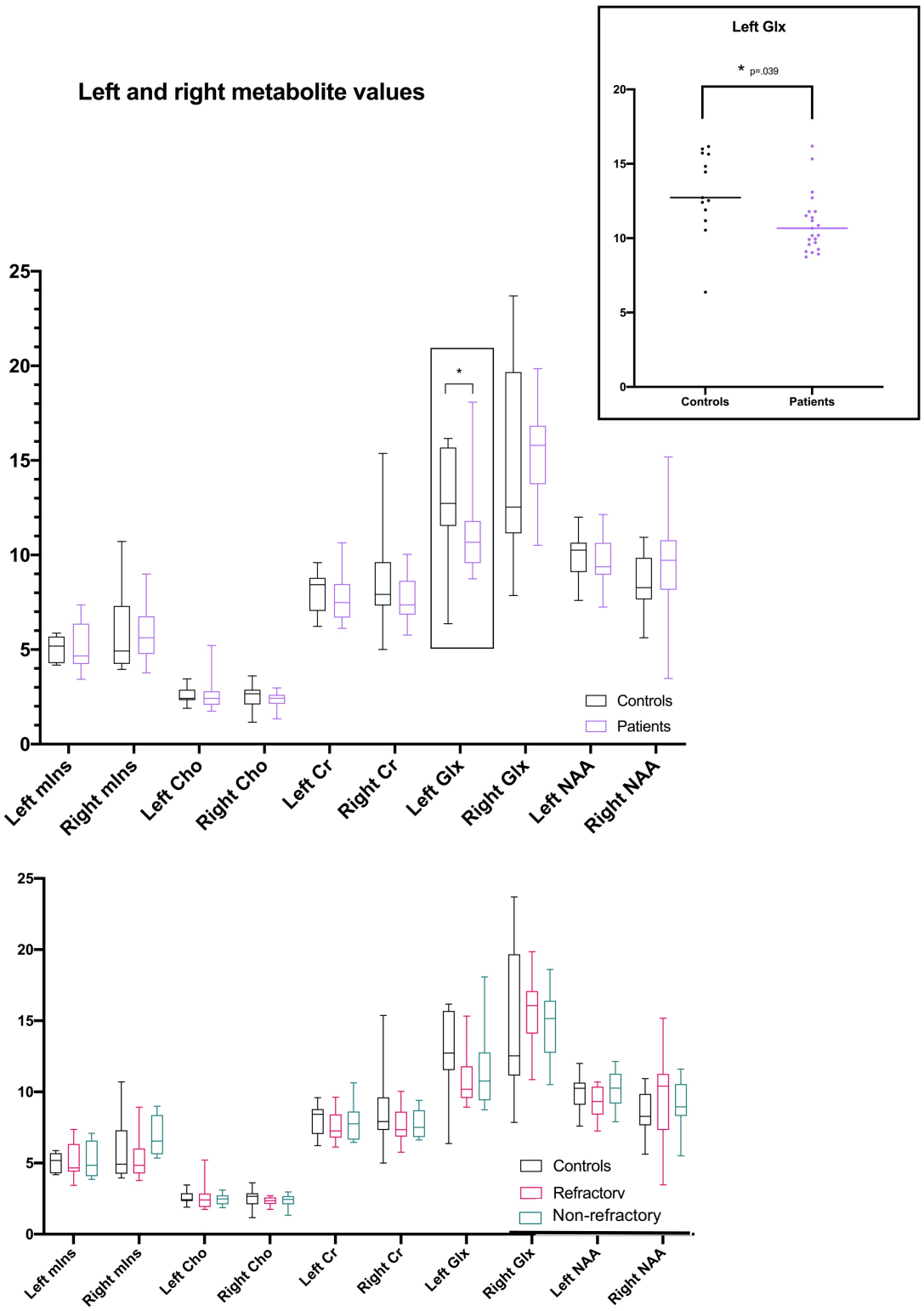

Figure 6.3 Group comparisons between MRS metabolite values for controls vs patients (top) and controls vs refractory vs non-refractory patients (bottom). Highlighted is left Glx individual values showing significance between patients and controls.

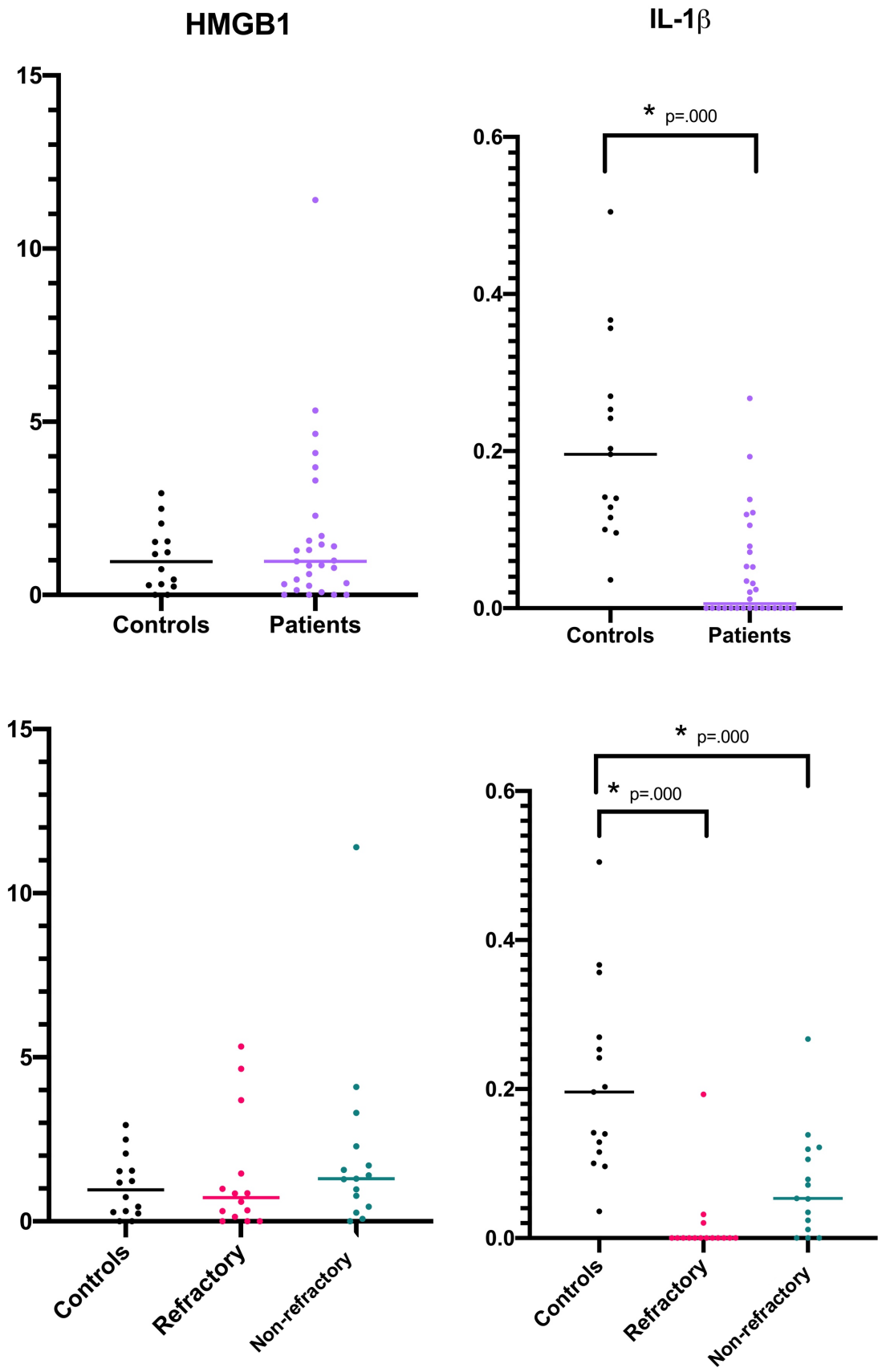

Figure 6.4 Left – HMGB1 concentration levels for controls vs patients (above left) and controls vs refractory vs non-refractory (bottom left). Right – Il-1B concentration levels for controls vs patients (above right) showing significant difference between controls and patients and for controls vs refractory vs non-refractory patients (bottom right) showing significance between controls and refractory and controls and non-refractory patients.

6.4 Discussion

In the present study, we analysed thalamic changes in patients with both refractory and non-refractory focal epilepsy using volumetric analysis, DKI measures, and MRS metabolite markers. We additionally investigated peripheral markers of inflammation, serum levels of HMGB1 and IL-1ß in patient groups.

Group analysis revealed no significant differences between thalamic volumes in patient groups though there was a trend toward a reduction in volumes in patient groups. DKI analysis showed a decrease in axial kurtosis in the right thalamus only in non-refractory patients relative to refractory patients. A reduction was seen in left thalamic Glx of patients compared to controls, along with a reduction of IL-1ß in patients compared to controls, and in refractory and non-refractory patients compared to controls. There was no significant difference in groups in serum HMGB1 levels, though there was a mild increase in non-refractory patients.

6.4.1 Thalamic volumes

Mean thalamic volumes were moderately reduced in patient groups, though not significantly. A reduction in thalamic volume has typically been seen in patients with focal epilepsy (Dreifuss *et al*., 2001; Keller, Richardson, Schoene-Bake, *et al*., 2015), and has been suggested as a biomarker for post-surgical outcome as a reduced thalamic volume has been seen in patients who continued to experience persistent seizures following resective surgery (Keller, Richardson, O'Muircheartaigh, *et al*., 2015; Keller, Richardson, Schoene-Bake, *et al*., 2015). Our data supports this previous work, and when investigating between patient groups, we do see a slight reduction in volume particularly in the refractory patient group, though again this difference does not reach statistical significance. On the other hand, previous studies have also attempted to find differences in thalamic volumes and failed to find significance, such as Park et al. (2018) who investigated thalamic volumes in patients with TLE with hippocampal sclerosis, extra-TLE, and juvenile myoclonic epilepsy. Our work suggests there is a trend toward a reduction in thalamic volume, particularly in patients with refractory epilepsy, however, the small, heterogenous nature of our sample must be considered.

6.4.2 DKI values

This is the first study to investigate the thalamus in focal epilepsy specifically using DKI, and as such there is a lack of literature in this area. In this study, we have seen a significant reduction in thalamic AK in patients with non-refractory focal epilepsy, with a trend toward reduced kurtosis values for all patient groups. A reduction in GM kurtosis values has been seen in a number of patient groups including Alzheimer's disease and mild cognitive impairment (Falangola *et al*., 2013; Gong *et al*., 2013). In these studies, a significant reduction in both MK and RK was found in the patient groups and was attributed to neuron loss or an increase of extra-cellular space. Reduced global GM has also been found in patients with TLE (Gao *et al*., 2012; Bonilha *et al*., 2015), though not specific to the thalamus. Here we have investigated the thalamus due to its previously discussed role in almost all epilepsies. A reduction in kurtosis values has been linked to a less restricted diffusion environment (Hui *et al*., 2008), and particularly related to an increase in extracellular space (Gong *et al*., 2013). RK is thought to be more sensitive to extracellular space as it measures diffusion perpendicular to the direction of axons (Steven, Zhuo and Melhem, 2014), while AK is thought to me more related to intracellular space due to its measurement of diffusion along the length of the axons (Hui *et al*., 2008). A decrease in AK has thought to be related to decreased tissue homogeneity, or a reduction in the size or number of axons and dendrites (Hui *et al*., 2008). However, it is important to note that these metrics are not able to specifically look at these diffusion compartments, and that a voxel includes the signal from a number of cells. Therefore, we cannot say with absolute specificity which diffusion compartment these metrics are measuring.

This work also supports the notion that DKI is more sensitive to GM properties than standard DTI (Gao *et al*., 2012; Bonilha *et al*., 2015), as no differences were found using DTI measures, though it is important to note that we only found significance in one DKI metric between the patient groups.

6.4.3 Metabolite values

The only metabolite showing significance between groups was a decrease in Glx in the left thalamus of patients. Glx is a sum metabolite consisting of glutamine and glutamate, the main excitatory neurotransmitter in the brain (Godlewska *et al*., 2019).

Epilepsy is thought to be caused, at least in part, by an inhibitory-excitatory imbalance in neurotransmitters (Doelken *et al*., 2010), and increased levels of Glu have been demonstrated in the thalamus in patients with idiopathic generalised epilepsy (Helms *et al*., 2006; Doelken *et al*., 2010) and in focal epilepsy (Woermann *et al*., 1999; Savic *et al*., 2000). It is important to note that many studies often use metabolite ratios, as the individual metabolites can be difficult to resolve. When reporting an increase in Glx, many studies are actually reporting an increase in the Glx/NAA ratio, which may have been caused by an increase a decrease in NAA and an increase in Glx, or by decreases in both NAA and Glx. Savic et al. (2000), also measured metabolic levels using ratios, and so it is difficult to elucidate whether there was an increase or reduction in the absolute concentration of Glx in patients with focal epilepsy. Alternatively, a detailed study into glutamate metabolism revealed a reduction in Glu and Glx in the seizure focus in patients with refractory mTLE (Bartnik-Olson *et al*., 2017). The authors also measured metabolic turnover of Glu and found no differences between patients and controls, and therefore suggested that the reduction of Glu and Glx in their study was reflective of neuronal loss or simplification rather than a reduced oxidative metabolism. Furthermore, there is a known effect of medication on levels of Glx. Lamotrigine has been shown to reduce Glx concentrations (Choi and Morrell, 2003) and valproate has been seen to causes changes in some studies (Petroff, Mattson and Rothman, 2000; Ziyeh *et al*., 2002).

With respect to other metabolites, we expected to see a reduction in NAA and increase in inflammatory metabolites in patients, as NAA is a marker of neuronal dysfunction, and its reduction in patient groups is a common finding. We also expected to see an increase in the inflammatory metabolites, mIns, Cho, and Cr, due to their evidence as inflammatory markers, which was not found. A major limitation of the MRS aspect of the present study is sample size – particularly due to the loss of MRS data due to quality issues. However, previous literature surrounding mIns, Cho and Cr is inconclusive, and it may be that the role of these metabolites in focal epilepsy are not well characterised. Furthermore, anti-epileptic medication has been known to affect peripheral inflammatory markers (Kim *et al*., 2010; Zayed *et al*., 2011; Shi *et al*., 2018), and so may also display an effect on the concentrations of these metabolites. Additionally, while MRS has been argued as an informative method for studying

epilepsy, its specificity in relation to this data is questionable (Pan and Kuzniecky, 2015). As previously mentioned, this cohort is highly heterogenous, with varying epileptic loci across patients. Due to the nature of single-voxel MRS, we were able to scan the thalamus only in all patients. Multi-voxel MRS may be more informative in this cohort, however while we remain unsure of the epileptic locus in many of these patients, even this method may not be particularly reliable.

6.4.4 Serum analysis

A trend toward an increase in serum HMGB1 in non-refractory patients was seen in the present data along with a slight decrease in serum HMGB1 in refractory patients. Serum HMGB1 is thought to be a marker of either neuroinflammation or neuronal loss, both of which would lead to an increase in serum HMGB1. A further unexpected finding was a reduction in serum IL-1ß in patients compared to controls, which was also seen once patient groups were separated. We expected to see an increase in serum IL-1ß in patient groups as per the previous literature (Ravizza *et al*., 2006, 2008). However, similarly to Glx, anti-epileptic medication has been shown to have a reductive effect on levels of serum IL-1ß. In particular, levetiracetam (Kim *et al*., 2010) and lamotrigine (Shi *et al*., 2018) have both been shown to reduce levels of serum IL-1ß, and an effect of valproate has also been suggested (Zayed *et al*., 2011). Again, we have a number of patients who were taking these medications at time of scanning, and therefore this is possibly the explanation for the reduction of serum IL-1ß in both patient groups relative to controls and may explain the reduction of serum HMGB1 in patients, and potentially the levels of inflammatory metabolites – assuming that these markers are all linked. However, it is important to note that it is likely patients were taking AEDs in previously mentioned studies and so it is questionable whether AED effects can explain this result. More likely, it is due to the heterogeneity of the cohort and small sample size driving these counterintuitive findings in the present study.

6.4.5 Conclusions

Due to limitations with both data and analysis in this study, it is difficult to draw clear conclusions. We rather suggest that these methods may prove beneficial in the understanding of treatment outcome given a larger sample size.

7 Fiber Ball White Matter Modelling in longstanding focal epilepsy

7.1 Introduction

Despite being classically considered to be a grey matter disorder, increasing evidence demonstrates cerebral white matter pathology in focal epilepsy. Epilepsy is a systems disorder of brain networks and is characterised by various neuropathological processes in the cerebral white matter, both in lesional and non-lesional cases (Concha *et al*., 2010; Reeves *et al*., 2016; Deleo *et al*., 2018). Identifying and characterising these changes using non-invasive imaging techniques is important as this will provide deeper insights into the mechanisms of pathology in individual patients and potentially inform clinical and surgical decision making. For example, reconstruction of white matter structural networks and connectivity using diffusion MRI (dMRI) has been demonstrated to be an effective imaging biomarker of postoperative outcome in focal epilepsy (Bonilha *et al*., 2013; Bonilha and Keller, 2015; Keller, Richardson, O'Muircheartaigh, *et al*., 2015; Keller *et al*., 2017). Diffusion tensor imaging (DTI) and extensions of which, such as diffusion kurtosis imaging (DKI), have been widely used to study white matter alterations in patients with focal epilepsy. Typical findings show a pattern of reduced fractional anisotropy (FA) and increased mean diffusivity (MD) in patients with focal epilepsy (Concha, Beaulieu and Gross, 2005; Gross, Concha and Beaulieu, 2006; McDonald *et al*., 2008), and a more widespread pattern of altered kurtosis metrics, suggesting an increased sensitivity of DKI in detecting WM abnormalities in epilepsy (Lee *et al*., 2014; Bonilha *et al*., 2015; Glenn *et al*., 2016). However, while both DTI and DKI are reasonably sensitive to changes in white matter microstructure, these parameters only describe the tissue environment in terms of diffusion physics, rather than in biological parameters. They therefore lack

microstructural specificity, making biological interpretation difficult (Fieremans, Jensen and Helpern, 2011). To overcome this limitation, several diffusion methods have been proposed that more directly relate parameters with clear biological meanings to the diffusion MRI signal (Jelescu and Budde, 2017; Novikov, Kiselev and Jespersen, 2018). These must necessarily introduce assumptions and approximations that explicitly connect water diffusion to microstructure. The simplest of such methods are based on the assumption that there are two non-exchanging water compartments within brain white matter: a fast (which models the less hindered extra-axonal water) and a slow (which models the more restricted intra-axonal water) diffusion compartment (Assaf *et al*., 2004; Fieremans, Jensen and Helpern, 2011; Kleban *et al*., 2020).

The recently developed Fiber Ball Imaging (FBI) is one such two-compartment dMRI method (Jensen, Russell Glenn and Helpern, 2016; Moss *et al*., 2019). FBI offers the ability to estimate the fibre orientation distribution function (fODF) of white matter fibre bundles along with related axon-specific microstructural parameters. This is achieved by using strong diffusion weightings (b-value >> 2000 s/mm2) to suppress the signal from the more mobile extra-axonal water pool. Thus, by employing high b-values FBI only needs to model the intra-axonal compartment, a major advantage of FBI over other two-compartment models. The main assumption of FBI is that water diffusion inside axons is accurately described by regarding axons as thin, straight, impermeable tubes. Compelling experimental evidence indicates that this is indeed a good approximation at least for myelinated axons (McKinnon *et al*., 2017; Moss *et al*., 2019; Veraart, Fieremans and Novikov, 2019). Besides the fODF, FBI also allows estimation of the fractional anisotropy of the intra-axonal space (FAA) and ζ (a property related to the axonal water fraction; AWF). Fiber Ball White Matter Modelling (FBWM; (McKinnon, Helpern and Jensen, 2018)) builds upon the principles of FBI, but uses both high and low diffusion weightings to model the extra-axonal space as well as the intra-axonal space. FBWM therefore allows the estimation of additional microstructural parameters including the intrinsic intra-axonal diffusivity (Da), the mean extra-axonal diffusivity (MDe), the radial ($D_{e,\perp}$) and axial ($D_{e,\parallel}$) extra-axonal diffusivity, the fractional anisotropy of the extra-axonal space (FAE), and the AWF (Table 7.1). FBWM requires more data and more assumptions than FBI so

that there is a natural division between the two. Specifically, FBWM is built by combining FBI and DKI data. Distinguishing FBI, DKI, and FBWM parameters emphasizes that they each have different biophysical underpinnings. FBI and FBWM have not previously been applied in patient cohorts.

Parameter	Acronym	Meaning	Biological interpretation
Axonal water fraction (FBWM)	AWF	Amount of intra-axonal water divided by the total amount of MRI-visible water within a voxel. Decreases if intra-axonal water decreases, if extra-axonal water increases (edema), or both	Potential loss of axons, edema
Intra-axonal diffusivity (FBWM)	D_a	Diffusivity of water molecules along the length of the axons	Changes in the intra-axonal compartment (e.g. axonal beading – the formation of a series of swellings along the axon (Datar *et al.*, 2019))
Mean extra-axonal diffusivity (FBWM)	MD_e	Mean diffusivity of water within the extra-axonal compartment. This compartment includes glial cells and extra-cellular space	Analogous to MD but only for extra-axonal water
Radial extra-axonal diffusivity (FBWM)	$D_{e,\perp}$	Radial diffusivity of the extra-axonal compartment. Perpendicular to the direction of highest extra-axonal diffusivity	Analogous to RD but for extra-axonal compartment
Axial extra-axonal diffusivity (FBWM)	$D_{e,\parallel}$	Axial diffusivity of the extra-axonal compartment in the direction of highest extra-axonal diffusivity	Analogous to AD but for extra-axonal compartment
Intra-axonal fractional anisotropy (Pure FBI)	FAA	The fractional anisotropy of just the water within of the intra-axonal compartment. Reflects the geometrical arrangement – if all axons in the same direction, this value is high	Analogous to regular FA, but typically has higher values as intra-axonal water is more organized than extra-axonal water.
Extra-axonal fractional anisotropy (FBWM)	FAE	Fractional anisotropy of just the water within extra-axonal compartment	Analogous to regular FA, but typically has lower values as extra-axonal water is less organized than intra-axonal water. High values could represent tight packing of axons

			Parameter could be affected by myelination thickness
Zeta (Pure FBI)	ζ	Equal to the AWF divided by the square root of the intra-axonal diffusivity (D_a) Scaled version of the AWF	Since D_a is often fairly constant across voxels, ζ is usually strongly correlated with AWF, but it is easier to measure

Table 10 Diffusion parameters determined by FBI and FBWM, their biophysical meanings and potential biological interpretations.

Diffusion tractography provides the ability to reconstruct and assess diffusion characteristics averaged over whole white matter fibre bundles and along the longitudinal axis of tracts (along-tract). Along-tract analysis permits investigation of regionally specific alterations that may be more sensitive to regional pathology than averaging diffusion characteristics over entire tracts, particularly as tissue characteristics vary considerably along white matter tracts (Figure 2.5). This is particularly important for the in-vivo assessment of neuropathology in neurological disorders as some pathological alterations occur in circumscribed regions of tracts, which may be overlooked when averaging diffusion metrics over entire tracts (Keller *et al*., 2017). Along-tract approaches have demonstrated increased sensitivity for the identification of diffusion abnormalities in patients with temporal lobe epilepsy, (Concha *et al*., 2012; Kreilkamp *et al*., 2017, 2019), high levels of sensitivity and specificity for the prediction of postoperative outcome (Keller *et al*., 2017), and greater yield of diffusion changes using DKI over conventional DTI (Glenn *et al*., 2016). The use of FBI and FBWM combined with along-tract tractography offers the ability to investigate regional white matter tissue alterations with diffusion parameters that are biologically specific, which has not previously been possible using standard DTI approaches.

The modelling of several diffusion parameters with interpretable biological meaning may offer the development of new, non-invasive biomarkers of pharmacoresistance in epilepsy. It is unclear why 30% of patients with focal epilepsy do not attain seizure control despite anti-epileptic drug (AED) treatment (Kwan and Brodie, 2000). The identification of a non-invasive imaging biomarker of treatment outcome would allow earlier stratification to more personalised treatment methods. However, there have been limited insights into the mechanisms and markers underlying pharmacoresistance using advanced MRI methods. Markers of hippocampal neuronal-glial changes have

been associated with pharmacoresistance in patients with temporal lobe epilepsy using MR spectroscopy (Campos *et al*., 2010; Pimentel-Silva *et al*., 2020). Other studies have reported increased white matter and grey matter volumetric changes in patients with refractory relative to non-refractory focal epilepsy using morphometric techniques applied to T1-weighted images (Bilevicius *et al*., 2010; Kim *et al*., 2017), with further differences demonstrated in functional connectivity between refractory and non-refractory patients (Pressl *et al*., 2019). However, characterisation of diffusion properties between patient groups using advanced methods that offer biological interpretation has not, to our knowledge, been performed. DTI and other traditional diffusion imaging methods provide indirect information about the underlying cellular microstructure. Diffusion metrics such as FA and MD represent the diffusion dynamics of all underlying compartments mixed together. Biophysical models, such as FBWM, attempt to separate the diffusion dynamics into different compartments (i.e., intra-axonal and extra-axonal) to get a more specific understanding of changes happening in the underlying microstructure. This strategy is particularly useful when studying disease processes that affect microstructural compartments differently and could provide novel insights into pharmacoresistance in epilepsy.

In the present study we have investigated intra-axonal and extra-axonal white matter diffusion alterations in patients with focal epilepsy by combining FBI and FBWM with an along-tract tractography approach. By specifically recruiting patients with either refractory or non-refractory focal epilepsy, we sought to determine whether changes in the microscopic white matter environment may be a marker of pharmacoresistance. We expected to find differences between patient groups in FBI and FBWM metrics which have a more easily understandable biological basis compared to standard DTI.

7.2 Methods

3.1.2 Participants

3.2.2 MR Acquisition

3.3 MR preprocessing

3.3.1.2 dMRI preprocessing for diffusion map generation

3.3.1.3 dMRI preprocessing for tractography

3.3.3 White matter fibre tract segmentation

3.5.3 Statistical analysis

7.3 Results

There was no significant difference between refractory and non-refractory groups in the number of patients with (refractory = 9, 60%; non-refractory = 10, 67%) and without (refractory = 6, 40%; non-refractory = 5, 33%) radiologically diagnosed lesions that were considered to be not incidental (Appendix Table 10.3; $\chi 2 = 0.14$, $p = 0.70$). There was no significant difference in age ($t = 0.62$, $p = 0.54$), age of onset of epilepsy ($t = 0.02$, $p = 0.99$) or duration of epilepsy ($t = 0.71$, $p = 0.54$) between refractory and non-refractory patient groups.

Parameter	Tract	Controls	Refractory	αFWE	Min p-value	t-value	Cohen's d
AWF	L ST PREM	0.56 (0.04)	0.50 (0.07)	0.001125	0.000537	-3.91	1.39
FAE	R ICP	0.18 (0.10)	0.26 (0.10)	0.002152	0.001075	3.65	-1.30
MD_e	R ICP	0.97 (0.20)	1.39 (0.45)	0.002295	7.40E-05	4.64	-1.65
	L SCP	1.17 (0.13)	1.45 (0.23)	0.000558	0.000292	4.14	-1.47
$D_{e,\parallel}$	R ICP	1.30 (0.26)	1.82 (0.61)	0.002143	0.00017	4.34	-1.54
	L SCP	1.76 (0.26)	2.22 (0.39)	0.000665	0.000386	4.03	-1.43
	L ST PREM	1.36 (0.10)	1.56 (0.20)	0.001006	0.000451	3.97	-1.41
$D_{e,\perp}$	R AF	0.74 (0.05)	0.83 (0.08)	0.000969	0.000503	3.93	-1.40
	L ATR	0.77 (0.03)	0.82 (0.05)	0.001134	0.000104	4.52	-1.61
	L FPT	0.71 (0.05)	0.79 (0.07)	0.000745	3.70E-05	4.89	-1.74
	L ICP	0.71 (0.08)	0.87 (0.19)	0.002178	0.001242	3.59	-1.28
	R ICP	0.81 (0.18)	1.17 (0.39)	0.00254	5.00E-05	4.79	-1.70
	L T PREM	0.74 (0.02)	0.79 (0.05)	0.000724	0.000315	4.11	-1.46
FAA	R ICP	0.28 (0.14)	0.48 (0.07)	0.002887	2.00E-06	6.03	-2.14
ζ	R CG	0.32 (0.02)	0.29 (0.02)	0.000618	0.000516	-3.92	1.39
	R ICP	0.15 (0.08)	0.21 (0.05)	0.002866	0.000377	4.04	-1.44
	R ILF	0.24 (0.03)	0.19 (0.03)	0.000944	0.000479	-3.95	1.40
	R SLF III	0.39 (0.02)	0.36 (0.02)	0.000781	0.000219	-4.24	1.51
	R UF	0.23 (0.03)	0.18 (0.03)	0.001022	0.000909	-3.71	1.32
		Controls	Non-refractory				
D_a	L STR	2.10 (0.27)	2.50 (0.31)	6.00E-04	0.000565	-3.89	1.38
$D_{e,\parallel}$	R T PAR	1.18 (0.05)	1.30 (0.10)	0.000451	0.000163	-4.35	1.55
	R T OCC	1.21 (0.06)	1.37 (0.13)	0.000484	0.000171	-4.33	1.54
$D_{e,\perp}$	L ATR	0.76 (0.03)	0.85 (0.06)	0.000758	3.00E-06	-5.81	2.06
	L T PREM	0.69 (0.03)	0.75 (0.04)	0.000754	0.000199	-4.28	1.52

FA	CC1	0.37 (0.04)	0.31 (0.05)	0.002028	0.000699	3.81	-1.35
FAA	R STR	0.61 (0.02)	0.65 (0.03)	0.000539	0.000229	-4.23	1.50
MD	L ATR	0.91 (0.05)	0.98 (0.04)	0.000683	0.000113	-4.48	1.59
		Refractory	Non-refractory				
MD_e	R CST	1.11 (0.07)	1.02 (0.05)	0.001903	0.001867	3.44	-1.22
	R ICP	1.36 (0.13)	1.17 (0.21)	0.001822	0.000732	3.79	-1.35
$D_{e,\parallel}$	R ICP	1.86 (0.20)	1.63 (0.25)	0.003316	0.001363	3.56	-1.26
$D_{e,\perp}$	L FPT	0.79 (0.05)	0.71 (0.03)	0.000809	5.60E-05	4.74	-1.69
	R ICP	1.11 (0.17)	0.94 (0.23)	0.002599	0.000789	3.76	-1.34
FA	R SCP	0.44 (0.05)	0.37 (0.05)	0.003208	0.001382	3.55	-1.26
FAA	L OR	0.63 (0.03)	0.67 (0.03)	0.000264	0.000237	-4.21	1.50
	L T OCC	0.62 (0.02)	0.67 (0.03)	0.000253	0.00011	-4.50	1.60
MD	R CST	1.14 (0.08)	1.01 (0.08)	0.00058	1.10E-05	5.33	-1.89
	L FPT	1.04 (0.05)	0.93 (0.05)	0.000512	1.90E-05	5.15	-1.83
	R ICP	1.13 (0.09)	1.04 (0.12)	0.003937	0.002445	3.33	-1.18
	L POPT	1.08 (0.08)	0.96 (0.08)	0.000644	0.00013	4.43	-1.58
	R POPT	1.22 (0.11)	1.05 (0.10)	0.000544	8.40E-05	4.59	-1.63
ζ	MCP	0.44 (0.05)	0.36 (0.07)	0.005229	0.001876	3.43	-1.22
	R SCP	0.32 (0.05)	0.26 (0.06)	0.003404	0.001244	3.59	-1.28

Table 11 FBWM significant differences between patients with refractory epilepsy, non-refractory epilepsy and controls. The mean (standard deviation) of the individual diffusion parameter, minimum p-value and its corresponding α value, t statistic, and Cohen's d for the peak of each significant tract are provided. Diffusivities are expressed in units of μm2/ms, while ζ values are in units of ms1/2/ μm; all other quantities are dimensionless. Abbreviations for parameters are provided in Table 7.1 and for tracts in Table 3.2.

All significant differences in FBI and FBWM parameters between patients with refractory epilepsy, non-refractory epilepsy and controls are tabulated in Table 7.2. Significant differences between patients with refractory epilepsy and controls are illustrated in Figure 7.1. Significant differences were observed for seven diffusion measures over twelve tracts and effect sizes for significantly different regions were large (d = ± 1 or greater). Inspection of the along-tract values for both groups demonstrate that refractory patients showed consistent diffusion alterations over the entire length of tracts and statistical analysis revealed only the peak difference between groups. In putative measures of intra-axonal diffusivity, patients with refractory epilepsy had significantly reduced AWF in a region of the left striatoprefrontal tract (ST PREM) and reduced ζ in regions of the right cingulum (CG), right inferior longitudinal fascicule (ILF), right superior longitudinal fascicle segment III (SLF III), and right uncinate fascicle (UF) relative to controls. Increased ζ was seen in a region of the right inferior cerebellar peduncle (ICP). There were more widespread changes

in putative measures of extra-axonal diffusivity, including increases in MDe and De,II in regions of the right ICP, left superior cerebellar peduncle (SCP), and in the left ST PREM in De,II only. Additional De,⊥ increases were observed in the right arcuate fascicle (AF), left anterior thalamic radiation (ATR), left frontopontine tract (FPT), and left and right ICP. Significantly increased FAA and FAE was also observed within the right ICP in refractory patients compared to controls.

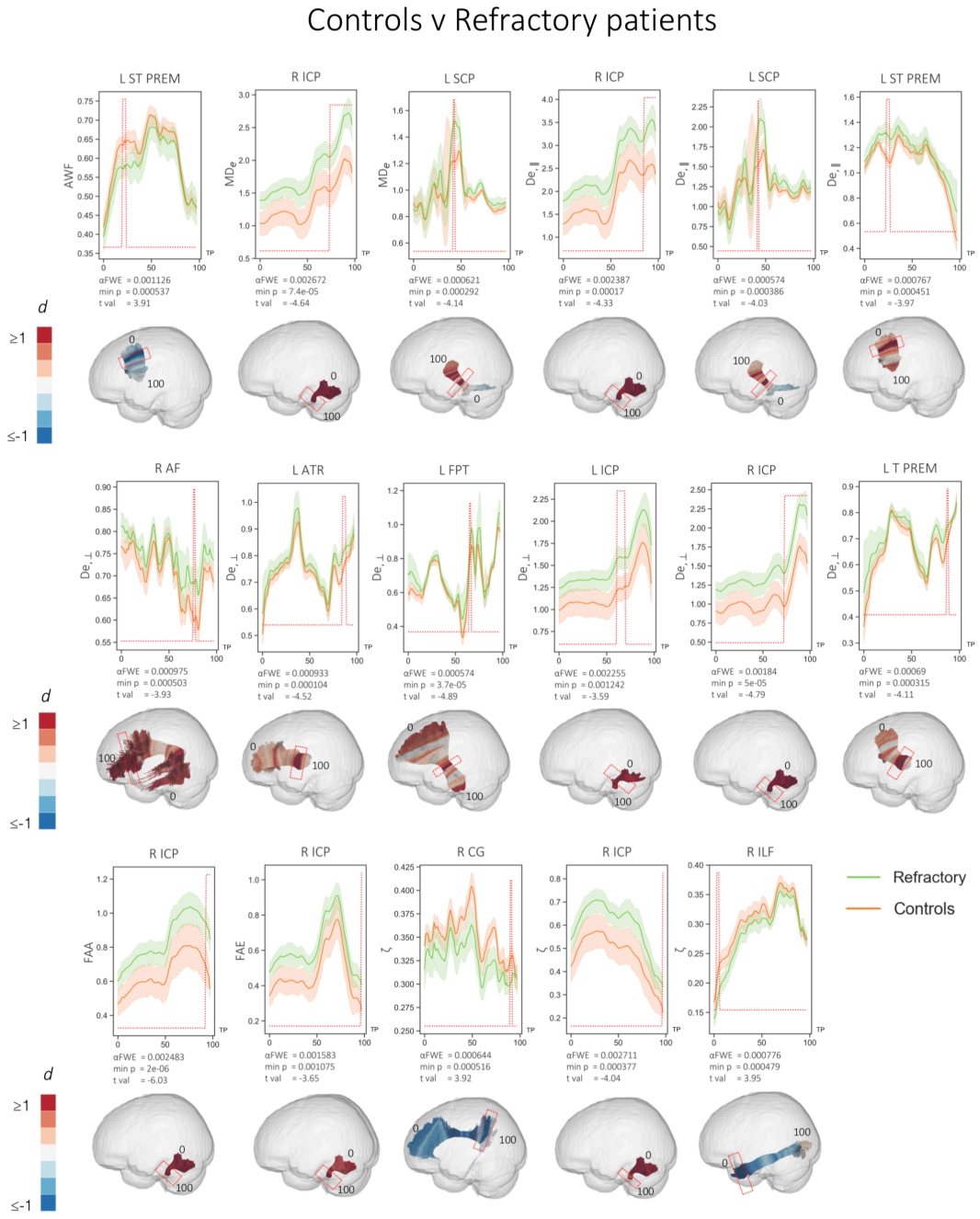

Figure 7.1 Statistically significant (red peaks) along-tract differences in FBWM diffusion properties in refractory patients compared to controls. 3D plots show Cohen's d values projected onto the relevant tracts with significant region highlighted by red boxes. Effect sizes greater than and equal to 1 are shown in dark red, with those less than and equal to −1 shown in dark blue. Significantly different ζ in regions of the right SLF III and right UF not

illustrated (see Table 4). Diffusivities are expressed in units of μm2/ms, while ζ values are in units of ms1/2/μm; all other quantities are dimensionless. TP = tract points.

Significant differences in FBI and FBWM parameters between patients with non-refractory epilepsy and controls are illustrated in Figure 7.2. Patients with non-refractory epilepsy showed substantially fewer diffusion alterations and smaller effect sizes. Significant differences were observed for six diffusion measures over six tracts. Patients had significantly increased values of the following parameters compared to controls: Da in a region of the left superior thalamic radiations (STR), De,II of the right thalamoparietal (T PAR) and right thalamo-occipital (T OCC) tracts, increased De,⊥ of the left ATR and left thalamopremotor (T PREM) tracts, and FAA of the right STR.

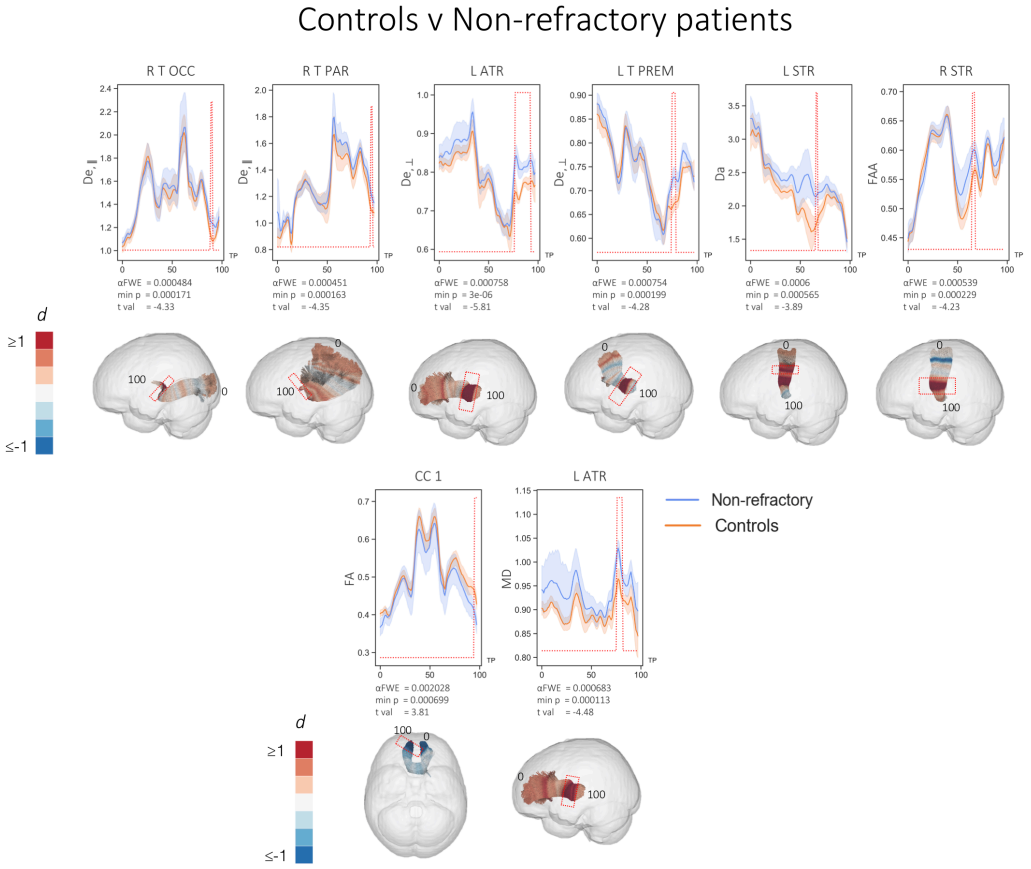

Figure 7.2 Statistically significant (red peaks) along-tract differences in FBWM diffusion properties in nonrefractory patients relative to controls. 3D plots show Cohen's d values projected onto the relevant tracts with significant region highlighted by red boxes. Effect sizes greater than and equal to 1 are shown in dark red, with those less than and equal to –1 shown in dark blue. Diffusivities are expressed in units of μm2/ms, while ζ values are in units of ms1/2/μm; all other quantities are dimensionless. TP = tract points

In direct comparisons between patient groups, patients with refractory epilepsy showed evidence of significantly increased putative measures of extra-axonal

diffusivity compared to patients with non-refractory epilepsy (Figure 7.3). These were manifest as significantly increased MDe in regions within the right corticospinal tract (CST) and right ICP, increased De,II in right ICP, and increased De,⊥ in regions of the left FPT, right and right ICP. Patients with refractory epilepsy also had significantly increased ζ in regions of the middle cerebellar peduncle (MCP) and right SCP. Significantly reduced FAA was observed in regions of the left optic radiation (OR) and left T OCC in refractory patients.

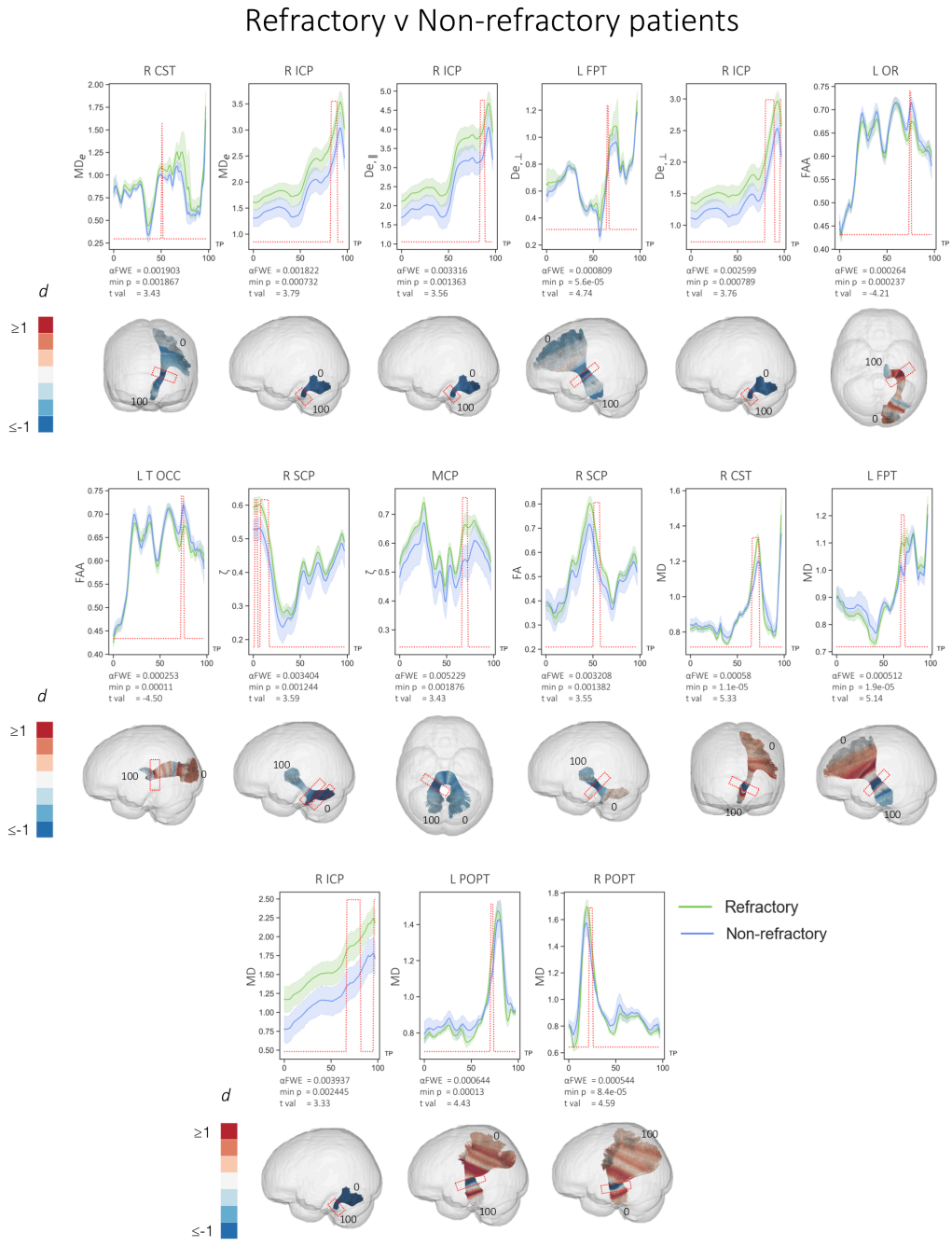

Figure 7.3 Statistically significant (red peaks) along-tract differences in FBWM diffusion properties in refractory patients relative to nonrefractory patients. 3D plots show Cohen's d values projected onto the relevant tracts with

significant region highlighted by red boxes. Effect sizes greater than and equal to 1 are shown in dark red, with those less than and equal to −1 shown in dark blue. Diffusivities are expressed in units of μm2/ms, while ζ values are in units of ms1/2/μm; all other quantities are dimensionless. TP = tract points

Analysis of conventional DTI metrics showed limited and more spatially restricted diffusion changes. There were no significant differences in FA or MD between refractory patients and controls. Non-refractory patients had significantly decreased FA in the rostrum of the corpus callosum (CC1) and increased MD in a region of the left ATR compared to controls (Figure 7.2). Direct comparisons between patient groups revealed significantly reduced FA in non-refractory patients in the right SCP and increased MD in refractory patients in regions of the right CST, left FPT, right ICP, left and right parieto-occipital pontine tracts (POPTs) (Figure 7.3).

7.4 Discussion

This study is the first to apply FBI and FBWM to a clinical population. We have used this advanced dMRI method together with along-tract tractography to investigate white matter microstructural changes in patients with longstanding focal epilepsy. By using FBI and FBWM, we are able make inferences about the biological processes underlying tissue diffusion changes, which has previously been difficult to do using conventional DTI. As expected, we found differences between patient groups and controls, and in accordance with previous literature we found increases in diffusivity parameters in patient groups. Relative to controls, refractory patients had significant increases in the putatative extra-axonal measures of MDe, De,II, and De,⊥ across several WM tracts. Conversely, patients with non-refractory epilepsy had limited statistically significant increases in extra-axonal diffusion measures compared to controls; this contrast in extra-axonal diffusion between patient groups was exemplified in direct comparisons, which demonstrated significantly greater measures of extra-axonal diffusion in refractory patients. Analysis of FBI and FBWM diffusion measures revealed more changes than conventional DTI metrics. We discuss the biological and clinical significance of these findings before highlighting pertinent methodological issues.

7.4.1 Biological and clinical implications

The FBI/FBWM two compartment model permits separation of intra-axonal and extra-axonal water diffusion. MDe is a measure of extra-axonal diffusivity, which is

similar to MD but only for the extra-axonal diffusion compartment. Similarly, $D_{e,\perp}$ is analogous to RD using conventional DTI, but for the extra-axonal compartment. An increase in extra-axonal space has been argued to reflect an increase in neuroinflammation via microglial activation (Schwartz *et al*., 2006; Pasternak *et al*., 2012). Neuroinflammation is known to have an important role in epilepsy (Amhaoul, Staelens and Dedeurwaerdere, 2014). Neuroinflammation has been studied extensively using positron emission tomography (PET), specifically using the radioligands (R)-[11C]PK11195 and 18F-PBR111 as measures of translocator protein (TSPO), which is upregulated in the context of activated glial cells (Scott *et al*., 2017). PET-derived measures of neuroinflammation have been validated in rat models of TLE – kainic acid-induced status epilepticus – where increased TSPO expression has been associated with increased microglial activation determined using immunohistochemistry (Amhaoul *et al*., 2015). In people with well circumscribed and phenotyped focal epilepsy, neuroinflammatory changes have been demonstrated in regions beyond the presumed seizure focus. For example, increased TSPO uptake has been demonstrated in temporal and extra-temporal lobe regions, ipsilateral and contralateral to the presumed seizure focus, in patients with TLE (Hirvonen *et al*., 2012; Gershen *et al*., 2015b). Increased neuroinflammatory changes have been reported in a case study of focal epilepsy using post-ictal PET (Butler *et al*., 2016). Interestingly, previous work has demonstrated increased uptake of (R)-[11C]PK11195 in rats with persistent seizures despite phenobarbital treatment compared to rats that responded well to treatment (Bogdanović *et al*., 2014). Taken together, these findings suggest that neuroinflammatory changes in local and distal brain regions are associated with refractory seizures, which may be considered consistent with the widespread extra-axonal water diffusion changes observed in the present study. Given that we preferentially observed increased extra-axonal diffusion in refractory patients we suggest that imaging measures sensitive to the extra-axonal space may be a biomarker of pharmacoresistance. However, in human epilepsy studies it is difficult to discern whether increased extra-axonal space and / or neuroinflammatory processes are a cause or consequence of active seizures. Nevertheless, it is interesting that patients with non-refractory epilepsy who had not experienced seizures for an average of over three years (Appendix Table 10.3) also showed evidence of more restricted pattern of extra-axonal diffusion compared to controls (Figure 7.2).

An alternative explanation is that increased extra-axonal space is directly due to axonal degeneration (Rodríguez-Cruces and Concha, 2015). Reduced myelin content and axonal density of myelinated and non-myelinated axons has been reported in refractory focal epilepsy (Garbelli *et al*., 2012), and reduced cumulative axonal membrane circumference is associated with reduced FA in WM tracts in close proximity to the epileptogenic zone (Concha *et al*., 2010). Reduced axonal density inherently generates increased extra-axonal space (Rodríguez-Cruces and Concha, 2015), and this process could be driving increased extra-axonal diffusion in patients with epilepsy. Most studies examining axonal density in refractory focal epilepsy naturally restrict analysis to the presumed epileptogenic zone (given the opportunity to perform histological studies on resected specimens). Whether the same neuropathology extends to axons more widely across the brain as we have shown here is a more contentious issue. We report extra-axonal diffusivity alterations across many WM tracts that are presumably not part of the epileptogenic zone. The underlying histological cause of these changes remain unknown.

We additionally report increases in regional white matter MD in patients with refractory epilepsy compared to those with non-refractory epilepsy. MD is a measure of all diffusion which is directionally averaged and may in itself be a marker of cellularity, oedema and necrosis (Alexander *et al*., 2011). Increased MD is often reported in many dMRI studies of epilepsy (McDonald *et al*., 2008; Concha *et al*., 2009; Jiang *et al*., 2017). Moreover, MD was found to be superior to other conventional diffusion metrics in predicting postoperative seizure outcome from preoperative DTI in patients with TLE (Keller *et al*., 2017). The results presented here suggest that the previously widespread observed changes in WM diffusivity using conventional DTI in patients with refractory focal epilepsy are largely driven by the extra-axonal diffusivity component.

7.4.2 Conclusions

This is the first clinical application of FBI and FBWM. The two-compartment diffusion model has provided the means to separate intra-axonal and extra-axonal diffusion alterations in patients with longstanding epilepsy. The strongest findings

were with parameters sensitive to extra-axonal diffusion, which may suggest significant neuroinflammatory processes and / or axonal degeneration. This work demonstrates that these changes are more widespread in patients with refractory epilepsy compared to those with well-controlled seizures located along eloquent white matter tracts not considered to be part of the epileptogenic zone in patients with focal seizures.

8 Discussion

In this work, we sought to characterise changes in patients with both newly diagnosed and longstanding focal epilepsy using advanced neuroimaging and serum analysis methods. DTI and DKI were used to investigate grey matter regions of interest (thalamic nuclei, hippocamps, amygdala, and parahippocampal gyrus) and white matter tracts in both patients with newly diagnosed and longstanding focal epilepsy. In order to infer biological meaning to diffusion parameters, we employed MRS and serum analysis, and a newly developed diffusion MRI technique, FBI. These techniques allowed us to characterise, further than previously possible, the microstructural environment underlying focal epilepsy and suggest biological mechanisms driving these changes.

8.1 Summary of results

8.1.1 Diffusion imaging in newly diagnosed focal epilepsy

DKI analysis of GM in patients with newly diagnosed epilepsy revealed significant changes between both patients who went on to become refractory and those who became non-refractory and controls, which were restricted to thalamic nuclei. Typically, reductions in DKI metrics were seen in patient groups relative to controls. No significant differences in grey matter were seen between patient groups in direct comparisons.

Analysis of WM revealed widespread alterations in both patient groups compared to controls across all DKI and DTI metrics. Furthermore, changes were found in direct patient comparisons in AK and FA only. Again, a reduction in DKI metrics and increases in DTI metrics were found in patient groups.

8.1.2 Diffusion imaging in longstanding focal epilepsy

GM analysis revealed significant changes in DKI metrics between non-refractory patients and controls in the thalamic nuclei and parahippocampal gyrus. In direct patient comparisons, lower AK values were seen in non-refractory patients in several thalamic nuclei, and the right amygdala and parahippocampal gyrus. No significant differences were found between refractory patients and controls.

In WM, we revealed changes in both DKI and DTI metrics across both patient groups relative to controls. This analysis revealed multiple significant differences in direct patient group comparisons, with more widespread changes in DTI metrics. Typically, patients with refractory epilepsy showed higher DKI and DTI values relative to non-refractory patients.

8.1.3 Investigation into thalamic changes in longstanding focal epilepsy

Volumetric analysis revealed no significant differences in thalamic volumes. DKI analysis demonstrated a significant difference in the thalamus between refractory and non-refractory patients, with lower AK found in non-refractory patients. In MRS analysis, a reduction in left Glx was found in patients compared to controls, while serum analysis revealed a reduction of IL-1ß in patients compared to controls and in refractory and non-refractory patients compared to controls.

Correlational analysis was extremely revealing in this study, with correlations found between many outcome measures. Correlations were revealed between both left and right thalamic volumes and a number of diffusion parameters of the thalamus, with a reduction in volume being related to an increase in DTI metrics and a decrease in DKI metrics. Additionally, serum HMGB1 levels were correlated with both left and right thalamic volumes, with an increase in serum HMGB1 linked to a decrease in volume. Left thalamic Cho was correlated with right thalamic RD and FA and both left

thalamic mIns and serum HMGB1 were correlated with right kurtosis metrics. An increase in left thalamic mIns and serum HMGB1 were related to a decrease in kurtosis values. Additionally, serum HMGB1 was positively correlated with thalamic mIns.

8.1.4 Fiber ball white matter modelling in longstanding focal epilepsy

FBI analysis of WM tracts revealed significant differences between refractory patients and controls, with significant increases in extra-axonal diffusion measures across several tracts. Patients with non-refractory epilepsy displayed only limited statistically significant increases in extra-axonal diffusion measures compared to controls. This difference translated to direct patient comparisons, with refractory patients demonstrating significantly greater measures of extra-axonal diffusivity relative to non-refractory patients. Furthermore, FBI measures were substantially more revealing than standard DTI measures.

8.2 Discussion and comparison of results across experimental chapters

Patients with NDfE demonstrated a general reduction in DKI values compared to controls. Moreover, this was further seen in patients who went on to become refractory compared to those who went on to become non-refractory. We suggested that these findings related to a less restricted diffusion environment – as expected in patient groups. A similar result was seen using FBWM in patients with longstanding epilepsy. In this study, we found that patients displayed increases in measures of extra-axonal diffusivity – again further found in patients with refractory compared to non-refractory epilepsy. This increase in extra-cellular space was suggested to be linked to an increase in inflammatory processes, cell loss, or axonal degeneration. From these results, we can begin to suggest that these abnormal processes potentially leading to differences in treatment response may begin at the onset of disease.

Investigation into GM changes found alterations restricted to the thalamic nuclei in patients with NDfE. In those with longstanding focal epilepsy, GM changes were more widespread, including the parahippocampal gyri. It is possible that alterations in GM become more widespread during disease progression, however it is important to note that direct conclusions cannot be drawn from these different cohorts.

Conversely to expectations, a general reduction in DKI values was found in non-refractory patients with longstanding epilepsy. This is also at odds to findings from other studies included in this thesis. These unexpected findings may be due to issues with heterogeneity within the cohort, or due to differences in methodology.

8.3 Methodological discussion and limitations

8.3.1 Use of DKI over DTI

DKI offers many advantages over standard DTI including the ability to provide information on crossing fibers (Lazar *et al*., 2008) and non-isotropic environments such as GM (Gao *et al*., 2012; Arab *et al*., 2018). This is due to DKI not sharing the assumption of DTI of a Gaussian distribution of water diffusion (Jensen and Helpern, 2010). This allows for a more detailed description of the microstructural environment than previously possible with DTI. In this body of work, we have demonstrated DKI changes in multiple white matter tracts and in GM in patients with both newly diagnosed and longstanding focal epilepsy. Further, we were able to demonstrate differences between patients with refractory and non-refractory epilepsy, including at the point of diagnosis. This supports previous literature and suggests that DKI is sensitive to changes in both regional white matter and grey matter (Gao *et al*., 2012; Bonilha *et al*., 2015).

Studies employing DKI in epilepsy have tended to reveal more widespread changes in DKI compared to DTI measures in both white and grey matter (Gao *et al*., 2012; Zhang *et al*., 2013, 2016; Bonilha *et al*., 2015; Glenn *et al*., 2016). In this thesis, we have demonstrated findings which both supports, and oppose, this literature. In terms of GM, which was studied in the thalamus, we found changes in DKI which could not be seen with DTI (Chapter 6). Similarly, in patients with newly diagnosed epilepsy, more widespread changes were seen across DKI metrics compared to DTI metrics (Chapter 4). These findings support previous work and suggest that DKI is more sensitive to changes in patients with focal epilepsy (Gao *et al*., 2012; Bonilha *et al*., 2015). However, in patients with longstanding focal epilepsy, we demonstrated more widespread changes in DTI rather than DKI metrics (Chapter 5). Previous literature has suggested that the presence of more widespread DKI changes is indicative of its position as a more sensitive method than DTI (Gao *et al*., 2012; Bonilha *et al*., 2015).

Although here we found DKI has revealed fewer changes in patients with longstanding epilepsy, these may be more accurate to the underlying microstructural abnormalities than the changes revealed by DTI. Certainly, DKI provides a better model of the diffusion environment (Jensen and Helpern, 2010), and so changes found with this method can be said to be intrinsically more biologically meaningful. Therefore, DKI may be superior to DTI for revealing a biomarker for pharmacoresistence in longstanding epilepsy.

8.3.2 Use of Fiber Ball Imaging

While FBI and FBWM are recently developed techniques that have not been previously applied to clinical populations, other dMRI two-/multi-compartment models have been employed in clinical contexts to further understand the cerebral microstructural environment. Free-water imaging approaches have been proposed for detecting neuroinflammatory markers in disorders known to have neuroinflammatory components including schizophrenia (Pasternak *et al*., 2012), Parkinson's disease (Planetta *et al*., 2016), and concussion (Pasternak *et al*., 2014). Neurite Orientation Dispersion and Density Imaging (NODDI) (Zhang *et al*., 2012) has been used to demonstrate alterations in intracellular volume fraction, a marker of neurite density, in malformed brain regions causing epilepsy (Winston *et al*., 2014) and in widespread temporal and extratemporal brain regions in TLE (Winston *et al*., 2020). Other work has reported that NODDI-derived orientation dispersion index maps reveal cortical and subcortical abnormalities in patients with non-lesional focal epilepsy (Rostampour *et al*., 2018). Multi-compartment models are better able to understand the biological processes driving changes in diffusion parameters (Winston *et al*., 2020). By modelling diffusion with two-/multi-compartment models, evidence suggests that improved detection of focal abnormalities and further insights into the underlying microstructure of the brain is possible.

While these models have provided important insights into microstructural brain changes associated with neuropathology, there are notable issues with many dMRI tissue models. These include problems with nonlinear fitting algorithms, on which many of these models are based, which can lead to increased computational times, sensitivity to noise and imaging artefacts, and issues related to the accuracy of the

underlying idealizations (Novikov, Kiselev and Jespersen, 2018). FBWM mitigates these difficulties with a two-compartment model based on well supported assumptions and a simple computational scheme involving a straightforward linear transformation of the dMRI signal together with a one-dimensional numerical optimisation. Further, FBWM improves substantially upon the White Matter Tract Integrity (WMTI) method (Fieremans, Jensen and Helpern, 2011). The WMTI method assumes that all axons in a given voxel are approximately aligned in the same direction, which creates issues in regions of crossing fibres. FBWM overcomes this by using the fODF from FBI rather than assuming a particular geometric arrangement of axons and, as such, should more accurately model regions with crossing fibres.

8.3.3 Use of along-tract rather than whole tract methods

Rather than averaging diffusion metrics over each reconstructed white matter tract we chose to utilise an along-tract approach. Given that white matter tissue diffusional characteristics vary long the length of tracts, it is advantageous to capture this variation in clinical studies as averaging across whole tracts may obscure regionally specific and pathologically relevant diffusion alterations (Figure 2.5). Tissue characteristics may vary along the length of tracts (Johnson *et al*., 2014) therefore it is likely that tissue abnormalities in focal epilepsies also vary along tracts. Indeed, only by quantifying diffusion changes along tracts did a previous study identify preoperative markers of excellent and suboptimal postoperative seizure outcomes in patients with refractory TLE (Keller *et al*., 2017). In this thesis, we see inconsistent regional differences in diffusion metrics within tracts, particularly in FBI metrics (Figure 7.2), and as such, we would be unable to identify significant differences in tract characteristics if diffusion measures were averages over entire tracts.

8.3.4 Use of MRS

MRS allows for the characterisation of the metabolic environment within the brain. In this thesis, we were able to not only quantitively measure metabolite values within the thalamus of patients with epilepsy, but also correlate these values with other outcome measures. This allowed us to make further inferences about the biological underpinning of diffusion changes than previously possible. However, there were significant limitations with the use of MRS in this work. We expected to find

alterations in metabolites known to be markers of neuronal dysfunction and neuroinflammation, as per previous literature (Connelly *et al*., 1994; Gadian *et al*., 1994; Kirov *et al*., 2018), which we were unable to demonstrate. Accurate analysis of MRS values requires collection of high-quality spectra (Figure 8.1). This can be difficult to achieve, particularly in patient populations, due to the propensity to move during the scan. Any metabolite values which fall outside of a quality threshold must be removed prior to analysis (Provencher, 2019). As a consequence of this quality control, our sample sized reduced, which may have affected our ability to replicate findings from previous literature.

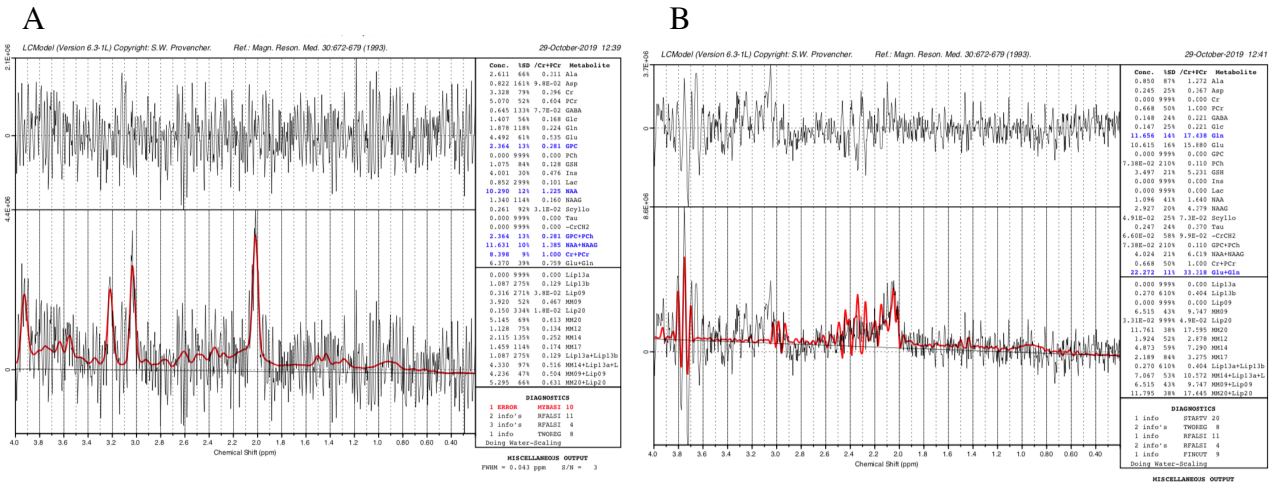

Figure 8.1: Output from LCModel. A is an example of high-quality spectra which was used for analysis. B is an example of low quality spectra which was removed from analysis. Decisions were made about low quality spectra with relation to the height and width of the NAA peak and its relativity to the Cho and Cr peaks. Additionally, we hoped to see a %SD for most of the metabolites, but particularly the sum metabolites or GPC+Pch (Cho), NAA+NAAG, Cr+PCr (Cr) and Glu+Gln (Glx).

8.3.5 Use of serum measures

Similarly to MRS analysis, serum analysis allowed us to further investigate the biological meaning of diffusion parameters. We expected to find an increase in serum HMGB1 and IL-1ß in patient groups relative to controls as per previous literature (Ravizza *et al*., 2006, 2008; Maroso *et al*., 2010; Zurolo *et al*., 2011; Iori *et al*., 2013), which was not demonstrated. Rather, we revealed a significant decrease in IL-1ß in patient groups. The major limitation with studying these serum markers in patients with epilepsy is the interaction with some anti-epileptic medications. Levetiracetam (Kim *et al*., 2010), lamotrigine (Shi *et al*., 2018), and valproate (Zayed *et al*., 2011) have all been found to reduce levels of serum IL-1ß and we suggested this was the

main reason for this finding. Again, a limitation of this analysis was small sample size. A non-significant trend toward an increase in serum HMGB1 was found in patients relative to controls, and we suggest with a larger, more homogenous sample size this trend may reach significance.

A further limitation of this method is the effect of systemic inflammation or infective processes in the population of patients. As these measures are a peripheral rather than direct marker of inflammation, they are subject to change due to any inflammatory process currently happening within the body – including unrelated inflammations or infections. Indeed, a higher prevalence of many conditions has been found in patients with epilepsy (Keezer, Sisodiya and Sander, 2016), of which some will themselves be related to inflammation. Thus, the cause behind an increase in peripheral inflammatory markers cannot be attributed to simply the presence of epilepsy alone.

8.3.6 Further limitations

The main advantage of recruiting a heterogeneous sample is time-efficient, easier recruitment leading to results that are generalisable to a large population (Jager, Putnick and Bornstein, 2017). However, the results become difficult to apply to a specific population, which is particularly relevant when searching for a biomarker for pharmacoresistance in focal epilepsy. Patients in this body of work were experiencing a range of seizure types, were taking a range of anti-epileptic medication, and were at varying points in their disease timelines. We suggest that this has led to findings which oppose previous literature, particularly in MRS and serum analysis, where sample sizes were reduced further due to poor quality.

It is important to note the heterogenous nature of epilepsies in general when discussing this work. Epilepsy is not one single disorder and it is unlikely that any two patients experience the same symptoms across their disease progression. Additionally, as seen in Chapter 4, seizure freedom and pharmacoresistance can be transitory. A patient may be seizure free for many years and still relapse into refractoriness. According to the ILAE definition of pharmacoresistance (Kwan *et al.*, 2010), a patient is pharmacoresistant if they have trialed two AED therapies and not achieved seizure freedom. However, a patient may have trialled three therapies and been seizure free

for many years. It is therefore difficult to classify patients reliably into both epilepsy type and outcome to treatment response.

Similar to many studies in this field, the majority of this work has focused on patients with longstanding focal epilepsy. Studying patients at this time point leads to difficulties establishing whether damage revealed is a cause or consequence of prolonged seizures (Kälviäinen and Salmenperä, 2002). Literature in this area has previously proved inconclusive, with some studies failing to find a correlation between damage and severity or duration of seizures, while others have suggested likewise. Although we have also included patients with newly diagnosed epilepsy in this work, the patients are from two separate cohorts, and were scanned using different hardware and protocols. It is therefore difficult to compare between these patient groups and so we are not able to add extensively to this debate.

8.4 Future work

This body of work is unique in its inclusion of patients with both newly diagnosed and longstanding focal epilepsy. Although we have been able to identify several alterations in patients with both newly diagnosed and longstanding focal epilepsy, this work could be built upon with a longitudinal design. In the present work, we studied two separate cohorts, limiting our ability to compare changes along the course of epilepsy. Studying a single cohort of patients from diagnosis to later on in disease progression, as is suggested in De Bézenac *et al*. (2019), would allow for changes to be monitored in relation to disease severity, duration, and treatment along the disease progression.

The use of FBI in this body of work is novel and has revealed changes in patients from which we can infer clear biological meaning. To improve the ability to infer biological meaning from changes in FBI metrics, we suggest a study employing histological analysis of resected tissue Studies combining histological findings with neuroimaging findings have previously been conducted in patients with temporal lobe epilepsy (Eriksson *et al*., 2007; Stefanits *et al*., 2017; Peixoto-Santos *et al*., 2020). These studies have revealed correlations between several neuroimaging parameters and histological findings. By combining FBI with histological analysis, it may be possible to support the assumptions made by FBI regarding extra- and intra- axonal space. Evidence

supporting the biological processes underlying FBI metric changes could allow for the development of a biomarker for pharmacoresistance which is biologically meaningful.

Further insights could be gained from FBI by employing more advanced network and tractography approaches. Epilepsy is now widely considered a network disorder (De Bézenac *et al*., 2019; Kreilkamp *et al*., 2021), and much work is now focusing on this analysis. Future work could make use of the fODFs generated directly from FBI. These are expected to yield improved tractography results over fODFs from standard DTI (Jensen, Russell Glenn and Helpern, 2016; McKinnon, Helpern and Jensen, 2018). The combination of these methods could provide key information which has not previously been accessible.

This body of work has implications not just for epilepsy research, but for research into other neurological disorders. As previously discussed, two-/multi- compartment models have provided insights in a number of clinical contexts. Free-water imaging has revealed neuroinflammatory markers in schizophrenia (Pasternak *et al*., 2012), Parkinson's disease (Planetta *et al*., 2016), and concussion (Pasternak *et al*., 2014), NODDI has been used in multiple contexts including epilepsy (Winston *et al*., 2014, 2020), and the WMTI method has been employed in multiple sclerosis (Ngamsombat *et al*., 2020) and glaucoma (Sun *et al*., 2020). The advantage of FBI over these other two-/multi-compartment models has been previously discussed and as such, FBI could be relatively easily employed in these contexts and more, providing valuable insights into a range of clinical disorders.

There are many directions in which this work could be taken. This is a rapidly advancing field and our understanding of changes in patients with both newly diagnosed and longstanding focal epilepsy has increased greatly in the past year (Hatton *et al*., 2020; Leek *et al*., 2020; Winston *et al*., 2020; Kreilkamp *et al*., 2021). This work has demonstrated how microstructural alterations can be studied and biological meaning can be inferred from diffusional parameters, providing valuable information about the progression of focal epilepsy.

9 References

Aasly, J. *et al*. (1999) 'Proton magnetic resonance spectroscopy of brain biopsies from patients with intractable epilepsy', *Epilepsy Research*. doi: 10.1016/S0920-1211(99)00011-X.

Abou-Khalil, B. (2007) 'An update on determination of language dominance in screening for epilepsy surgery: The Wada test and newer noninvasive alternatives', *Epilepsia*. doi: 10.1111/j.1528-1167.2007.01012.x.

Ahmadi, M. E. *et al*. (2009) 'Side matters: Diffusion tensor imaging tractography in left and right temporal lobe epilepsy', *American Journal of Neuroradiology*, 30(9), pp. 1740–1747. doi: 10.3174/ajnr.A1650.

Äikiä, M. *et al*. (1999) 'Predictors of seizure outcome in newly diagnosed partial epilepsy: Memory performance as a prognostic factor', *Epilepsy Research*. doi: 10.1016/S0920-1211(99)00059-5.

Alelú-Paz, R. and Giménez-Amaya, J. M. (2008) 'The mediodorsal thalamic nucleus and schizophrenia', *Journal of Psychiatry and Neuroscience*.

Alexander, A. L. *et al*. (2011) 'Characterization of Cerebral White Matter Properties Using Quantitative Magnetic Resonance Imaging Stains', *Brain Connectivity*. doi: 10.1089/brain.2011.0071.

Alonazi, B. K. *et al*. (2019) 'Resting-state functional brain networks in adults with a new diagnosis of focal epilepsy', *Brain and Behavior*. doi: 10.1002/brb3.1168.

Amhaoul, H. *et al*. (2015) 'Neurobiology of Disease Brain inflammation in a chronic epilepsy model : Evolving pattern of the translocator protein during epileptogenesis', 82, pp. 526–539. doi: 10.1016/j.nbd.2015.09.004.

Amhaoul, H., Staelens, S. and Dedeurwaerdere, S. (2014) 'Imaging brain inflammation in epilepsy', *Neuroscience*. IBRO, 279, pp. 238–252. doi: 10.1016/j.neuroscience.2014.08.044.

Andersson, J. L. R. and Sotiropoulos, S. N. (2016) 'An integrated approach to correction for off-resonance effects and subject movement in diffusion MR imaging', *NeuroImage*. doi: 10.1016/j.neuroimage.2015.10.019.

Annegers, J. F. *et al*. (1998) 'A population-based study of seizures after traumatic brain injuries', *New England Journal of Medicine*. doi: 10.1056/NEJM199801013380104.

Annegers, J. F., Hauser, W. A. and Elveback, L. R. (1979) 'Remission of Seizures

and Relapse in Patients with Epilepsy', *Epilepsia*. doi: 10.1111/j.1528-1157.1979.tb04857.x.

Arab, A. *et al*. (2018) 'Principles of diffusion kurtosis imaging and its role in early diagnosis of neurodegenerative disorders', *Brain Research Bulletin*. doi: 10.1016/j.brainresbull.2018.01.015.

Aroniadou-Anderjaska, V. *et al*. (2008) 'Pathology and pathophysiology of the amygdala in epileptogenesis and epilepsy', *Epilepsy Research*. doi: 10.1016/j.eplepsyres.2007.11.011.

Arts, W. F. M. *et al*. (1999) 'The early prognosis of epilepsy in childhood: The prediction of a poor outcome. The Dutch Study of Epilepsy in Childhood', *Epilepsia*. doi: 10.1111/j.1528-1157.1999.tb00770.x.

Assaf, Y. *et al*. (2004) 'New modeling and experimental framework to characterize hindered and restricted water diffusion in brain white matter', *Magnetic Resonance in Medicine*. doi: 10.1002/mrm.20274.

Assaf, Y. and Basser, P. J. (2005) 'Composite hindered and restricted model of diffusion (CHARMED) MR imaging of the human brain', *NeuroImage*, 27(1), pp. 48–58. doi: 10.1016/j.neuroimage.2005.03.042.

Aydin, H. *et al*. (2012) 'Value of proton-MR-spectroscopy in the diagnosis of temporal lobe Epilepsy; Correlatıon of metabolite alterations with electroencephalography', *Iranian Journal of Radiology*. doi: 10.5812/iranjradiol.6686.

Baker, G. A. *et al*. (1997) 'Quality of life of people with epilepsy: A European study', *Epilepsia*. doi: 10.1111/j.1528-1157.1997.tb01128.x.

Barbas, H., García-Cabezas, M. Á. and Zikopoulos, B. (2013) 'Frontal-thalamic circuits associated with language.', *Brain and language*. doi: 10.1016/j.bandl.2012.10.001.

Barker, P. B. and Lin, D. D. M. (2006) 'In vivo proton MR spectroscopy of the human brain', *Progress in Nuclear Magnetic Resonance Spectroscopy*. doi: 10.1016/j.pnmrs.2006.06.002.

Bartnik-Olson, B. L. *et al*. (2017) 'Glutamate metabolism in temporal lobe epilepsy as revealed by dynamic proton MRS following the infusion of [U13-C] glucose', *Epilepsy Research*. doi: 10.1016/j.eplepsyres.2017.07.010.

Basser, P. J., Mattiello, J. and Lebihan, D. (1994) 'Estimation of the Effective Self-

Diffusion Tensor from the NMR Spin Echo', *Journal of Magnetic Resonance, Series B*. doi: 10.1006/jmrb.1994.1037.
Basser, P. J., Mattiello, J. and LeBihan, D. (1994) 'MR diffusion tensor spectroscopy and imaging', *Biophysical Journal*. doi: 10.1016/S0006-3495(94)80775-1.
Basser, P. J. and Pierpaoli, C. (2011) 'Microstructural and physiological features of tissues elucidated by quantitative-diffusion-tensor MRI', *Journal of Magnetic Resonance*. doi: 10.1016/j.jmr.2011.09.022.
Baulac, S. *et al*. (2015) 'Familial focal epilepsy with focal cortical dysplasia due to DEPDC5 mutations', *Annals of Neurology*. doi: 10.1002/ana.24368.
Beghi, E. *et al*. (2010) 'Recommendation for a definition of acute symptomatic seizure', *Epilepsia*. doi: 10.1111/j.1528-1167.2009.02285.x.
Beghi, E. and Tognoni, G. (1988) 'Prognosis of Epilepsy in Newly Referred Patients: A Multicenter Prospective Study: Collaborative Group for the Study of Epilepsy Principal Investigators*', *Epilepsia*. doi: 10.1111/j.1528-1157.1988.tb03712.x.
Behrens, T. E. J. *et al*. (2003) 'Non-invasive mapping of connections between human thalamus and cortex using diffusion imaging', *Nature Neuroscience*. doi: 10.1038/nn1075.
Benarroch, E. E. (2008) 'N-Acetylaspartate and N-acetylaspartylglutamate: Neurobiology and clinical significance', *Neurology*. doi: 10.1212/01.wnl.0000311267.63292.6c.
Berg, A. T., Shinnar, S., *et al*. (2001) 'Early development of intractable epilepsy in children: A prospective study', *Neurology*. doi: 10.1212/WNL.56.11.1445.
Berg, A. T., Shinnar, Shlomo, *et al*. (2001) 'Two-year remission and subsequent relapse in children with newly diagnosed epilepsy', *Epilepsia*. doi: 10.1046/j.1528-1157.2001.21101.x.
Berkovic, S. F. *et al*. (2006) 'Human epilepsies: interaction of genetic and acquired factors', *Trends in Neurosciences*. doi: 10.1016/j.tins.2006.05.009.
Bernasconi, N. *et al*. (1999) 'Entorhinal cortex in temporal lobe epilepsy: A quantitative MRI study', *Neurology*. doi: 10.1212/wnl.52.9.1870.
Bernasconi, N. *et al*. (2000) 'Morphometric MRI analysis of the parahippocampal region in temporal lobe epilepsy', in *Annals of the New York Academy of Sciences*. doi: 10.1111/j.1749-6632.2000.tb06752.x.

Bernasconi, N. *et al*. (2001) 'Entorhinal cortex atrophy in epilepsy patients exhibiting normal hippocampal volumes', *Neurology*. doi: 10.1212/WNL.56.10.1335.

Bernasconi, N., Andermann, F., *et al*. (2003) 'Entorhinal cortex MRI assessment in temporal, extratemporal, and idiopathic generalized epilepsy', *Epilepsia*. doi: 10.1046/j.1528-1157.2003.64802.x.

Bernasconi, N., Bernasconi, A., *et al*. (2003) 'Mesial temporal damage in temporal lobe epilepsy: A volumetric MRI study of the hippocampus, amygdala and parahippocampal region', *Brain*. doi: 10.1093/brain/awg034.

Bernhardt, B. C., Worsley, K. J., *et al*. (2009) 'Longitudinal and cross-sectional analysis of atrophy in pharmacoresistant temporal lobe epilepsy', *Neurology*. doi: 10.1212/01.wnl.0000345969.57574.f5.

Bernhardt, B. C., Rozen, D. A., *et al*. (2009) 'Thalamo-cortical network pathology in idiopathic generalized epilepsy: Insights from MRI-based morphometric correlation analysis', *NeuroImage*. doi: 10.1016/j.neuroimage.2009.01.055.

Bernhardt, B. C., Bonilha, L. and Gross, D. W. (2015) 'Network analysis for a network disorder: The emerging role of graph theory in the study of epilepsy', *Epilepsy and Behavior*. doi: 10.1016/j.yebeh.2015.06.005.

Bertram, E. H. *et al*. (1998) 'Functional anatomy of limbic epilepsy: A proposal for central synchronization of a diffusely hyperexcitable network', in *Epilepsy Research*. doi: 10.1016/S0920-1211(98)00051-5.

Bertram, E. H. *et al*. (2001) 'The midline thalamus: Alterations and a potential role in limbic epilepsy', *Epilepsia*. doi: 10.1046/j.1528-1157.2001.042008967.x.

De Bézenac, C. *et al*. (2019) 'Investigating imaging network markers of cognitive dysfunction and pharmacoresistance in newly diagnosed epilepsy: A protocol for an observational cohort study in the UK', *BMJ Open*. doi: 10.1136/bmjopen-2019-034347.

Le Bihan, D. *et al*. (1986) 'MR imaging of intravoxel incoherent motions: Application to diffusion and perfusion in neurologic disorders', *Radiology*. doi: 10.1148/radiology.161.2.3763909.

Bilevicius, E. *et al*. (2010) 'Antiepileptic drug response in temporal lobe epilepsy: A clinical and MRI morphometry study', *Neurology*. doi: 10.1212/WNL.0b013e3181fc29dd.

Blumcke, I. *et al*. (2017) 'Histopathological findings in brain tissue obtained during epilepsy surgery', *New England Journal of Medicine*. doi: 10.1056/NEJMoa1703784.

Blümcke, I. *et al*. (2011) 'The clinicopathologic spectrum of focal cortical dysplasias: A consensus classification proposed by an ad hoc Task Force of the ILAE Diagnostic Methods Commission', *Epilepsia*. doi: 10.1111/j.1528-1167.2010.02777.x.

Blümcke, I. and Spreafico, R. (2012) 'Cause matters: A neuropathological challenge to human epilepsies', in *Brain Pathology*. doi: 10.1111/j.1750-3639.2012.00584.x.

Bogdanović, R. M. *et al*. (2014) '(R)-[11C]PK11195 brain uptake as a biomarker of inflammation and antiepileptic drug resistance: Evaluation in a rat epilepsy model', *Neuropharmacology*. doi: 10.1016/j.neuropharm.2014.05.002.

Bonilha, L. *et al*. (2013) 'Presurgical connectome and postsurgical seizure control in temporal lobe epilepsy', *Neurology*, 81(19), pp. 1704–1710. doi: 10.1212/01.wnl.0000435306.95271.5f.

Bonilha, L. *et al*. (2015) 'Altered Microstructure in Temporal Lobe Epilepsy: A Diffusional Kurtosis Imaging Study', *American Journal of Neuroradiology*, 36(4), pp. 719–724. doi: 10.3174/ajnr.A4185.

Bonilha, L. and Keller, S. S. (2015) 'Quantitative MRI in refractory temporal lobe epilepsy: relationship with surgical outcomes.', *Quantitative imaging in medicine and surgery*, 5(2), pp. 204–24. doi: 10.3978/j.issn.2223-4292.2015.01.01.

Brenner, R. E. *et al*. (1993) 'The proton NMR spectrum in acute EAE: The significance of the change in the Cho:Cr ratio', *Magnetic Resonance in Medicine*. doi: 10.1002/mrm.1910290605.

Briellmann, R. S. *et al*. (2002) 'Seizure-associated hippocampal volume loss: A longitudinal magnetic resonance study of temporal lobe epilepsy', *Annals of Neurology*. doi: 10.1002/ana.10171.

Brodie, M. J. *et al*. (2012) 'Patterns of treatment response in newly diagnosed epilepsy', *Neurology*. doi: 10.1212/WNL.0b013e3182563b19.

Brorson, L. O. and Wranne, L. (1987) 'Long-Term Prognosis in Childhood Epilepsy: Survival and Seizure Prognosis', *Epilepsia*. doi: 10.1111/j.1528-1157.1987.tb03651.x.

Broyd, S. J. *et al*. (2009) 'Default-mode brain dysfunction in mental disorders: A

systematic review', *Neuroscience and Biobehavioral Reviews*. doi: 10.1016/j.neubiorev.2008.09.002.
Bürgel, U. *et al*. (1999) 'Mapping of histologically identified long fiber tracts in human cerebral hemispheres to the MRI volume of a reference brain: Position and spatial variability of the optic radiation', *NeuroImage*. doi: 10.1006/nimg.1999.0497.
Butler, T. *et al*. (2016) 'Transient and chronic seizure-induced inflammation in human focal epilepsy', *Epilepsia*. doi: 10.1111/epi.13457.
Calcagnotto, M. E., Barbarosie, M. and Avoli, M. (2000) 'Hippocampus-entorhinal cortex loop and seizure generation in the young rodent limbic system', *Journal of Neurophysiology*. doi: 10.1152/jn.2000.83.5.3183.
Camfield, C. *et al*. (1993) 'Outcome of childhood epilepsy: A population-based study with a simple predictive scoring system for those treated with medication', *Journal of Pediatrics*. doi: 10.1016/S0022-3476(09)90008-7.
Campos, B. A. G. *et al*. (2010) 'Proton MRS may predict AED response in patients with TLE', *Epilepsia*. doi: 10.1111/j.1528-1167.2009.02379.x.
Campos, B. M. *et al*. (2015) 'White matter abnormalities associate with type and localization of focal epileptogenic lesions', *Epilepsia*. doi: 10.1111/epi.12871.
Capizzano, A. A. *et al*. (2002) 'Multisection proton MR spectroscopy for mesial temporal lobe epilepsy', *American Journal of Neuroradiology*.
Casetta Granieri, E., Monetti, V.C., Gilli, G., Tola, M.R., Paolino, E., Govoni, V., Iezzi, E., I. *et al*. (1999) 'Early predictors of intractability in childhood epilepsy: a community-based case-control study in Copparo, Italy.', *Acta neurologica Scandinavica*.
Cendes, F. *et al*. (1993) 'Mri volumetric measurement of amygdala and hippocampus in temporal lobe epilepsy', *Neurology*. doi: 10.1212/wnl.43.4.719.
Cendes, F. *et al*. (1997) 'Normalization of neuronal metabolic dysfunction after surgery for temporal lobe epilepsy: Evidence from proton MR spectroscopic imaging', *Neurology*. doi: 10.1212/WNL.49.6.1525.
Cendes, F. *et al*. (2016) 'Neuroimaging of epilepsy', in *Handbook of Clinical Neurology*. doi: 10.1016/B978-0-444-53486-6.00051-X.
Centeno, M. *et al*. (2014) 'Structural changes in the temporal lobe and piriform cortex in frontal lobe epilepsy', *Epilepsy Research*. doi: 10.1016/j.eplepsyres.2014.03.001.

Chang, L. *et al*. (2013) 'Magnetic resonance spectroscopy to assess neuroinflammation and neuropathic pain', *Journal of Neuroimmune Pharmacology*. doi: 10.1007/s11481-013-9460-x.

Chanraud, S. *et al*. (2010) 'MR diffusion tensor imaging: A window into white matter integrity of the working brain', *Neuropsychology Review*. doi: 10.1007/s11065-010-9129-7.

Chen, Y. *et al*. (2021) 'Probabilistic mapping of thalamic nuclei and thalamocortical functional connectivity in idiopathic generalised epilepsy', *Human Brain Mapping*. doi: 10.1002/hbm.25644.

Chernov, M. F. *et al*. (2009) 'Role of proton magnetic resonance spectroscopy in preoperative evaluation of patients with mesial temporal lobe epilepsy', *Journal of the Neurological Sciences*. doi: 10.1016/j.jns.2009.07.004.

Child, N. D. and Benarroch, E. E. (2013) 'Anterior nucleus of the thalamus:Functional organization and clinical implications', *Neurology*. doi: 10.1212/01.wnl.0000436078.95856.56.

Choi, H. and Morrell, M. J. (2003) 'Review of lamotrigine and its clinical applications in epilepsy', *Expert Opinion on Pharmacotherapy*. doi: 10.1517/14656566.4.2.243.

Christensen, J. *et al*. (2009) 'Long-term risk of epilepsy after traumatic brain injury in children and young adults: a population-based cohort study', *The Lancet*. doi: 10.1016/S0140-6736(09)60214-2.

Coan, A. C. *et al*. (2009) 'Seizure frequency and lateralization affect progression of atrophy in temporal lobe epilepsy', *Neurology*. doi: 10.1212/WNL.0b013e3181b783dd.

Colnaghi, S. *et al*. (2017) 'Parahippocampal involvement in mesial temporal lobe epilepsy with hippocampal sclerosis: A proof of concept from memory-guided saccades', *Frontiers in Neurology*. doi: 10.3389/fneur.2017.00595.

Concha, L. *et al*. (2009) 'White-matter diffusion abnormalities in temporal-lobe epilepsy with and without mesial temporal sclerosis', *Journal of Neurology, Neurosurgery and Psychiatry*, 80(3), pp. 312–319. doi: 10.1136/jnnp.2007.139287.

Concha, L. *et al*. (2010) 'In vivo diffusion tensor imaging and histopathology of the fimbria-fornix in temporal lobe epilepsy', *Journal of Neuroscience*. doi: 10.1523/JNEUROSCI.1619-09.2010.

Concha, L. *et al*. (2012) 'Spatial patterns of water diffusion along white matter tracts in temporal lobe epilepsy', *Neurology*. doi: 10.1212/WNL.0b013e31826170b6.
Concha, L., Beaulieu, C. and Gross, D. W. (2005) 'Bilateral limbic diffusion abnormalities in unilateral temporal lobe epilepsy', *Annals of Neurology*. doi: 10.1002/ana.20334.
Connelly, A. *et al*. (1994) 'Magnetic resonance spectroscopy in temporal lobe epilepsy', *Neurology*. doi: 10.1212/wnl.44.8.1411.
da Costa Leite, C. and Castillo, M. (2016) *Diffusion Weighted and Diffusion Tensor Imaging: A Clinical Guide*. Edited by C. da C. Leite, C. da C. Leite, and M. Castillo. Stuttgart: Georg Thieme Verlag. doi: 10.1055/b-003-129431.
Datar, A. *et al*. (2019) 'The Roles of Microtubules and Membrane Tension in Axonal Beading, Retraction, and Atrophy', *Biophysical Journal*. doi: 10.1016/j.bpj.2019.07.046.
Deleo, F. *et al*. (2018) 'Histological and MRI markers of white matter damage in focal epilepsy', *Epilepsy Research*. doi: 10.1016/j.eplepsyres.2017.11.010.
Diaz-Arrastia, R. *et al*. (2003) 'Increased risk of late posttraumatic seizures associated with inheritance of APOE ε4 allele', *Archives of Neurology*. doi: 10.1001/archneur.60.6.818.
Díaz, B. *et al*. (2012) 'Dysfunction of the auditory thalamus in developmental dyslexia', *Proceedings of the National Academy of Sciences of the United States of America*. doi: 10.1073/pnas.1119828109.
Dibbens, L. M. *et al*. (2013) 'Mutations in DEPDC5 cause familial focal epilepsy with variable foci', *Nature Genetics*. doi: 10.1038/ng.2599.
Doelken, M. T. *et al*. (2008) '1H-MRS profile in MRI positive- versus MRI negative patients with temporal lobe epilepsy', *Seizure*. doi: 10.1016/j.seizure.2008.01.008.
Doelken, M. T. *et al*. (2010) 'Multi-voxel magnetic resonance spectroscopy at 3 T in patients with idiopathic generalised epilepsy', *Seizure*. doi: 10.1016/j.seizure.2010.07.005.
Dreifuss, S. *et al*. (2001) 'Volumetric measurements of subcortical nuclei in patients with temporal lobe epilepsy', *Neurology*. doi: 10.1212/WNL.57.9.1636.
Dubé, C. M. *et al*. (2010) 'Epileptogenesis provoked by prolonged experimental febrile seizures: Mechanisms and biomarkers', *Journal of Neuroscience*. doi: 10.1523/JNEUROSCI.0551-10.2010.

Duncan, J. S. (1996) 'Magnetic resonance spectroscopy', *Epilepsia*. doi: 10.1111/j.1528-1157.1996.tb00622.x.
Epilepsy Action UK (2019) 'Epilepsy facts and terminology'.
Epilepsy, C. G. for the S. of (1992) 'Prognosis of Epilepsy in Newly Referred Patients: A Multicenter Prospective Study of the Effects of Monotherapy on the Long-Term Course of Epilepsy', *Epilepsia*. doi: 10.1111/j.1528-1157.1992.tb02281.x.
Eriksson, S. H. *et al*. (2007) 'Correlation of quantitative MRI and neuropathology in epilepsy surgical resection specimens-T2 correlates with neuronal tissue in gray matter', *NeuroImage*. doi: 10.1016/j.neuroimage.2007.04.051.
Falangola, M. F. *et al*. (2008) 'Age-related non-Gaussian diffusion patterns in the prefrontal brain', *Journal of Magnetic Resonance Imaging*, 28(6), pp. 1345–1350. doi: 10.1002/jmri.21604.
Falangola, M. F. *et al*. (2013) 'Non-Gaussian diffusion MRI assessment of brain microstructure in mild cognitive impairment and Alzheimer's disease', *Magnetic Resonance Imaging*. doi: 10.1016/j.mri.2013.02.008.
Farquharson, S. *et al*. (2013) 'White matter fiber tractography: Why we need to move beyond DTI', *Journal of Neurosurgery*. doi: 10.3171/2013.2.JNS121294.
Ficker, D. M. *et al*. (1998) 'Population-based study of the incidence of sudden unexplained death in epilepsy', *Neurology*, 51(5), pp. 1270–1274. doi: 10.1212/WNL.51.5.1270.
Fieremans, E., Jensen, J. H. and Helpern, J. A. (2011) 'White matter characterization with diffusional kurtosis imaging', *NeuroImage*, 58(1), pp. 177–188. doi: 10.1016/j.neuroimage.2011.06.006.
Fischl, B. (2012) 'FreeSurfer', *NeuroImage*. doi: 10.1016/j.neuroimage.2012.01.021.
Fisher, R. *et al*. (2010) 'Electrical stimulation of the anterior nucleus of thalamus for treatment of refractory epilepsy', *Epilepsia*. doi: 10.1111/j.1528-1167.2010.02536.x.
Fisher, R. S. *et al*. (2005) 'Epileptic seizures and epilepsy: Definitions proposed by the International League Against Epilepsy (ILAE) and the International Bureau for Epilepsy (IBE)', *Epilepsia*. doi: 10.1111/j.0013-9580.2005.66104.x.
Fisher, R. S. *et al*. (2014) 'ILAE Official Report: A practical clinical definition of epilepsy', *Epilepsia*. doi: 10.1111/epi.12550.
Fisher, R. S. *et al*. (2017) 'Instruction manual for the ILAE 2017 operational

classification of seizure types', *Epilepsia*. doi: 10.1111/epi.13671.
Fu, L. *et al*. (2017) 'Therapeutic effects of anti-HMGB1 monoclonal antibody on pilocarpine-induced status epilepticus in mice', *Scientific Reports*. doi: 10.1038/s41598-017-01325-y.
Fuerst, D. *et al*. (2003) 'Hippocampal sclerosis is a progressive disorder: A longitudinal volumetric MRI study', *Annals of Neurology*. doi: 10.1002/ana.10509.
Gadian, D. G. *et al*. (1994) 'H magnetic resonance spectroscopy in the investigation of intractable epilepsy', *Acta Neurologica Scandinavica*. doi: 10.1111/j.1600-0404.1994.tb05202.x.
Gallagher, M. and Chiba, A. A. (1996) 'The amygdala and emotion', *Current Opinion in Neurobiology*. doi: 10.1016/S0959-4388(96)80076-6.
Gao, Y. *et al*. (2012) 'Diffusion abnormalities in temporal lobes of children with temporal lobe epilepsy: A preliminary diffusional kurtosis imaging study and comparison with diffusion tensor imaging', *NMR in Biomedicine*. doi: 10.1002/nbm.2809.
Garbelli, R. *et al*. (2012) 'Blurring in patients with temporal lobe epilepsy: Clinical, high-field imaging and ultrastructural study', *Brain*. doi: 10.1093/brain/aws149.
Garcia, M. *et al*. (2009) 'Valproate-induced metabolic changes in patients with epilepsy: Assessment with 1H-MRS', *Epilepsia*. doi: 10.1111/j.1528-1167.2008.01801.x.
Geerts, A. T. *et al*. (2010) 'Course and outcome of childhood epilepsy: A 15-year follow-up of the Dutch Study of Epilepsy in Childhood', *Epilepsia*. doi: 10.1111/j.1528-1167.2010.02546.x.
Gershen, L. D. *et al*. (2015a) 'Neuroinflammation in temporal lobe epilepsy measured using positron emission tomographic imaging of translocator protein', *JAMA Neurology*, 72(8), pp. 882–888. doi: 10.1001/jamaneurol.2015.0941.
Gershen, L. D. *et al*. (2015b) 'Neuroinflammation in temporal lobe epilepsy measured using positron emission tomographic imaging of translocator protein', *JAMA Neurology*. doi: 10.1001/jamaneurol.2015.0941.
Gill, S. S. *et al*. (1989) 'Brain metabolites as 1H NMR markers of neuronal and glial disorders', *NMR in Biomedicine*. doi: 10.1002/nbm.1940020505.
Gilliam, F. (2002) 'Optimizing health outcomes in active epilepsy', *Neurology*. doi: 10.1212/wnl.58.8_suppl_5.s9.

Glenn, G. R. *et al*. (2016) 'Epilepsy-related cytoarchitectonic abnormalities along white matter pathways', *Journal of Neurology, Neurosurgery and Psychiatry*, 87(9), pp. 930–936. doi: 10.1136/jnnp-2015-312980.

Gloveli, T., Schmitz, D. and Heinemann, U. (1998) 'Interaction between superficial layers of the entorhinal cortex and the hippocampus in normal and epileptic temporal lobe', in *Epilepsy Research*. doi: 10.1016/S0920-1211(98)00050-3.

Goddard, G. V. (1967) 'Development of epileptic seizures through brain stimulation at low intensity', *Nature*. doi: 10.1038/2141020a0.

Godlewska, B. R. *et al*. (2019) 'Changes in brain Glx in depressed bipolar patients treated with lamotrigine: A proton MRS study', *Journal of Affective Disorders*. doi: 10.1016/j.jad.2018.12.092.

Gong, J. *et al*. (2017) 'Microstructural alterations of white matter in juvenile myoclonic epilepsy', *Epilepsy Research*. doi: 10.1016/j.eplepsyres.2017.04.002.

Gong, N. J. *et al*. (2013) 'Correlations between microstructural alterations and severity of cognitive deficiency in Alzheimer's disease and mild cognitive impairment: A diffusional kurtosis imaging study', *Magnetic Resonance Imaging*. doi: 10.1016/j.mri.2012.10.027.

Goodridge, D. M. G. and Shorvon, S. D. (1983) 'Epileptic seizure in a population of 6000. II: Treatment and prognosis', *British Medical Journal*. doi: 10.1136/bmj.287.6393.645.

Gourfinkel-An, I. *et al*. (2004) 'Monogenic idiopathic epilepsies', *Lancet Neurology*. doi: 10.1016/S1474-4422(04)00706-9.

Greve, D. N. and Fischl, B. (2009) 'Accurate and robust brain image alignment using boundary-based registration', *NeuroImage*. doi: 10.1016/j.neuroimage.2009.06.060.

Gross, D. W., Concha, L. and Beaulieu, C. (2006) 'Extratemporal white matter abnormalities in mesial temporal lobe epilepsy demonstrated with diffusion tensor imaging', *Epilepsia*, 47(8), pp. 1360–1363. doi: 10.1111/j.1528-1167.2006.00603.x.

Hagler Jr., D. J. *et al*. (2009) 'diffusion tensor atlas : Application to temporal lobe epilepsy', *Human brain mapping*, 30(5), pp. 1535–1547. doi: 10.1002/hbm.20619.Automated.

Haneef, Z., Levin, H. S. and Chiang, S. (2015) 'Brain graph topology changes associated with anti-epileptic drug use', *Brain Connectivity*. doi:

10.1089/brain.2014.0304.
Hansen, B. and Jespersen, S. N. (2016) 'Kurtosis fractional anisotropy, its contrast and estimation by proxy', *Scientific Reports*. doi: 10.1038/srep23999.
Hardus, P. *et al*. (2000) 'Concentric contraction of the visual field in patients with temporal lobe epilepsy and its association with the use of vigabatrin medication', *Epilepsia*. doi: 10.1111/j.1528-1157.2000.tb00212.x.
Harrison, N. A. *et al*. (2015) 'Quantitative magnetization transfer imaging as a biomarker for effects of Systemic inflammation on the brain', *Biological Psychiatry*. doi: 10.1016/j.biopsych.2014.09.023.
Hatton, S. N. *et al*. (2020) 'White matter abnormalities across different epilepsy syndromes in adults: An ENIGMA-Epilepsy study', *Brain*. doi: 10.1093/brain/awaa200.
Hauser, E. *et al*. (1996) 'Prognosis of childhood epilepsy in newly referred patients', *Journal of Child Neurology*. doi: 10.1177/088307389601100307.
He, X. *et al*. (2015) 'Reduced thalamocortical functional connectivity in temporal lobe epilepsy', *Epilepsia*. doi: 10.1111/epi.13085.
Heida, J. G. and Pittman, Q. J. (2005) 'Causal links between brain cytokines and experimental febrile convulsions in the rat', *Epilepsia*. doi: 10.1111/j.1528-1167.2005.00294.x.
Helbig, I. *et al*. (2008) 'Navigating the channels and beyond: unravelling the genetics of the epilepsies', *The Lancet Neurology*. doi: 10.1016/S1474-4422(08)70039-5.
Helms, G. *et al*. (2006) 'Increased thalamus levels of glutamate and glutamine (Glx) in patients with idiopathic generalised epilepsy', *Journal of Neurology, Neurosurgery and Psychiatry*. doi: 10.1136/jnnp.2005.074682.
Henry, T. R. *et al*. (1990) 'Quantifying interictal metabolic activity in human temporal lobe epilepsy', *Journal of Cerebral Blood Flow and Metabolism*. doi: 10.1038/jcbfm.1990.128.
Hirvonen, J. *et al*. (2012) 'Increased in vivo expression of an inflammatory marker in temporal lobe epilepsy', *Journal of Nuclear Medicine*. doi: 10.2967/jnumed.111.091694.
Hitiris, N. *et al*. (2007) 'Predictors of pharmacoresistant epilepsy', *Epilepsy Research*. doi: 10.1016/j.eplepsyres.2007.06.003.

Hodaie, M. *et al*. (2002) 'Chronic anterior thalamus stimulation for intractable epilepsy', *Epilepsia*. doi: 10.1046/j.1528-1157.2002.26001.x.
Holt, R. L. *et al*. (2011) 'Structural connectivity of the frontal lobe in children with drug-resistant partial epilepsy', *Epilepsy and Behavior*. doi: 10.1016/j.yebeh.2011.03.016.
Hui, E. S. *et al*. (2008) 'Towards better MR characterization of neural tissues using directional diffusion kurtosis analysis', *NeuroImage*. doi: 10.1016/j.neuroimage.2008.04.237.
Iglesias, J. E. *et al*. (2018) 'A probabilistic atlas of the human thalamic nuclei combining ex vivo MRI and histology', *NeuroImage*. doi: 10.1016/j.neuroimage.2018.08.012.
ILAE (1989) 'Proposal for Revised Classification of Epilepsies and Epileptic Syndromes.', *Epilepsia*, 30(4), pp. 389–399. doi: 10.1111/j.1528-1157.1989.tb05316.x.
International, I. (2017) 'HMGB1 ELISA Protocol', pp. 0–8.
Iori, V. *et al*. (2013) 'Receptor for Advanced Glycation Endproducts is upregulated in temporal lobe epilepsy and contributes to experimental seizures', *Neurobiology of Disease*. doi: 10.1016/j.nbd.2013.03.006.
Ishida, S. *et al*. (2013) 'Mutations of DEPDC5 cause autosomal dominant focal epilepsies', *Nature Genetics*. doi: 10.1038/ng.2601.
Jager, J., Putnick, D. L. and Bornstein, M. H. (2017) 'II. MORE THAN JUST CONVENIENT: THE SCIENTIFIC MERITS OF HOMOGENEOUS CONVENIENCE SAMPLES', *Monographs of the Society for Research in Child Development*. doi: 10.1111/mono.12296.
Jallon, P. and Picard, F. (2001) 'Bodyweight gain and anticonvulsants: A comparative review', *Drug Safety*. doi: 10.2165/00002018-200124130-00004.
Janak, P. H. and Tye, K. M. (2015) 'From circuits to behaviour in the amygdala', *Nature*. doi: 10.1038/nature14188.
Jelescu, I. O. and Budde, M. D. (2017) 'Design and validation of diffusion MRI models of white matter', *Frontiers in Physics*. doi: 10.3389/fphy.2017.00061.
Jenkinson, M. *et al*. (2002) 'Improved optimization for the robust and accurate linear registration and motion correction of brain images', *NeuroImage*. doi: 10.1016/S1053-8119(02)91132-8.

Jenkinson, M. and Smith, S. (2001) 'A global optimisation method for robust affine registration of brain images', *Medical Image Analysis*. doi: 10.1016/S1361-8415(01)00036-6.

Jensen, J. H. and Helpern, J. A. (2010) 'MRI quantification of non-Gaussian water diffusion by kurtosis analysis', *NMR in Biomedicine*. doi: 10.1002/nbm.1518.

Jensen, J. H., Russell Glenn, G. and Helpern, J. A. (2016) 'Fiber ball imaging', *NeuroImage*. Elsevier Inc., 124, pp. 824–833. doi: 10.1016/j.neuroimage.2015.09.049.

Jiang, Y. *et al*. (2017) 'Investigation of altered microstructure in patients with drug refractory epilepsy using diffusion tensor imaging', *Neuroradiology*. Neuroradiology, 59(6), pp. 597–608. doi: 10.1007/s00234-017-1835-x.

Johansen-Berg, H. *et al*. (2005) 'Functional-anatomical validation and individual variation of diffusion tractography-based segmentation of the human thalamus', *Cerebral Cortex*. doi: 10.1093/cercor/bhh105.

Johnson, G. D., Kuzniecky, R. I. and Pell, G. S. (2005) 'Principles of Magnetic Resonance Imaging', in *Magnetic Resonance in Epilepsy: Neuroimaging Techniques*. Second.

Johnson, R. T. *et al*. (2014) 'Diffusion properties of major white matter tracts in young, typically developing children', *NeuroImage*. doi: 10.1016/j.neuroimage.2013.11.025.

Jokeit, H., Okujava, M. and Woermann, F. G. (2001) 'Memory fMRI lateralizes temporal lobe epilepsy', *Neurology*. doi: 10.1212/WNL.57.10.1786.

Jong, S. P. *et al*. (2006) 'High mobility group box 1 protein interacts with multiple Toll-like receptors', *American Journal of Physiology - Cell Physiology*. doi: 10.1152/ajpcell.00401.2005.

Jooma, R. *et al*. (1995) 'Seizure control and extent of mesial temporal resection', *Acta Neurochirurgica*. doi: 10.1007/BF01404946.

Josephson, C. B., Jetté, N. and Jett, N. (2017) 'International Review of Psychiatry Psychiatric comorbidities in epilepsy Psychiatric comorbidities in epilepsy', *International Review of Psychiatry*, 29(5), pp. 409–424. doi: 10.1080/09540261.2017.1302412.

Jutila, L. *et al*. (2001) 'MR volumetry of the entorhinal, perirhinal, and temporopolar cortices in drug-refractory temporal lobe epilepsy', in *American Journal of*

Neuroradiology.

Kairiss, E. W., Racine, R. J. and Smith, G. K. (1984) 'The development of the interictal spike during kindling in the rat', *Brain Research*. doi: 10.1016/0006-8993(84)91185-5.

Kälviäinen, R. and Salmenperä, T. (2002) 'Do recurrent seizures cause neuronal damage? A series of studies with MRI volumetry in adults with partial epilepsy', in *Progress in Brain Research*. doi: 10.1016/S0079-6123(02)35026-X.

Keezer, M. R., Sisodiya, S. M. and Sander, J. W. (2016) 'Comorbidities of epilepsy: Current concepts and future perspectives', *The Lancet Neurology*. Elsevier Ltd, 15(1), pp. 106–115. doi: 10.1016/S1474-4422(15)00225-2.

Keller, Simon S. *et al*. (2002) 'Voxel-based morphometric comparison of hippocampal and extrahippocampal abnormalities in patients with left and right hippocampal atrophy', *NeuroImage*. doi: 10.1006/nimg.2001.1072.

Keller, S S *et al*. (2002) 'Voxel based morphometry of grey matter abnormalities in patients with medically intractable temporal lobe epilepsy: effects of side of seizure onset and epilepsy duration.', *Journal of neurology, neurosurgery, and psychiatry*, 73(6), pp. 648–55. Available at: http://www.ncbi.nlm.nih.gov/pubmed/12438464 (Accessed: 6 October 2016).

Keller, S. S. *et al*. (2007) 'Persistent seizures following left temporal lobe surgery are associated with posterior and bilateral structural and functional brain abnormalities', *Epilepsy Research*. doi: 10.1016/j.eplepsyres.2007.02.005.

Keller, S. S., Richardson, M. P., O'Muircheartaigh, J., *et al*. (2015) 'Morphometric MRI alterations and postoperative seizure control in refractory temporal lobe epilepsy', *Human Brain Mapping*. doi: 10.1002/hbm.22722.

Keller, S. S., Richardson, M. P., Schoene-Bake, J. C., *et al*. (2015) 'Thalamotemporal alteration and postoperative seizures in temporal lobe epilepsy', *Annals of Neurology*. doi: 10.1002/ana.24376.

Keller, S. S. *et al*. (2017) 'Preoperative automated fibre quantification predicts postoperative seizure outcome in temporal lobe epilepsy', *Brain*, 140(1), pp. 68–82. doi: 10.1093/brain/aww280.

Keller, S. S. and Roberts, N. (2008) 'Voxel-based morphometry of temporal lobe epilepsy: An introduction and review of the literature', *Epilepsia*, 49(5), pp. 741–757. doi: 10.1111/j.1528-1167.2007.01485.x.

Khan, N. *et al*. (1997) 'Thalamic glucose metabolism in temporal lobe epilepsy measured with 18F-FDG positron emission tomography (PET)', *Epilepsy Research*. doi: 10.1016/S0920-1211(97)00049-1.
Kim, H. C. *et al*. (2017) 'Can we predict drug response by volumes of the corpus callosum in newly diagnosed focal epilepsy?', *Brain and Behavior*. doi: 10.1002/brb3.751.
Kim, J. E. *et al*. (2010) 'Levetiracetam inhibits interleukin-1β inflammatory responses in the hippocampus and piriform cortex of epileptic rats', *Neuroscience Letters*. doi: 10.1016/j.neulet.2010.01.018.
Kinomura, S. *et al*. (1996) 'Activation by attention of the human reticular formation and thalamic intralaminar nuclei', *Science*. doi: 10.1126/science.271.5248.512.
Kirov, I. I. *et al*. (2018) 'Whole brain neuronal abnormalities in focal quantified with proton MR spectroscopy', *Epilepsy Research*. doi: 10.1016/j.eplepsyres.2017.11.017.
Kleban, E. *et al*. (2020) 'Strong diffusion gradients allow the separation of intra- and extra-axonal gradient-echo signals in the human brain', *NeuroImage*. doi: 10.1016/j.neuroimage.2020.116793.
Klein, P. *et al*. (2018) 'Commonalities in epileptogenic processes from different acute brain insults: Do they translate?', *Epilepsia*. doi: 10.1111/epi.13965.
Ko, T. S. and Holmes, G. L. (1999) 'EEG and clinical predictors of medically intractable childhood epilepsy', *Clinical Neurophysiology*. doi: 10.1016/S1388-2457(99)00068-1.
Kosif, R. (2016) 'The Thalamus: A Review of its Functional Anatomy', *Medical Research Archives*, 4(8). doi: 10.18103/mra.v4i8.740.
Kovesdi, E. *et al*. (2012) 'Acute minocycline treatment mitigates the symptoms of mild blast-induced traumatic brain injury', *Frontiers in Neurology*. doi: 10.3389/fneur.2012.00111.
Kramer, M. A. and Cash, S. S. (2012) 'Epilepsy as a disorder of cortical network organization', *Neuroscientist*. doi: 10.1177/1073858411422754.
Kreilkamp, B. A. K. *et al*. (2017) 'Automated tractography in patients with temporal lobe epilepsy using TRActs Constrained by UnderLying Anatomy (TRACULA)', *NeuroImage: Clinical*. The Authors, 14, pp. 67–76. doi: 10.1016/j.nicl.2017.01.003.
Kreilkamp, B. A. K. *et al*. (2019) 'Comparison of manual and automated fiber

quantification tractography in patients with temporal lobe epilepsy', *NeuroImage: Clinical*. Elsevier, 24(September), p. 102024. doi: 10.1016/j.nicl.2019.102024.
Kreilkamp, B. A. K. *et al*. (2021) 'Altered structural connectome in non-lesional newly diagnosed focal epilepsy: Relation to pharmacoresistance', *NeuroImage: Clinical*. doi: 10.1016/j.nicl.2021.102564.
Kumar, V. J. *et al*. (2017) 'Functional anatomy of the human thalamus at rest', *NeuroImage*, 147(December 2016), pp. 678–691. doi: 10.1016/j.neuroimage.2016.12.071.
Kwan, P. *et al*. (2010) 'Definition of drug resistant epilepsy: Consensus proposal by the ad hoc Task Force of the ILAE Commission on Therapeutic Strategies', *Epilepsia*. doi: 10.1111/j.1528-1167.2009.02397.x.
Kwan, P. and Brodie, M. J. (2000) 'Early Identification of Refractory Epilepsy', *New England Journal of Medicine*. doi: 10.1056/nejm200002033420503.
Kwan, P. and Brodie, M. J. (2006) 'Refractory epilepsy: Mechanisms and solutions', *Expert Review of Neurotherapeutics*. doi: 10.1586/14737175.6.3.397.
Lallement, G *et al*. (1991) '[Involvement of glutamatergic system of amygdala in generalized seizures induced by soman: comparison with the hippocampus].', *Comptes rendus de l'Academie des sciences. Serie III, Sciences de la vie*.
Lallement, Guy *et al*. (1991) 'Effects of soman-induced seizures on different extracellular amino acid levels and on glutamate uptake in rat hippocampus', *Brain Research*. doi: 10.1016/0006-8993(91)91539-D.
Lambert, C. *et al*. (2017) 'Defining thalamic nuclei and topographic connectivity gradients in vivo', *NeuroImage*. doi: 10.1016/j.neuroimage.2016.08.028.
Law, N., Smith, M. L. and Widjaja, E. (2018) 'Thalamocortical connections and executive function in pediatric temporal and frontal lobe epilepsy', *American Journal of Neuroradiology*. doi: 10.3174/ajnr.A5691.
Lazar, M. *et al*. (2008) 'Estimation of the orientation distribution function from diffusional kurtosis imaging', *Magnetic Resonance in Medicine*. doi: 10.1002/mrm.21725.
Lee, C.-Y. *et al*. (2014) 'Diffusional kurtosis imaging reveals a distinctive pattern of microstructural alternations in idiopathic generalized epilepsy', *Acta Neurologica Scandinavica*, 130(3), pp. 148–155. doi: 10.1111/ane.12257.
Lee, C. Y. *et al*. (2013) 'Microstructural integrity of early- Versus late-Myelinating

white matter tracts in medial temporal lobe epilepsy', *Epilepsia*, 54(10), pp. 1801–1809. doi: 10.1111/epi.12353.
Leek, N. J. *et al*. (2020) 'Thalamohippocampal atrophy in focal epilepsy of unknown cause at the time of diagnosis', *European Journal of Neurology*. doi: 10.1111/ene.14565.
Li, G., Liang, X. and Lotze, M. T. (2013) 'HMGB1: The central cytokine for all lymphoid cells', *Frontiers in Immunology*. doi: 10.3389/fimmu.2013.00068.
Li, M. C. H. and Cook, M. J. (2018) 'Deep brain stimulation for drug-resistant epilepsy', *Epilepsia*. doi: 10.1111/epi.13964.
Liao, W. *et al*. (2011) 'Default mode network abnormalities in mesial temporal lobe epilepsy: A study combining fMRI and DTI', *Human Brain Mapping*. doi: 10.1002/hbm.21076.
Liu, H. *et al*. (2009) 'Task-free presurgical mapping using functional magnetic resonance imaging intrinsic activity: Laboratory investigation', *Journal of Neurosurgery*. doi: 10.3171/2008.10.JNS08846.
Liu, J. Y. W. *et al*. (2014) 'High-throughput, automated quantification of white matter neurons in mild malformation of cortical development in epilepsy', *Acta Neuropathologica Communications*. doi: 10.1186/2051-5960-2-72.
Liu, R. S. N. *et al*. (2002) 'Seizure-associated hippocampal volume loss: A longitudinal magnetic resonance study of temporal lobe epilepsy', *Annals of Neurology*, 52(6), pp. 861–861. doi: 10.1002/ana.10408.
Liu, R. S. N. *et al*. (2005) 'Cerebral damage in epilepsy: A population-based longitudinal quantitative MRI study', *Epilepsia*. doi: 10.1111/j.1528-1167.2005.51603.x.
Loprinzi, P. D. (2019) 'The effects of physical exercise on parahippocampal function', *Physiology International*. doi: 10.1556/2060.106.2019.10.
Lowenstein, D. H. (2009) 'Epilepsy after head injury: An overview', in *Epilepsia*. doi: 10.1111/j.1528-1167.2008.02004.x.
MacDonald, B. K. *et al*. (2000) 'Factors predicting prognosis of epilepsy after presentation with seizures', *Annals of Neurology*. doi: 10.1002/1531-8249(200012)48:6<833::AID-ANA3>3.0.CO;2-U.
MacIntosh, B. J. and Graham, S. J. (2013) 'Magnetic resonance imaging to visualize stroke and characterize stroke recovery: A review', *Frontiers in Neurology*. doi:

10.3389/fneur.2013.00060.
Mai, J. K. and Paxinos, G. (2012) *The human nervous system [electronic book] / edited by Jürgen K. Mai, George Paxinos, Online access with subscription: Elsevier (Sciencedirect Freedom Collection)*.
Maier, M. *et al*. (2000) 'Schizophrenia, temporal lobe epilepsy and psychosis: An in vivo magnetic resonance spectroscopy and imaging study of the hippocampus/amygdala complex', *Psychological Medicine*. doi: 10.1017/S0033291799001993.
Malekmohammadi, M., Elias, W. J. and Pouratian, N. (2015) 'Human thalamus regulates cortical activity via spatially specific and structurally constrained phase-amplitude coupling', *Cerebral Cortex*. doi: 10.1093/cercor/bht358.
Maroso, M. *et al*. (2010) 'Toll-like receptor 4 and high-mobility group box-1 are involved in ictogenesis and can be targeted to reduce seizures', *Nature Medicine*. doi: 10.1038/nm.2127.
Marson, A. *et al*. (2005) 'Immediate versus deferred antiepileptic drug treatment for early epilepsy and single seizures: A randomised controlled trial', *Lancet*. doi: 10.1016/S0140-6736(05)66694-9.
Masterton, R. A., Carney, P. W. and Jackson, G. D. (2012) 'Cortical and thalamic resting-state functional connectivity is altered in childhood absence epilepsy', *Epilepsy Research*. doi: 10.1016/j.eplepsyres.2011.12.014.
Mattson, R. H., Cramer, J. A. and Collins, J. F. (1996) 'Prognosis for total control of complex partial and secondarily generalized tonic clonic seizures', *Neurology*. doi: 10.1212/WNL.47.1.68.
McDonald, C. R. *et al*. (2008) 'Diffusion tensor imaging correlates of memory and language impairments in temporal lobe epilepsy', *Neurology*, 71(23), pp. 1869–1876. doi: 10.1212/01.wnl.0000327824.05348.3b.
McGill, M. L. *et al*. (2012) 'Default mode network abnormalities in idiopathic generalized epilepsy', *Epilepsy and Behavior*. doi: 10.1016/j.yebeh.2012.01.013.
McKenna, F. F. *et al*. (2019) 'Diffusion kurtosis imaging of gray matter in schizophrenia', *Cortex*. doi: 10.1016/j.cortex.2019.08.013.
McKinnon, E. T. *et al*. (2017) 'Dependence on b-value of the direction-averaged diffusion-weighted imaging signal in brain', *Magnetic Resonance Imaging*. doi: 10.1016/j.mri.2016.10.026.

McKinnon, E. T., Helpern, J. A. and Jensen, J. H. (2018) 'Modeling white matter microstructure with fiber ball imaging', *NeuroImage*. Elsevier Ltd, 176(December 2017), pp. 11–21. doi: 10.1016/j.neuroimage.2018.04.025.

McLean, M. A. and Cross, J. J. (2009) 'Magnetic resonance spectroscopy: Principles and applications in neurosurgery', *British Journal of Neurosurgery*. doi: 10.1080/02688690802491673.

Meiners, L. C. *et al*. (2000) 'Proton magnetic resonance spectroscopy of temporal lobe white matter in patients with histologically proven hippocampal sclerosis', *Journal of Magnetic Resonance Imaging*. doi: 10.1002/(SICI)1522-2586(200001)11:1<25::AID-JMRI4>3.0.CO;2-Z.

Merboldt, K. D., Hanicke, W. and Frahm, J. (1985) 'Self-diffusion NMR imaging using stimulated echoes', *Journal of Magnetic Resonance (1969)*. doi: 10.1016/0022-2364(85)90111-8.

Miettinen, R. *et al*. (1998) 'Hippocampal damage after injection of kainic acid into the rat entorhinal cortex', *Brain Research*. doi: 10.1016/S0006-8993(98)00915-9.

Miller, J. W. and Goodkin, H. P. (2014) *Epilepsy*, *Epilepsy*. doi: 10.1002/9781118456989.

Mintzer, S. (2010) 'Metabolic consequences of antiepileptic drugs', *Current Opinion in Neurology*. doi: 10.1097/WCO.0b013e32833735e7.

Mirski, M. A. *et al*. (1997) 'Anticonvulsant effect of anterior thalamic high frequency electrical stimulation in the rat', *Epilepsy Research*. doi: 10.1016/S0920-1211(97)00034-X.

Mirski, M. A. and Ferrendelli, J. A. (1986) 'Anterior thalamic mediation of generalized pentylenetetrazol seizures', *Brain Research*. doi: 10.1016/0006-8993(86)91511-8.

Mirski, M. A. and Ferrendelli, J. A. (1987) 'Interruption of the connections of the mammillary bodies protects against generalized pentylenetetrazol seizures in guinea pigs', *Journal of Neuroscience*. doi: 10.1523/jneurosci.07-03-00662.1987.

Moeller, F. *et al*. (2011) 'Functional connectivity in patients with idiopathic generalized epilepsy', *Epilepsia*. doi: 10.1111/j.1528-1167.2010.02938.x.

Mohan, M. *et al*. (2018) 'The long-term outcomes of epilepsy surgery', *PLoS ONE*. doi: 10.1371/journal.pone.0196274.

Mohanraj, R. and Brodie, M. J. (2013) 'Early predictors of outcome in newly

diagnosed epilepsy', *Seizure*. doi: 10.1016/j.seizure.2013.02.002.
Morel, A. (2007) *Stereotactic Atlas of the Human Thalamus and Basal Ganglia*, *Stereotactic Atlas of the Human Thalamus and Basal Ganglia*. doi: 10.3109/9781420016796.
Moss, H. G. *et al*. (2019) 'Optimization of data acquisition and analysis for fiber ball imaging', *NeuroImage*. doi: 10.1016/j.neuroimage.2019.07.005.
Mountford, C. E. *et al*. (2010) 'Neurospectroscopy: The past, present and future', *Chemical Reviews*. doi: 10.1021/cr900250y.
Mtui, E., Gruener, G. and FitzGerald, M. J. T. (2011) *Clinical Neuroanatomy and Neuroscience*. 6th Editio. Elsevier Saunders.
Najdenovska, E. *et al*. (2018) 'In-vivo probabilistic atlas of human thalamic nuclei based on diffusion-weighted magnetic resonance imaging', *Scientific Data*. doi: 10.1038/sdata.2018.270.
Ngamsombat, C. *et al*. (2020) 'Axonal damage in the optic radiation assessed by white matter tract integrity metrics is associated with retinal thinning in multiple sclerosis', *NeuroImage: Clinical*. doi: 10.1016/j.nicl.2020.102293.
Novikov, D. S., Kiselev, V. G. and Jespersen, S. N. (2018) 'On modeling', *Magnetic Resonance in Medicine*. doi: 10.1002/mrm.27101.
O'Dwyer, R. *et al*. (2010) 'Differences in corpus callosum volume and diffusivity between temporal and frontal lobe epilepsy', *Epilepsy and Behavior*. doi: 10.1016/j.yebeh.2010.06.049.
Ohye, C. and Shibazaki, T. (2001) 'Behavior of Thalamic Neurons in the Movement Disorders — Tremor and Dystonia', in *Basal Ganglia and Thalamus in Health and Movement Disorders*. doi: 10.1007/978-1-4615-1235-6_25.
Van Paesschen, W. *et al*. (1998) 'Longitudinal quantitative hippocampal magnetic resonance imaging study of adults with newly diagnosed partial seizures: One-year follow-up results', *Epilepsia*. doi: 10.1111/j.1528-1157.1998.tb01432.x.
Pan, J. W. and Kuzniecky, R. I. (2015) 'Utility of magnetic resonance spectroscopic imaging for human epilepsy.', *Quantitative imaging in medicine and surgery*. doi: 10.3978/j.issn.2223-4292.2015.01.03.
Pardoe, H. R. *et al*. (2017) 'Structural brain changes in medically refractory focal epilepsy resemble premature brain aging', *Epilepsy Research*. doi: 10.1016/j.eplepsyres.2017.03.007.

Pardoe, H. R., Berg, A. T. and Jackson, G. D. (2013) 'Sodium valproate use is associated with reduced parietal lobe thickness and brain volume', *Neurology*. doi: 10.1212/WNL.0b013e318292a2e5.

Park, K. M. *et al*. (2018) 'Reduction of ipsilateral thalamic volume in temporal lobe epilepsy with hippocampal sclerosis', *Journal of Clinical Neuroscience*. doi: 10.1016/j.jocn.2018.06.025.

Pascente, R. *et al*. (2016) 'Cognitive deficits and brain myo-Inositol are early biomarkers of epileptogenesis in a rat model of epilepsy', *Neurobiology of Disease*. Elsevier Inc., 93, pp. 146–155. doi: 10.1016/j.nbd.2016.05.001.

Pasternak, O. *et al*. (2009) 'Free water elimination and mapping from diffusion MRI', *Magnetic Resonance in Medicine*, 62(3), pp. 717–730. doi: 10.1002/mrm.22055.

Pasternak, O. *et al*. (2012) 'Excessive extracellular volume reveals a neurodegenerative pattern in schizophrenia onset.', *The Journal of Neuroscience*, 32(48), pp. 17365–72. doi: 10.1523/JNEUROSCI.2904-12.2012.

Pasternak, O. *et al*. (2014) 'Hockey concussion education project, Part 2. Microstructural white matter alterations in acutely concussed ice hockey players: A longitudinal free-water MRI study - Clinical article', *Journal of Neurosurgery*. doi: 10.3171/2013.12.JNS132090.

Paudel, Y. N. *et al*. (2018) 'HMGB1: A common biomarker and potential target for TBI, neuroinflammation, epilepsy, and cognitive dysfunction', *Frontiers in Neuroscience*. doi: 10.3389/fnins.2018.00628.

Pauletti, A. *et al*. (2017) 'Targeting oxidative stress improves disease outcomes in a rat model of acquired epilepsy', *Brain*. doi: 10.1093/brain/awx117.

Pedersen, M. *et al*. (2016) 'Abnormal Brain Areas Common to the Focal Epilepsies: Multivariate Pattern Analysis of fMRI', *Brain Connectivity*. doi: 10.1089/brain.2015.0367.

Pegg, E. J. *et al*. (2021) 'Functional network topology in drug resistant and well-controlled idiopathic generalized epilepsy: a resting state functional MRI study', *Brain Communications*. doi: 10.1093/braincomms/fcab196.

Peixoto-Santos, J. E. *et al*. (2020) 'Histological correlates of hippocampal magnetization transfer images in drug-resistant temporal lobe epilepsy patients', *NeuroImage: Clinical*. doi: 10.1016/j.nicl.2020.102463.

Pereira, F. R. S. *et al*. (2010) 'Asymmetrical hippocampal connectivity in mesial temporal lobe epilepsy: Evidence from resting state fMRI', *BMC Neuroscience*. doi: 10.1186/1471-2202-11-66.

Perucca, P. *et al*. (2017) 'Real-world utility of whole exome sequencing with targeted gene analysis for focal epilepsy', *Epilepsy Research*. doi: 10.1016/j.eplepsyres.2017.02.001.

Perucca, P. and Gilliam, F. G. (2012) 'Adverse effects of antiepileptic drugs', *The Lancet Neurology*. doi: 10.1016/S1474-4422(12)70153-9.

Petroff, O. A., Mattson, R. H. and Rothman, D. L. (2000) 'Proton MRS: GABA and glutamate.', *Advances in neurology*.

Picard, F. *et al*. (2014) 'DEPDC5 mutations in families presenting as autosomal dominant nocturnal frontal lobe epilepsy', *Neurology*. doi: 10.1212/WNL.0000000000000488.

Pimentel-Silva, L. R. *et al*. (2020) 'Interactions between in vivo neuronal-glial markers, side of hippocampal sclerosis, and pharmacoresponse in temporal lobe epilepsy', *Epilepsia*. doi: 10.1111/epi.16509.

Pitkänen, A. *et al*. (1998) 'Amygdala damage in experimental and human temporal lobe epilepsy', in *Epilepsy Research*. doi: 10.1016/S0920-1211(98)00055-2.

Pitkänen, A. and Engel, J. (2014) 'Past and Present Definitions of Epileptogenesis and Its Biomarkers', *Neurotherapeutics*. doi: 10.1007/s13311-014-0257-2.

Planetta, P. J. *et al*. (2016) 'Free-water imaging in Parkinson's disease and atypical parkinsonism', *Brain*. doi: 10.1093/brain/awv361.

Plant, G. T. and Sergott, R. C. (2011) 'Understanding and interpreting vision safety issues with vigabatrin therapy', *Acta Neurologica Scandinavica*. doi: 10.1111/j.1600-0404.2011.01601.x.

Pohlmann-Eden, B. (2011) 'Conceptual relevance of new-onset epilepsy', *Epilepsia*. doi: 10.1111/j.1528-1167.2011.03142.x.

Pressl, C. *et al*. (2019) 'Resting state functional connectivity patterns associated with pharmacological treatment resistance in temporal lobe epilepsy', *Epilepsy Research*. doi: 10.1016/j.eplepsyres.2018.11.002.

Provencher, S. (2019) *LCModel & LCMgui User's Manual*.

Provencher, S. W. (1993) 'Estimation of metabolite concentrations from localized in vivo proton NMR spectra', *Magnetic Resonance in Medicine*. doi:

10.1002/mrm.1910300604.
R&D Systems Inc (2017) 'Quantikine ® HS ELISA Human IL-1β/IL-1F2 Immunoassay', pp. 1–13.
Racine, R. J. *et al*. (1988) 'The effects of various lesions and knife-cuts on septal and amygdala kindling in the rat', *Brain Research*. doi: 10.1016/0006-8993(88)90826-8.
Rajagopalan, V. *et al*. (2017) 'A Basic Introduction to Diffusion Tensor Imaging Mathematics and Image Processing Steps', *Brain Disorders & Therapy*. doi: 10.4172/2168-975x.1000229.
RajMohan, V. and Mohandas, E. (2007) 'The limbic system', *Indian Journal of Psychiatry*. doi: 10.4103/0019-5545.33264.
Ramantani, G. and Holthausen, H. (2017) 'Epilepsy after cerebral infection: review of the literature and the potential for surgery', *Epileptic Disorders*. doi: 10.1684/epd.2017.0916.
Ramli, N. *et al*. (2015) 'Neuroimaging in refractory epilepsy. Current practice and evolving trends', *European Journal of Radiology*. Elsevier Ireland Ltd, 84(9), pp. 1791–1800. doi: 10.1016/j.ejrad.2015.03.024.
Rasmussen, T. and Feindel, W. (1991) 'Temporal Lobectomy with Amygdalectomy and Minimal Hippocampal Resection: Review of 100 Cases', *Canadian Journal of Neurological Sciences / Journal Canadien des Sciences Neurologiques*. doi: 10.1017/S0317167100032807.
Ravizza, T. *et al*. (2006) 'The IL-1β system in epilepsy-associated malformations of cortical development', *Neurobiology of Disease*. doi: 10.1016/j.nbd.2006.06.003.
Ravizza, T. *et al*. (2008) 'Innate and adaptive immunity during epileptogenesis and spontaneous seizures: Evidence from experimental models and human temporal lobe epilepsy', *Neurobiology of Disease*. doi: 10.1016/j.nbd.2007.08.012.
Ravizza, T. *et al*. (2018) 'High Mobility Group Box 1 is a novel pathogenic factor and a mechanistic biomarker for epilepsy', *Brain, Behavior, and Immunity*. doi: 10.1016/j.bbi.2017.10.008.
Ravizza, T. and Vezzani, A. (2006) 'Status epilepticus induces time-dependent neuronal and astrocytic expression of interleukin-1 receptor type I in the rat limbic system', *Neuroscience*. doi: 10.1016/j.neuroscience.2005.07.063.
Ravizza, T. and Vezzani, A. (2018) 'Pharmacological targeting of brain inflammation in epilepsy: Therapeutic perspectives from experimental and clinical

studies', *Epilepsia Open*. doi: 10.1002/epi4.12242.
Reeves, C. *et al*. (2016) 'Combined Ex Vivo 9.4T MRI and Quantitative Histopathological Study in Normal and Pathological Neocortical Resections in Focal Epilepsy', *Brain Pathology*. doi: 10.1111/bpa.12298.
Rezayev, A. *et al*. (2018) 'Bilateral thalamocortical abnormalities in focal cortical dysplasia', *Brain Research*. doi: 10.1016/j.brainres.2018.05.005.
Riley, J. D. *et al*. (2010) 'Altered white matter integrity in temporal lobe epilepsy: Association with cognitive and clinical profiles', *Epilepsia*. doi: 10.1111/j.1528-1167.2009.02508.x.
Rodríguez-Cruces, R. and Concha, L. (2015) 'White matter in temporal lobe epilepsy: clinico-pathological correlates of water diffusion abnormalities.', *Quantitative imaging in medicine and surgery*, 5(2), pp. 264–26478. doi: 10.3978/j.issn.2223-4292.2015.02.06.
Ross, A. J. and Sachdev, P. S. (2004) 'Magnetic resonance spectroscopy in cognitive research', *Brain Research Reviews*. doi: 10.1016/j.brainresrev.2003.11.001.
Rostampour, M. *et al*. (2018) 'Detection of structural abnormalities of cortical and subcortical gray matter in patients with MRI-negative refractory epilepsy using neurite orientation dispersion and density imaging', *Physica Medica*. doi: 10.1016/j.ejmp.2018.03.005.
Rugg-Gunn, F. J. and Stapley, H. B. (2017) *EPILEPSY 2017 From Bench to Bedside: A Practical Guide to Epilepsy*. International League Against Epilepsy.
Ryan, N. S. *et al*. (2013) 'Magnetic resonance imaging evidence for presymptomatic change in thalamus and caudate in familial Alzheimer's disease', *Brain*. doi: 10.1093/brain/awt065.
Salanova, V. *et al*. (2015) 'Long-term efficacy and safety of thalamic stimulation for drug-resistant partial epilepsy', *Neurology*. doi: 10.1212/WNL.0000000000001334.
Salmenperä, T. *et al*. (2005) 'Hippocampal damage in newly diagnosed focal epilepsy: A prospective MRI study', *Neurology*. doi: 10.1212/01.WNL.0000148643.36513.2A.
Sama, M. A. *et al*. (2008) 'Interleukin-1β-dependent signaling between astrocytes and neurons depends critically on astrocytic calcineurin/NFAT activity', *Journal of Biological Chemistry*. doi: 10.1074/jbc.M800148200.
Saukkonen, A. *et al*. (1994) 'Do seizures cause neuronal damage? A MRI study in

newly diagnosed and chronic epilepsy', *NeuroReport*. doi: 10.1097/00001756-199412300-00055.

Savic, I. *et al*. (2000) 'In vivo measurements of glutamine + glutamate (Glx) and N-acetyl aspartate (NAA) levels in human partial epilepsy', *Acta Neurologica Scandinavica*. doi: 10.1034/j.1600-0404.2000.102003179.x.

Schmahmann, J. D. (2003) 'Vascular syndromes of the thalamus', *Stroke*. doi: 10.1161/01.STR.0000087786.38997.9E.

Schurr, J. *et al*. (2017) 'Mild Malformation of Cortical Development with Oligodendroglial Hyperplasia in Frontal Lobe Epilepsy: A New Clinico-Pathological Entity', *Brain Pathology*. doi: 10.1111/bpa.12347.

Schwarcz, R., Eid, T. and Du, F. (2000) 'Neurons in layer III of the entorhinal cortex. A role in epileptogenesis and epilepsy?', in *Annals of the New York Academy of Sciences*. doi: 10.1111/j.1749-6632.2000.tb06735.x.

Schwartz, M. *et al*. (2006) 'Microglial phenotype: Is the commitment reversible?', *Trends in Neurosciences*. doi: 10.1016/j.tins.2005.12.005.

Scott, G. *et al*. (2017) 'Microglial positron emission tomography (PET) imaging in epilepsy: Applications, opportunities and pitfalls', *Seizure*. doi: 10.1016/j.seizure.2016.10.023.

Serres, S. *et al*. (2009) 'Systemic inflammatory response reactivates immune-mediated lesions in rat brain', *Journal of Neuroscience*. doi: 10.1523/JNEUROSCI.0406-09.2009.

Shi, S. *et al*. (2018) 'Effect of lamotrigine on cognitive function and serum inflammatory factors in patients with depression of recurrent bipolar disorder', *Pakistan journal of pharmaceutical sciences*.

Shih, T. M., Duniho, S. M. and McDonough, J. H. (2003) 'Control of nerve agent-induced seizures is critical for neuroprotection and survival', *Toxicology and Applied Pharmacology*. doi: 10.1016/S0041-008X(03)00019-X.

Sillanpää, M. (1993) 'Remission of Seizures and Predictors of Intractability in Long-Term Follow-Up', *Epilepsia*. doi: 10.1111/j.1528-1157.1993.tb02114.x.

Sillanpää, M., Haataja, L. and Shinnar, S. (2004) 'Perceived impact of childhood-onset epilepsy on quality of life as an adult', *Epilepsia*. doi: 10.1111/j.0013-9580.2004.44203.x.

Simister, R. J. *et al*. (2007) 'Proton magnetic resonance spectroscopy of

malformations of cortical development causing epilepsy', *Epilepsy Research*. doi: 10.1016/j.eplepsyres.2007.02.002.

De Simoni, M. G. *et al*. (2000) 'Inflammatory cytokines and related genes are induced in the rat hippocampus by limbic status epilepticus', *European Journal of Neuroscience*. doi: 10.1046/j.1460-9568.2000.00140.x.

Sivakanthan, S. *et al*. (2016) 'The evolving utility of diffusion tensor tractography in the surgical management of temporal lobe epilepsy: a review', *Acta Neurochirurgica*. Acta Neurochirurgica, 158(11), pp. 2185–2193. doi: 10.1007/s00701-016-2910-5.

Skjei, K. L. *et al*. (2015) 'Clinical and histopathological outcomes in patients with SCN1A mutations undergoing surgery for epilepsy', *Journal of Neurosurgery: Pediatrics*. doi: 10.3171/2015.5.PEDS14551.

Smith, S. M. *et al*. (2004) 'Advances in functional and structural MR image analysis and implementation as FSL', in *NeuroImage*. doi: 10.1016/j.neuroimage.2004.07.051.

So, M. and Ryvlin, M. (eds) (2015) *MRI-Negative Epilepsy*. Cambridge: Cambridge University Press. doi: 10.1017/CBO9781139525312.

Soares, D. P. and Law, M. (2009) 'Magnetic resonance spectroscopy of the brain: review of metabolites and clinical applications', *Clinical Radiology*. doi: 10.1016/j.crad.2008.07.002.

Soares, J. M. *et al*. (2013) 'A hitchhiker's guide to diffusion tensor imaging', *Frontiers in Neuroscience*. doi: 10.3389/fnins.2013.00031.

Sousa, H. T. de, Brito, J. and Magro, F. (2018) 'New cross-sectional imaging in IBD', *Current Opinion in Gastroenterology*, 34(4), pp. 194–207. doi: 10.1097/MOG.0000000000000440.

Squire, L. R., Stark, C. E. L. and Clark, R. E. (2004) 'The medial temporal lobe', *Annual Review of Neuroscience*. doi: 10.1146/annurev.neuro.27.070203.144130.

Stefanits, H. *et al*. (2017) 'Seven-Tesla MRI of Hippocampal Sclerosis: An in Vivo Feasibility Study with Histological Correlations', *Investigative Radiology*. doi: 10.1097/RLI.0000000000000388.

Steinlein, O. K. *et al*. (1995) 'A missense mutation in the neuronal nicotinic acetylcholine receptor α4 subunit is associated with autosomal dominant nocturnal frontal lobe epilepsy', *Nature Genetics*. doi: 10.1038/ng1095-201.

Stephen, L. J. *et al*. (2006) 'Pharmacological outcomes in older people with newly diagnosed epilepsy', *Epilepsy and Behavior*. doi: 10.1016/j.yebeh.2005.11.007.
Steriade, M. (1997) *Thalamus: Experimental and clinical aspects*. Elsevier.
Steven, A. J., Zhuo, J. and Melhem, E. R. (2014) 'Diffusion kurtosis imaging: An emerging technique for evaluating the microstructural environment of the brain', *American Journal of Roentgenology*. doi: 10.2214/AJR.13.11365.
Suarez, R. O. *et al*. (2014) 'Passive fMRI mapping of language function for pediatric epilepsy surgical planning: Validation using Wada, ECS, and FMAER', *Epilepsy Research*. doi: 10.1016/j.eplepsyres.2014.09.016.
Sun, Z. *et al*. (2020) 'Diffusion Kurtosis Imaging Reveals Optic Tract Damage That Correlates with Clinical Severity in Glaucoma', in *Proceedings of the Annual International Conference of the IEEE Engineering in Medicine and Biology Society, EMBS*. doi: 10.1109/EMBC44109.2020.9176192.
Swenson, R. (2006) 'Thalamic Organization', in *Review of Clinical and Functional Neuroscience*. http://www.dartmouth.edu/.
Symms, M. *et al*. (2004) 'A review of structural magnetic resonance neuroimaging', *Journal of Neurology, Neurosurgery and Psychiatry*. doi: 10.1136/jnnp.2003.032714.
Tabesh, A. *et al*. (2011) 'Estimation of tensors and tensor-derived measures in diffusional kurtosis imaging', *Magnetic Resonance in Medicine*, 65(3), pp. 823–836. doi: 10.1002/mrm.22655.
Taylor, D. G. and Bushell, M. C. (1985) 'The spatial mapping of translational diffusion coefficients by the NMR imaging technique', *Physics in Medicine and Biology*. doi: 10.1088/0031-9155/30/4/009.
Thijs, R. D. *et al*. (2019) 'Epilepsy in adults', *The Lancet*. doi: 10.1016/S0140-6736(18)32596-0.
Thomas, R. H. and Berkovic, S. F. (2014) 'The hidden genetics of epilepsy - A clinically important new paradigm', *Nature Reviews Neurology*. doi: 10.1038/nrneurol.2014.62.
Thompson, P. J. and Duncan, J. S. (2005) 'Cognitive decline in severe intractable epilepsy', *Epilepsia*. doi: 10.1111/j.1528-1167.2005.00279.x.
Thudium, M. O. *et al*. (2010) 'The basal temporal approach for mesial temporal surgery: Sparing the meyer loop with navigated diffusion tensor tractography',

Neurosurgery. doi: 10.1227/NEU.0b013e3181f7424b.

Tournier, J. D., Calamante, F. and Connelly, A. (2007) 'Robust determination of the fibre orientation distribution in diffusion MRI: Non-negativity constrained super-resolved spherical deconvolution', *NeuroImage*. doi: 10.1016/j.neuroimage.2007.02.016.

Tschampa, H. J. *et al*. (2015) 'Proton magnetic resonance spectroscopy in focal cortical dysplasia at 3 T', *Seizure*, 32, pp. 23–29. doi: 10.1016/j.seizure.2015.08.008.

Urenjak, J. *et al*. (1993) 'Proton nuclear magnetic resonance spectroscopy unambiguously identifies different neural cell types', *Journal of Neuroscience*. doi: 10.1523/jneurosci.13-03-00981.1993.

Varella, P. P. V. *et al*. (2011) 'Relationship between fluid-attenuated inversion-recovery (FLAIR) signal intensity and inflammatory mediator ' s levels in the hippocampus of patients with temporal lobe epilepsy and mesial temporal sclerosis', 69(1), pp. 91–99.

Varoglu, A. O. *et al*. (2009) 'Prognosis of patients with mesial temporal lobe epilepsy due to hippocampal sclerosis', *Epilepsy Research*. doi: 10.1016/j.eplepsyres.2009.03.001.

Veraart, J., Fieremans, E. and Novikov, D. S. (2019) 'On the scaling behavior of water diffusion in human brain white matter', *NeuroImage*. doi: 10.1016/j.neuroimage.2018.09.075.

Vezzani, A. *et al*. (1999) 'Interleukin-1β immunoreactivity and microglia are enhanced in the rat hippocampus by focal kainate application: Functional evidence for enhancement of electrographic seizures', *Journal of Neuroscience*. doi: 10.1523/jneurosci.19-12-05054.1999.

Vezzani, A. *et al*. (2000) 'Powerful anticonvulsant action of IL-1 receptor antagonist on intracerebral injection and astrocytic overexpression in mice', *Proceedings of the National Academy of Sciences of the United States of America*. doi: 10.1073/pnas.190206797.

Vezzani, A. *et al*. (2016) 'Infections, inflammation and epilepsy', *Acta Neuropathologica*. doi: 10.1007/s00401-015-1481-5.

van Vliet, E. A., Aronica, E. and Gorter, J. A. (2015) 'Blood-brain barrier dysfunction, seizures and epilepsy', *Seminars in Cell and Developmental Biology*. doi: 10.1016/j.semcdb.2014.10.003.

Walker, M. C. (2015) 'Hippocampal sclerosis: Causes and prevention', *Seminars in Neurology*. doi: 10.1055/s-0035-1552618.
Wasserthal, J. *et al*. (2019) 'Combined tract segmentation and orientation mapping for bundle-specific tractography', *Medical Image Analysis*. Elsevier B.V., 58, p. 101559. doi: 10.1016/j.media.2019.101559.
Wasserthal, J., Neher, P. F. and Maier-Hein, K. H. (2018) 'Tract orientation mapping for bundle-specific tractography', *Lecture Notes in Computer Science (including subseries Lecture Notes in Artificial Intelligence and Lecture Notes in Bioinformatics)*, 11072 LNCS, pp. 36–44. doi: 10.1007/978-3-030-00931-1_5.
Wasserthal, J., Neher, P. and Maier-Hein, K. H. (2018) 'TractSeg - Fast and accurate white matter tract segmentation', *NeuroImage*. Elsevier Ltd, 183(July), pp. 239–253. doi: 10.1016/j.neuroimage.2018.07.070.
Watanabe, Y. and Funahashi, S. (2012) 'Thalamic mediodorsal nucleus and working memory', *Neuroscience and Biobehavioral Reviews*. doi: 10.1016/j.neubiorev.2011.05.003.
Weber, R. A. *et al*. (2015) 'Diffusional kurtosis and diffusion tensor imaging reveal different time-sensitive stroke-induced microstructural changes', *Stroke*. doi: 10.1161/STROKEAHA.114.006782.
Weintraub, D. *et al*. (2007) 'Psychiatric and behavioral side effects of the newer antiepileptic drugs in adults with epilepsy', *Epilepsy and Behavior*. doi: 10.1016/j.yebeh.2006.08.008.
Weissinger, F. *et al*. (2000) 'Optical imaging reveals characteristic seizure onsets, spread patterns, and propagation velocities in hippocampal-entorhinal cortex slices of juvenile rats', *Neurobiology of Disease*. doi: 10.1006/nbdi.2000.0298.
West, S. *et al*. (2019) 'Surgery for epilepsy', *Cochrane Database of Systematic Reviews*. doi: 10.1002/14651858.CD010541.pub3.
Whelan, C. D. *et al*. (2018) 'Structural brain abnormalities in the common epilepsies assessed in a worldwide ENIGMA study', *Brain*. doi: 10.1093/brain/awx341.
Wiebe, S. *et al*. (2001) 'A Randomized, Controlled Trial of Surgery for Temporal-Lobe Epilepsy', *New England Journal of Medicine*. doi: 10.1056/nejm200108023450501.
Wieser, H. G. (2000) 'Mesial temporal lobe epilepsy versus amygdalar epilepsy: Late seizure recurrence after initially successful amygdalotomy and regained seizure

control following hippocampectomy', *Epileptic Disorders*.
Wild, J. M. *et al*. (2007) 'Vigabatrin and epilepsy: Lessons learned', *Epilepsia*. doi: 10.1111/j.1528-1167.2007.01133.x.
Winer, J. A. (1992) 'The Functional Architecture of the Medial Geniculate Body and the Primary Auditory Cortex', in. doi: 10.1007/978-1-4612-4416-5_6.
Winston, G. P. *et al*. (2014) 'Advanced diffusion imaging sequences could aid assessing patients with focal cortical dysplasia and epilepsy', *Epilepsy Research*. Elsevier B.V., 108(2), pp. 336–339. doi: 10.1016/j.eplepsyres.2013.11.004.
Winston, G. P. (2015) 'The potential role of novel diffusion imaging techniques in the understanding and treatment of epilepsy.', *Quantitative imaging in medicine and surgery*, 5(2), pp. 279–27987. doi: 10.3978/j.issn.2223-4292.2015.02.03.
Winston, G. P. *et al*. (2020) 'Microstructural imaging in temporal lobe epilepsy: Diffusion imaging changes relate to reduced neurite density', *NeuroImage: Clinical*. doi: 10.1016/j.nicl.2020.102231.
Woermann, F. G. *et al*. (1999) 'Short echo time single-voxel 1H magnetic resonance spectroscopy in magnetic resonance imaging-negative temporal lobe epilepsy: Different biochemical profile compared with hippocampal sclerosis', *Annals of Neurology*. doi: 10.1002/1531-8249(199903)45:3<369::AID-ANA13>3.0.CO;2-Q.
Wozny, C. *et al*. (2005) 'Entorhinal cortex entrains epileptiform activity in CA1 in pilocarpine-treated rats', *Neurobiology of Disease*. doi: 10.1016/j.nbd.2005.01.016.
Wu, H. *et al*. (2018) 'Emerging Role of High Mobility Group Box-1 in Thrombosis-Related Diseases', *Cellular Physiology and Biochemistry*. doi: 10.1159/000490818.
Yasuda, C. L. *et al*. (2019) 'Predicting the Outcome of Surgical Interventions for Epilepsy Using Imaging Biomarkers', *Imaging Biomarkers in Epilepsy*, pp. 169–180. doi: 10.1017/9781316257951.017.
Yasuda, C. L. and Cendes, F. (2012) 'Neuroimaging for the prediction of response to medical and surgical treatment in epilepsy', *Expert Opinion on Medical Diagnostics*. doi: 10.1517/17530059.2012.683408.
Yeatman, J. D. *et al*. (2012) 'Tract Profiles of White Matter Properties: Automating Fiber-Tract Quantification', *PLoS ONE*. doi: 10.1371/journal.pone.0049790.
Yendiki, A. *et al*. (2011) 'Automated probabilistic reconstruction of white-matter pathways in health and disease using an atlas of the underlying anatomy', *Frontiers in Neuroinformatics*. doi: 10.3389/fninf.2011.00023.

Yogarajah, M. *et al*. (2009) 'Defining Meyers looptemporal lobe resections, visual field deficits and diffusion tensor tractography', *Brain*. doi: 10.1093/brain/awp114.
Zahr, N. M. *et al*. (2014) 'Imaging Neuroinflammation? A Perspective from MR Spectroscopy', *Brain Pathology*. doi: 10.1111/bpa.12197.
Zayed, N. *et al*. (2011) 'Valproic acid suppresses interleukin-1β-induced microsomal prostaglandin E 2 synthase-1 expression in chondrocytes through upregulation of NAB1', *Journal of Rheumatology*. doi: 10.3899/jrheum.100907.
Zhang, C. H. *et al*. (2015) 'Thalamocortical relationship in epileptic patients with generalized spike and wave discharges - A multimodal neuroimaging study', *NeuroImage: Clinical*. doi: 10.1016/j.nicl.2015.07.014.
Zhang, H. *et al*. (2012) 'NODDI: Practical in vivo neurite orientation dispersion and density imaging of the human brain', *NeuroImage*. Elsevier Inc., 61(4), pp. 1000–1016. doi: 10.1016/j.neuroimage.2012.03.072.
Zhang, X. *et al*. (2011) 'Social network theory applied to resting-state fMRI connectivity data in the identification of epilepsy networks with iterative feature selection', *Journal of Neuroscience Methods*. doi: 10.1016/j.jneumeth.2011.04.020.
Zhang, Y. *et al*. (2013) 'A preliminary study of epilepsy in children using diffusional kurtosis imaging', *Clinical Neuroradiology*, 23(4), pp. 293–300. doi: 10.1007/s00062-013-0212-3.
Zhang, Y. *et al*. (2016) 'A diffusional kurtosis imaging study of idiopathic generalized epilepsy with unilateral interictal epileptiform discharges in children', *Journal of Neuroradiology*. Elsevier Masson SAS, 43(5), pp. 339–345. doi: 10.1016/j.neurad.2016.05.001.
Zhang, Z. *et al*. (2009) 'Impaired attention network in temporal lobe epilepsy: A resting FMRI study', *Neuroscience Letters*. doi: 10.1016/j.neulet.2009.04.040.
Zhao, J. *et al*. (2017) 'Therapeutic potential of an anti-high mobility group box-1 monoclonal antibody in epilepsy', *Brain, Behavior, and Immunity*. doi: 10.1016/j.bbi.2017.02.002.
Zhou, X. *et al*. (2019) 'Disruption and lateralization of cerebellar–cerebral functional networks in right temporal lobe epilepsy: A resting-state fMRI study', *Epilepsy and Behavior*. doi: 10.1016/j.yebeh.2019.03.020.
Zhu, H. and Barker, P. B. (2010) 'MR spectroscopy and spectroscopic imaging of the brain', *Methods in Molecular Biology*. doi: 10.1007/978-1-61737-992-5_9.

Zhuo, J. *et al*. (2012) 'Diffusion kurtosis as an in vivo imaging marker for reactive astrogliosis in traumatic brain injury', *NeuroImage*. doi: 10.1016/j.neuroimage.2011.07.050.

Ziyeh, S. *et al*. (2002) 'Valproate-induced encephalopathy: Assessment with MR imaging and 1H MR spectroscopy', *Epilepsia*. doi: 10.1046/j.1528-1157.2002.42201.x.

Zurolo, E. *et al*. (2011) 'Activation of toll-like receptor, RAGE and HMGB1 signalling in malformations of cortical development', *Brain*. doi: 10.1093/brain/awr032.